Abteilung Zoologie und Endokrinologie der Universität Ulm
und
Abteilung Zentrales Nervensystem der Boehringer Ingelheim
Pharma GmbH & Co.KG

Die Beteiligung verschiedener a-Synuklein Oligomere in der Entstehung der Parkinson Krankheit

Dissertation (kumulativ) zur Erlangung des Doktorgrades Dr. rer. nat.
der Fakultät für Naturwissenschaften der Universität Ulm

vorgelegt von
Karin Danzer
aus Biberach/Riß

2007

Amtierender Dekan: Prof. Dr. Klaus-Dieter Spindler

Erstgutachter: apl. Prof. Dr. Wolfgang Weidemann
Zweitgutachter:

Tag der Promotion:

Die Arbeiten im Rahmen der vorgelegten Dissertation wurden in der Abteilung Zentrales Nervensystem der Boehringer Ingelheim Pharma GmbH & Co. KG durchgeführt und von Herrn Dr. Marcus Kostka betreut.

Ulm, den 2. Juli 2007

„*Die Naturwissenschaft braucht der Mensch zum Erkennen, die Religion zum Handeln, weil wir mit unseren Willensentscheidungen nicht warten können, bis die Erkenntnisse vollständig, und bis wir allwissend geworden sind.*“

Max Planck (1858-1947), dt. Physiker

Inhaltsverzeichnis

1 Einleitung

1.1 Die Parkinson Krankheit

Die Parkinson Krankheit (PK) wurde erstmals 1817 von James Parkinson beschrieben (Parkinson, 1817).

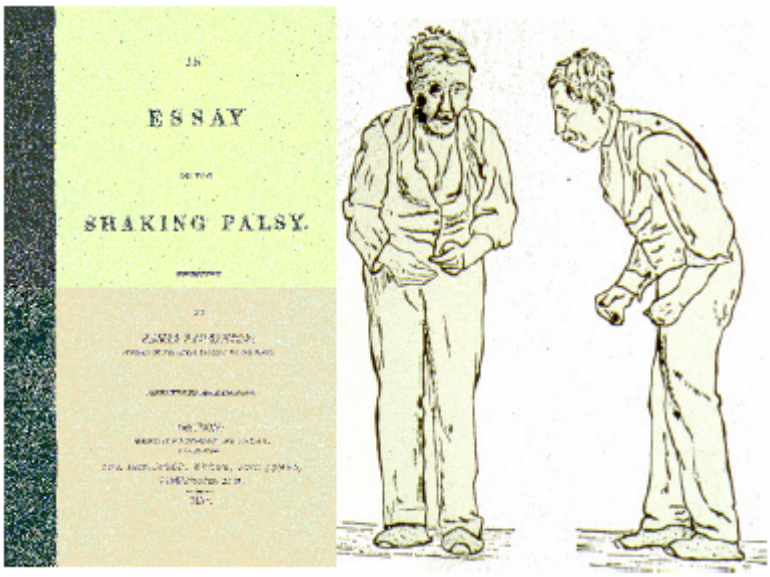

Abbildung 1: Erste Beschreibung der Symptome eines Parkinson Patienten durch James Parkinson

Sie beginnt im Allgemeinen zwischen dem 50. und 60. Lebensjahr und betrifft rund 1-2% der europäischen Bevölkerung ab einem Alter von 65 Jahren. Damit ist der Morbus Parkinson die zweithäufigste neurodegenerative Erkrankung nach dem Morbus Alzheimer. Charakteristisch für die Parkinson Krankheit ist eine progressive Reduktion der dopaminergen Neuronen in der Substantia nigra, die zu einer dopaminergen Minderinnervation des Striatums führt. Ab einem Verlust von ca. 60 % der neuromelaninhaltigen Neuronen oder einer Dopaminreduktion von ca. 80 % im Striatum kommt es zu den charakteristischen Symptomen, wie Tremor (unwillkürliches Zittern), Rigor (Muskelsteifheit) und Bradykinese/Akinese (langsame/fehlende Bewegung)(Bernheimer et al., 1973; McGeer et al., 1988; Fearnley und Lees, 1991). Dieser Verlust an dopaminergen Neuronen kann mittels Positronen-Emissions-Tomographie (PET) dargestellt werden. Dabei wird die Dopamintransporterdichte durch die Bindung von ^{18}F-Dopa an den Dopaminrezeptor

gemessen. Je nach Stärke der radioaktiven Strahlung können die Regionen des Gehirns in unterschiedlichen Farbabstufungen dargestellt werden (vgl. Abb. 2).

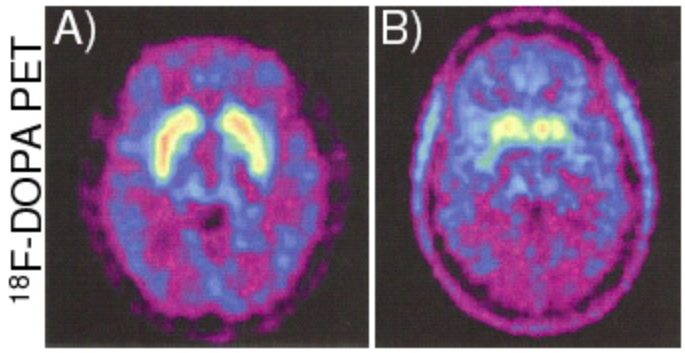

Abbildung 2: ^{18}F-Dopa PET Analyse eines Parkinsonpatientengehirns im Vergleich zum gesunden Menschengehirn

A) Kontrollgehirn eines gesunden Menschens mit normaler Aufnahme von ^{18}F-Dopa im Striatum (starke Gelbfärbung) B) Gehirn eines Parkinsonpatienten mit verminderter Aufnahme von ^{18}F-Dopa im Striatum (abgeschwächte Gelbfärbung) (Dekker et al., 2004)

Neben der Substantia nigra sind bei der Parkinson Krankheit auch andere Hirnareale wie der cholinerge dorsale motorische Vaguskern, der noradrenerge Locus coeruleus, der serotonerge Nucleus raphe dorsalis und Nucleus basalis meynert betroffen. Dies bedeutet, dass bei der Parkinson Krankheit keinesfalls, wie oft zu lesen ist, nur das dopaminerge System befallen ist. Auch dort kommt es in den entsprechenden Hirnarealen zur Degeneration von serotonergen, noradrenergen und cholinergen Neuronen. Deshalb kann es sowohl im frühen als auch im späten Krankheitsstadium zu nicht-motorischen Symptomen wie Halluzination, Depression, Angststörung und Demenz kommen (Galvin et al., 2001; Galvin et al., 1999; Braak et al., 2003)

Das histopathologische Charakteristikum der Parkinson Krankheit ist das Auftreten von eosinophilen, intrazellulären, fibrillären Einschlusskörperchen, so genannten Lewy-Körperchen und Lewy-Neuriten (Lewy und Lewandowski, 1912). Diese fibrillären Ablagerungen, ebenso wie die Degeneration dopaminerger Neuronen, treten bereits 10 bis 15 Jahre vor Beginn der ersten klinischen Symptomatik auf. So konnten Braak und Kollegen an post mortem Hirngewebe zeigen, dass sich Lewy-Körperchen und Lewy-Neuriten zunächst im Hirnstammgebiet und im Bulbus olfaktorius befinden. Braaks Studien deuten darauf hin, dass sich diese

Einschlusskörperchen im weiteren Krankheitsverlauf weiter zum Mittelhirn und bis zum Kortex ausbreiten (Braak et al., 2003).

Mindestens 90% der Parkinson Krankheitsfälle treten sporadisch auf, als Hauptrisikofaktor wird das Alter angesehen. Steigender oxidativer Stress im höheren Lebensalter wird hierfür als ursächlicher Faktor diskutiert. Dabei könnten verschiedene Umweltfaktoren eine Rolle spielen, jedoch ist deren Relevanz noch nicht vollständig geklärt (Langston, 1998; Brooks et al., 1999; Betarbet et al., 2000; Logroscino, 2005; Chade et al., 2006). Ungefähr 10% der Krankheitsfälle rechnet man familiären Formen zu (Gasser, 2001), denen Mutationen bestimmter Gene zugrunde liegen. Bis zum heutigen Zeitpunkt wurden 13 krankheitsverursachende Genloci und Gene identifiziert, die als PARK Gene bezeichnet werden (vgl. Tabelle 1).

Locus	Gen	Chromo-som	Proteinfunktion	Vererbung	Referenz	Lewy Körperchen
PARK 1	α–Syn Punkt-mutation	4q21	u.a. Stabilisierung und Freisetzung synaptischer Vesikel	dominant	Polymero poulos et al 1997	+
PARK 2	Parkin	6q25-27	Ubiquitin Ligase	rezessiv	Kitada et al 1998	- / (+)*
PARK 3	unbekannt	2p13	unbekannt	dominant	Gasser et al. 1998	+
PARK 4	α–Syn genomische Multiplikationen	4q21	s.o.	dominant	Singleton et al 2003	+
PARK 5	UCH-L1	4p14-15	Ubiquitin-Hydrolase/ Ligase	dominant	Leroy et al 1998	unbekannt
PARK 6	PINK-1	1q35-36	mitochondriale Protein Kinase	rezessiv	Valente et al 2004; Gandhi et al 2006	+
PARK 7	DJ-1	1p36	oxidative Stressantwort	rezessiv	Bonifati et al. 2003	unbekannt
PARK 8	LRRK2	12p11.2-q13.1	Protein Kinase	dominant	Paisan Ruiz et al. 2004; Zimprich et al. 2004	+
PARK 9 Kufor-Rakeb-syndrom	P-type ATPase, (ATP13A2)	1p36	lysosomale Typ 5 P-ATPase	rezessiv	Ramirez et al.2006; Najim al-Din et al. 1994; Williams et al. 2005	unbekannt
PARK 10	unbekannt	1p32	unbekannt	dominant	Hicks et al. 2002	unbekannt
PARK 11	unbekannt	2q36-q37	unbekannt	rezessiv	Pankratz et al. 2003	unbekannt
PARK 12	unbekannt	Xq21-q25	unbekannt	dominant	Pankratz et al. 2003	unbekannt
PARK 13	HTRA2/Omi	2p12	HtrA2/Omi Stress-regulierte Serin Endoprotease	dominant	Strauss et al. 2005	+

Tabelle 1: Bekannte Gene und Loci, die mit vererbter Parkinson Krankheit assoziiert sind, * wenige Ausnahmefälle (Farrer et al., 2001)

Auch bei den bisher genauer untersuchten Mutationen in den PARK Genen treten nahezu immer (Ausnahme bei Mutationen des Parkingens) Lewy-Körperchen und Lewy-Neuriten auf. Wie Spillantini und Kollegen 1997 zeigen konnten, bestehen diese Ablagerungen hauptsächlich aus einem zytoplasmatischen Protein namens α-Synuklein (α-Syn) (Spillantini et al., 1997) (vgl. Abb. 3).

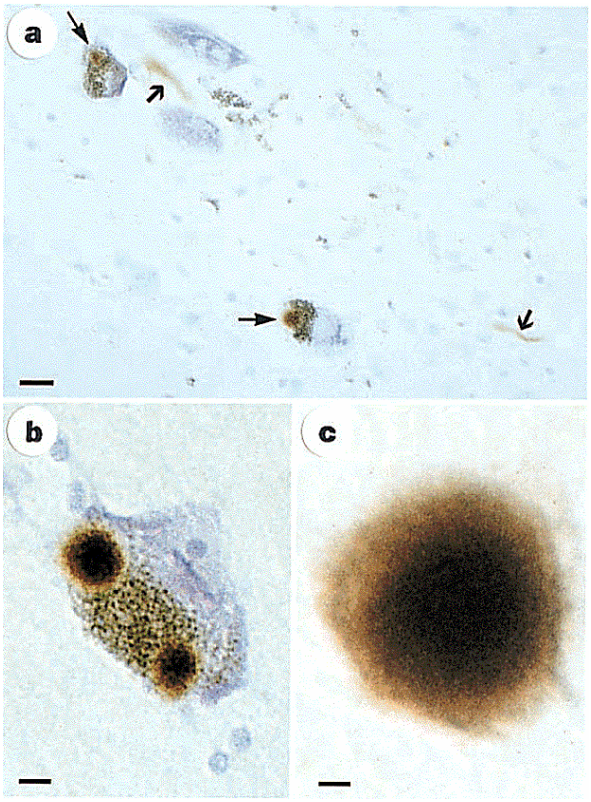

Abbildung 3: Lewy Körperchen und Lewy Neuriten

a) Zwei pigmentierte Neurone, die jeweils ein α-Syn positives Lewy Körperchen enthalten (dünne Pfeile). Lewy Neuriten (dicke Pfeile) sind ebenfalls immunpositiv. Maßstab 20 µm. b) pigmentiertes Neuron mit zwei Lewy Körperchen, Maßstab 8 µm. c) extrazelluläres Lewy Körperchen, Maßstab 4 µm. Aus Goedert 2001a

1.2 α-Syn: Lokalisierung und Struktur

1.2.1 Lokalisierung

α-Syn ist ein nahezu ungefaltetes und hoch lösliches Protein, das seinen Namen in seiner Erstbeschreibung aufgrund seiner Lokalisierung in der Synapse und im Nukleus erhalten hat (Maroteaux et al., 1988). Nachfolgende Studien beschreiben α-Syn jedoch als ausschließlich zytoplasmatisches Protein, das sich an präsynaptischen Endigungen akkumuliert (Jakes et al., 1994; Masliah et al., 1996; Petersen et al., 1999).

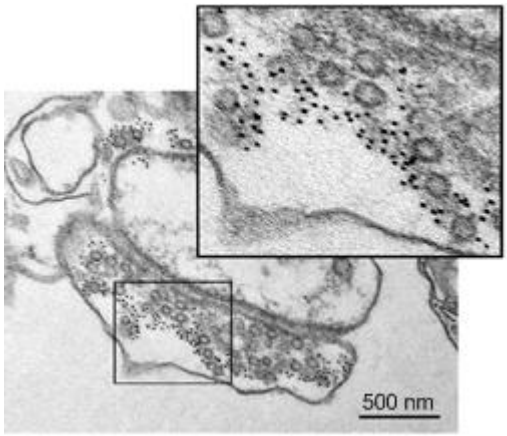

Abbildung 4: Lokalisation von α-Syn in präsynaptischen Endigungen

Elektronenmikroskopische Aufnahmen von Synaptosomen aus dem Rattengehirn, die zeigen, dass α-Syn hauptsächlich in präsynaptischen Endigungen lokalisiert ist, aus Clayton et al. 1999

α-Syn gehört zur Familie der Synukleine. Diese Proteinfamilie beinhaltet hauptsächlich α-, β- und γ-Syn (Lavedan, 1998). Ein weiter entferntes Mitglied dieser Familie ist das Retina-spezifische Paralog Synoretin (Surguchov et al., 1999). Die drei Homologe α-, β- und γ-Syn sind zwischen 127 und 140 Aminosäuren lang und zu 55-62 % identisch.

α-, β-und γ-Syn-Gene werden in hohem Maße im Gehirn exprimiert, andere Gewebe zeigen ein geringeres Expressionsniveau (vgl. Tabelle 1). Die Verteilung der Proteine innerhalb des Gehirns unterscheidet sich nur geringfügig (vgl. Tabelle 2) (Nakajo et al., 1994; Iwai et al., 1995). Spezifisch für γ-Syn wurde neben der Expression in verschiedenen Hirnarealen auch Überexpression in Brust- und Ovariar-Tumoren gefunden (Lavedan, 1998).

Table 1. Tissue Expression of the Human Synuclein Genes

	Pancreas	Kidney	Skeletal muscle	Liver	Lung	Placenta	Brain	Heart
α	+	+	++	–	+	+	++++	++
β	–	–	+	–	–	–	++++	–
γ	+	+	++	+	–	–	++++	++

The relative expression, determined by Northern blot analysis of different tissues, is indicated for a particular gene but cannot be compared here between genes: α-synuclein (Ueda et al. 1993, 1994); β-synuclein (Jakes et al. 1994; E. Leroy. pers. comm.); γ-synuclein (Lavedan et al. 1998b).

Tabelle 2: Northernblot Analyse, die die relative Expression der Synukleine in verschiedenen Geweben zusammenfasst, aus Lavedan 1998

Table 2. Expression of the Human Synuclein Genes in the Brain

	Thalamus	Subthalamic nucleus	Substantia nigra	Hippocampus	Corpus callosum	Caudate nucleus	Amygdala
α	++	+	+++	+++	++	+++	+++
β	++	–	++	++	–	+	++
γ	+++	+++	+++	++	+	++	+++

The relative expression, determined by Northern blot analysis of different tissues, is indicated for a particular gene but cannot be compared here between genes: α- and β-synuclein (E. Leroy, pers. comm.); γ-synuclein (Lavedan et al. 1998b).

Tabelle 3: Expression der Synukleine in verschiedenen Hirnarealen, aus Lavedan 1998

Bis vor kurzem wurde α-Syn als ausschließlich intrazelluläres Protein betrachtet, das hauptsächlich im Zytosol und teilweise auch membrangebunden in Vesikelfraktionen zu finden ist (George et al., 1995; Lee et al., 2002). Neuere Studien wiesen α-Syn darüber hinaus auch in der humanen Gehirn-Rückenmarks-Flüssigkeit und im Blutplasma nach (Borghi et al., 2000; El Agnaf et al., 2003).

1.2.2 Struktur

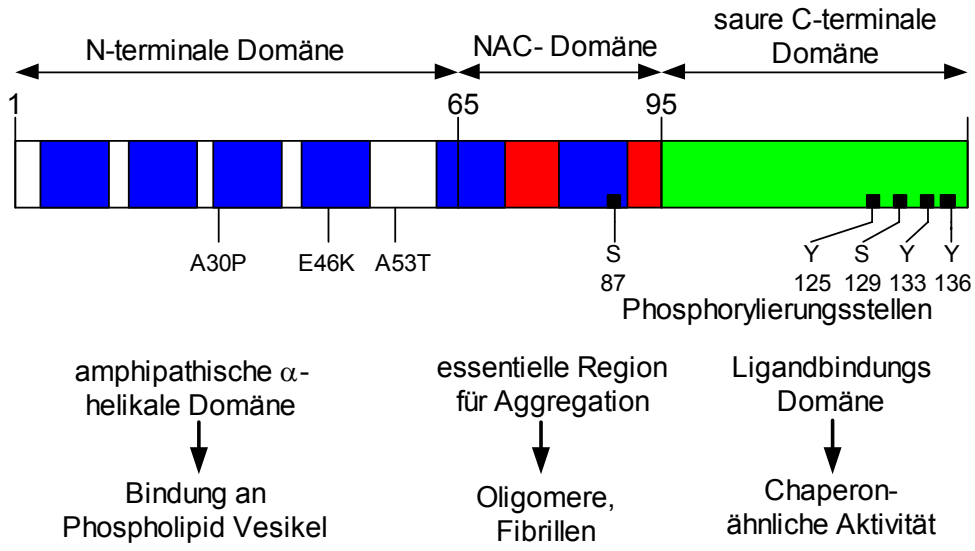

Abbildung 5: Schematische Darstellung der humanen α-Syn Sequenz mit Domänen

Die Proteinsequenz von α-Syn kann in drei Domänen eingeteilt werden (Abb. 5)

1.2.2.1 N-terminale Domäne

Die hoch konservierte N-terminale Domäne (Aminosäuren 1-65) enthält sechs Kopien einer unvollendeten 11 Aminosäure langen sich wiederholenden Sequenz, wobei es sich hier um leichte Variationen der KTKEGV-Konsensus-Sequenz handelt (Goedert, 2001a).

Diese Domäne liegt in Lösung in einer ungeordneten Struktur vor und ermöglicht die Bindung an Phospholipid Vesikel und Membranen, wodurch der N-Terminus des Proteins eine α-helikale Konformation erfährt. Die amphipatischen α-Helixes ähneln der Lipidbindungsdomäne von Klasse A2 Apolipoproteinen (Davidson et al., 1998).

1.2.2.2 NAC Domäne

Die zentrale hydrophobe Domäne von α-Syn (Aminosäuren 66-95) ist als NAC Domäne (non amyloid component of plaques) (Ueda et al., 1993) bekannt. Interessanterweise wurde diese Domäne erstmals aus senilen Plaques von Alzheimer-Patienten isoliert. Erst später wurde deutlich, dass es sich hier um einen wichtigen Teil des α-Syn handelt, der eine entscheidende Rolle für das biochemische und biophysikalische Verhalten der Proteins hat. Damit vermutete man erstmals eine

Rolle von α-Syn im Zusammenhang mit neurodegenerativen Erkrankungen. Die NAC Domäne stellt aufgrund ihrer Hydrophobizität den hoch amyloidogenen Teil des Moleküls dar, der für die Aggregation des Proteins essentiell ist.

Aminosäuresequenzanalysen verschiedener amyloidogener Proteine haben ergeben, dass sie eine gemeinsame ähnliche hydrophobe Region besitzen (Han et al., 1995; El Agnaf et al., 1998a; Uversky und Fink, 2002b). Hier handelt es sich um eine Konsensus Sequenz (^{66}VGGAVVAGV^{74}), die reich an Glycin, Alanin und Valin ist (Du et al., 2003; Du et al., 2006). Mehrere Studien weisen darauf hin, dass diese konservierte Sequenz für die Proteinaggregation essentiell ist (Uversky et al., 2002b; Florio et al., 2003; DeMarco und Daggett, 2004; Tjernberg et al., 1999; Balbach et al. 2000). Bei α-Syn liegt diese Konsensussequenz in der Nähe der Sequenzwiederholungen (KTKEGV-Motiv) innerhalb der NAC Domäne. Interessanterweise fehlt bei dem nächsten Homolog ß-Syn, das keine Aggregationsneigung zeigt (Bodles et al., 2000; Hashimoto et al., 2001; Uversky et al., 2002c), ein Teil dieser Konsensus-Sequenz und eine Sequenzwiederholung (KTKEGV-Motiv) innerhalb der NAC Domäne. El Agnaf et al. konnte in einer Studie zeigen, dass ein kurzes Peptidstück von α-Syn (^{68}GAVVT^{72}) in der Lage ist, die Bildung von Oligomeren und Fibrillen *in vitro* zu inhibieren. Dieser Aggregationsinhibitor war überdies fähig, in α-Syn überexprimierenden Zellen die durch das Protein hervorgerufene Toxizität aufzuheben (El Agnaf et al., 2004). Diese Studien machen deutlich, dass α-Syn eine Aminosäuresequenz besitzt, welche das Aggregieren von Proteinen favorisiert.

1.2.2.3 C-terminale Domäne

Der C-Terminus von α-Syn (Aminosäuren 96-140) ist negativ geladen, da er hauptsächlich aus sauren Aminosäureresten besteht (George, 2002). Man nimmt an, dass der negativ geladene C-Terminus die Aggregation inhibiert, da C-terminal verkürzte α-Syn Formen eine stärkere Neigung zur Aggregation zeigen (Crowther et al., 1998; McLean et al., 2001; McLean und Hyman, 2002; Murray et al., 2003). Jedoch lassen mehrere Studien vermuten, dass die C-terminale Domäne andererseits zur Metall induzierten Aggregation von α-Syn beiträgt (Paik et al., 1999; Ostrerova-Golts et al., 2000; Paik et al., 2000; Golts et al., 2002). Gerade in der Substantia nigra, die in der Parkinson Krankheit am meisten vom fortschreitenden

dopaminergen Neuronenverlust betroffen ist, findet man eine erhöhte Konzentrationen an Eisen (Connor et al., 1995; Zecca et al., 2002; Zecca et al., 2003; Gotz et al., 2004; Smith et al., 2005). Als weitere aggregationsbeeinflussende Faktoren werden posttranslationale Modifikationen diskutiert. Dazu gehören unter anderem Phosphorylierungen (Okochi et al., 2000), Glykosylierungen (McLean et al., 2002) und Nitrierungen (Takahashi et al., 2002).

1.3 Physiologische Funktion von α-Syn

Die physiologische Funktion von α-Syn ist bis zum heutigen Zeitpunkt noch nicht vollständig geklärt. Es wird diskutiert, dass α-Syn sowohl eine Rolle in der synaptischen Plastizität, in der Dopaminfreisetzung als auch in der Generierung von synaptischen Vesikeln spielt. Darüber hinaus gibt es neuere Hinweise, dass α-Syn eine Chaperonfunktion besitzen könnte.

Untersuchungen an Zebrafinken wiesen schon früh auf eine Funktion von α-Syn in der synaptischen Plastizität hin. So wurde bei Zebrafinken während der kritischen Phase des Lernens von Balzliedern eine erhöhte neuronale Expression von α-Syn gefunden (George et al., 1995). Dieses regulierte Expressionsmuster und der Befund, dass das Protein in Gehirnregionen, die mit Lernprozessen assoziiert sind, am stärksten exprimiert ist, unterstützen diese Annahme.

α-Syn scheint für die Aufrechterhaltung der Vesikelhomöostase und des Vesikelpools, sowie bei der Speicherung von Dopamin und Regulation der synaptischen Vesikelgröße eine wichtige Rolle zu spielen. Diese Befunde sprechen für eine Beteiligung des α-Syn in der synaptischen Übertragung (Abeliovich et al., 2000; Cabin et al., 2002; Liu et al., 2004; Yavich et al., 2004). Weiterhin wird diese Funktion durch den Befund unterstützt, dass α-Syn die Aktivität des Dopamintransporters inhibiert (Wersinger und Sidhu, 2003).

Die Sequenzhomologie von α-Syn zu anderen Chaperonen (z.B. 14-3-3 Chaperon (Ostrerova et al., 1999) oder HSP 27) und sein nativ ungefalteter Zustand, lieferten erste Hinweise für eine Chaperonfunktion des Proteins. Weitere Argumente, die die Chaperonfunktion unterstützen, sind zum einen Studien, die gezeigt haben, dass α-

Syn mit einer Mehrzahl von Liganden und zellulären Proteinen interagieren kann (Ostrerova et al., 1999; Xu et al., 2002). Einen Überblick zeigt Abb. 6.

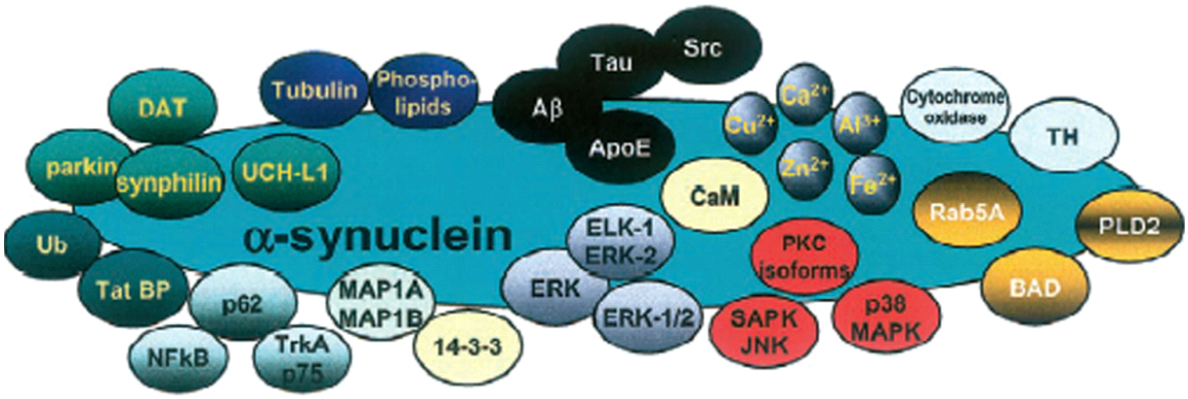

Abbildung 6: Proteine, die mit α-Syn interagieren oder kolokalisieren, aus Dev et al 2003

Zum anderen konnte in Protein-Rückfaltungs-Studien eine *in vitro* Chaperon-Aktivität des α-Syn gezeigt werden. Es wird vermutet, dass eine saure C-terminale Domäne (Aminosäuren 125-140) für die Chaperon-ähnliche Aktivität verantwortlich ist (Souza et al., 2000).

Das sicherlich überzeugendste Argument für die Chaperonfunktion des α-Syn stellt die Studie von Chandra et al. dar (2005). α-Syn konnte die Funktion eines Co-chaperons (CSPα), das maßgeblich an der synaptischen Übertragung beteiligt ist, übernehmen. CSPα defiziente Mäuse zeigen starke progressive neurodegenerative Störungen, die mit einer signifikanten Reduktion an synaptischen SNARE-Komplexen einhergehen. SNARE-Proteine haben eine entscheidende Funktion bei der Vesikelfreisetzung in den synaptischen Spalt, bei der Vesikelwiederverwertung und der synaptischen Integrität. Insbesondere scheint dabei CSPα eine Schlüsselrolle in der Faltung und Rückfaltung von SNARE-Komplexen zu spielen. Interessanterweise konnte durch Überexpression von α-Syn in diesen Mäusen der defekte Zusammenbau von SNARE Komplexen aufgehoben werden. Die Studie von Chandra et al. (2005) liefert damit einen wichtigen Hinweis für eine mögliche Chaperonfunktion des α-Syn und macht deutlich, dass α-Syn als „Hilfs-Chaperon“ fungieren kann.

1.4 Pathophysiologie von α-Syn und Aggregation

Mit der Entdeckung einer Mutation auf dem α-Syn-Gen (A53T) (Polymeropoulos et al., 1997), die für seltene familiäre Formen der Parkinson Krankheit ursächlich verantwortlich ist, wurde erstmals die Bedeutung von α-Syn bei der Entstehung der Parkinson Krankheit ersichtlich. Im selben Jahr identifizierte Spilliantini et al. α-Syn als Hauptkomponente von Lewy-Körperchen (Spillantini et al., 1997). Mit diesen Befunden von 1997 wuchs die Bedeutung von α-Syn in der Parkinson Krankheit enorm und prägte die nachfolgende Forschung grundlegend. Inzwischen sind drei Punktmutationen (A53T: (Polymeropoulos et al., 1997); A30P: (Kruger et al., 1998); E46K: (Zarranz et al., 2004)) im α-Syn-Gen bekannt, die alle zur familiären Form von Parkinson führen.

Ein weiterer Meilenstein zum Verständnis der Parkinson-Entstehung war die Entdeckung von chromosomalen Triplikationen (Singleton et al., 2003) und Duplikationen (Ibanez et al., 2004; Chartier-Harlin et al., 2004) im α-Syn-Gen bei Parkinson Familien. Dabei wurde deutlich, dass Träger einer Triplikation früher an der Parkinson Krankheit erkranken als Träger einer Duplikation. Die Menge an α-Syn determiniert also hauptsächlich sowohl Krankheitsbeginn, als auch den Schweregrad der Parkinson Krankheit. Es handelt sich hier somit um einen Gen-Dosis-Effekt. Polymorphismen in der Promoterregion dieses Gens, die zu einer verstärkten Synthese von α-Syn führen, tragen ebenfalls zu einer erhöhten Empfindlichkeit bei, an Morbus Parkinson zu erkranken (Kruger et al., 1999; Maraganore et al., 2006). Damit wird deutlich, dass auch ohne Mutationen im α-Syn-Gen, das wildtyp α-Syn die Parkinson Krankheit auslösen kann. Es wird vermutet, dass bei einer erhöhten Menge an α-Syn die Aggregation des Proteins zunimmt und dass dies ein auslösender Faktor sein könnte.

α-Syn spielt nicht nur in der Parkinson Krankheit eine wichtige Rolle, es gibt eine ganze Reihe neurodegenerativen Erkrankungen, die Ablagerungen bzw. Aggregate von α-Syn in Form von Lewy-Körperchen enthalten. Sie werden zusammenfassend als Synukleinopathien bezeichnet. Dazu gehören unter anderem die multiple Systematrophie, die Demenz mit Lewy-Körperchen und Neurodegeneration mit Eisenablagerungen Typ 1 (Goedert, 2001a; Goedert, 2001b). Insgesamt wird eine duale Rolle von α-Syn in der Neurodegeneration deutlich: die normale Funktion von

α-Syn hilft dabei, synaptische Aktivität und Integrität zu verstärken, wohingegen mutiertes α-Syn oder eine abnormale Akkumulation des wildtyp α-Syn zu Neurodegeneration führt.

α-Syn liegt in Lewy-Körperchen als fibrilläres Protein vor. Die Vorstufen von Fibrillen stellen Oligomere dar. Im Detail stellt man sich die Bildung von Oligomeren und Fibrillen folgendermaßen vor: Die Aggregation vom Monomer bis zur Fibrille verläuft schrittweise über verschiedene Stadien (vgl. Schema Abb.7). Dabei werden verschiedene Intermediate gebildet, die entweder über Protofibrillen weiter zu unlöslichen Fibrillen aggregieren oder auf dem Oligomer-Stadium verbleiben bzw. als amorphe Aggregate enden (Hoyer et al., 2002; Caughey und Lansbury, 2003; Munishkina et al., 2003). Diese Bildung von Oligomeren oder Fibrillen geht mit deutlichen Konformationsänderungen von einer ungefalteten Struktur zu einer ß-Faltblatt-Konformation einher.

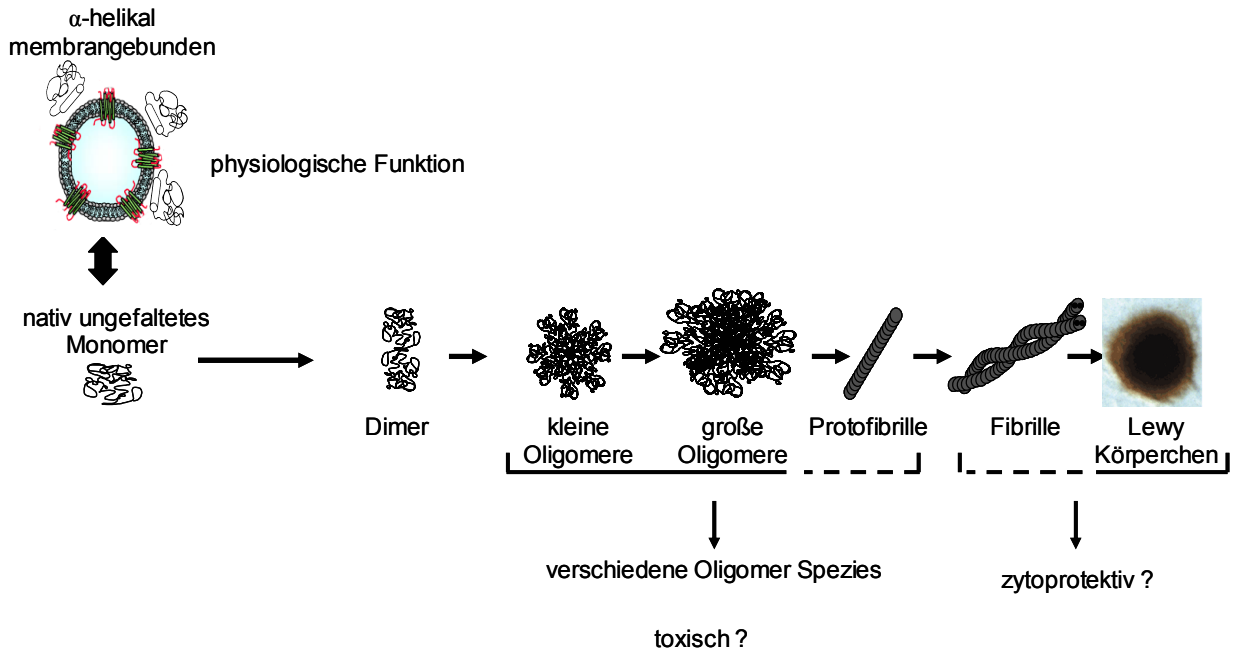

Abbildung 7: Schematische Darstellung der α-Syn Aggregation

In vitro Studien haben gezeigt, dass die Aggregation von α-Syn ein nukleationsabhängiger Prozess ist. Bei einem vorhandenen Aggregationskeim lagern sich Monomere an, wodurch die Aggregation deutlich beschleunigt wird (Wood et al., 1999; Conway et al., 2000b). Weiterhin gibt es *in vitro* Studien, die darauf hindeuten, dass die mutanten A53T, A30P und E46K Proteine zu einer gesteigerten

Aggregation im Vergleich zum wildtyp α-Syn führen. A53T und E46K Mutationen fördern anscheinend die Ausbildung von Fibrillen, wohingegen die A30P Mutation zu einer Akkumulation von Oligomeren führt (Conway et al., 1998; El Agnaf et al., 1998b; Narhi et al., 1999; Giasson et al., 1999; Wood et al., 1999; Conway et al., 2000b; Li et al., 2001; Greenbaum et al., 2005; Pandey et al., 2006).

Letztendlich kann *in vitro* die Aggregation von α-Syn auch durch verschiedene Milieubedingungen beeinflusst werden. Als aggregationsfördernde Faktoren werden ein niedriger pH-Wert (Hashimoto et al., 1998), eine erhöhte Temperatur (Hashimoto et al., 1998), eine erhöhte Proteinkonzentration von α-Syn (Hashimoto et al., 1998), ein so genanntes „molecular crowding“ (Uversky et al., 2002a) und eine erhöhte Konzentration von Metallionen (Uversky et al., 2001b) angesehen.

1.5 Oligomere und Fibrillen von α-Syn

Die Aggregation von α-Syn scheint eine entscheidende Rolle in der Parkinson Krankheit zu spielen. Als man fibrilläres α-Syn in Lewy-Körperchen fand, ging man zunächst von der Annahme aus, dass Fibrillen toxisch für Neuronen sind. Dass jedoch auch deren Vorstufen, die Oligomere, in der Pathogenese der Parkinson Krankheit eine wichtige Rolle spielen könnten, wurde zunächst außer Acht gelassen. Mittlerweile gibt es eine zunehmende Anzahl an Belegen dafür, dass eher die nicht fibrillären Oligomere und Protofibrillen die pathogene Spezies in der Parkinson Krankheit darstellen (Masliah et al., 2000; Goldberg und Lansbury, Jr., 2000; Conway et al., 2000b). Zum einen führt eine Überexpression von α-Syn in Zellkultur zu Apoptose und Schädigung von Zellorganellen, ohne Ausbildung von Fibrillen (Gosavi et al., 2002). Zum anderen zeigt eine Co-Expression von HSP70 und α-Syn in einem Drosophila-Tiermodell einen verminderten Zelltod, jedoch ohne die Anzahl an Einschlusskörperchen zu verändern (Auluck et al., 2002). Die fibrilläre Form von α-Syn kann typischerweise bei der Autopsie von Parkinson Patienten beobachtet werden (Park und Lansbury, Jr., 2003) und könnte deshalb auch neuroprotektiv sein. Vor kurzem wurde eine Substanz gefunden, die die Bildung von Einschlusskörperchen in einem Zellkulturmodell der Huntington Krankheit und der Parkinson Krankheit fördert (Bodner et al., 2006). Interessanterweise erniedrigt diese Substanz die toxischen Auswirkungen von Huntingtin und α-Syn, während es zu einer Zunahme von Einschlusskörperchen kommt.

Im Laufe der letzen Jahre wurden mehrere Mechanismen vorgeschlagen, die eventuell Konsequenzen von α-Syn Aggregaten bzw. Oligomeren sein könnten. Dazu gehören: erhöhter ER-Stress (Smith et al., 2005), oxidativer Stress, veränderte Chaperon-Aktivität (Chandra et al., 2005), Dysfunktion des Ubiquitin-Proteasom-Systems (Tanaka et al., 2001; Stefanis et al., 2001; Petrucelli et al., 2002; Snyder et al., 2003; Lindersson et al., 2004), Defekte im Mitochondrium und im Golgi-Apparat (Hsu et al., 2000; Gosavi et al., 2002; Song et al., 2004; Moore et al., 2005), gestörter axonaler Transport (Outeiro und Lindquist, 2003; Dalfo et al., 2004a; Dalfo et al., 2004b; Cooper et al., 2006), Vesikel Permeabilisierung (Volles et al., 2001; Volles und Lansbury, Jr., 2002) und lysosomale Defekte (Stefanis et al., 2001; Cuervo et al., 2004). Einige dieser Mechanismen wurden bisher nur in zellfreien Systemen untersucht (Stefanis et al., 2001; Volles et al., 2001; Volles et al., 2002; Cuervo et al., 2004), andere hat man bisher nur für mutiertes α-Syn gefunden (Stefanis et al., 2001; Cuervo et al., 2004; Tanaka et al., 2001).

Von all diesen möglichen Auswirkungen der α-Syn Aggregate wird angenommen, dass sie in der Initiation bzw. Progression der Neurodegeneration eine Schlüsselrolle spielen. Es bleibt jedoch bislang unklar, welche oligomere Formen in direktem Zusammenhang mit einer α-Syn vermittelten Toxizität stehen.

1.6 Zielsetzung der Arbeit

Obwohl es immer mehr Hinweise darauf gibt, dass α-Syn Oligomere die pathologisch relevanten Formen in der Entstehung der Parkinson Krankheit sind, ist es bisher noch unzulänglich verstanden, welche dieser Oligomere toxisch sind und wie sie ihre schädliche Wirkung entfalten.

Das Hauptziel dieser Arbeit ist es daher, den Einfluss verschiedener oligomerer Formen von α-Syn auf Zellen zu untersuchen.

In der Literatur werden verschiedene Protokolle beschrieben, um aus rekombinantem α-Syn Oligomere herzustellen. Es ist jedoch einerseits unklar, ob sich Oligomere voneinander strukturell unterscheiden und andererseits, ob diese Oligomere in Zellkultur bioaktiv sind. Außerdem verwenden alle bisher beschriebenen Protokolle hoch mikromolare Protein Konzentrationen. Zu diesem Zweck sollten zunächst

verschiedene Protokolle entwickelt werden, um aus rekombinantem α-Syn *in vitro* bei niedrigen Proteinkonzentrationen Oligomere herzustellen. Diese Oligomere sollten dann mittels hochsensitiver Techniken im pico- bis femtomolaren Bereich charakterisiert werden. Desweiteren sollte untersucht werden, welche zellulären Effekte diese *in vitro* hergestellten Oligomere in humanen Zellen hervorrufen. Um den Einfluss verschiedener α-Syn Oligomere auf α-Syn überexprimierende und nicht-überexprimierende Zellen vergleichen zu können, sollten stabile α-Syn überexprimierende neuronale Zelllinen hergestellt werden.

Zusätzlich sollte auch der Einfluss von α-Syn Oligomeren auf Signaltransduktionswege am Beispiel der Autophoshorylierungsaktivität verschiedener Proteinkinasen untersucht werden. Dazu sollten mittels einer neuen Protein-Chip-Technology putative Kinasen *in vitro* identifiziert werden, die durch Oligomereinfluss eine veränderte Autophosphorylierungsaktivität aufweisen. Ein weiteres Ziel war es, diese veränderte Kinaseaktivität auch in Proteinextrakten aus α-Syn transgenen Tieren zu bestätigen.

2 Material und Methoden

Das verwendete Material und die in der vorliegenden Arbeit angewandten Methoden sind in den Studien der Kapitel 3.1-3.3 ausführlich dargestellt. Die konfokalen Einzelmolekülspektroskopie und deren Analysemethoden wurden in dieser Form für α-Syn noch nicht angewandt, daher soll diese spezielle Methode hier ausführlich erklärt werden.

2.1 Konfokale Einzelmolekülspektroskopie

Das grundlegende theoretisch-analytische Konzept der fluoreszenzbasierten Korrelationsspektroskopie wurde bereits vor mehr als 30 Jahren zur Untersuchung chemischer Reaktionen und molekularer Diffusionsprozesse entwickelt (Magde et al. 1972, Ehrenberg und Rigler 1974, Aragon und Pecora 1975). Es basiert auf der Messung von Signalfluktuationen einer kleinen Anzahl von Molekülen in einem Messvolumen. Erst die Einführung des konfokalen Aufbaus der Fluoreszenz-Korrelations-Spektroskopie („fluorescence correlation spectroscopy“, FCS) (Rigler et al. 1993, Eigen und Rigler 1994) ermöglichte die praktische Anwendung dieses Konzepts auf die Analyse einzelner Moleküle. Damit erschloss sich eine Vielzahl analytischer Anwendungen im Bereich der Grundlagenforschung, so dass sich die FCS im Laufe der späten 90er Jahre zunehmend als Methode zur Untersuchung dynamischer Prozesse bei kleinsten, d.h. submikromolaren Konzentrationen etablierte (Schwille et al. 1997a). In der Fluoreszenz-Korrelations-Spektroskopie (FCS) werden Moleküle anhand ihrer Fluoreszenzemission charakterisiert. Dazu wird das Licht eines Anregungslasers durch ein Mikroskopobjektiv hoher numerischer Apertur auf einen Brennpunkt mit einem Durchmesser von weniger als 1 µm fokussiert. Die Fluoreszenzemission wird durch dasselbe Objektiv gesammelt und konfokal über eine Lochblende auf einen hochempfindlichen Einzelphotonendetektor, eine sogenannte Avalanche-Photodiode (APD), abgebildet (Abb. 8). Im Rahmen der meisten Anwendungen der klassischen FCS werden Fluktuationen in der lokalen Teilchenkonzentration aufgrund der Brownschen Molekularbewegung genutzt, um den Diffusionskoeffizienten von Partikeln und damit ihre Größe zu bestimmen. Bei einer Konzentration von 1 nM befindet sich dabei in einem Messvolumen von ca. 1 femtoliter im zeitlichen Mittel etwa ein Molekül. Die relative Fluktuation der Konzentration dieser Moleküle in einem offenen Lösungssystems ist dabei um so

größer, je kleiner die Konzentration der Partikel ist. Die Stärke der Korrelationanalyse liegt daher gerade in der Untersuchung nano- bis subpicomolarer Konzentrationen. Die zeitlichen Signalfluktuationen lassen sich dabei durch die Korrelationsfunktion G(τ) charakterisieren, die mathematisch betrachtet die Selbstähnlichkeit eines Signals zum Zeitpunkt t verglichen mit dem Zeitpunkt t+τ angibt (Schwille et al. 1997a). Eine technische Weiterentwicklung stellt die Kreuzkorrelations-FCS dar, die die zeitliche Korrelation zweier anhand ihrer Emissionsspektren unterscheidbarer Molekülspezies im selben Messvolumen analysiert und damit besonders geeignet zur quantitativen Analyse intermolekularer Bindungsprozesse ist (Schwille et al. 1997b). Eine zur FCS-Analyse komplementäre Möglichkeit, die im konfokalen Messaufbau gemessenen Fluoreszenzfluktuationen analytisch zu nutzen, besteht in eine Analyse der Helligkeitsfluktuationen in konsekutiven Zeitsegmenten („bins“) mittels der Fluoreszenz-Intensitäts-Verteilungs-Analyse („fluorescence intensity distribution analysis“, FIDA). Dieses Verfahren ist besonders geeignet, verschiedene Molekülspezies hinsichtlich ihrer Helligkeit zu charakterisieren und zu unterscheiden (Kask et al. 1999, Kask et al. 2000). FIDA gibt so indirekt Informationen über die Partikelgröße.

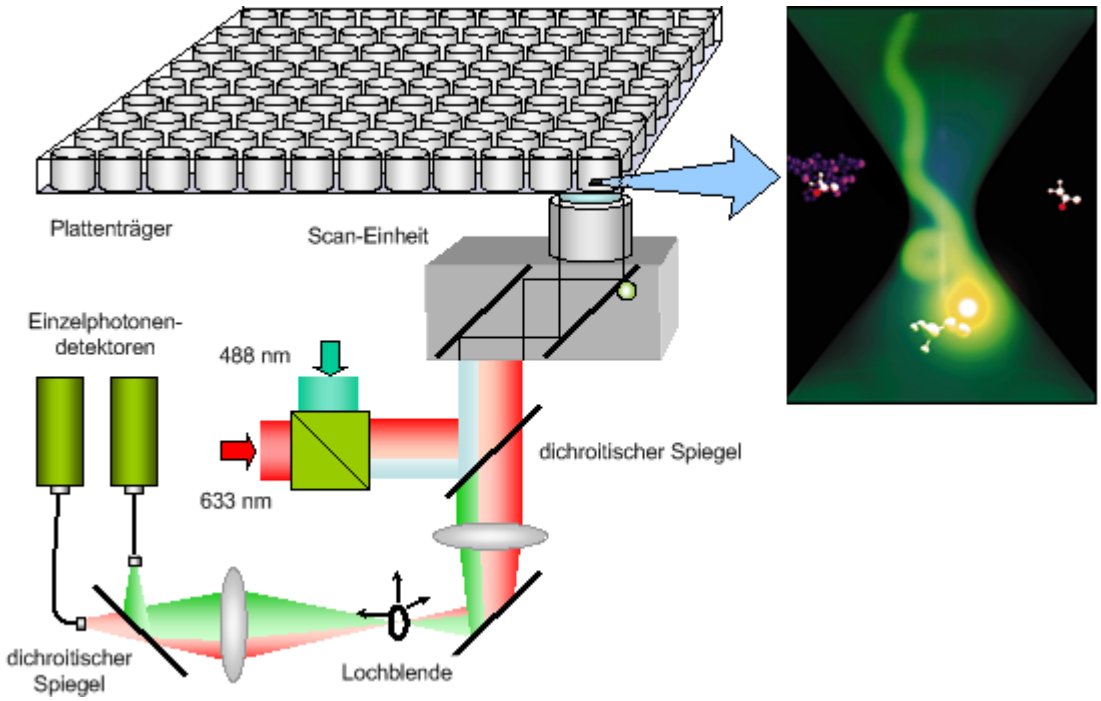

Abbildung 8: Schematische Darstellung eines konfokalen Systems zur Einzelmolekülspektroskopie

3 Ergebnisse

3.1 Single particle characterization of pore forming α-Synuclein aggregates

Marcus Kostka[1#], Tobias Högen[2#], Karin M. Danzer[1#], Matthias Habeck[2], Andreas Wirth[3], Richard Wagner[4], Charles G. Glabe[5], Sabine Finger[1], Udo Heinzelmann[1], Patrick Garidel[1], Wenzhen Duan[5], Christopher A. Ross[5], Hans Kretzschmar[2] and Armin Giese[2]

[1]CNS Research, Boehringer Ingelheim Pharma GmbH & Co KG, Germany; [2]Zentrum für Neuropathologie und Prionforschung, Ludwig-Maximilians-Universität München, Germany; [3]Ionovation GmbH, Osnabrück, Germany; [4]Abteilung Biophysik, Universität Osnabrück, Germany; [5]Department of Molecular Biology and Biochemistry, University of California, Irvine, CA 92697-3900. USA; [5]Division of Neurobiology, Department of Psychiatry, Johns Hopkins University School of Medicine, CMSC 8-121, 600 North Wolfe Street, Baltimore, Maryland 21287, USA

[#] these authors contributed equally, submitted to European Molecular Biology organisation (EMBO) on 13th May, 2007

Abstract

Aggregation of α-synuclein (α-syn) is a key event in the pathology of several neurodegenerative diseases including Parkinson´s disease. Recent findings suggest that oligomers represent the principal toxic aggregate species. We used confocal single molecule fluorescence techniques such as SIFT and atomic force microscopy to monitor α-syn oligomer formation at nanomolar protein concentrations. Ethanol was used to influence the folding of α-syn and trigger aggregation, which resulted in small oligomers ("intermediate I"). Under these conditions, Fe^{3+} at low micromolar concentrations dramatically increased aggregation and resulted in formation of larger oligomers ("intermediate II"). Both oligomer species appeared to be on-pathway to amyloid fibrils and could seed amyloid formation measured by thioflavinT binding. Notably, Fe^{3+}-induced oligomers could also form ion-permeable pores in a planar lipid bilayer assay. Both an anti-α-syn-antibody and the oligomer-specific antibody A11 inhibited pore formation. Moreover, baicalein and N´-benzylidene-benzohydrazide anti-prion compounds were able to inhibit oligomer formation. Baicalein also inhibited α-syn-dependent toxicity in cell-culture. Our results further elucidate the role of toxic oligomer species in neurodegenerative diseases and provide new approaches for drug discovery.

3.2 Different species of alpha synuclein oligomers induce calcium influx and seeding

Karin M. Danzer[1], Dorothea Haasen[2], Anne R. Karow[1],Simon Moussaud[1]; Matthias Habeck[3],Hans Kretzschmar[3]; Armin Giese[3], Bastian Hengerer[1] and Marcus Kostka[1]

[1]CNS Research Boehringer Ingelheim Pharma GmbH & Co KG, 88397 Biberach, Germany; [2]Integrated Drug Discovery, Boehringer Ingelheim Pharma GmbH & Co KG, 88397 Biberach, Germany; [3]Zentrum für Neuropathologie und Prionforschung, Ludwig-Maximilians Universität München, Germany

accepted by Journal of Neuroscience, 21st June, 2007

Abstract:

Aggregation of α-synuclein (α-syn) has been linked to the pathogenesis of Parkinsons Disease (PD) and other neurodegenerative diseases. Increasing evidence suggests that prefibrillar oligomers and protofibrils, rather than mature fibrils of α-syn, are the pathogenic species in PD. Despite extensive effort on studying oligomerisation of α-syn, no studies have compared different oligomer species directly on a single particle level and investigated their biological effects on cells. In this study we applied a novel highly sensitive single molecule detection system that allowed a direct comparison of different oligomer types. Furthermore, we studied biological effects of different oligomer types on cells. For this purpose, we developed new oligomerisation protocols, that enabled the use of these different oligomers in cell culture. We found that all of our three aggregation protocols resulted in heterogeneous populations of oligomers. Some types of oligomers induced cell death via disruption of cellular ion homeostasis by a presumably pore-forming mechanism. Other oligomer types could directly enter the cell resulting in increased α-syn aggregation. Based on our results we propose that under various physiological conditions heterogeneous populations of oligomeric forms will co-exist in an equilibrium. These different oligomer types lead directly or indirectly to cell damage. Our data indicate that inhibition of early α-syn aggregation events would consequently prevent all α-syn oligomer related toxicities. This has important implications for the development of disease modifying drugs for the treatment of PD and other synucleinopathies.

3.3 Functional protein kinase arrays reveal inhibition of p-21 activated kinase 4 by α-synuclein oligomers

Karin M. Danzer[1]*, Cathrin Schnack[1]*, Andrew Sutcliffe[2], Bastian Hengerer[1] and Frank Gillardon[1]

[1]Boehringer Ingelheim Pharma GmbH & Co KG, 88397 Biberach, Germany ; [2]Procognia Limited, Maidenhead, Berkshire SL6 7RJ, UK

*these authors contributed equally, revised version submitted to Journal of Neurochemistry on 28th June, 2007

Abstract:

There is increasing evidence that aggregation of α-synuclein contributes to the functional and structural deterioration in the central nervous system of Parkinson's disease patients and transgenic animal models. α-Synuclein binds to various cellular proteins and aggregated α-synuclein species may affect their physiological function. In the present study, we used protein arrays spotted with 178 active human kinases for a large scale analysis of the effects of recombinant α-synuclein on kinase activities. Incubation with globular α-synuclein oligomers significantly inhibited autophosphorylation of p21-activated kinase 4 compared to treatment with monomeric α-synuclein or β-synuclein. A concentration-dependent inhibition was also observed in a solution-based kinase assay. To show *in vivo* relevance, we analyzed brainstem protein extracts from α-synuclein(A30P) transgenic mice where accumulation of α-synuclein oligomers has been demonstrated. By immunoblotting using a phospho-specific antibody, we detected a significant decline in phosphorylation of LIM kinase 1, a physiological substrate for p21-activated kinase 4. Suppression of p21-activated kinase activity by amyloid-ß oligomers has recently been reported in Alzheimer's disease. Thus, p21-activated kinases may represent a target for various neurotoxic protein oligomers, and signalling deficits may contribute to the behavioural defects in chronic neurodegenerative diseases.

4 Zusammenfassung

Wie in der Zielsetzung (Kapitel 1.6) ausführlich dargelegt, ist diese Arbeit der wesentlichen Fragestellung nachgegangen, welchen Einfluss verschiedene oligomere α-Syn Formen auf Zellen haben. Eine ausführliche Beschreibung der durchgeführten Studien, sowie deren Ergebnisse und Diskussion finden sich in Kapitel 3.1-3.3, sowie in den Anhängen. Im Nachfolgenden sollen die wesentlichen Ergebnisse zusammengefasst dargestellt werden.

4.1 Ergebnisse

In der Studie von Kapitel 3.1 wurde mittels der konfokalen Einzelmolekülspektroskopie (Scanning For Intensely Fluorescent Targets (SIFT)) zum ersten Mal die Bildung von α-Syn Oligomeren in niederen nano- bis picomolaren Konzentrationen untersucht. Bisher wurde angenommen, dass es eine kritische Proteinkonzentration gäbe, unterhalb derer keine Oligomerisierung von α-Syn möglich sei (Wood et al., 1999). Die Anwendung der fluoreszenzbasierten Einzelmolekülspektroskopie ermöglichte jedoch die Analyse und Charakterisierung einzelner Oligomer-Moleküle. Dazu wurde zunächst das α-Syn Protein in *E. coli* exprimiert und mittels verschiedenerer biochemischer Methoden bis zu etwa 95% gereinigt. Der monomere Status des Proteins wurde mittels Analyse mit einem Rasterkraftmikroskop (Atomic Force Microscope (AFM)) bestimmt. Als nächster Schritt wurde ein Protokoll entwickelt, um das α-Syn im 96-well Format bei nanomolaren Proteinkonzentrationen zum oligomerisieren zu bringen. Tatsächlich war es durch Zugabe von Ethanol möglich, kleine α-Syn Oligomere auch bei geringen Konzentrationen herzustellen und zu detektieren. Durch zusätzliches Hinzufügen von Eisenchlorid nahmen diese Ethanol-induzierten Oligomere an Größe zu und konnten aufgrund des Größenunterschieds von den kleineren Oligomeren unterschieden werden. Die reine Eisenchloridzugabe ohne Ethanol im Kontrollansatz führte zu keiner Induktion der Aggregation. Um die Daten aus der fluoreszenzbasierten Einzelmolekülspektroskopie mit einer fluoreszenzunabhängigen Einzelpartikel-Detektionsmethode zu bestätigen, und die verschiedenen Oligomerpopulationen näher zu charakterisieren, wurde eine Analyse mittels AFM durchgeführt. Die AFM-Ergebnisse unterstützen die Fluoreszenz basierenden Befunde. So konnten ebenfalls kleine Ethanol-induzierte Oligomere und größere

Oligomere nachgewiesen werden, die durch die synergistische Wirkung von Ethanol und Eisen entstanden waren. Zum einfacheren Verständnis wurden die kleinen Ethanol-induzierten Oligomere Intermediate 1, die größeren Oligomere, die durch den Einfluss von Ethanol und Eisen entstanden sind, Intermediate 2 genannt. Es wurden mit AFM sowohl fluoreszenzmarkierte als auch unmarkierte Oligomere analysiert, um einen Einfluss der Fluorophormarkierung im Aggregationsprozess auszuschließen. Unabhängig von einem Fluoreszenzfluorophor konnten in Morphologie und Größe ununterscheidbare Oligomere nachgewiesen werden. Diese Ergebnisse bestätigten ein gleiches Aggregationsverhalten von fluoreszenzmarkiertem und unmarkiertem α-Syn. Da bisher oligomere Proteinformen auch mit einer Porenbildung in Zusammenhang gebracht wurden, sollte im Anschluss an die Einzelmolekülanalysen die hergestellten oligomere Formen daraufhin untersucht werden. Die Studie von Kapitel 3.1 zeigte, dass nur die größeren Oligomere (Intermediate 2) in der Lage waren, Poren in einer synthetischen Doppelmembran auszubilden. Koapplizierte Antikörper gegen monomeres α-Syn konnten die Porenbildung in diesem Testsystem inhibieren. Demgegenüber zeigte ein Kontroll-Antikörper gegen das Amyloid-ß-Peptid (6E10) keine Wirkung. Zwei Argumente belegen, dass oligomere Formen an der Porenbildung beteiligt waren. Einerseits verhinderte ein Oligomer-spezifischer Antikörper (A11) die Porenbildung. Andererseits wurden in dem gleichen Ansatz größere oligomere Formen mit Hilfe des AFM und SIFT nachgewiesen, die nicht im Kontrollansatz zu finden waren. In weiteren Versuchen wurde der Fragestellung nachgegangen, ob es sich bei den Intermediaten 1 und 2 um oligomere Zwischenprodukte handelt, die durch weitere Aggregation amyloide Fibrillen ausbilden können. Dies wurde durch die Verwendung des Fluoreszenzfarbstoffs Thioflavin T ermittelt, der an amyloide Strukturen binden kann und so indirekt ein Maß der Aggregation darstellt. Beide Intermediate konnten als Keim fungieren und die Bildung von amyloiden Strukturen drastisch beschleunigen, was ein Beleg dafür ist, dass es sich bei diesen Intermediaten um Zwischenprodukte im Entstehungsprozess von Fibrillen handelt. In darauf aufbauenden Experimenten wurden mehrere Substanzen aus der Gruppe der N-Benzyliden-Benzohydrazide auf eine potentiell aggregationshemmende Wirkung hin untersucht. Aus dieser Substanzgruppe konnte mittels konfokaler Einzelmolekülspektroskopie eine wirksame Substanz identifiziert werden, die dosisabhängig die Aggregation von α-Syn inhibierte. Dabei handelt es sich um einen

Wirkstoff, der auch die Bildung von Prionaggregaten blockiert. Auch für eine andere Substanz namens Baicalein wurde schon in früheren Studien gezeigt, dass dieses die Bildung von α-Syn Fibrillen inhibiert (Zhu et al., 2004). Mit der angewandten fluoreszenzbasierten Einzelpartikeldetektionsmethode konnte für Baicalein bestätigt werden, dass es auch hier die Bildung von kleinen α-Syn Oligomeren inhibiert. In einer vorangegangenen Studie wurde berichtet, dass die induzierbare Überexpression einer mutierten α-Syn Form in einem Zellkulturmodell zu ER Stress, mitochondrialer Dysfunktion und letztlich zum Zelltod führt (Smith et al., 2005). In der Studie von Kapitel 3.1 konnte gezeigt werden, dass Baicalein die Bildung von kleinen α-Syn Oligomeren nicht nur im zellfreien Versuchsaufbau blockiert, sondern auch in diesem Zellkulturmodell in der Lage war, den durch α-Syn vermittelten Zelltod aufzuheben.

Bei der Studie von Kapitel 3.2 wurden strukturell verschiedene α-Syn Oligomere hergestellt und charakterisiert, sowie deren Effekte auf Zellen untersucht. Ausgehend von der vorherigen Studie (Kapitel 3.1), wurde die Tatsache genutzt, dass Ethanol die Oligomerisierung von α-Syn beschleunigt. Da nach der Oligomerpräparation die verbleibende Ethanolkonzentration nachfolgende Zellkulturexperimente beeinflussen würde, musste das Protokoll zur Oligomerherstellung aus der Studie von Kapitel 3.1 angepasst und optimiert werden. Es wurden deshalb basierend auf der in Studie von Kapitel 3.1 beschrieben Methode und veröffentlichten Beobachtungen drei neue Protokolle zu Oligomerherstellung entwickelt. Zunächst wurden alle Oligomeransätze in ethanolhaltigem Natriumphosphatpuffer angesetzt. In der ersten Methode wurden die Ansätze sechs Tage inkubiert und wurden so für Zellkulturexperimente eingesetzt. Diese Art von Oligomeren wurde Typ A genannt. In der zweiten Methode wurde nur kurz (24h) inkubiert und der Aggregationsprozess zusätzlich durch Rühren beschleunigt. Diese Oligomerart wurde Typ B genannt. Als drittes wurde nach der Inkubation über Nacht Ultrafiltration benutzt. Diese Oligomerart wurde Typ C genannt. Basierend auf den Entdeckungen aus der Studie von Kapitel 3.1, dass eine Eisenzugabe die Partikelgröße von Ethanol-induzierten Oligomere vergrößert, wurde der Einfluss von Eisen auf alle drei Oligomere Arten (A, B, C) untersucht. Die eisenfreien Oligomere wurden Typ 1 und die eisenhaltige Oligomere wurden Typ 2 genannt. Wie auch schon in der vorigen Studie (Kapitel 3.1) beschrieben, erfolgte eine Charakterisierung der Oligomere mittels konfokaler Einzelmolekülspektroskopie

und AFM. Alle drei Aggregationsprotokolle zeigten heterogene Populationen von Oligomeren. Diese konnten aufgrund unterschiedlicher Größe und Morphologie unterschieden werden. Zusätzlich konnten jeder Oligomerpopulation unterschiedliche biologische Effekte zugeordnet werden. Eine Oligomerpopulation (Typ A) bestand aus kleinen, globulären und protofibrillären, sowie aus ringförmigen Strukturen. Diese Oligomerpopulation bewirkte in Neuroblastomazellen einen Anstieg der intrazellulären Kalziumspiegel. Kobalt-sensitive Kalziumkanäle konnten dabei als Ursache für den Kalziumanstieg ausgeschlossen werden. Wie Versuche in kalziumfreiem extrazellulären Medium zeigten, handelte es sich hier um einen Einstrom von extrazellulärem Kalzium. Darüber hinaus konnte auch eine Depolarisation von primären Neuronen nach der Zugabe der Oligomere Typ A beobachtet werden. Letztendlich führte eine Behandlung mit dieser Oligomerpopulation zur Apoptose und zum Zelltod. Die zweite Oligomerpopulation Typ B bestand hauptsächlich aus amorphen Strukturen. Oligomere vom Typ B waren in der Lage direkt in Zellen einzudringen und dort als Aggregationskeim zu wirken. Dies führte zu einer beschleunigten Aggregation des intrazellulären α-Syn, wie Colokalisierungsstudien zeigten. Die dritte Oligomerpopulation Typ C bestand aus großen, globulären und protofibrillären Partikeln. Diese Oligomere waren ebenfalls in der Lage, direkt in Zellen zu internalisieren und dort eine beschleunigte Aggregation des intrazellulären α-Syn hervorzurufen. Für die Oligomerpopulationen Typ B und Typ C konnte im Gegensatz zum Typ A keine Beeinflussung der intrazellulären Kalziumspiegel beobachtet werden. Zusammenfassend waren durch die neu entwickelten Protokolle zur Oligomerherstellung drei unterschiedliche Arten an Oligomeren entstanden, die entweder direkt zum Zelltod führen können oder indirekt über einen Seeding-Effekt vermutlich zu Zellschädigung führen könnten.

Wie in der Einleitung ausführlich erläutert, bindet α-Syn an verschiedene zelluläre Proteine. Es wird deshalb angenommen, dass aggregiertes α-Syn deren physiologische Funktion beeinträchtigen könnte. Die Studie von Kapitel 3.3 widmete sich deshalb der Frage, welchen Einfluss α-Syn Oligomeren, die in der Studie von Kapitel 3.2 näher charakterisiert wurden, auf die Autophosporylierungsaktivität verschiedener Proteinkinasen haben. Dazu wurden so genannte „Proteinarrays“ von der Firma Procognia verwendet, auf welche 178 aktive humane Kinasen aufgetragen sind. Diese Proteinarrays ermöglichten eine große Anzahl gleichzeitiger Analysen

der Autophosphorylierungsaktivität verschiedener Kinasen nach Oligomerinkubation. Im Gegensatz zu monomerem α-Syn und ß-Syn inhibierte eine Inkubation mit globulären α-Syn Oligomeren vom Typ A signifikant die Autophosphorylierungsaktivität von p21 aktivierter Kinase 4 (PAK4). Dieser Effekt konnte auch konzentrationsabhängig in „solution-based“ Kinase Versuchen beobachtet werden. Um diesen Effekt auch in einem Tiermodell zu bestätigen, wurden Proteinextrakte aus dem Gehirnstamm von α-Syn[A30P] transgenen Mäusen analysiert. In diesen Tieren konnte in einer früheren Studie bereits aggregiertes α-Syn nachgewiesen werden (Freichel et al., 2006). Die LIM Kinase 1 (LIMK1) stellt ein physiologisches Substrat der PAK4 dar. Mittels Western-Blot unter Verwendung von Antikörpern gegen phosphoryliertes LIMK1(Thr508) und gegen gesamtes LIMK1 war es möglich, eine signifikante Reduktion des Verhältnisses von phosphoryliertem LIMK1 zu Gesamt-LIMK1 in α-Syn[A30P] überexprimierenden Tieren verglichen mit nicht transgenen Kontrollen nachzuweisen. Es konnte also sowohl in einem zellfreien System als auch in einem transgenen Tiermodell eine Beeinträchtigung des PAK4-LIMK1 Signalweges nachgewiesen werden.

4.2 Diskussion

Die Aggregation von α-Syn spielt eine wichtige Rolle in der Pathogenese der Parkinson Krankheit und anderen Synukleinopathien. Immer mehr Hinweise deuten darauf hin, dass die Neurotoxizität von α-Syn hauptsächlich durch oligomere oder protofibrilläre Proteinformen verursacht wird (Lashuel und Lansbury, Jr., 2006). In der Studie von Kapitel 3.1 wurden erstmalig verschiedene α-Syn Oligomere bei niederen nanomolaren Proteinkonzentrationen hergestellt und mittels der Einzelmoleküldetektionsmethoden AFM und SIFT detektiert und näher charakterisiert. Im Gegensatz zu vorangegangenen Studien, die aufgrund von Verwendung von klassischen biophysikalischen oder biochemischen Methoden wie z.B. CD-Spektroskopie (Yamin et al., 2003), Fourier-Transformations-Infrarot-Spektroskopie (Uversky et al., 2001a), Messung der Thioflavin-T-Fluoreszenz (Conway et al., 2000b) und Gelelektrophorese (Cappai et al., 2005) hohe Proteinkonzentrationen (meist im millimolaren Konzentrationsbereich) verwendeten, ermöglicht diese konfokale Einzelmolekülspektroskopietechnik die Charakterisierung von einzelnen Oligomeren in nanomolaren Proteinkonzentrationen ohne den nativen Zustand der Oligomere zu beeinflussen. Dieses Verfahren wurde in den

vergangenen Jahren auch zur Charakterisierung von anderen oligomeren Formen, wie z.B. Prionprotein und Huntingtin angewandt und hat sich dort als hoch sensitive Methode zur Analyse von Proteinaggregaten herausgestellt (Bieschke et al., 2000; Giese et al., 2000; Giese et al., 2004; Levin et al., 2005; Behrends et al., 2006).

In der vorliegenden Arbeit wurde die Tatsache genutzt, dass Ethanol die Proteinfaltung von α-Syn beeinflusst und so die Oligomerisierung von α-Syn deutlich beschleunigt (Munishkina et al., 2003). Auf diese Weise konnten kleine Oligomere schon nach wenigen Stunden detektiert werden, während andere Studien erst nach längeren Inkubationszeiten und bzw. oder unter Verwendung von hohen Proteinkonzentrationen Oligomerisierung von α-Syn beobachten konnten (Kayed et al., 2003; Lindersson et al., 2004). Wie schon früher in der Literatur beschrieben, beschleunigen Metallionen wie z.B. Eisen die Bildung von oligomeren α-Syn Formen *in vitro* (Uversky et al., 2001b). Diese Tatsache wurde in den vorliegenden Studien genutzt. Es konnte ein synergistischer Effekt von Ethanol und Eisen beobachtet werden, der die Oligomerisierung von α-Syn weiter voranschreiten ließ. Im Gegensatz zu vorigen Studien jedoch, wurden hier physiologische Serumkonzentrationen an $FeCl^{3+}$ von 10-20 µM verwendet.

Ein kritischer Punkt stellt der mögliche Einfluss des konjugierten Fluorophores auf das Aggregationsverhalten von α-Syn dar. Es konnte jedoch in der Studie von Kapitel 3.1 gezeigt werden, dass der konjugierte Fluorophor die Aggregation von α-Syn nicht beeinflusst. Mittels AFM-Analyse konnten Oligomere von gleicher Größe und Morphologie von fluoreszenzmarkiertem und unmarkiertem α-Syn nachgewiesen werden. AFM stellt hier ein gut geeignetes fluoreszenzunabhängiges Einzelmoleküldetektionssystem dar, das in mehren Studien zuvor genutzt wurde, um verschiedene morphologische Strukturen während der Aggregation von α-Syn nachzuweisen (Conway et al., 2000a; Volles et al., 2001; Ding et al., 2002; Lashuel et al., 2002b; Rochet et al., 2004). Die Ergebnisse der Studie aus Kapitel 3.1 zeigen, dass die hier angewandte konfokale Einzelmolekülspektroskopie geeignet ist, effizient und systematisch im Hochdurchsatz nach α-Syn Oligomerisierungsinhibitoren zu suchen und hierbei eventuell pharmakologische interessante Substanzen zu identifizieren. So konnte die Substanz Baicalein nicht nur die Oligomerisierung des α-Syn *in vitro* hemmen, sondern war darüber hinaus in

der Lage, eine α-Syn vermittelte Toxizität in Zellkultur aufzuheben. Derartige Hemmstoffe könnten zukünftig dazu beitragen, den Krankheitsverlauf der Parkinson Krankheit zu verändern und so derzeitige Therapiemöglichkeiten zu verbessern.

In der Studie von Kapitel 3.2 wurde der Fragestellung nachgegangen, ob sich α-Syn Oligomere strukturell unterscheiden und welchen Einfluss oligomere Formen von α-Syn auf humane und murine Zellen haben. Die Ergebnisse der Studie von Kapitel 3.2 illustrieren und belegen, dass es durch Veränderungen im Aggregationsprotokoll möglich ist, die Oligomerentstehung von α-Syn zu lenken. Es konnte gezeigt werden, dass je nachdem, welche Aggregationsbedingungen gewählt werden, jeweils verschiedene heterogene Oligomerpopulationen (hier mit Typ A, B, C bezeichnet) entstehen, denen biologische Effekte auf Zellen vom Anstieg des intrazellulären Kalziums über Seeding-Eigenschaften bis hin zum Zelltod zugeordnet werden konnten. Die Heterogenität der einzelnen Oligomerpopulationen steht im Gegensatz zu Arbeiten von Kayed et al, da in diesen Studien ausschließlich homogene Oligomerpopulationen entstanden sind (Kayed et al., 2003; Demuro et al., 2005). Jedoch variieren die Aggregationsbedingungen von Kayed et al. zu den Bedingungen der vorliegenden Arbeit deutlich. Um eine homogene Oligomerpräparationen zu erhalten, ist es laut Kayed et al. eines der wichtigsten Faktoren, die α-Syn Aggregation mit einer komplett solvatierten Stammlösung zu beginnen, welche frei von jeglichen Aggregationskeimen ist (Kayed und Glabe, 2006). In den Oligomerisierungsansätzen der vorliegenden Arbeit jedoch kann das Vorhandensein kleiner Mengen an Aggregationskeimen nicht ausgeschlossen werden, welche die Bildung von heterogenen Oligomerpopulationen favorisieren. Es wird allerdings angenommen, dass die Beobachtungen der vorliegenden Arbeit eher einer physiologischen Situation entsprechen, da Aggregationskeime und vor-aggregierte Proteinen auch *in vivo* vorkommen können. Unsere Befunde weisen deshalb darauf hin, dass auch unter verschiedenen physiologischen Bedingungen heterogene Populationen an Oligomeren gebildet werden könnten. Die Oligomerpopulation Typ A bewirkte in Zellen einen Anstieg der intrazellulären Kalziumspiegel. Es wurden mehrere Mechanismen vorgeschlagen, die für den intrazellulären Kalziumanstieg durch verschiedene amyloide Proteine verantwortlich sein könnten. Dazu gehören eine erhöhte Permeabilität der Zellmembran (Demuro et al. 2005), ein Einbau von Oligomeren in die Membran, was zur Porenbildung führt

(Lashuel und Lansbury, 2006; Kawahara et al., 2000; Arispe et al., 2004), und eine direkte Interaktion der Oligomere mit Membrankomponenten, welche die Membranstruktur destabilisieren (Avdulov et al., 1997; Green et al., 2004; Mason et al., 1996; Müller et al., 1995). Obwohl eine erhöhte Membranpermeabilität oder ein Membran destabilisierender Mechanismus durch Bindung an Membrankomponenten nicht ausgeschlossen werden kann, unterstützen zwei Ergebnisse der vorliegenden Arbeit eine Porenbildung in Membranen. Einerseits konnte ein porenbildender Mechanismus von α-Syn Oligomeren unter Verwendung von synthetischen Lipid-Doppelmembranen beobachtet werden (Studie aus Kapitel 3.1). Andererseits führte eine Zugabe von Oligomeren Typ A zu einem von Kalziumkanal-unabhängigen Kalziumeinstrom (Studie aus Kapitel 3.2). Darüber hinaus gibt es Hinweise aus der Literatur, dass synthetische Vesikel durch protofibrilläres α-Syn über einen poren-bildenden Mechanismus permeabilisiert werden können (Lashuel et al., 2002, Volles et al., 2001, Volles und Lansbury, 2002). Damit unterstützen die Daten der vorliegenden Arbeit die Amyloide-Porenhypothese, die von Lashuel und Lansbury vorgeschlagen wurde (Lashuel und Lansbury, 2006). Allerdings lassen diese *in vitro* Untersuchungen die Frage offen, ob oligomere Porenbildung auch in Zellen stattfindet. Kanalbildende bakterielle Proteintoxine sind in der Natur bereits bekannt (Orlova et al., 2000; Valeva et al., 1997, Wallace et al., 2000). Ein Vergleich der von den Oligomeren Typ A ausgelösten Depolarisation und des Kalziumeinstroms in Neuronen mit der Wirkung des bakteriellen kanalbildenen Toxins Gramicidin, zeigten deutlich ein vergleichbares Profil. Dies unterstützt die Annahme, dass ein Porenmechanismus für den Kalziumeinstrom auch in zellulären Systemen verantwortlich sein könnte.

Andere Oligomerarten Typ B und Typ C waren in der Lage, in Zellen einzudringen und dort als Aggregationskeim zu wirken. Eine beschleunigte Aggregation durch das Hinzufügen von vorhandenen Aggregationskeimen (Seeding) wurde zuvor nur in zellfreien Studien beschrieben (Hoyer et al., 2002). In der vorliegenden Arbeit konnte erstmals gezeigt werden, dass es durch Zugabe von Oligomerern möglich ist, eine beschleunigte Aggregation des intrazellulären α-Syn hervorzurufen (Studie von Kapitel 3.2). Diese Effekte könnten auch in Parkinson Patienten auftreten, jedoch gibt es bis dato noch keinen Beleg dafür. Allerdings könnte der Seeding-Mechanismus eine sinnvolle Erklärung für die angenommene schrittweise Ausbreitung der Lewy-

Körperchen-Pathologie in den Gehirnen von Parkinson Patienten sein (Braak et al., 2003). Eine Reduzierung der frühen Aggregationsereignisse würde folglich auch die im Krankheitsverlauf späteren Gehirnareale vor einer α-Syn vermittelten Toxizität schützen. Dies hätte wichtige Auswirkungen für die Entwicklung von Arzneistoffen, die den Krankheitsverlauf der Parkinson Krankheit und anderen Synukleinopathien verändern.

Die Studie von Kapitel 3.3 widmete sich der Frage, ob α-Syn Oligomere Einfluss auf Signaltransduktionswege haben, die weitere Faktoren für eine Entstehung der Parkinson Krankheit sein könnten. Dies wurde am Beispiel von veränderten Autophoshorylierungsaktivitäten von verschiedenen Kinasen untersucht. Mittels Kinome 1.0 arrays konnte die Kinaseaktivität von 178 aktiven humanen Kinasen gleichzeitig analysiert werden. Die Ergebnisse der Studie von Kapitel 3.3 zeigen, dass α-Syn Oligomere signifikant die Autophosphorylierungsaktivität von PAK4 inhibierten. Es sind bis dato wenig Substrate von PAK4 bekannt, jedoch konnte gezeigt werden, dass LIMK1 ein Haupteffektormolekül von PAK4 darstellt, das von PAK4 phosphoryliert und aktiviert wird (Dan et al., 2001). Interessanterweise zeigten die Ergebnisse der Studie von Kapitel 3.3 eine signifikante Reduktion der LIMK1 Phosphorylierung in Gerhirnextrakten von transgenen α-Syn [A30P] überexprimierenden Mäusen. In diesen Mäusen wurde zuvor eine Akkumulation von α-Syn Oligomeren nachgewiesen (Freichel et al., 2006), daher ist es sehr wahrscheinlich, dass aggregiertes α-Syn auch *in vivo* eine Inhibierung des PAK4-LIMK1 Signalweges hervorruft. Die funktionellen Konsequenzen eines PAK4 bzw. LIMK1 Aktivitätsverlusts sind eindeutig: PAK4 defiziente murine Embryos zeigen schwere Störungen im Herzen und Nervensystem. Es liegt hier ein gestörtes Neuritenwachstum und eine gestörte neuronale Migration vor, was vermutlich durch die Rolle von PAK4 in der Regulation des Zytoskeletts und Ausbildung von Filopodien zustande kommt. Es kommt in diesen Mäusen daher zu einer embryonalen Letalität am Tag 11.5 (Qu et al., 2003). Mäusen, denen das Gen für das PAK4 Substrat LIMK1 entfernt wurde, sind nicht letal. Jedoch zeigen LIMK1 defiziente Mäuse eine ungewöhnliche Spine Morphologie und veränderte postsynaptische Ströme (Meng et al., 2002). Interessanterweise zeigen LIMK1 defiziente Mäuse ähnliche motorische Störungen und Lerndefizite wie transgene α-Syn [A30P] überexprimierende Mäuse (Freichel et al., 2006). Eine Reduktion der

PAK Aktivität durch Aß Oligomere, welche bei der Alzheimerschen Krankheit eine wichtige Rolle spielen, wurde kürzlich in Gehirnextrakten von Alzheimer Patienten und transgenen Amyloid Precursor Protein überexprimierenden Mäusen entdeckt (Zhao et al., 2006). Eine Inhibierung der PAK Aktivität könnte also die Folge von mehreren neurotoxischen Protein Oligomeren sein und so zu Defiziten in Signaltransduktionswegen führen und damit verstärkt zu neurodegenerativen Krankheiten beitragen.

5 Literaturverzeichnis

1. Abeliovich A, Schmitz Y, Farinas I, Choi-Lundberg D, Ho WH, Castillo PE, Shinsky N, Verdugo JM, Armanini M, Ryan A, Hynes M, Phillips H, Sulzer D, and Rosenthal A (2000) Mice lacking alpha-synuclein display functional deficits in the nigrostriatal dopamine system. Neuron, 25, 239-252.

2. Alper T, Cramp WA, Haig DA, and Clarke MC (1967) Does the scrapie agent replicate without nucleic acid? Nature, 214, 764-766.

3. Auluck PK, Chan HY, Trojanowski JQ, Lee VM, and Bonini NM (2002) Chaperone suppression of alpha-synuclein toxicity in a Drosophila model for Parkinson's disease. Science, 295, 865-868.

4. Balbach JJ, Ishii Y, Antzutkin ON, Leapman RD, Rizzo NW, Dyda F, Reed J, and Tycko R (2000) Amyloid fibril formation by Aβ16-22, a seven-residue fragment of the Alzheimer's beta-amyloid peptide, and structural characterization by solid state NMR. Biochemistry, 39, 13748–13759.

5. Behrends C, Langer CA, Boteva R, Bottcher UM, Stemp MJ, Schaffar G, Rao BV, Giese A, Kretzschmar H, Siegers K, and Hartl FU (2006) Chaperonin TRiC promotes the assembly of polyQ expansion proteins into nontoxic oligomers. Mol Cell, 23, 887-897.

6. Bernheimer H, Birkmayer W, Hornykiewicz O, Jellinger K, and Seitelberger F (1973) Brain dopamine and the syndromes of Parkinson and Huntington. Clinical, morphological and neurochemical correlations. J Neurol Sci, 20, 415-455.

7. Betarbet R, Sherer TB, MacKenzie G, Garcia-Osuna M, Panov AV, and Greenamyre JT (2000) Chronic systemic pesticide exposure reproduces features of Parkinson's disease. Nat Neurosci, 3, 1301-1306.

8. Bieschke J, Giese A, Schulz-Schaeffer W, Zerr I, Poser S, Eigen M, and Kretzschmar H (2000) Ultrasensitive detection of pathological prion protein aggregates by dual-color scanning for intensely fluorescent targets. Proc Natl Acad Sci U S A, 97, 5468-5473.

9. Bodles AM, Guthrie DJ, Harriott P, Campbell P, and Irvine GB (2000) Toxicity of non-abeta component of Alzheimer's disease amyloid, and N-terminal fragments thereof, correlates to formation of beta-sheet structure and fibrils. Eur J Biochem, 267, 2186-2194.

10. Bodner RA, Outeiro TF, Altmann S, Maxwell MM, Cho SH, Hyman BT, McLean PJ, Young AB, Housman DE, and Kazantsev AG (2006) Pharmacological promotion of inclusion formation: a therapeutic approach for Huntington's and Parkinson's diseases. Proc Natl Acad Sci U S A, 103, 4246-4251.

11. Bonifati V, Rizzu P, Squitieri F, Krieger E, Vanacore N, van Swieten JC, Brice A, van Duijn CM, Oostra B, Meco G, and Heutink P (2003) DJ-1(PARK7), a novel gene for autosomal recessive, early onset parkinsonism. Neurol Sci, 24,159-60.

12. Borghi R, Marchese R, Negro A, Marinelli L, Forloni G, Zaccheo D, Abbruzzese G, and Tabaton M (2000) Full length alpha-synuclein is present in cerebrospinal fluid from Parkinson's disease and normal subjects. Neuroscience Letters, 287, 65-67.

13. Braak H, Del TK, Rub U, de Vos RA, Jansen Steur EN, and Braak E (2003) Staging of brain pathology related to sporadic Parkinson's disease. Neurobiol Aging, 24, 197-211.

14. Brooks AI, Chadwick CA, Gelbard HA, Cory-Slechta DA, and Federoff HJ (1999) Paraquat elicited neurobehavioral syndrome caused by dopaminergic neuron loss. Brain Res, 823, 1-10.

15. Cabin DE, Cole NB, Orrison B, Chen A, Ellis CE, Nussbaum RL, Murphy D, Shimazu K, Gottschalk W, Lu B, McIlwain KL, and Paylor R (2002) Synaptic vesicle depletion correlates with attenuated synaptic responses to prolonged repetitive stimulation in mice lacking alpha-synuclein. Journal of Neuroscience, 22, 8797-8807.

16. Cappai R, Tew DJ, Smith DP, Galatis D, Sharples RA, Curtain CC, Ali FE, Cherny RA, Culvenor JG, Masters CL, Barnham KJ, Hill AF, Leek SL, Williamson NA, and Bottomley SP (2005) Dopamine promotes alpha-synuclein aggregation into SDS-resistant soluble oligomers via a distinct folding pathway. FASEB Journal, 19, 1377-1379.

17. Caughey B and Lansbury PT (2003) Protofibrils, pores, fibrils, and neurodegeneration: separating the responsible protein aggregates from the innocent bystanders. Annu Rev Neurosci, 26, 267-298.

18. Chade AR, Kasten M, and Tanner CM (2006) Nongenetic causes of Parkinson's disease. J Neural Transm Suppl, 147-151.

19. Chandra S, Gallardo G, Südhof TC, Fernbndez C, and Schl³ter OM (2005) alpha-Synuclein cooperates with CSP-alpha in preventing neurodegeneration. Cell, 123, 383-396.

20. Chartier-Harlin MC, Kachergus J, Roumier C, Mouroux V, Douay X, Lincoln S, Levecque C, Larvor L, Andrieux J, Hulihan M, Waucquier N, Defebvre L, Amouyel P, Farrer M, and Destee A (2004) Alpha-synuclein locus duplication as a cause of familial Parkinson's disease. Lancet, 364, 1167-1169.

21. Clayton DF and George JM (1999) Synucleins in synaptic plasticity and neurodegenerative disorders, Journal of Neuroscience Research, 58, 120-129

22. Connor JR, Snyder BS, Arosio P, Loeffler DA, and LeWitt P (1995) A quantitative analysis of isoferritins in select regions of aged, parkinsonian, and Alzheimer's diseased brains. J Neurochem, 65, 717-724.

23. Conway KA, Harper JD, and Lansbury PT (1998) Accelerated in vitro fibril formation by a mutant alpha-synuclein linked to early-onset Parkinson disease. Nat Med, 4, 1318-1320.

24. Conway KA, Harper JD, and Lansbury PT, Jr. (2000a) Fibrils formed in vitro from alpha-synuclein and two mutant forms linked to Parkinson's disease are typical amyloid. Biochemistry, 39, 2552-2563.

25. Conway KA, Lee SJ, Rochet JC, Ding TT, Williamson RE, and Lansbury PT, Jr. (2000b) Acceleration of oligomerization, not fibrillization, is a shared property of both alpha-synuclein mutations linked to early-onset Parkinson's disease: implications for pathogenesis and therapy. Proc Natl Acad Sci U S A, 97, 571-576.

26. Cooper AA, Gitler AD, Cashikar A, Haynes CM, Hill KJ, Bhullar B, Liu K, Xu K, Strathearn KE, Liu F, Cao S, Caldwell KA, Caldwell GA, Marsischky G, Kolodner RD, Labaer J, Rochet JC, Bonini NM, and Lindquist S (2006) {alpha}-Synuclein Blocks ER-Golgi Traffic and Rab1 Rescues Neuron Loss in Parkinson's Models. Science.

27. Crowther RA, Jakes R, Spillantini MG, and Goedert M (1998) Synthetic filaments assembled from C-terminally truncated alpha-synuclein. FEBS Lett, 436, 309-312.

28. Cuervo AM, Stafanis L, Fredenburg R, Lansbury PT, and Sulzer D (2004) Impaired degradation of mutant alpha-synuclein by chaperone-mediated autophagy. Science, 305, 1292-1295.

29. Dalfo E, Barrachina M, Rosa JL, Ambrosio S, and Ferrer I (2004a) Abnormal alpha-synuclein interactions with rab3a and rabphilin in diffuse Lewy body disease. Neurobiol Dis, 16, 92-97.

30. Dalfo E, Gomez-Isla T, Rosa JL, Nieto BM, Cuadrado TM, Barrachina M, Ambrosio S, and Ferrer I (2004b) Abnormal alpha-synuclein interactions with Rab

proteins in alpha-synuclein A30P transgenic mice. J Neuropathol Exp Neurol, 63, 302-313.

31. Dan C, Kelly A, Bernard O, and Minden A (2001) Cytoskeletal changes regulated by the PAK4 serine/threonine kinase are mediated by LIM kinase 1 and cofilin. J Biol Chem, 276, 32115-32121.

32. Davidson WS, Jonas A, Clayton DF, and George JM (1998) Stabilization of alpha-synuclein secondary structure upon binding to synthetic membranes. J Biol Chem, 273, 9443-9449.

33. Dekker MC, Eshuis SA, Maguire RP, Veenma-van der Duijn L, Pruim J, Snijders PJ, Oostra BA, van Duijn CM, and Leenders KL (2004) PET neuroimaging and mutations in the DJ-1 gene. J Neural Transm, 111, 1575-81.

34. DeMarco ML and Daggett V (2004) From conversion to aggregation: protofibril formation of the prion protein. Proc Natl Acad Sci U S A, 101, 2293-2298.

35. Demuro A, Parker I, Glabe CG, Mina E, Kayed R, and Milton SC (2005) Calcium dysregulation and membrane disruption as a ubiquitous neurotoxic mechanism of soluble amyloid oligomers. J Biol Chem, 280, 17294-17300.

36. Dev KK, Hofele K, Barbieri S, Buchman VL, and Van Der Putten H (2003) Part II: alpha-synuclein and its molecular pathophysiological role in neurodegenerative disease. Neuropharmacology, 45, 14-44.

37. Ding TT, Lee SJ, Rochet JC, and Lansbury PT, Jr. (2002) Annular alpha-synuclein protofibrils are produced when spherical protofibrils are incubated in solution or bound to brain-derived membranes. Biochemistry, 41, 10209-10217.

38. Du HN, Li HT, Zhang F, Lin XJ, Shi JH, Shi YH, Ji LN, Hu J, Lin DH, and Hu HY (2006) Acceleration of alpha-synuclein aggregation by homologous peptides. FEBS Lett, 580, 3657-3664.

39. Du HN, Luo XY, Li HT, Zhou JW, Hu HY, Tang L, and Hu J (2003) A peptide motif consisting of glycine, alanine, and valine is required for the fibrillization and cytotoxicity of human alpha-synuclein. Biochemistry, 42, 8870-8878.

40. Ehrenberg M, Rigler R (1974) Rotational Brownian motion and fluorescence intensity fluctuations. Chem Phys, 4, 390.

41. Eigen M, Rigler R (1994) Sorting single molecules: application to diagnostics and evolutionary biotechnology. Proc Natl Acad Sci USA, 91, 5740–5747.

42. El Agnaf OM, Bodles AM, Guthrie DJ, Harriott P, and Irvine GB (1998a) The N-terminal region of non-A beta component of Alzheimer's disease amyloid is responsible for its tendency to assume beta-sheet and aggregate to form fibrils. Eur J Biochem, 258, 157-163.

43. El Agnaf OM, Paleologou KE, Greer B, Abogrein AM, King JE, Salem SA, Fullwood NJ, Benson FE, Hewitt R, Ford KJ, Martin FL, Harriott P, Cookson MR, and Allsop D (2004) A strategy for designing inhibitors of alpha-synuclein aggregation and toxicity as a novel treatment for Parkinson's disease and related disorders. FASEB J.

44. El Agnaf OM, Salem SA, Paleologou KE, Cooper LJ, Fullwood NJ, Gibson MJ, Curran MD, Court JA, Mann DM, Ikeda S, Cookson MR, Hardy J, and Allsop D (2003) Alpha-synuclein implicated in Parkinson's disease is present in extracellular biological fluids, including human plasma. FASEB J, 17, 1945-1947.

45. El Agnaf OMA, Wallace A, Jakes R, and Curran MD (1998b) Effects of the mutations Ala30 to Pro and Ala53 to Thr on the physical and morphological properties of alpha-synuclein protein implicated in Parkinson's disease. FEBS Letters, 440, 67-70.

46. Fearnley JM and Lees AJ (1991) Ageing and Parkinson's disease: substantia nigra regional selectivity. Brain, 114 (Pt 5), 2283-2301.

47. Florio T, Paludi D, Villa V, Principe DR, Corsaro A, Millo E, Damonte G, D'Arrigo C, Russo C, Schettini G, and Aceto A (2003) Contribution of two conserved glycine residues to fibrillogenesis of the 106-126 prion protein fragment. Evidence that a soluble variant of the 106-126 peptide is neurotoxic. J Neurochem, 85, 62-72.

48. Freichel C, Neumann M, Ballard T, Muller V, Woolley M, Ozmen L, Borroni E, Kretzschmar HA, Haass C, Spooren W, and Kahle PJ (2006) Age-dependent cognitive decline and amygdala pathology in alpha-synuclein transgenic mice. Neurobiol Aging.

49. Galvin JE, Lee VM, Schmidt ML, Tu PH, Iwatsubo T, and Trojanowski JQ (1999) Pathobiology of the Lewy body. Adv Neurol, 80, 313-324.

50. Galvin JE, Lee VM, and Trojanowski JQ (2001) Synucleinopathies: clinical and pathological implications. Arch Neurol, 58, 186-190.

51. Gandhi S, Muqit MM, Stanyer L, Healy DG, Abou-Sleiman PM, Hargreaves I, Heales S, Ganguly M, Parsons L, Lees AJ, Latchman DS, Holton JL, Wood NW, and Revesz T (2006) PINK1 protein in normal human brain and Parkinson's disease. Brain, 129, 1720-31.

52. Gasser T, Muller-Myhsok B, Wszolek Z K, Oehlmann R, Calne DB, Bonifati V, Bereznai B, Fabrizio E, Vieregge P, and Horstmann RD (1998) A susceptibility locus for Parkinson's disease maps to chromosome 2p13. Nat Genet, 18, 262-265.

53. Gasser T (2001) Genetics of Parkinson's disease. J Neurol, 248, 833-840.

54. George JM (2001) The synucleins. Genome Biol, 3, 3002.1-3002.6.

55. George JM, Jin H, Woods WS, and Clayton DF (1995) Characterization of a novel protein regulated during the critical period for song learning in the zebra finch. Neuron, 15, 361-372.

56. Giasson BI, Uryu K, Trojanowski JQ, and Lee VM (1999) Mutant and wild type human alpha-synucleins assemble into elongated filaments with distinct morphologies in vitro. J Biol Chem, 274, 7619-7622.

57. Giese A, Bieschke J, Eigen M, and Kretzschmar HA (2000) Putting prions into focus: application of single molecule detection to the diagnosis of prion diseases. Arch Virol Suppl, 161-171.

58. Giese A, Levin J, Bertsch U, and Kretzschmar H (2004) Effect of metal ions on de novo aggregation of full-length prion protein. Biochemical and Biophysical Research Communications, 320, 1240-1246.

59. Goedert M (2001a) Alpha-synuclein and neurodegenerative diseases. Nat Rev Neurosci, 2, 492-501.

60. Goedert M (2001b) Parkinson's disease and other alpha-synucleinopathies. Clin Chem Lab Med, 39, 308-312.

61. Goldberg MS and Lansbury PT, Jr. (2000) Is there a cause-and-effect relationship between alpha-synuclein fibrillization and Parkinson's disease? Nat Cell Biol, 2, E115-E119.

62. Golts N, Snyder H, Frasier M, Theisler C, Choi P, and Wolozin B (2002) Magnesium inhibits spontaneous and iron-induced aggregation of alpha-synuclein. J Biol Chem, 277, 16116-16123.

63. Gosavi N, Lee HJ, Lee JS, Patel S, and Lee SJ (2002) Golgi fragmentation occurs in the cells with prefibrillar alpha-synuclein aggregates and precedes the formation of fibrillar inclusion. J Biol Chem, 277, 48984-48992.

64. Gotz ME, Double K, Gerlach M, Youdim MB, and Riederer P (2004) The relevance of iron in the pathogenesis of Parkinson's disease. Ann N Y Acad Sci, 1012, 193-208.

65. Greenbaum EA, Graves CL, Mishizen-Eberz AJ, Lupoli MA, Lynch DR, Englander SW, Axelsen PH, and Giasson BI (2005) The E46K mutation in alpha-synuclein increases amyloid fibril formation. J Biol Chem, 280, 7800-7807.

66. Han H, Weinreb PH, and Lansbury PT, Jr. (1995) The core Alzheimer's peptide NAC forms amyloid fibrils which seed and are seeded by beta-amyloid: is NAC a common trigger or target in neurodegenerative disease? Chem Biol, 2, 163-169.

67. Hashimoto M, Hsu LJ, Sisk A, Xia Y, Takeda A, Sundsmo M, and Masliah E (1998) Human recombinant NACP/α-synuclein is aggregated and fibrillated in vitro: Relevance for lewy body disease. Brain Research, 799, 301-306.

68. Hashimoto M, Rockenstein E, Mante M, Mallory M, and Masliah E (2001) beta-synuclein inhibits alpha-synuclein aggregation: A possible role as an anti-Parkinsonian factor. Neuron, 32, 213-223.

69. Hicks AA, Petursson H, Jonsson T, Stefansson H, Johannsdottir HS, Sainz J, Frigge ML, Kong A, Gulcher JR, Stefansson K, and S. Sveinbjornsdottir (2002) A susceptibility gene for late-onset idiopathic Parkinson's disease. Ann Neurol, 52, 549-55.

70. Hoyer W, Antony T, Cherny D, Heim G, Jovin TM, and Subramaniam V (2002) Dependence of alpha-synuclein aggregate morphology on solution conditions. J Mol Biol, 322, 383-393.

71. Hsu LJ, Sagara Y, Arroyo A, Rockenstein E, Sisk A, Mallory M, Wong J, Takenouchi T, Hashimoto M, and Masliah E (2000) alpha-synuclein promotes mitochondrial deficit and oxidative stress. American Journal of Pathology, 157, 401-410.

72. Ibanez P, Bonnet AM, Debarges B, Lohmann E, Tison F, Pollak P, Agid Y, Durr A, and Brice PA (2004) Causal relation between [alpha]-synuclein gene duplication and familial Parkinson's disease. The Lancet, 364, 1169-1171.

73. Iwai A, Masliah E, Yoshimoto M, Ge N, Flanagan L, de Silva HA, Kittel A, and Saitoh T (1995) The precursor protein of non-A beta component of Alzheimer's disease amyloid is a presynaptic protein of the central nervous system. Neuron, 14, 467-475.

74. Jakes R, Spillantini MG, and Goedert M (1994) Identification of two distinct synucleins from human brain. FEBS Letters, 345, 27-32.

75. Kask P, Palo K, Ullmann D, Gall K (1999) Fluorescence-intensity distribution analysis and its application in biomolecular detection technology. Proc Natl.Acad Sci USA, 96, 13756-13761.

76. Kask P, Palo K, Fay N, Brand L, Mets U, Ullmann D, Jungmann J, Pschorr J, Gall K (2000) Two-dimensional fluorescence intensity distribution analysis: theory and applications. J Biophys, 78, 1703-1713.

77. Kayed R, Head E, Thompson JL, McIntire TM, Milton SC, Cotman CW, and Glabe CG (2003) Common structure of soluble amyloid oligomers implies common mechanism of pathogenesis. Science, 300, 486-489.

78. Kayed R, Glabe CG (2006) Conformation-dependent anti-amyloid oligomer antibodies. Methods Enzymol, 413, 326-44.

79. Kitada T, Asakawa S, Minoshima S, Mizuno Y, and Shimizu N (2000) Molecular cloning, gene expression, and identification of a splicing variant of themouse parkin gene. Mamm Genome, 11, 417-421.

80. Kruger R, Kuhn W, Muller T, Woitalla D, Graeber M, Kosel S, Przuntek H, Epplen JT, Schols L, and Riess O (1998) Ala30Pro mutation in the gene encoding alpha-synuclein in Parkinson's disease. Nat Genet, 18, 106-108.

81. Kruger R, Vieira-Saecker AM, Kuhn W, Berg D, Muller T, Kuhnl N, Fuchs GA, Storch A, Hungs M, Woitalla D, Przuntek H, Epplen JT, Schols L, and

Riess O (1999) Increased susceptibility to sporadic Parkinson's disease by a certain combined alpha-synuclein/apolipoprotein E genotype. Ann Neurol, 45, 611-617.

82. Langston JW (1998) Epidemiology versus genetics in Parkinson's disease: progress in resolving an age-old debate. Ann Neurol, 44, S45-S52.

83. Lashuel HA, Hartley D, Petre BM, Walz T, and Lansbury PT, Jr. (2002a) Neurodegenerative disease: amyloid pores from pathogenic mutations. Nature, 418, 291.

84. Lashuel HA and Lansbury PT, Jr. (2006) Are amyloid diseases caused by protein aggregates that mimic bacterial pore-forming toxins? Q Rev Biophys, 39, 167-201.

85. Lashuel HA, Petre BM, Wall J, Simon M, Nowak RJ, Walz T, and Lansbury PT, Jr. (2002b) Alpha-synuclein, especially the Parkinson's disease-associated mutants, forms pore-like annular and tubular protofibrils. J Mol Biol, 322, 1089-1102.

86. Lavedan C (1998) The synuclein family. Genome Res, 8, 871-880.

87. Lee HJ, Choi C, and Lee SJ (2002) Membrane-bound alpha-synuclein has a high aggregation propensity and the ability to seed the aggregation of the cytosolic form. J Biol Chem, 277, 671-678.

88. Leroy E, Boyer R, Auburger G, Leube B, Ulm G, Mezey E, Harta G, Brownstein MJ, Jonnalagada S, Chernova T, et al. (1998). The ubiquitin pathway in Parkinson's disease. Nature, 395, 451-452.

89. Levin J, Bertsch U, Kretzschmar H, and Giese A (2005) Single particle analysis of manganese-induced prion protein aggregates. Biochemical and Biophysical Research Communications, 329, 1200-1207.

90. Lewy F and Lewandowski M&AG (1912) Handbuch der Neurologie, 3, 920-933.

91. Li J, Uversky VN, and Fink AL (2001) Effect of familial Parkinson's disease point mutations A30P and A53T on the structural properties, aggregation, and fibrillation of human alpha-synuclein. Biochemistry, 40, 11604-11613.

92. Lindersson E, Beedholm R, Hojrup P, Moos T, Gai W, Hendil KB, and Jensen PH (2004) Proteasomal inhibition by alpha-synuclein filaments and oligomers. J Biol Chem, 279, 12924-12934.

93. Liu S, Ninan I, Antonova I, Battaglia F, Trinchese F, Narasanna A, Kolodilov N, Dauer W, Hawkins RD, and Arancio O (2004) alpha-Synuclein produces a long-lasting increase in neurotransmitter release. EMBO J.

94. Logroscino G (2005) The role of early life environmental risk factors in Parkinson disease: what is the evidence? Environ Health Perspect, 113, 1234-1238.

95. Magde D, Elson EL, Webb WW (1972) Thermodynamic fluctuations in a reacting system-measurement by fluorescence correlation spectroscopy. Phys Rev Lett, 29, 705–711.

96. Maraganore DM, de AM, Elbaz A, Farrer MJ, Ioannidis JP, Kruger R, Rocca WA, Schneider NK, Lesnick TG, Lincoln SJ, Hulihan MM, Aasly JO, Ashizawa T, Chartier-Harlin MC, Checkoway H, Ferrarese C, Hadjigeorgiou G, Hattori N, Kawakami H, Lambert JC, Lynch T, Mellick GD, Papapetropoulos S, Parsian A, Quattrone A, Riess O, Tan EK, and Van BC (2006) Collaborative analysis of alpha-synuclein gene promoter variability and Parkinson disease. JAMA, 296, 661-670.

97. Maroteaux L, Campanelli JT, and Scheller RH (1988) Synuclein: a neuron-specific protein localized to the nucleus and presynaptic nerve terminal. J Neurosci, 8, 2804-2815.

98. Masliah E, Iwai A, Mallory M, Ueda K, and Saitoh T (1996) Altered presynaptic protein NACP is associated with plaque formation and neurodegeneration in Alzheimer's disease. Am J Pathol, 148, 201-210.

99. Masliah E, Rockenstein E, Veinbergs I, Mallory M, Hashimoto M, Takeda A, Sagara Y, Sisk A, and Mucke L (2000) Dopaminergic loss and inclusion body formation in alpha-synuclein mice: Implications for neurodegenerative disorders. Science, 287, 1265-1269.

100. McGeer PL, Itagaki S, Akiyama H, and McGeer EG (1988) Rate of cell death in parkinsonism indicates active neuropathological process. Ann Neurol, 24, 574-576.

101. McLean PJ and Hyman BT (2002) An alternatively spliced form of rodent alpha-synuclein forms intracellular inclusions in vitro: role of the carboxy-terminus in alpha-synuclein aggregation. Neurosci Lett, 323, 219-223.

102. McLean PJ, Kawamata H, and Hyman BT (2001) Alpha-synuclein-enhanced green fluorescent protein fusion proteins form proteasome sensitive inclusions in primary neurons. Neuroscience, 104, 901-912.

103. Meng Y, Zhang Y, Tregoubov V, Janus C, Cruz L, Jackson M, Lu WY, MacDonald JF, Wang JY, Falls DL, and Jia Z (2002) Abnormal spine morphology and enhanced LTP in LIMK-1 knockout mice. Neuron, 35, 121-133.

104. Moore DJ, West AB, Dawson VL, and Dawson TM (2005) Molecular pathophysiology of Parkinson's disease. Annu Rev Neurosci, 28, 57-87.

105. Munishkina LA, Phelan C, Uversky VN, and Fink AL (2003) Conformational behavior and aggregation of alpha-synuclein in organic solvents: modeling the effects of membranes. Biochemistry, 42, 2720-2730.

106. Murray IV, Giasson BI, Quinn SM, Koppaka V, Axelsen PH, Ischiropoulos H, Trojanowski JQ, and Lee VM (2003) Role of alpha-synuclein carboxy-terminus on fibril formation in vitro. Biochemistry, 42, 8530-8540.

107. Nakajo S, Shioda S, Nakai Y, and Nakaya K (1994) Localization of phosphoneuroprotein 14 (PNP 14) and its mRNA expression in rat brain determined by immunocytochemistry and in situ hybridization. Brain Res Mol Brain Res, 27, 81-86.

108. Narhi L, Wood SJ, Steavenson S, Jiang Y, Wu GM, Anafi D, Kaufman SA, Martin F, Sitney K, Denis P, Louis JC, Wypych J, Biere AL, and Citron M (1999) Both familial Parkinson's disease mutations accelerate alpha-synuclein aggregation. J Biol Chem, 274, 9843-9846.

109. Okochi M, Walter J, Kahle PJ, Haass C, Koyama A, Baba M, Iwatsubo T, Meijer L, and Nakajo S (2000) Constitutive phosphorylation of the Parkinson's disease associated alpha- synuclein. J Biol Chem, 275, 390-397.

110. Ostrerova N, Petrucelli L, Farrer M, Mehta N, Choi P, Hardy J, and Wolozin B (1999) alpha-Synuclein shares physical and functional homology with 14-3-3 proteins. J Neurosci, 19, 5782-5791.

111. Ostrerova-Golts N, Petrucelli L, Hardy J, Lee JM, Farer M, and Wolozin B (2000) The A53T alpha-synuclein mutation increases iron-dependent aggregation and toxicity. J Neurosci, 20, 6048-6054.

112. Outeiro TF and Lindquist S (2003) Yeast cells provide insight into alpha-synuclein biology and pathobiology. Science, 302, 1772-1775.

113. Paik SR, Shin HJ, and Lee JH (2000) Metal-catalyzed oxidation of alpha-synuclein in the presence of copper(II) and hydrogen peroxide. Archives of Biochemistry and Biophysics, 378, 269-277.

114. Paik SR, Shin HJ, Lee JH, Chang CS, and Kim J (1999) Copper(II)-induced self-oligomerization of alpha-synuclein. Biochem J, 340 (Pt 3), 821-828.

115. Paisan-Ruiz C, Jain S, Evans EW, Gilks WP, Simon J, van der Brug M, de Munain AL, Aparicio S, Gil AM, Khan N, et al. (2004) Cloning of the gene containing mutations that cause PARK8-linked Parkinson's disease. Neuron, 44, 595-600.

116. Pandey N, Schmidt RE, and Galvin JE (2006) The alpha-synuclein mutation E46K promotes aggregation in cultured cells. Exp Neurol, 197, 515-520.

117. Pankratz N, Nichols WC, Uniacke SK, Halter C, Rudolph A, Shults C, Conneally PM, and Foroud T (2003) Significant linkage of Parkinson disease tochromosome 2q36-37. Am J Hum Genet, 72, 1053-7.

118. Park JY and Lansbury PT, Jr. (2003) Beta-synuclein inhibits formation of alpha-synuclein protofibrils: a possible therapeutic strategy against Parkinson's disease. Biochemistry, 42, 3696-3700.

119. Parkinson J (1817) An Essay on the Shaking Palsy. Sherwood, Neely & Jones.

120. Petersen K, Olesen OF, and Mikkelsen JD (1999) Developmental expression of alpha-synuclein in rat hippocampus and cerebral cortex. Neuroscience, 91, 651-659.

121. Petrucelli L, O'Farrell C, Lockhart PJ, Baptista M, Kehoe K, Vink L, Choi P, Wolozin B, Farrer M, Hardy J, and Cookson MR (2002) Parkin protects against the toxicity associated with mutant alpha-synuclein: proteasome dysfunction selectively affects catecholaminergic neurons. Neuron, 36, 1007-1019.

122. Polymeropoulos MH, Lavedan C, Leroy E, Ide SE, Dehejia A, Dutra A, Pike B, Root H, Rubenstein J, Boyer R, Stenroos ES, Chandrasekharappa S, Athanassiadou A, Papapetropoulos T, Johnson WG, Lazzarini AM, Duvoisin RC, Di

IG, Golbe LI, and Nussbaum RL (1997) Mutation in the alpha-synuclein gene identified in families with Parkinson's disease. Science, 276, 2045-2047.

123. Pountney DL, Voelcker NH, and Gai WP (2005) Annular alpha-synuclein oligomers are potentially toxic agents in alpha-synucleinopathy. Hypothesis. Neurotox Res, 7, 59-67.

124. Qu J, Li X, Novitch BG, Zheng Y, Kohn M, Xie JM, Kozinn S, Bronson R, Beg AA, and Minden A (2003) PAK4 kinase is essential for embryonic viability and for proper neuronal development. Mol Cell Biol, 23, 7122-7133.

125. Ramirez A, Heimbach A, Grundemann J, Stiller B, Hampshire D, Cid LP, Goebel I, Mubaidin AF, Wriekat AL, Roeper J, Al-Din A, Hillmer AM, Karsak M, Liss B, Woods CG, Behrens MI, Kubisch C. (2006) Hereditary parkinsonism with dementia is caused by mutations in ATP13A2, encoding a lysosomal type 5 P-type ATPase. Nat Genet, 38, 1184–1191.

126. Rigler R, Mets U, Widengren J, Kask P (1993) Fluorescence correlation spectroscopy with high countrate and low background: analysis of translational diffusion. Eur Biophys J, 22, 169–175.

127. Rochet JC, Outeiro TF, Conway KA, Ding TT, Volles MJ, Lashuel HA, Bieganski RM, Lindquist SL, and Lansbury PT (2004) Interactions Among alpha-Synuclein, Dopamine, and Biomembranes: Some Clues for Understanding Neurodegeneration in Parkinson's Disease. J Mol Neurosci, 23, 23-34.

128. Schwille P, Bieschke J, Oehlenschläger F (1997) Kinetic investigations by fluorescence correlation spectroscopy: The analytical and diagnostic potential of diffusion studies. Biophys Chem, 66, 211–228.

129. Schwille P, Meyer-Almes FJ, Rigler R (1997) Dual–color fluorescence cross–correlation spectroscopy for multicomponent diffusional analysis in solution. J Biophys, 72, 1878–1886.

130. Singleton AB, Farrer M, Johnson J, Singleton A, Hague S, Kachergus J, Hulihan M, Peuralinna T, Dutra A, Nussbaum R, Lincoln S, Crawley A, Hanson M, Maraganore D, Adler C, Cookson MR, Muenter M, Baptista M, Miller D, Blancato J, Hardy J, and Gwinn-Hardy K (2003) alpha-Synuclein locus triplication causes Parkinson's disease. Science, 302, 841.

131. Smith WW, Jiang H, Pei Z, Tanaka Y, Morita H, Sawa A, Dawson VL, Dawson TM, and Ross CA (2005) Endoplasmic reticulum stress and mitochondrial cell death pathways mediate A53T mutant alpha-synuclein-induced toxicity. Hum Mol Genet, 14, 3801-3811.

132. Snyder H, Mensah K, Theisler C, Lee J, Matouschek A, and Wolozin B (2003) Aggregated and monomeric alpha-synuclein bind to the S6' proteasomal protein and inhibit proteasomal function. J Biol Chem, 278, 11753-11759.

133. Song DD, Shults CW, Sisk A, Rockenstein E, and Masliah E (2004) Enhanced substantia nigra mitochondrial pathology in human alpha-synuclein transgenic mice after treatment with MPTP. Exp Neurol, 186, 158-172.

134. Souza JM, Giasson BI, Lee VM, and Ischiropoulos H (2000) Chaperone-like activity of synucleins. FEBS Lett, 474, 116-119.

135. Spillantini MG, Schmidt ML, Lee VMY, Trojanowski JQ, Jakes R, and Goedert M (1997) alpha-synuclein in Lewy bodies. Nature, 388, 839-840.

136. Stefanis L, Larsen KE, Rideout HJ, Sulzer D, and Greene LA (2001) Expression of A53T mutant but not wild-type alpha-synuclein in PC12 cells induces alterations of the ubiquitin-dependent degradation system, loss of dopamine release, and autophagic cell death. J Neurosci, 21, 9549-9560.

137. Strauss KM, Martins LM, Plun-Favreau H, Marx FP, Kautzmann S, Berg D, Gasser T, Wszolek Z, Müller T, Bornemann A, Wolburg H, Downward J, Riess O, Schulz JB, and Krüger R (2005) Loss of function mutations in the gene encoding Omi/HtrA2 in Parkinson's disease. Human Molecular Genetics, 14, 2099-2111.

138. Surguchov A, Surgucheva I, Solessio E, and Baehr W (1999) Synoretin--A new protein belonging to the synuclein family. Mol Cell Neurosci, 13, 95-103.

139. Takahashi T, Yamashita H, Nakamura T, Nagano Y, and Nakamura S (2002) Tyrosine 125 of alpha-synuclein plays a critical role for dimerization following nitrative stress. Brain Res, 938, 73-80.

140. Tanaka Y, Engelender S, Igarashi S, Rao RK, Wanner T, Tanzi RE, Sawa A, Dawson L, Dawson TM, and Ross CA (2001) Inducible expression of mutant alpha-synuclein decreases proteasome activity and increases sensitivity to mitochondria-dependent apoptosis. Hum Mol Genet, 10, 919-926.

141: Tjernberg LO, Callaway DJE, Tjernberg A, Hahnet S, Lilliehook C, Terenius L, Thyberg J, and Nordstedt C (1999) A molecular model of Alzheimer amyloid beta-peptide fibril formation, J Biol Chem, 274, 12619-12625.

142. Tsigelny IF, Bar-On P, Sharikov Y, Crews L, Hashimoto M, Miller MA, Keller SH, Platoshyn O, Yuan JX, and Masliah E (2007) Dynamics of alpha-synuclein aggregation and inhibition of pore-like oligomer development by beta-synuclein. FEBS J, 274, 1862-1877.

143. Ueda K, Fukushima H, Masliah E, Xia Y, Iwai A, Yoshimoto M, Otero DA, Kondo J, Ihara Y, and Saitoh T (1993) Molecular cloning of cDNA encoding an unrecognized component of amyloid in Alzheimer disease. Proc Natl Acad Sci U S A, 90, 11282-11286.

144. Uversky VN, Cooper M, Bower KS, Li J, and Fink AL (2002a) Accelerated alpha-synuclein fibrillation in crowded milieu. FEBS Lett, 515, 99-103.

145. Uversky VN and Fink AL (2002b) Amino acid determinants of alpha-synuclein aggregation: putting together pieces of the puzzle. FEBS Lett, 522, 9-13.

146. Uversky VN, Li J, and Fink AL (2001a) Evidence for a partially folded intermediate in alpha-synuclein fibril formation. J Biol Chem, 276, 10737-10744.

147. Uversky VN, Li J, and Fink AL (2001b) Metal-triggered structural transformations, aggregation, and fibrillation of human alpha-synuclein. A possible molecular NK between Parkinson's disease and heavy metal exposure. J Biol Chem, 276, 44284-44296.

148. Uversky VN, Li J, Souillac P, Millett IS, Doniach S, Jakes R, Goedert M, and Fink AL (2002c) Biophysical properties of the synucleins and their propensities to fibrillate: inhibition of alpha-synuclein assembly by beta- and gamma-synucleins. J Biol Chem, 277, 11970-11978.

149. Valente EM, Abou-Sleiman PM, Caputo V, Muqit MM, Harvey K, Gispert S, Ali Z, Del Turco D, Bentivoglio AR, Healy DG, et al. (2004) Hereditary early-onset Parkinson's disease caused by mutations in PINK1. Science, 304, 1158-1160.

150. Volles MJ and Lansbury PT, Jr. (2002) Vesicle permeabilization by protofibrillar alpha-synuclein is sensitive to Parkinson's disease-linked mutations and occurs by a pore-like mechanism. Biochemistry, 41, 4595-4602.

151. Volles MJ, Lee SJ, Rochet JC, Shtilerman MD, Ding TT, Kessler JC, and Lansbury PT, Jr. (2001) Vesicle permeabilization by protofibrillar alpha-synuclein: implications for the pathogenesis and treatment of Parkinson's disease. Biochemistry, 40, 7812-7819.

152. Wersinger C and Sidhu A (2003) Attenuation of dopamine transporter activity by alpha-synuclein. Neurosci Lett, 340, 189-192.

153. Williams DR, Hadeed A, Al-Din AS, Wreikat AL, and Lees AJ (2005) Kufor Rakeb Disease: Autosomal recessive, levodopa-responsive parkinsonism with pyramidaldegeneration, supranuclear gaze palsy, and dementia. Mov. Disord, 20, 1264–1271.

154. Wood SJ, Wypych J, Steavenson S, Louis JC, Citron M, and Biere AL (1999) alpha-synuclein fibrillogenesis is nucleation-dependent. Implications for the pathogenesis of Parkinson's disease. J Biol Chem, 274, 19509-19512.

155. Xu J, Kao SY, Lee FJ, Song W, Jin LW, and Yankner BA (2002) Dopamine-dependent neurotoxicity of alpha-synuclein: a mechanism for selective neurodegeneration in Parkinson disease. Nat Med, 8, 600-606.

156. Yamin G, Glaser CB, Uversky VN, and Fink AL (2003) Certain metals trigger fibrillation of methionine-oxidized alpha-synuclein. J Biol Chem, 278, 27630-27635.

157. Yavich L, Tanila H, Vepsalainen S, and Jakala P (2004) Role of alpha-synuclein in presynaptic dopamine recruitment. J Neurosci, 24, 11165-11170.

158. Zarranz JJ, Alegre J, Gomez-Esteban JC, Lezcano E, Ros R, Ampuero I, Vidal L, Hoenicka J, Rodriguez O, Atares B, Llorens V, Gomez TE, del Ser T, Munoz DG, and de Yebenes JG (2004) The new mutation, E46K, of alpha-synuclein causes Parkinson and Lewy body dementia. Ann Neurol, 55, 164-173.

159. Zecca L, Fariello R, Riederer P, Sulzer D, Gatti A, and Tampellini D (2002) The absolute concentration of nigral neuromelanin, assayed by a new sensitive method, increases throughout the life and is dramatically decreased in Parkinson's disease. FEBS Lett, 510, 216-220.

160. Zecca L, Zucca FA, Wilms H, and Sulzer D (2003) Neuromelanin of the substantia nigra: a neuronal black hole with protective and toxic characteristics. Trends Neurosci, 26, 578-580.

161. Zhao L, Ma QL, Calon F, Harris-White ME, Yang F, Lim GP, Morihara T, Ubeda OJ, Ambegaokar S, Hansen JE, Weisbart RH, Teter B, Frautschy SA, and Cole GM (2006) Role of p21-activated kinase pathway defects in the cognitive deficits of Alzheimer disease. Nat Neurosci, 9, 234-242.

162. Zhu M, Rajamani S, Kaylor J, Han S, Zhou F, and Fink AL (2004) The flavonoid baicalein inhibits fibrillation of alpha-synuclein and disaggregates existing fibrils. J Biol Chem, 279, 26846-26857.

163. Zimprich A, Biskup S, Leitner P, Lichtner P, Farrer M, Lincoln S, Kachergus J, Hulihan M, Uitti RJ, Calne DB, et al. (2004) Mutations in LRRK2 cause autosomal-dominant parkinsonism with pleomorphic pathology. Neuron, 44, 601-607.

6 Manuskriptstatus

Die eigenen Anteile und Anteile der Koautoren aus den Kapiteln 3.1-3.3 werden nachfolgend beschrieben.

Kapitel 3.1:

Kostka* M., Högen* T., Danzer*, K.M. et al. (2007): Single particle characterization of pore forming α-Synuclein aggregates

*Autoren teilen sich die Erstautorenschaft. Eingereicht am 13. Mai bei *European Molecular Biology organisation (EMBO)*

Die konzeptionellen Grundlagen zu diesem Projekt, die Ideenfindung, sowie die Gesamtplanung und Organisation erfolgte in gleichwertiger Arbeitsteilung von Dr. Marcus Kostka, Dr. Armin Giese, Tobias Högen und mir. Das Protein wurde von mir gereinigt und gemeinsam mit Tobias Högen mit einem Fluoreszenzfarbstoff markiert. Die Aggregationsversuche habe ich zusammen mit Tobias Högen geplant und durchgeführt. Für die Auswertung der konfokalen Einzelmolekülspektroskopie war Tobias Högen verantwortlich. Die α-Syn Oligomere für die AFM Analyse habe ich hergestellt, deren Analyse mittels AFM hat Udo Heinzelmann durchgeführt. Die Versuche zur Porenbildung von α-Syn Oligomeren wurden von der Arbeitsgruppe um Andreas Wirth durchgeführt und ausgewertet. Die Thioflavin T Versuche habe ich zusammen mit Dr. Marcus Kostka geplant. Sabine Finger war für die Durchführung der Experimente verantwortlich. Die Testung der Substanzen auf anti-aggregatorische Wirkung wurde von Matthias Habeck durchgeführt und ausgewertet. Die Zellkulturexperimente wurden von der Arbeitsgruppe um Christopher Ross durchgeführt. Tobias Högen und ich waren am Entstehen des Manuskriptes beteiligt. Den Hauptteil haben Dr. Marcus Kostka und Dr. Armin Giese verfasst.

Kapitel 3.2:

Danzer K.M. et al. (2007): Different species of alpha synuclein oligomers induce calcium influx and seeding

Zur Publikation angenommen am 21.06.2007 bei *Journal of Neuroscience*

In dieser Arbeit habe ich die gesamte Planung der Einzelexperimente, sowie Entwicklung der Oligomerisierungsprotokolle selbstständig durchgeführt. Das Protein wurde von mir gereinigt und mit einem Fluoreszenzfarbstoff markiert. Alle Oligomerpräparationen, sowie große Teile derer Charakterisierung mittels AFM wurden von mir durchgeführt und ausgewertet. Unterstützende Hilfe bei der AFM Aufnahmen leistete hier Anne Karow. Die Durchführung der einzelmolekülspektroskopischen Messungen habe ich unter technischer Anleitung von Matthias Habeck durchgeführt. Die Auswertung der Einzelmolekülanalysen erfolgte durch Matthias Habeck. Die stabil überexprimierenden α-Syn neuronalen Zelllinien für alle zellulären Versuche wurden von mir hergestellt und charakterisiert. Alle Versuche zur Messung des intrazellulären Kalziumgehalts wurden von mir geplant, durchgeführt und ausgewertet. Die Seeding-Experimente, sowie die anschließenden Immunfluoreszenzen wurden von mir geplant, durchgeführt und ausgewertet. Darüber hinaus habe ich das Manuskript selbstständig verfasst. Dr. Marcus Kostka leistete dabei unterstützende Hilfe und ermöglichte alle durchgeführten Versuche.

Kapitel 3.3:

Danzer*, K.M., Schnack* C. et al.: Functional protein kinase arrays reveal inhibition of p-21 activated kinase 4 by α-synuclein oligomers

*Autoren teilen sich die Erstautorenschaft. Überarbeitete Version eingereicht am 28. Juni 2007 bei *Journal of Neurochemistry*

Bei dieser Arbeit war ich an der Planung der Experimente maßgeblich beteiligt. Alle verwendeten α-Syn Oligomere wurden von mir hergestellt. Deren Charakterisierung

mittels AFM, SIFT und Western Blot wurden von mir größtenteils durchgeführt und ausgewertet. Cathrin Schnack war für die Durchführung und Auswertung der Kinome 1.0 Protein Array Versuche und Kinase assays verantwortlich.

Die Analyse der transgenen Mausextrakte mittels Immunoblot wurden im Labor von Dr. Frank Gillardon durchgeführt und ausgewertet. Das Manuskript wurde von Dr. Frank Gillardon und mir verfasst.

Hiermit bestätige ich diese Angaben zum Eigenanteil von Karin Danzer an den vorgelegten Publikationen bzw. Manuskripten:

Betreuer der vorgelegten Dissertation: _____ (Dr. Marcus Kostka)

7 Abkürzungsverzeichnis und Anglizismen

Viele wissenschaftliche Begriffe entstammen dem englischen Wortschatz und können nur schwer ins Deutsche übersetzt werden. Die hieraus verwendeten Begriffe und Abkürzungen sind im folgenden erläutert:

AFM	atomic force microscope, Rasterkraftmikroskop
α-Syn[A30P]	familiäre Punktmutation an Position 30 von α-Syn, Austausch von Alanin nach Prolin
α -Syn[E46K]	familiäre Punktmutation an Position 46 von α-Syn, Austausch von Glutaminsäure nach Lysin
α -Syn[A53T]	familiäre Punktmutation an Position 53 von α-Syn, Austausch von Alanin nach Threonin
Amyloid precursor protein	Amyloid Vorläufer Protein
AS	Aminosäure
CD-Spektroskopie	Circular Dichroism, Zirkulardichroismus
CSPα	Cystein String Protein α
C-terminal	am Carboxy-Ende eines Proteins gelegen
FCS	Fluorescence Correlation Spectroscopy, Fluoreszenz-Korrelations-Spektroskopie
FIDA	Fluorescence Intensity Distribution Analysis, Fluoreszenz-Intensitäts-Verteilungs-Analyse
LIMK1	LIM Kinase 1
NAC	non amyloid component, nicht amyloide Komponente
N-terminal	am Aminoende eines Proteins gelegen
PAK	p21 aktivierte Kinase

PET	Positronen-Emissions-Tomographie
PK	Parkinson Krankheit
Protein Kinase array	Protein Chip, auf den auf kleinster Fläche aktive Kinasen aufgetragen sind
Seeding	beschleunigte Aggregation aufgrund eines vorhandenen Aggregationskeimes
SIFT	Scanning for Intensely Fluorescent Targets
SNARE-Proteine	soluble NSF attachment receptor: Schlüsselfaktoren in der Fusion von biologischen Membranen. Diese Transmembranproteine bilden sehr stabile Komplexe, welche jeweils aus vier SNARE-Proteinen bestehen. Dabei steht NSF für N-Ethylmaleinimid-sensitiver Faktor
Spine	synaptische Endigungen am Axon
Western-Blot	durch ein elektrisches Feld erzielter Protein-Transfer vom Gel auf Membranen

Bezeichnung	Abkürzung	Einbuchstabencode
Alanin	Ala	A
Arginin	Arg	R
Asparagin	Asn	N
Asparaginsäure	Asp	D
Cystein	Cys	C
Glutamin	Gln	Q
Glutaminsäure	Glu	E
Glycin	Gly	G
Histidin	His	H
Isoleucin	Ile	I
Leucin	Leu	L
Lysin	Lys	K
Methionin	Met	M
Phenylalanin	Phe	F
Prolin	Pro	P
Serin	Ser	S
Threonin	Thr	T
Tryptophan	Trp	W
Tyrosin	Tyr	Y
Valin	Val	V

8 Anhang

Single particle characterization of pore forming α-Synuclein oligomers

Marcus Kostka[1*#], Tobias Högen[2#], Karin M. Danzer[1#], Matthias Habeck[2], Andreas Wirth[3], Richard Wagner[4], Charles G. Glabe[5], Sabine Finger[1], Udo Heinzelmann[1], Patrick Garidel[1], Wenzhen Duan[6], Christopher A. Ross[6], Hans Kretzschmar[2], and Armin Giese[2*]

[1] CNS Research, Boehringer Ingelheim Pharma GmbH & Co KG, Germany
[2] Zentrum für Neuropathologie und Prionforschung, Ludwig-Maximilians-Universität München, Germany
[3] Ionovation GmbH, Osnabrück, Germany
[4] Department of Biophysics, University of Osnabrück, Germany
[5] Department of Molecular Biology and Biochemistry, University of California, Irvine, CA 92697-3900. USA
[6] Division of Neurobiology, Department of Psychiatry, Johns Hopkins University School of Medicine, Baltimore, Maryland 21287, USA

 # MK, TH, and KMD contributed equally

* Corresponding authors:

Dr. Armin Giese
Zentrum für Neuropathologie und Prionforschung
Ludwig-Maximilians-Universität München
Feodor Lynen-Str. 23
81377 München, Germany
Tel. ++49-89-2180-78048
Fax ++49-89-2180-78037
Email Armin.Giese@med.uni-muenchen.de

Dr. Marcus Kostka
Boehringer Ingelheim Pharma GmbH & Co KG, Germany
CNS Research
Birkendorferstr. 65
88397 Biberach, Germany
Tel. ++49-7351-54-5415
Fax ++49-7351-54-98928
Email Marcus.Kostka@bc.boehringer-ingelheim.com

Character count: 55,036

Running title: α-Synuclein oligomers

Abstract

Aggregation of α-synuclein (α-syn) is a key event in the pathology of several neurodegenerative diseases including Parkinson´s disease. Recent findings suggest that oligomers represent the principal toxic aggregate species. We used confocal single molecule fluorescence techniques such as SIFT and atomic force micrcoscopy to monitor α-syn oligomer formation at nanomolar protein concentrations. Ethanol was used to influence the folding of α-syn and trigger aggregation, which resulted in small oligomers ("intermediate I"). Under these conditions, Fe^{3+} at low micromolar concentrations dramatically increased aggregation and resulted in formation of larger oligomers ("intermediate II"). Both oligomer species appeared to be on-pathway to amyloid fibrils and could seed amyloid formation measured by thioflavinT binding. Notably, Fe^{3+}-induced oligomers could also form ion-permeable pores in a planar lipid bilayer assay. Both an anti-α-syn-antibody and the oligomer-specific antibody A11 inhibited pore formation. Moreover, baicalein and N´-benzylidene-benzohydrazide anti-prion compounds were able to inhibit oligomer formation. Baicalein also inhibited α-syn-dependent toxicity in cell-culture. Our results further elucidate the role of toxic oligomer species in neurodegenerative diseases and provide new approaches for drug discovery.

Introduction

All common neurodegenerative diseases are characterized by the formation and deposition of fibrillar aggregates of specific proteins such as tau protein and amyloid beta-peptide in Alzheimer´s disease, prion protein in prion diseases, and α-synculein (α-syn) in Parkinson´s disease (PD), dementia with Lewy bodies, and multiple system atrophy (Koo *et al.*, 1999; Muchowski, 2002). PD is the most common movement disorder and, after Alzheimer's disease, the second most common neurodegenerative brain disorder. It affects about 1% of people beyond 65 years of age (Forman *et al.*, 2005). Pathologically, PD it is characterized by degeneration of dopaminergic neurons in the substantia nigra, which leads to disruption of neuronal systems responsible for motor functions (Braak *et al.*, 2003).

Initial evidence for a central role of α-syn in the pathogenesis of PD came from the discovery of point mutations in the α-syn gene in families with familial PD (Polymeropoulos *et al.*, 1997; Kruger *et al.*, 1998). Subsequently, α-syn has been identified as the major component of Lewy bodies and in Lewy neurites, which are characteristic deposits of aggregated protein in PD, dementia with Lewy bodies, and Lewy body variant of Alzheimer's disease, and as the major component of the glial cytoplasmatic inclusions that characterize multiple system atrophy (Spillantini *et al.*, 1997; Irizarry *et al.*, 1998; Goedert, 2001). So far, three different point mutations have been described in the α-syn gene (Polymeropoulos *et al.*, 1997; Kruger *et al.*, 1998; Zarranz *et al.*, 2004). Further evidence for a fundamental role of α-syn in the pathogenesis of PD came from the recent observation that an increased gene dose in PD patients caused by a duplication or triplication of the α-syn gene is sufficient to trigger disease (Singleton *et al.*, 2003; Ibanez *et al.*, 2004; Chartier-Harlin *et al.*, 2004).

The transformation of amyloidogenic proteins from the monomeric state into fibrillar aggregates seems to progress via intermediates that have been termed protofibrils, protofilaments or oligomers (Goldberg and Lansbury, Jr., 2000; Conway *et al.*, 2001; Volles *et al.*, 2001; Kayed *et al.*, 2003; Sanchez *et al.*, 2003; Cole *et al.*, 2005). Although the cause of neurodegeneration in PD is not fully understood, recent findings suggests that small oligomers rather than the fibrillar amyloid deposits of α-syn represent the principal toxic species (Kayed *et al.*, 2004). Overexpression of human α-syn can cause apoptosis, damage of cell organelles and enhance susceptibility to oxidative stress in the absence of detectable fibril formation (Gosavi *et al.*, 2002).

It has been shown that certain soluble α-syn oligomers share a common structure with oligomers derived from other amyloidogenic proteins, such as the amyloid-ß peptide, amylin,

insulin, prion protein and others, implying a common mechanism of pathogenesis (Bucciantini *et al.*, 2002; Kayed *et al.*, 2003; Bucciantini *et al.*, 2004). One mechanism of oligomer toxicity that has been proposed is the formation of pores that lead to permeabilization of lipid bilayers (Kayed *et al.*, 2004). Additionally, oligomeric forms were found to inhibit the proteasome leading to decreased protein degradation and increased oxidative stress (Tanaka *et al.*, 2001; Lindersson *et al.*, 2005). Moreover, it has been shown that α-syn overexpression in various mammalian cells results in reduced viability (Smith *et al.*, 2005).

In the aggregation process from the monomeric protein to the endstage amyloid fibril, different distinct intermediates like globular oligomers and protofibrils have been proposed (Conway *et al.*, 2000c; Uversky *et al.*, 2001a; Kayed *et al.*, 2003; Glabe, 2006; Fink, 2006). So far, it remains unclear which oligomer species harbour toxic properties.

Several lines of evidence indicate that iron ions play an important role in PD pathogenesis. In PD patients, a correlation between increased iron levels and severity of neuropathological changes has been observed (Gotz *et al.*, 2004). Furthermore, the neurons that are affected most severely in PD are located in the substantia nigra and locus coeruleus. These brain areas are enriched with neuromelanin that sequesters reactive metals, mainly iron (Connor *et al.*, 1995; Zecca *et al.*, 2003; Smith *et al.*, 2005). Interestingly, iron chelators showed neuroprotective activity against proteasome-inhibitor induced, MPTP-induced and 6-hydroxydopamine-induced nigral degeneration (Ben-Shachar *et al.*, 1991; Kaur *et al.*, 2003; Zhang *et al.*, 2005; Smith *et al.*, 2005). Additionally, it has been suggested that iron can induce the formation of intracellular α-syn aggregates and trigger α-syn oligomerization in cells (Ostrerova-Golts *et al.*, 2000; Matsuzaki *et al.*, 2004; Hasegawa *et al.*, 2004; Cole *et al.*, 2005). Taken together, these findings implicate iron ions in generation of α-syn aggregates and in disease progression in PD. However, the underlying molecular events have not been elucidated so far. Therefore, the aim of our study was to improve the understanding of the molecular events in the pathological processes underlying the formation and toxicity of α-syn oligomers and the role of iron in PD.

To quantify and characterize α-syn aggregates at the single particle level, we used fluorescently labelled α-syn and applied fluorescence correlation spectroscopy (FCS), fluorescence intensity distribution analysis (FIDA) as well as scanning for intensely fluorescent targets (SIFT) in a confocal single molecule detection system. In recent years, FCS, FIDA, and SIFT have been recognized as methods that allow highly sensitive analysis of protein aggregation in neurodegenerative diseases such as prion diseases, synucleinopathies,

and polyQ diseases at the molecular level (Post *et al.*, 1998; Giese *et al.*, 2000; Bieschke *et al.*, 2000; Giese *et al.*, 2004; Giese *et al.*, 2005; Behrends *et al*., 2006). FCS is based on the analysis of fluctuations in fluorescence caused by the diffusion of fluorescently labelled molecules at nanomolar to picomolar concentrations through an open detection volume of approximately 1 femtoliter that is created by a focussed laser beam. From these fluctuations, the concentration and the diffusion time can be calculated. In addition, the molecular brightness of fluorescent particles can be obtained (Schwille *et al.*, 1997a; Kask *et al.*, 2000). When molecules labelled with two different fluorophores form complexes, the amount of complex formation can be easily monitored by cross-correlation analysis in a dual-color set-up (Schwille *et al.*, 1997b). Moreover, aggregate formation can be analysed with high sensitivity by SIFT analysis (Giese *et al.*, 2000; Bieschke *et al.*, 2000).

Results and Discussion

Single particle detection and characterization of α-synuclein oligomers

Oligomerization of α-syn appears to play an important role in the pathogenesis of PD and other synucleinopathies. It could be shown that this aggregation process can be influenced by various factors including low pH, high salt, high temperature, divalent and trivalent ions, pesticides, TMAO, polycations, GAG´s, and alcohols (Munishkina *et al.*, 2003; Munishkina *et al.*, 2004). Organic solvents (e.g. ethanol at a concentration of 5-25%) can induce the generation of a partially folded intermediate and accelerate amyloid formation, whereas higher concentrations of ethanol resulted in the formation of a different oligomer species unable to form amyloid (Munishkina *et al.*, 2003). Thus, this approach can be used as a model system to study aggregation pathways of α-syn *in vitro*. However, high concentrations of α-syn have been used in these studies. Therefore, we asked whether this effect can also been seen at low protein concentrations in the nanomolar range, as we reasoned that oligomeric α-syn aggregation intermediates might be kinetically trapped under these conditions, as amyloid formation is known to be highly inefficient at low α-syn concentrations. Moreover, nanomolar protein concentrations allow efficient oligomer characterization by confocal single particle fluorescence techniques.

We used α-syn labeled with fluorescent dyes to monitor the aggregations process with a single particle approach that has also been used to detect huntingtin and prion protein oligomers (Giese *et al.*, 2004; Levin *et al.*, 2005; Piening *et al.*, 2006; Behrends *et al.*, 2006). After four hours incubation of 10-20 nM α-syn at room temperature virtually no oligomeric forms were

observed. In contrast, when ethanol was added at concentrations of 5-20%, small oligomers could be detected by FCS, cross-correlation analysis, and FIDA (Fig.1). Diffusion times obtained for these oligomers by cross-correlation analysis indicated that the oligomers consisted on average of approximately 20 monomers. This was confirmed by the detection of particles with a corresponding increase in particle brightness by FIDA analysis (Supplement, table S1). When the sample was diluted in ethanol-free buffer, the process was reversible (data not shown). In contrast to oligomers formed at ethanol concentrations >30%, aggregation at intermediate concentrations of ethanol could be blocked by the addition of detergents such as NP40 and by BSA (Fig.1D), which corroborates that different oligomer species are formed depending on the concentration of ethanol. At the low concentration of α-syn used in our assay, no formation of amyloid-like large aggregates was detectable by highly sensitive SIFT analysis (Giese *et al.*, 2005). This indicates that aggregation may be kinetically trapped at the level of small oligomers under these conditions.

It has been described that BSA can bind the acidic C-terminal domain of α-syn (El-Agnaf *et al.*, 2004). Therefore we tested if BSA could block oligomer formation. Indeed, 0,01 % BSA was sufficient to block oligomerization completely (Fig.1D).

Effect of metal ions on synuclein oligomer formation

Epidemiological studies suggest an involvement of heavy metals in the etiology of PD (Zayed *et al.*, 1990; Rybicki *et al.*, 1993; Gorell *et al.*, 1997). It has been reported that metal ions such as iron and aluminum can accelerate amyloid formation from α-syn (Uversky *et al.*, 2001b) and influence aggregation behavior of various amyloidogenic proteins (Paik *et al.*, 1999; Capanni *et al.*, 2004). In addition, several groups showed that metal ions can trigger the generation of oligomeric α-syn forms *in vitro* (Paik *et al.*, 1999; Uversky *et al.*, 2001b; Yamin *et al.*, 2003; Lowe *et al.*, 2004; Capanni *et al.*, 2004; Cole *et al.*, 2005). In contrast to other groups that used a combination of high protein and high metal ion concentrations, we studied the influence of Fe^{3+} concentrations close to physiological serum levels (10-20 μM) on the aggregation process with nanomolar α-syn concentrations. First, we screened various metal ions (Fe^{3+}, Al^{3+}, Cu^{2+}, Mn^{2+}, Ca^{2+}) in our assay. Of the metal ions tested, only Fe^{3+} and to a lesser extend Al^{3+} resulted in an increase in aggregation (Fig. 2a, Fig. S2).

Notably, Fe^{3+} (and to a lesser extent Al^{3+}) resulted in the formation of significantly larger oligomers that were detectable as a high-intensity signal in scanned measurements by SIFT analysis (Fig. 2 and Fig. S2). Diffusion time analysis is not useful for these large aggregates as these aggregates diffuse very slowly and are detected only inefficiently when no scanning

device is used. Brightness analysis by FIDA indicated formation of >100meres (Table S1). To distinguish these aggregates from the small oligomers described above, we termed the small ones intermediate I and the large ones intermediate II.

Importantly, Fe^{3+} only caused an effect on α-syn aggregation when added in the presence of intermediate concentrations of ethanol (Fig. 2b,c). Neither did Fe^{3+} affect aggregation of α-syn in the absence of ethanol, nor at concentrations of ethanol >30%. Moreover, addition of either NP40 or BSA, which specifically inhibited the formation of the intermediate I at intermediate concentrations of ethanol, also inhibited the effect of Fe^{3+}. This indicates that the effect of Fe^{3+} depends on the presence of the intermediate I species, which results in a synergistic effect of Fe^{3+} and ethanol on α-syn aggregation. To exclude that the observed effect of iron was related to the sodium phosphate buffer used in these experiments, we also analyzed aggregation in Tris buffer and obtained identical results (Fig. S3).

AFM analysis of intermediates I & II

In order to exclude an influence of the fluorescence label on the aggregation process we observed with confocal single particle fluorescence techniques, we chose AFM as a fluorescence-independent single particle detection method suited for low particle concentrations. The α-syn aggregates formed in the presence or absence of ethanol and/or Fe^{3+} were imaged by tapping mode atomic force microscopy. AFM has been shown to be a powerful method for the characterisation of protein aggregates (Colton RJ, 1998; Costa *et al.*, 2004). AFM has been used for the identification of the different morphological structures formed during α-syn aggregation (Conway *et al.*, 2000a; Volles *et al.*, 2001; Lashuel *et al.*, 2002; Ding *et al.*, 2002; Rochet *et al.*, 2004).

AFM images of dissolved non-labeled α-syn, incubated for 4 h at room temperature show globular features with a height between 0.9 – 1.9 nm. Based on their size distribution in the AFM images and their comparison with images of other similar peptides with a similar molecular weight (Conway *et al.*, 2000b; Quist *et al.*, 2005; Pountney *et al.*, 2005), these globular structures appear to be mostly monomers. Compared to freshly prepared protein samples, α-syn retained its globular structure over a period of several hours (4 h) with no significant change in the size distribution and without noteworthy aggregation. This is in agreement with (Quist *et al.*, 2005). The particle distribution was quite homogeneous. Assuming a cylindrical shape of the particle, the average calculated volume is around 200 nm^3 (Table S2). About 80 % of the particles were smaller than 300 nm^3, and just about 5 % had a volume between 400 – 500 nm^3.

The presence of 20 v% ethanol induced an increase of the particle size (Fig. 3). The average particle size was estimated with ~34 nm and the height 2.1 nm, with an average volume of 2500 nm^3 (Table S2). 75% of the particles were smaller than 3000 nm^3. The combination of 20% ethanol and 20µM $FeCl_3$ showed an average particle size of 70 nm and 6.4 nm height. The calculated volume of these particles was around 33000 nm^3 (Table S2).

To study the influence of fluorescence dyes on the aggregation process, we compared labeled and non-labeled α-syn. Coupling the fluorescence dye ALEXA-647 to the protein did not influence the oligomerization process (Fig. 3c, Table S2).

These data completely confirm the influence of ethanol and iron on the oligomerization process analysed by SIFT. In summary, the α-syn oligomers that have been formed in the presence of ethanol showed a ten-fold increase(intermediate I) and the combination with iron showed a hundred-fold increase in the particle size (intermediate II) compared to monomeric α-syn.

Seeding of intermediates I & II of α-synuclein oligmers

It has previously been shown that pre-formed aggregates of α-syn can seed the generation of amyloid fibrils from α-syn monomers arguing for a nucleation-dependent polymerization process (Wood *et al.*, 1999; Hoyer *et al.*, 2002). To analyze whether buffer conditions that favor formation of intermediate I and II oligomers at nanomolar concentrations of α-syn also accelerate amyloid formation at higher concentrations of α-syn, we used a Thioflavin T assay (Hoyer *et al.*, 2002;Yamin *et al.*, 2003). As expected (Munishkina *et al.*, 2003), both 20% ethanol and 20% ethanol/100 µM Fe^{3+} accelerate amyloid formation (Fig. 4a). Next, we wanted to test whether the intermediate I and II oligomers have seeding properties, which would provide further evidence that they are on-pathway to amyloid structures. The samples used for seeding experiments were generated by over night incubation of 0.1 mg/ml monomeric α-syn with 10% ethanol with or without 10 µM ferric chloride. As starting material for the different aggregation approaches monomeric α-syn (1mg/ml) containing 10% ETOH with or without 10 µM ferric chloride was used. Non-seeded samples (control reactions) and seeded samples were performed under these buffer conditions. The seeding was started by spiking with 10% (v/v) of pre-aggregated α-syn. This resulted in a reduced lag time and an increased thioflavinT fluorescence signal. Therefore, we conclude that both oligomer types can seed amyloid formation and are on-pathway to amyloid fibrils (Fig. 4).

Pore formation by iron-induced intermediate II oligomers

Goldberg and collegues proposed the model of annular protofibrils as toxic species in the aggregation process (Goldberg *et al.*, 2000). In agreement with this model, Mina *et al.* could isolate annular amyloid-ß structures from AD brain (pers. comm. C. Glabe). Pore formation has been described as a characteristic feature of various oligomeric protein aggregates (Volles *et al.*, 2001; Lashuel *et al.*, 2002; Volles and Lansbury, Jr., 2002; Kayed *et al.*, 2004; Pountney *et al.*, 2005). Therefore we were interested to test if the intermediate I or II oligomers were able to form pore-like structures. The planar lipid bilayer technique has been established as a powerful tool to obtain single channel recording from pores inserted into artificial membranes (Meuser *et al.*, 1999; Romer and Steinem, 2004; Hill *et al.*, 1998). After 3 h incubation of α-syn with pre-formed suv-liposomes, membrane vesicles were added to the *cis* chamber directly below the bilayer to induce membrane fusion. Changes in the electrical conductivity of the membrane in response to various α-syn samples were monitored. It could be shown that the bilayer was not affected by the various buffer components alone (Ethanol, BSA, Fe^{3+}, phosphate buffer) as well as by monomeric α-syn. Also the combination of α-syn and ethanol had no effect. Therefore, we concluded that the intermediate I form of α-syn did not form pores in this assay. The intermediate II form generated with Fe^{3+} and ethanol exhibited a reproducible effect on membrane conductivity (Fig. 5; Table 1). Pore formation in the bilayer was reproducibly observed at a success-rate of 12-15% (Table 1). These pores were permanently open. The distribution of conductance states obtained (Fig. 5b) indicates the presence of a smallest unit pore with a conductivity of about 50pS in 250 mM KCl.

The observed reversal potential in 250/20 mM KCl was V_{rev}= -21±2 mV (Fig. 5a), using the GHK approach this corresponds to an ion selectivity of $P_{Cl-}/ P_{K+} \cong 2.75$. The known Ca^{2+}-channel blocker cobalt did not show an effect on the pores formed. Importantly, similar results were obtained with non-labeled and labeled α-syn.

In agreement with the observed inhibitory effect of BSA on aggregation, BSA also inhibited pore formation in the bilayer assay (Table 1). To corroborate further that pore formation was α-syn dependent, we added an α-syn specific antibody (asy1, gift from Poul Henning Jensen, University of Aarhus, Denmark) and an anti-Aß antibody (6E10, Senetec) to the pre-incubation mix. As expected, only the anti-α-syn antibody was able to prevent pore formation (Table 2). To demonstrate that oligomers were responsible for the pore formation, the recently described oligomer specific antibody A11 (Kayed *et al.*, 2003) was added to the pre-incubation mix. This oligomer specific antibody also inhibited pore formation. Moreover, when applied to the *cis* chamber after integration of membrane pores into the lipid bilayer, the A11 antibody reduced conductivity by approximately 30%. Taken together, these results

indicate that A11-reactive oligomers were formed by the combined effect of ethanol and Fe^{3+} and provide evidence that A11-positive oligomers contribute to pore formation.

Compounds that inhibit synuclein oligomer formation also block toxicity in cell culture

It has been suggested that soluble oligomers share a common structure and may also share a common mechanism of toxicity (Kayed *et al.*, 2003; Kayed *et al.*, 2004). In this study we could confirm that the aggregation process of α-syn involves discrete intermediates of different size that could be detected and characterized with high sensitivity at the single particle level. The finding that certain intermediates exhibit potentially toxic properties such as pore formation suggests that the oligomerization process provides an attractive target for drug development, as the interaction of small compounds with these different intermediates may block the generation of toxic species. A major advantage of our single particle based fluorescence approach is that it lends itself to high-throughput screening applications. For example, a SIFT screening assay has recently been employed successfully in the search for new anti-prion compounds (Bertsch *et al.*, 2005). In a pilot study, we tested eight N'-benzylidene-benzohydrazide derivates that were identified as anti-prion compounds by us previously (Bertsch *et al.*, 2005). Some of these compounds were recently shown to also inhibit poly-Q aggregation (Schiffer *et al.*, 2007). In addition, we used baicalein which has previously been shown to inhibit fibrillation of α-syn (Zhu *et al.*, 2004). For compound testing, aggregation was induced by DMSO instead of ethanol as compound stock solutions were supplied in DMSO and because DMSO was shown to mimick the effect of ethanol in control experiments (Fig. S4). Baicalein at a concentration of 10 μM efficiently blocked aggregation in our assay system. Similarly, aggregation was inhibited by some of the tested NBB compounds. Interestingly, inhibitory activity was strictly dependent on the presence of two hydroxyl groups at the benzohydrazide ring indicating a well-defined structure-activity relationship (Fig. 6a+b).

Unfortunately the NBB compounds showed toxicity at low micromolar concentrations in our cell culture model for α-syn-dependent toxicity (see below), so that we were not able to confirm this *in vitro* activity in cell culture. However, baicalein showed no toxicity up to 10 μM in cell culture and could therefore be used to study a potential effect on α-syn-dependent toxicity. It has been shown previously that inducible expression of α-syn [A53T] in PC12 cells results in ER stress and mitochondrial dysfunction leading finally to cell death. This apoptotic mechanism could be partially blocked by a pan-caspase inhibitor (z-VAD) (Smith *et*

al., 2005). Interestingly, overexpression of the mutant E46K α-syn resulted in the same reversible toxicity.

Here, we show that baicalein, which blocks formation of small oligomeric forms in our cell-free system, is able to prevent cell death in a dose-dependant manner (Fig. 6c). This result suggests that α-syn aggregation might be involved in cell death in this model system. It is already known that baicalein can form a Schiff base with a lysine of α-syn preventing the fibrillization process (Zhu *et al.*, 2004). In that study, baicalein was also able to disaggregate existing fibrils in vitro to high molecular weight oligomer species. Here we used a cellular system where fibril formation has never been observed. Therefore, we exclude a role of fibril deaggregation activity of baicalein in this model. However, the binding of baicalein to the monomeric α-syn as it was proposed by Zhu et al. would also interfere with the α-syn aggregation process in our cell culture model preventing the generation of toxic oligomers. Taken together with our findings in the cell-free SIFT assay, this indicates that inhibition of α-syn oligomer formation is the most likely explanation for the effect of baicalein on α-syn mediated toxicity in our cell culture model system.

Conclusion

In summary, we used confocal single molecule fluorescence techniques such as SIFT in combination with atomic force micrcoscopy to analyse aggregation pathways and oligomer formation of alpha-synuclein. By this approach, we could characterize two different oligomer species that were both on-pathway to amyloid fibrils ("intermediate I" and "intermediate II") for the first time. Notably, "intermediate II" oligomers, which could be induced by low micromolar concentrations of ferric iron, could also form ion-permeable pores in a planar lipid bilayer assay. Both an anti-α-synuclein-antibody and the oligomer-specific antibody A11 inhibited this pore formation. Moreover, baicalein and N´-benzylidene-benzohydrazide anti-prion compounds were able to inhibit oligomer formation. Baicalein also inhibited α-syn-dependent toxicity in cell-culture. Thus, our results further elucidate the role of toxic oligomer species in neurodegenerative diseases and provide new approaches for drug discovery.

Materials and Methods

Expression and purification of recombinant wild-type α-synuclein

Expression and purification was preformed as described previously by Nuscher *et al.* (Nuscher *et al.*, 2004). Briefly, pET-5a /α-Synuclein wt plasmid (kind gift of Philipp Kahle,

LMU Munich) was used to transform *Escherichia coli* BL21(DE3) pLys, and expression was induced with isopropyl-ß-D-thiogalactopyranose (IPTG) for 4h. Cells were harvested, resuspended in 20mM Tris and 25mM NaCl, pH 8.0 and lysed by freezing in liquid nitrogen followed by thawing. After 30min of boiling, the lysate was centrifuged at 17600 g or 15 min at 4°C. Supernatant was filtered through 0.22µm filter (Millex-GV, Millipore Corp.,Bedford, MA, USA) before loaded into HiTrap Q HP (5ml) and eluted with a 25mM to 500mM NaCl salt gradient. The pooled α-syn peak was desalted by Superdex 200 HR10/30 gel filtration with 20mM Tris, 25mM NaCl, pH 8.0 running buffer. The pooled α-syn peak was concentrated using Vivaspin columns MWCO 5kD (Vivascience, Stonehouse, UK) and equilibrated to water. The protein concentration was determined with a BCA protein quantification kit (Pierce, Rockford, IL, USA). Samples were aliquoted und lyophilized.

Separation of monomeric and oligomeric α-synuclein

Size exclusion chromatography was performed as previously described (Volles et al. 2001). Briefly, a solution of purified recombinant α-syn (1-5 mg/ml) in 10 mM PBS, prepared from lyophilized protein, was filtered through a 0.22 µm filter. The filtrate was eluted from a Superdex 200 gel filtration column (Pharmazia) in PBS at a flow rate of 0.5 ml/min. The eluate was monitored at 215-280 nm.

Fluorescent labelling of α-synuclein

Protein labelling was performed with amino-reactive fluorescent dyes Alexa Fluor-488-O-succinimidylester and Alexa Fluor-647-O-succinimidylester (Molecular Probes, USA), respectively. Unbound fluorophores were separated by two filtration steps in PD10 Columns (Sephadex G25, Amersham Biosciences, Munich, Germany) equilibrated with 50mM sodium phosphate buffer, pH 7.0. Quality control of labelled α-syn was performed by mass spectroscopy and by FCS measurements on an Insight Reader (Evotec-Technologies, Germany). The typical labelling ratio achieved was approximately 1-2 dye molecules per α-syn molecule. In order to remove preformed aggregates, the stock solution of labelled α-syn was subjected to size exclusion chromatography (see above).

Confocal single particle analysis

FCS, FIDA, and SIFT measurements were carried out on an Insight Reader (Evotec-Technologies, Germany) with dual-colour excitation at 488nm and 633nm, using a 40x 1.2 NA microscope objective (Olympus, Japan) and a pinhole diameter of 70µm at FIDA setting.

Excitation power was 200 µW at 488 nm and 300 µW at 633 nm. Measurement time was 10 sec. Scanning parameters were set to 100 µm scan path length, 50 Hz beam scanner frequency, and 2000 µm positioning table movement. This is equivalent to approximately 10 mm/s scanning speed. All measurements were performed at room temperature. The fluorescence data was analysed by auto-correlation analysis using the FCSPPEvaluation software version 2.0 (Evotec-Technologies, Germany). Two-colour cross-correlation amplitudes G(0) (Schwille *et al.*, 1997b) and FIDA data were evaluated using the same software. For fluorescence intensity distribution analysis (FIDA) (Kask *et al.*, 1999; Kask *et al.*, 2000) and SIFT analysis (Bieschke *et al.*, 2000; Giese *et al.*, 2000), fluorescence from the two different fluorophores was recorded simultaneously with two single photon detectors. Photons were summed over time intervals of constant length (bins) using a bin length of 40 µs. The frequency of specific combinations of "green" and "red" photon counts was recorded in a two-dimensional intensity distribution histogram as described previously (Kask *et al.*, 2000; Bieschke *et al.*, 2000; Giese *et al.*, 2000). Evaluation of SIFT data in two-dimensional intensity distribution histograms was performed by summing up the numbers of high-intensity bins as described using a 2D-SIFT software module (Evotec-Technologies, Germany). For threshold setting, non-aggregated reference samples were used.

Aggregation assay

A 5-fold stock solution of fluorescently labelled α-syn was prepared by mixing α-syn labeled with Alexa-488 and α-syn labeled with Alexa-647. The concentrations of α-syn-Alexa-488 and α-syn-Alexa-647 were adjusted to approximately 10 molecules per focal volume and 15 molecules per focal volume, respectively. Quality control SIFT measurements were used to confirm that the stock solution was free of α-syn aggregates. Experiments were started by diluting the stock solution in 50mM sodium phosphate buffer, pH 7.0, or in 50mM Tris-HCl buffer, pH 7.0, respectively, containing ethanol concentrations of 0% to 50% and a final concentration of labelled α-syn of 10-20 nM in a total assay volume of 20 µl. $FeCl_3$ (Merck), $AlCl_3$, $CuCl_2$, $MnCl_2$, $CaCl_2$ (Sigma) were used at final concentrations of 0.1µM to 10 µM. In some experiments dimethylsulfoxid (DMSO, Sigma) was used instead of ethanol to induce α-syn aggregation. All experiments were performed in 96-well-plates with a cover slide bottom (Evotec-Technologies, Germany). To reduce evaporation, plates were sealed with adhesive film. Typically, aggregation was monitored for at least 5 hours in two to four independent samples for each experimental group.

Electrophysiology with planar lipid bilayers

Planar lipid bilayers were produced by the painting technique. A solution of 80mg/ml purified azolectin (Hinnah *et al*., 2002) in n-decan was applied to a hole (100µM diameter) in a Teflon septum, separating two bath chambers (volume 3ml each). Both chambers were equipped with magnetic stirrers. Through continuously lowering and then re-raising of the solution level the lipid layer across the hole was gradually thinned out until a bilayer was formed. This formation was monitored optically and by capacitance measurements. The resulting bilayers had a typical capacitance of 0.5µF/cm^2 and a resistance of >100GΩ. The noise was 3pA (r.m.s.) at 5kHz bandwidth. After the formation of a stable bilayer in 250mM KCl, 20mM Mops/Tris pH 7.0 in both chambers (= symmetrical conditions), the solutions were changed by perfusion to asymmetrical conditions 250mM/20mM KCl, 10mM Mops/Tris pH 7.0, *cis*/*trans*. An osmotic gradient of a channel-permeant solute, is – in addition to the absolute necessity of the channel in the vesicle being in the open state (Woodbury and Hall, 1988) - a prerequisite for fusion of membrane vesicles with the bilayer. To promote attachment of the membrane vesicles to the bilayer, $CaCl_2$ was added to the *cis* chamber to a concentration of 10mM (Niles and Cohen, 1987; Zimmerberg *et al.*, 1980). Membrane vesicles were then added to the *cis* chamber directly below the bilayer, affecting a slow flow of membrane vesicles along the bilayer surface. After fusion, the electrolytes were changed to the final composition.

The Ag/AgCl electrodes were connected to the chambers through 2 M KCl-agar bridges. The electrode of the *trans* compartment was directly connected to the headstage of a current amplifier (Axon Gene Clamp 500, Axon Instr.). Membrane potentials are referred to the *trans* compartment. The amplified currents were digitised at a sampling interval of 0.2 ms, filtered with a low-pass-filter at 5kHz and fed into an Digidata1200 A/D converter (Axon Instruments, Foster City, CA). For analysis, an analysis software („SCIP“ single channel investigation program) developed in our laboratory was used in combination with Origin 6.0 (Microcal Software Inc.).

Preparation of α-synculein aggregates for pore formation assay

α-syn and other chemical components were incubated in the presence of preformed liposomes (Ionovation, Osnabrück, Germany) with a mean diameter of 100 nm at room temperature. After 3 h samples were treated in an ultrasonic bath for 10 s. Then 1µl aliquots were added to the *cis* chamber of the bilayer setup. The *cis* chamber was stirred by a magnetic stir bar. When no fusion occurred for 5 min, another aliquot was added. Every 30 minutes, the chamber

solutions and the bilayer were rebuilt. After fusion of an α-syn-induced membrane leak, the electrolytes were changed to the final composition 250 mM KCl, 10 mM Mops/Tris, pH 7 in both chambers.

AFM

After incubation, samples were mixed gently to suspend any aggregates; 5-6 µL aliquots were placed on freshly cleaved mica (muscovite, Veeco Europe, Dourdan Cedex, France) and incubated for 80-90 s, after which mica was warily rinsed twice with 100 µL of filtered, deionized water to remove salt and loosely bound proteins. The micas were dried under dry N_2-gas. Images were obtained with a MultiMode^{TM} SPM (Veeco, Mannheim, Germany) equipped with an E-Scanner and operating in the TappingMode, using etched silicon NanoProbes (model FESP, Veeco Europe, Dourdan Cedex, France). Data were corrected with regard to the sample tip size (Colton *et al.*, 1998). Some typical values were: free oscillation amplitude, 0.8-1.8 V; drive frequency, 65-80 kHz; amplitude setpoint, 300-600 mV and scan rates 0.5-1.4 Hz. The measuring conditions were 39-42 % relative humidity and 21-23 °C.

Thioflavin T fluorescence assays

Thioflavin T (ThT) assay was modified from Munishkina et al. (2003). Briefly, α-syn (1mg/ml) was incubated in 20mM Tris-HCl and 0.1M NaCl, pH 7.4, containing 20µM ThT with ethanol and/or $FeCl_3$ as indicated. The sample volume of 150µl was pipetted into a 96-well-plate (black clear bottom, BD Bioscience) and Teflon coated magnetic stir bars with a diameter of 4mm were added to each well. The sample plate was covered with adhesive aluminium plate sealer and incubated in an Ascent Fluoroscan plate reader at 37°C with shaking at 540rpm. The fluorescence was measured at 15 min intervals with a sampling time of 100ms in the fluorescent plate reader in bottom read mode with excitation at 450nm and emission at 490 nm. Seeding was performed with preformed oligomers added at 10% v/v. Data were measured in duplicates or triplicates and averaged for evaluations.

Compound testing

NBB compounds were obtained from ChemBridge Corp., San Diego, CA. Baicalein was obtained from Fluka. Stock solutions (10mM) were prepared in DMSO. Compound screening was done at a concentration of 10 µM in a total assay volume of 20µL. Aggregation was induced by the addition of 1% DMSO to a mixture of α α-syn monomers

labelled with Alexa 488 or Alexa 647 at a final protein concentration of approximately 10nM in 50mM sodium phosphate at pH 7.0. Compounds were added together with DMSO.

Generation of inducible PC12 cell lines for expression of E46K mutant α-synuclein

Tet-off PC12 cells (Clontech, Palo Alto, CA), stably expressing tTA, were co-transfected with 4 μg of E46K mutant α-syn construct with 0.2 μg pTK-Hyg (Clontech, Palo Alto, CA) plasmid using Lipofectamine Plus (Life Technologies Inc., Gaithersburg, MD). The cells were selected in DMEM (GIBCO) with 5% fetal bovine serum (FBS), 10% horse serum, 100 μg/ml G418, 200 μg/ml hygromycin, 200 ng/ml doxycycline, 100 units/ml penicillin and 100 units/ml streptomycin. After 3-4 weeks of selection at 37°C in a humidified 5% CO2 incubator, G418/hygromycin-resistant colonies were isolated and screened for transgene expression by western blot analysis using an anti α-syn antibody (1:500, BD Pharmingen). We chose line 34 which was highly expressing E46K α-syn and consistent toxicity for this study. Cells were maintained in the presence of doxycycline (200 ng/ml). Expression of the mutant transgene and induction of differentiation were induced by withdrawing doxycycline and adding 50ng/ml NGF to medium at the same time. NGF and doxycyline were replenished every second day after differentiation.

LDH Assay

PC12 cells expressing E46K α-syn were treated with baicalein for six days. Cytotoxicity Detection Kit (Roche) was used for measurement of lactate dehydrogenase (LDH) released into the medium by dead cells. 25μl culture medium was transferred to 96 well plates for LDH assay. The LDH working solution was made freshly according to the manufacture's instructions. 25μl LDH working solution were added into the 25μl culture medium and incubated for 30 min at room temperature. Absorbency was read at 492nm with a plate reader (Molecular Devices Spectra Max 340 PC).

Acknowledgement

This work was supported by the Deutsche Forschungsgemeinschaft (Special Program Grant SFB596-B13 to HK and AG)

REFERENCES

1. Behrends C, Langer CA, Boteva R, Bottcher UM, Stemp MJ, Schaffar G, Rao BV, Giese A, Kretzschmar H, Siegers K, and Hartl FU (2006) Chaperonin TRiC promotes the assembly of polyQ expansion proteins into nontoxic oligomers. *Mol Cell* **23:** 887-897

2. Ben-Shachar D, Eshel G, Finberg JP, and Youdim MB (1991) The iron chelator desferrioxamine (Desferal) retards 6-hydroxydopamine-induced degeneration of nigrostriatal dopamine neurons. *J Neurochem* **56:** 1441-1444

3. Bertsch U, Bieschke J, Weber P, Kretzschmar HA, Giese A, Winklhofer KF, Hartl FU, Tatzelt J, Hirschberger T, and Tavan P (2005) Systematic identification of antiprion drugs by high-throughput screening based on scanning for intensely fluorescent targets. *J Virol* **79:** 7785-7791

4. Bieschke J, Giese A, Schulz-Schaeffer W, Zerr I, Poser S, Eigen M, and Kretzschmar H (2000) Ultrasensitive detection of pathological prion protein aggregates by dual-color scanning for intensely fluorescent targets. *Proc Natl Acad Sci U S A* **97:** 5468-5473

5. Braak H, Del TK, Rub U, de Vos RA, Jansen Steur EN, and Braak E (2003) Staging of brain pathology related to sporadic Parkinson's disease. *Neurobiol Aging* **24:** 197-211

6. Bucciantini M, Calloni G, Chiti F, Stefani M, Formigli L, Nosi D, and Dobson CM (2004) Prefibrillar amyloid protein aggregates share common features of cytotoxicity. *J Biol Chem* **279:** 31374-31382

7. Bucciantini M, Giannoni E, Chiti F, Baroni F, Formigli L, Zurdo J, Taddei N, Ramponi G, Dobson CM, and Stefani M (2002) Inherent toxicity of aggregates implies a common mechanism for protein misfolding diseases. *Nature* **416:** 507-511

8. Capanni C, Taddei N, Gabrielli S, Messori L, Orioli P, Chiti F, Stefani M, and Ramponi G (2004) Investigation of the effects of copper ions on protein aggregation using a model system. *Cell Mol Life Sci* **61:** 982-991

9. Chartier-Harlin MC, Kachergus J, Roumier C, Mouroux V, Douay X, Lincoln S, Levecque C, Larvor L, Andrieux J, Hulihan M, Waucquier N, Defebvre L, Amouyel P, Farrer M, and Destee A (2004) Alpha-synuclein locus duplication as a cause of familial Parkinson's disease. *Lancet* **364:** 1167-1169

10. Cole NB, Murphy DD, Lebowitz J, Di Noto L, Levine RL, and Nussbaum RL (2005) Metal-catalyzed oxidation of alpha-synuclein: helping to define the relationship between oligomers, protofibrils, and filaments. *J Biol Chem* **280:** 9678-9690

11. Colton RJ, Engel A, Frommer JE, Gaub HE, Gewirth A, Guckenberger R, Rabe J, Heckl WM, Parkinson B (1998) *Procedures in scanning probe microscopy.* John Wiley & Sons (Publisher), New York, USA, Weinheim, Germany

12. Connor JR, Snyder BS, Arosio P, Loeffler DA, and LeWitt P (1995) A quantitative analysis of isoferritins in select regions of aged, parkinsonian, and Alzheimer's diseased brains. *J Neurochem* **65:** 717-724

13. Conway KA, Harper JD, and Lansbury PT, Jr. (2000a) Fibrils formed in vitro from alpha-synuclein and two mutant forms linked to Parkinson's disease are typical amyloid. *Biochemistry* **39:** 2552-2563

14. Conway KA, Lee SJ, Rochet JC, Ding TT, Harper JD, Williamson RE, and Lansbury PT, Jr. (2000b) Accelerated oligomerization by Parkinson's disease linked alpha-synuclein mutants. *Ann N Y Acad Sci* **920:** 42-45

15. Conway KA, Lee SJ, Rochet JC, Ding TT, Williamson RE, and Lansbury PT, Jr. (2000c) Acceleration of oligomerization, not fibrillization, is a shared property of both alpha-synuclein mutations linked to early-onset Parkinson's disease: implications for pathogenesis and therapy. *Proc Natl Acad Sci U S A* **97:** 571-576

16. Conway KA, Rochet JC, Bieganski RM, and Lansbury PT, Jr. (2001) Kinetic stabilization of the alpha-synuclein protofibril by a dopamine-alpha-synuclein adduct. *Science* **294:** 1346-1349

17. Costa LT, Kerkmann M, Hartmann G, Endres S, Bisch PM, Heckl WM, and Thalhammer S (2004) Structural studies of oligonucleotides containing G-quadruplex motifs using AFM. *Biochem Biophys Res Commun* **313:** 1065-1072

18. Ding TT, Lee SJ, Rochet JC, and Lansbury PT, Jr. (2002) Annular alpha-synuclein protofibrils are produced when spherical protofibrils are incubated in solution or bound to brain-derived membranes. *Biochemistry* **41:** 10209-10217

19. El Agnaf OM, Paleologou KE, Greer B, Abogrein AM, King JE, Salem SA, Fullwood NJ, Benson FE, Hewitt R, Ford KJ, Martin FL, Harriott P, Cookson MR, and Allsop D (2004) A strategy for designing inhibitors of alpha-synuclein aggregation and toxicity as a novel treatment for Parkinson's disease and related disorders. *FASEB J* **18:** 1315-1317

20. Fink AL (2006) The aggregation and fibrillation of alpha-synuclein. *Acc Chem Res* **39:** 628-634

21. Forman MS, Lee VM, and Trojanowski JQ (2005) Nosology of Parkinson's disease: looking for the way out of a quagmire. *Neuron* **47:** 479-482

22. Giese A, Bader B, Bieschke J, Schaffar G, Odoy S, Kahle PJ, Haass C, and Kretzschmar H (2005) Single particle detection and characterization of synuclein co-aggregation. *Biochem Biophys Res Commun* **333:** 1202-1210

23. Giese A, Bieschke J, Eigen M, and Kretzschmar HA (2000) Putting prions into focus: application of single molecule detection to the diagnosis of prion diseases. *Arch Virol Suppl* 16: 161-171

24. Giese A, Levin J, Bertsch U, and Kretzschmar H (2004) Effect of metal ions on de novo aggregation of full-length prion protein. *Biochem Biophys Res Commun* **320:** 1240-1246

25. Glabe CG (2006) Common mechanisms of amyloid oligomer pathogenesis in degenerative disease. *Neurobiol Aging* **27:** 570-575

26. Goedert M (2001) Alpha-synuclein and neurodegenerative diseases. *Nat Rev Neurosci* **2:** 492-501

27 Goldberg MS and Lansbury PT, Jr. (2000) Is there a cause-and-effect relationship between alpha-synuclein fibrillization and Parkinson's disease? *Nat Cell Biol* **2:** E115-E119

28. Gorell JM, Johnson CC, Rybicki BA, Peterson EL, Kortsha GX, Brown GG, and Richardson RJ (1997) Occupational exposures to metals as risk factors for Parkinson's disease. *Neurology* **48:** 650-658

29. Gosavi N, Lee HJ, Lee JS, Patel S, and Lee SJ (2002) Golgi fragmentation occurs in the cells with prefibrillar alpha-synuclein aggregates and precedes the formation of fibrillar inclusion. *J Biol Chem* **277:** 48984-48992

30. Gotz ME, Double K, Gerlach M, Youdim MB, and Riederer P (2004) The relevance of iron in the pathogenesis of Parkinson's disease. *Ann N Y Acad Sci* **1012:** 193-208

31. Hasegawa T, Matsuzaki M, Takeda A, Kikuchi A, Akita H, Perry G, Smith MA, and Itoyama Y (2004) Accelerated alpha-synuclein aggregation after differentiation of SH-SY5Y neuroblastoma cells. *Brain Res* **1013:** 51-59

32. Hill K, Model K, Ryan MT, Dietmeier K, Martin F, Wagner R, and Pfanner N (1998) Tom40 forms the hydrophilic channel of the mitochondrial import pore for preproteins. Nature **395:** 516-521

33. Hinnah SC, Wagner R, Sveshnikova N, Harrer R, and Soll J (2002) The chloroplast protein import channel Toc75: pore properties and interaction with transit peptides. *Biophys J* **83:** 899-911

34. Hoyer W, Antony T, Cherny D, Heim G, Jovin TM, and Subramaniam V (2002) Dependence of alpha-synuclein aggregate morphology on solution conditions. *J Mol Biol* **322:** 383-393

35. Ibanez P, Bonnet AM, Debarges B, Lohmann E, Tison F, Pollak P, Agid Y, Durr A, and Brice PA (2004) Causal relation between alpha-synuclein gene duplication and familial Parkinson's disease. *The Lancet* **364:** 1169-1171

36. Irizarry MC, Growdon W, Gomez-Isla T, Newell K, Hyman BT, George JM, and Clayton DF (1998) Nigral and cortical Lewy bodies and dystrophic nigral neurites in Parkinson's disease and cortical Lewy body disease contain alpha-synuclein immunoreactivity. *J Neuropathol Exp Neurol* **57:** 334-337

37. Kask P, Palo K, Fay N, Brand L, Mets U, Ullmann D, Jungmann J, Pschorr J, and Gall K (2000) Two-dimensional fluorescence intensity distribution analysis: theory and applications. *Biophys J* **78:** 1703-1713

38. Kask P, Palo K, Ullmann D, and Gall K (1999) Fluorescence-intensity distribution analysis and its application in biomolecular detection technology. *Proc Natl Acad Sci U S A* **96:** 13756-13761

39. Kaur D, Yantiri F, Rajagopalan S, Kumar J, Mo JQ, Boonplueang R, Viswanath V, Jacobs R, Yang L, Beal MF, DiMonte D, Volitaskis I, Ellerby L, Cherny RA, Bush AI, and Andersen JK (2003) Genetic or pharmacological iron chelation prevents MPTP-induced neurotoxicity in vivo: a novel therapy for Parkinson's disease. *Neuron* **37:** 899-909

40. Kayed R, Edmonds B, Milton SC, Glabe CG, Sokolov Y, Hall JE, and McIntire TM (2004) Permeabilization of lipid bilayers is a common conformation-dependent activity of soluble amyloid oligomers in protein misfolding diseases. *J Biol Chem* **279:** 46363-46366

41. Kayed R, Head E, Thompson JL, McIntire TM, Milton SC, Cotman CW, and Glabe CG (2003) Common structure of soluble amyloid oligomers implies common mechanism of pathogenesis. *Science* **300:** 486-489

42. Koo EH, Lansbury PT, Jr., and Kelly JW (1999) Amyloid diseases: abnormal protein aggregation in neurodegeneration. *Proc Natl Acad Sci U S A* **96:** 9989-9990

43. Kruger R, Kuhn W, Muller T, Woitalla D, Graeber M, Kosel S, Przuntek H, Epplen JT, Schols L, and Riess O (1998) Ala30Pro mutation in the gene encoding alpha-synuclein in Parkinson's disease. *Nat Genet* **18:** 106-108

44. Lashuel HA, Petre BM, Wall J, Simon M, Nowak RJ, Walz T, and Lansbury PT, Jr. (2002) Alpha-synuclein, especially the Parkinson's disease-associated mutants, forms pore-like annular and tubular protofibrils. *J Mol Biol* **322:** 1089-1102

45. Levin J, Bertsch U, Kretzschmar H, and Giese A (2005) Single particle analysis of manganese-induced prion protein aggregates. *Biochem Biophys Res Commun* **329:** 1200-1207

46. Lindersson E, Beedholm R, Hojrup P, Moos T, Gai W, Hendil KB, and Jensen PH (2004) Proteasomal inhibition by alpha-synuclein filaments and oligomers. *J Biol Chem* **279:** 12924-12934

47. Lindersson E, Lundvig D, Petersen C, Madsen P, Nyengaard JR, Hojrup P, Moos T, Otzen D, Gai WP, Blumbergs PC, and Jensen PH (2005) p25alpha stimulates alpha-synuclein aggregation and is co-localized with aggregated alpha-synuclein in alpha-synucleinopathies. *J Biol Chem* **280:** 5703-5715

48. Lowe R, Pountney DL, Jensen PH, Gai WP, and Voelcker NH (2004) Calcium(II) selectively induces alpha-synuclein annular oligomers via interaction with the C-terminal domain. *Protein Sci* **13:** 3245-3252

49. Matsuzaki M, Hasegawa T, Takeda A, Kikuchi A, Furukawa K, Kato Y, and Itoyama Y (2004) Histochemical features of stress-induced aggregates in alpha-synuclein overexpressing cells. *Brain Res* **1004:** 83-90

50. Meuser D, Splitt H, Wagner R, and Schrempf H (1999) Exploring the open pore of the potassium channel from Streptomyces lividans. *FEBS Lett* **462:** 447-452

51. Muchowski PJ (2002) Protein misfolding, amyloid formation, and neurodegeneration: a critical role for molecular chaperones? *Neuron* **35:** 9-12

52. Munishkina LA, Henriques J, Uversky VN, and Fink AL (2004) Role of protein-water interactions and electrostatics in alpha-synuclein fibril formation. *Biochemistry* **43:** 3289-3300

53. Munishkina LA, Phelan C, Uversky VN, and Fink AL (2003) Conformational behavior and aggregation of alpha-synuclein in organic solvents: modeling the effects of membranes. *Biochemistry* **42:** 2720-2730

54. Niles WD, and Cohen FS (1987) Video fluorescence microscopy studies of phospholipid vesicle fusion with a planar phospholipid membrane. Nature of membrane-membrane interactions and detection of release of contents. *J Gen Physiol* **90:** 703-735

55. Nuscher B, Kamp F, Mehnert T, Odoy S, Haass C, Kahle PJ, and Beyer K (2004) Alpha-synuclein has a high affinity for packing defects in a bilayer membrane: a thermodynamics study. *J Biol Chem* **279:** 21966-21975

56. Ostrerova-Golts N, Petrucelli L, Hardy J, Lee JM, Farer M, and Wolozin B (2000) The A53T alpha-synuclein mutation increases iron-dependent aggregation and toxicity. *J Neurosci* **20:** 6048-6054

57. Paik SR, Shin HJ, Lee JH, Chang CS, and Kim J (1999) Copper(II)-induced self-oligomerization of alpha-synuclein. *Biochem J* **340:** 821-828

58. Piening N, Weber P, Hogen T, Beekes M, Kretzschmar H, Giese A (2006) Photo-induced crosslinking of prion protein oligomers and prions. Amyloid 13: 67-77

59. Polymeropoulos MH, Lavedan C, Leroy E, Ide SE, Dehejia A, Dutra A, Pike B, Root H, Rubenstein J, Boyer R, Stenroos ES, Chandrasekharappa S, Athanassiadou A, Papapetropoulos T, Johnson WG, Lazzarini AM, Duvoisin RC, Di IG, Golbe LI, and Nussbaum RL (1997) Mutation in the alpha-synuclein gene identified in families with Parkinson's disease. *Science* **276:** 2045-2047

60. Post K, Pitschke M, Schafer O, Wille H, Appel TR, Kirsch D, Mehlhorn I, Serban H, Prusiner SB, and Riesner D (1998) Rapid acquisition of beta-sheet structure in the prion protein prior to multimer formation. *Biol Chem* **379:** 1307-1317

61. Pountney DL, Voelcker NH, and Gai WP (2005) Annular alpha-synuclein oligomers are potentially toxic agents in alpha-synucleinopathy. Hypothesis. *Neurotox Res* **7:** 59-67

62. Quist A, Doudevski I, Lin H, Azimova R, Ng D, Frangione B, Kagan B, Ghiso J, and Lal R (2005) Amyloid ion channels: a common structural link for protein-misfolding disease. *Proc Natl Acad Sci U S A* **102:** 10427-10432

63. Rochet JC, Outeiro TF, Conway KA, Ding TT, Volles MJ, Lashuel HA, Bieganski RM, Lindquist SL, and Lansbury PT (2004) Interactions Among alpha-Synuclein, Dopamine, and Biomembranes: Some Clues for Understanding Neurodegeneration in Parkinson's Disease. *J Mol Neurosci* **23:** 23-34

64. Romer W and Steinem C (2004) Impedance analysis and single-channel recordings on nano-black lipid membranes based on porous alumina. *Biophys J* **86:** 955-965

65. Rybicki BA, Johnson CC, Uman J, and Gorell JM (1993) Parkinson's disease mortality and the industrial use of heavy metals in Michigan. *Mov Disord* **8:** 87-92:

66. Sanchez I, Mahlke C, and Yuan J (2003) Pivotal role of oligomerization in expanded polyglutamine neurodegenerative disorders. *Nature* **421:** 373-379

67. Schiffer NW, Broadley SA, Hirschberger T, Tavan P, Kretzschmar HA, Giese A, Haass C, Hartl FU, and Schmid B (2007) Identification of anti-prion compounds as efficient inhibitors of polyglutamine protein aggregation in a zebrafish model. *J Biol Chem* **282**: 9195-9203

68. Schwille P, Bieschke J, and Oehlenschlager F (1997a) Kinetic investigations by fluorescence correlation spectroscopy: the analytical and diagnostic potential of diffusion studies. *Biophys Chem* **66:** 211-228

69. Schwille P, Meyer-Almes FJ, and Rigler R (1997b) Dual-color fluorescence cross-correlation spectroscopy for multicomponent diffusional analysis in solution. *Biophys J* **72:** 1878-1886

70. Singleton AB, Farrer M, Johnson J, Singleton A, Hague S, Kachergus J, Hulihan M, Peuralinna T, Dutra A, Nussbaum R, Lincoln S, Crawley A, Hanson M, Maraganore D, Adler C, Cookson MR, Muenter M, Baptista M, Miller D, Blancato J, Hardy J, and Gwinn-Hardy K (2003) alpha-Synuclein locus triplication causes Parkinson's disease. *Science* **302:** 841

71. Smith WW, Jiang H, Pei Z, Tanaka Y, Morita H, Sawa A, Dawson VL, Dawson TM, and Ross CA (2005b) Endoplasmic reticulum stress and mitochondrial cell death pathways mediate A53T mutant alpha-synuclein-induced toxicity. *Hum Mol Genet* **14:** 3801-3811

72. Spillantini MG, Schmidt ML, Lee VMY, Trojanowski JQ, Jakes R, and Goedert M (1997) alpha-synuclein in Lewy bodies. *Nature* **388:** 839-840

73. Tanaka Y, Engelender S, Igarashi S, Rao RK, Wanner T, Tanzi RE, Sawa A, Dawson L, Dawson TM, and Ross CA (2001) Inducible expression of mutant alpha-synuclein decreases proteasome activity and increases sensitivity to mitochondria-dependent apoptosis. *Hum Mol Genet* **10:** 919-926

74. Uversky VN, Li J, and Fink AL (2001a) Evidence for a partially folded intermediate in alpha-synuclein fibril formation. *J Biol Chem* **276:** 10737-10744

75. Uversky VN, Li J, and Fink AL (2001b) Metal-triggered structural transformations, aggregation, and fibrillation of human alpha-synuclein. A possible molecular NK between Parkinson's disease and heavy metal exposure. *J Biol Chem* **276:** 44284-44296

76. Volles MJ and Lansbury PT, Jr. (2002) Vesicle permeabilization by protofibrillar alpha-synuclein is sensitive to Parkinson's disease-linked mutations and occurs by a pore-like mechanism. *Biochemistry* **41:** 4595-4602

77. Volles MJ, Lee SJ, Rochet JC, Shtilerman MD, Ding TT, Kessler JC, and Lansbury PT, Jr. (2001) Vesicle permeabilization by protofibrillar alpha-synuclein: implications for the pathogenesis and treatment of Parkinson's disease. *Biochemistry* **40:** 7812-7819

78. Wood SJ, Wypych J, Steavenson S, Louis JC, Citron M, and Biere AL (1999) alpha-synuclein fibrillogenesis is nucleation-dependent. Implications for the pathogenesis of Parkinson's disease. *J Biol Chem* **274:** 19509-19512

79. Woodbury DJ, and Hall JE (1988) Role of channels in the fusion of vesicles with a planar bilayer. *Biophys J* **54:** 1053-1063

80. Yamin G, Glaser CB, Uversky VN, and Fink AL (2003) Certain metals trigger fibrillation of methionine-oxidized alpha-synuclein. *J Biol Chem* **278:** 27630-27635

81. Zarranz JJ, Alegre J, Gomez-Esteban JC, Lezcano E, Ros R, Ampuero I, Vidal L, Hoenicka J, Rodriguez O, Atares B, Llorens V, Gomez TE, del Ser T, Munoz DG, and de Yebenes JG (2004) The new mutation, E46K, of alpha-synuclein causes Parkinson and Lewy body dementia. *Ann Neurol* **55:** 164-173

82. Zayed J, Ducic S, Campanella G, Panisset JC, Andre P, Masson H, and Roy M (1990) Environmental factors in the etiology of Parkinson's disease. *Can J Neurol Sci* **17:** 286-291

83. Zecca L, Zucca FA, Wilms H, and Sulzer D (2003) Neuromelanin of the substantia nigra: a neuronal black hole with protective and toxic characteristics. *Trends Neurosci* **26:** 578-580

84. Zhang X, Xie W, Qu S, Pan T, Wang X, and Le W (2005) Neuroprotection by iron chelator against proteasome inhibitor-induced nigral degeneration. *Biochem Biophys Res Commun* **333:** 544-549

85. Zhu M, Rajamani S, Kaylor J, Han S, Zhou F, and Fink AL (2004) The flavonoid baicalein inhibits fibrillation of alpha-synuclein and disaggregates existing fibrils. *J Biol Chem* **279:** 26846-26857

86. Zimmerberg J, Cohen FS, and Finkelstein A (1980) Micromolar Ca^{2+} stimulates fusion of lipid vesicles with planar bilayers containing a calcium-binding protein. Science **210:** 906-908

Figure Legends

Figure 1:

Ethanol induces oligomer formation of α-syn. A) Time course of oligomer formation was monitored by cross-correlation amplitude [G(0)] in a mixture of α-syn labeled with Alexa488 and α-syn labeled with Alexa647 in samples containing 5% ethanol (filled triangles), without ethanol (empty diamonds), and in the presence of 0.01% NP40 (empty squares) in non-scanned measurements. B) Normalized auto-correlation curves from the same experiment obtained after 4 hours of incubation show an increase in diffusion time (τ_{Diff}) in the presence of ethanol indicating oligomer formation. C) Formation of small oligomers is also evident in the 2D intensity distribution histograms obtained in the same experiment. D) Effect of different concentrations of ethanol and inhibitory effect of 0.01% NP40 and 0.01% BSA on the aggregation of α-syn. Shown is the mean + SEM of the cross-correlation amplitude in scanned measurements after > 3.5 hours of incubation from 12-17 independent determinations.

Figure 2:

Effect of Fe^{3+} and other metal ions on α-syn oligomerization. A) Aggregation was monitored by cross-correlation amplitude [G(0)] in a mixture of α-syn labeled with Alexa488 and α-syn labeled with Alexa647 in samples containing either no ethanol (empty bars), or 20% ethanol (black bars) in the presence of 5μM $FeCl_3$, $AlCl_3$, $CaCl_2$, $CuCl_2$, or $MnCl_2$, respectively, and in controls. Data were obtained after approximately 4 h of aggregation in triplicate measurements. Shown is the mean + SEM. The corresponding 2D intensity distribution histograms are provided in the supplement (Fig. S2). B) 2D intensity distribution histograms obtained in an independent experiment show that the synergistic action of ethanol and Fe^{3+} results in the formation of much larger aggregates than found with ethanol. Notably, Fe^{3+} alone does not induce aggregate formation. A detailed quantitative SIFT- and FIDA analysis of aggregate concentration and brightness is provided in the supplement (Table S1). C) Different concentrations of ethanol and Fe^{3+} were tested systematically in the presence and absence of 0.1% Np40 and 0.01% BSA, respectively. A synergistic effect on α-syn aggregation was found only in intermediate concentrations of ethanol. This effect was blocked both by NP40 and by BSA. Shown is the median of the cross-correlation amplitude [G(0)] in scanned measurements after > 3.5 hours of incubation for 5 (control), 2 (NP40), and 3 (BSA) independent experiments, respectively.

Figure 3:

AFM analysis of α-syn oligomers. A) Representative AFM image of a 2 x 2 µm scan in the height mode showing typical oligomers after incubation of 50 nM α-syn for 4 h at room temperature in the presence of 20% ethanol. The color-bar represents the height of the particle. B) AFM image obtained from a parallel incubation in the presence of 20% ethanol and 20µM $FeCl_3$. C) Quantitatve analysis of oligomer size distribution for labeled α-syn (hatched bars) and non-labeled α-syn (black bars) (mean + SD, n=20). The corresponding data regarding particle height and diameter are provided in the supplement (Table S2).

Figure 4:

Ethanol-induced α-syn oligomers are on pathway to amyloid fibrils. A) Aggregation of unlabelled α-syn (1mg/ml) was monitored at 37°C for 20 h in a Thioflavin T assay in the presence of 0% ethanol (empty diamonds), 20% ethanol (filled triangles) and 20% ethanol / 100µM Fe^{3+} (filled circles), respectively. Incubation was performed in a 96 well plate stirred with Teflon coated magnetic stir bars. Both 20% ethanol and 20% ethanol/100 µM Fe^{3+} accelerate amyloid formation. B) Seeding of amyloid formation by preformed intermediate I and intermediate II aggregates. Aggregation was performed in a 96 well plate stirred with a Teflon coated magnetic stir bar with unlabelled α-syn (1mg/ml) at 37°C. In control reactions containing 10% ethanol (filled squares) and 10% ethanol / 10µM $FeCl_3$ (filled diamonds), respectively, only slow formation of ThT-positive aggregates can be seen. Seeded aggregation was induced at t=0 with 10% (v/v) of α-syn pre-aggregated using the same buffer conditions, i.e. 10% ethanol (black crosses) and 10% ethanol / 10µM $FeCl_3$ (empty triangles). Shown is the mean of triplicate measurements.

Figure 5:

Electrophysiological analysis of poreforming ability of α-syn oligomers in the planar lipid bilayer system. A) Typical current-potential curve obtained in 250/20 mM KCl shows a reversal potential of approximately -20 mV. B) The distribution of conductance states obtained for different fusion events indicates the presence of a smallest unit pore with a conductivity of about 50pS in 250 mM KCl.

Figure 6:

N´-benzyliden-benzohydrazide (NBB) compounds and baicalein inhibit α-syn aggregation. A) Aggregation was induced in a mixture of α-syn labeled with Alexa488 and Alexa647, respectively, by 1% DMSO. The NBB-compound 10293G02 and baicalein at a concentration of 10 µM were capable of inhibiting α-syn aggregation. Shown are 2D intensity distribution histograms obtained after 4h of incubation in scanned measurements. B) Eight NBB derivatives were tested at final concentration of 10 µM in regard to inhibition of α-syn aggregation. The presence of two hydroxyl groups at the benzohydrazide ring correlates with activity. C) PC12 cells expressing E46K mutant α-syn were cultured in doxycyxline (Dox) containing medium. Mutant α-syn was induced by withdrawal of Dox and cell differentiation was induced by adding of NGF to the medium. Cells were induced and treated with baicalein at 10µM-3nM or a positive control compound (z-VAD at 50µM) for six days. LDH activity in the medium was measured by Cytotoxicity Detection Kit. The results are expressed as mean ± S.D. $p < 0.01$ compared with the value of the Dox(-) group (ANOVA with Scheffè post hoc tests).

Table 1:

Pore formation by α-syn aggregates. Aggregation mixtures as indicated were incubated for 3 h in the presence of preformed liposomes. Then, aliquots of 1µl of the reaction mixture were added to the *cis* chamber directly below the bilayer to induce membrane fusion. N indicates the total number of applications performed. Changes in the electrical conductivity of the membrane were monitored. Pore formation in the bilayer was reproducibly observed at a success-rate of 12-15% only for samples containing α-syn + 20% ethanol + 20 µM $FeCl_3$.

Table 2:

Inhibition of α-syn pore formation by the oligomer-specific antibody A11 and by the anti-synuclein antibody asy1. Experiments were performed as described in table 1. Aggregation of α-syn was induced by 20% ethanol + 20µM $FeCl_3$.

Figure 1

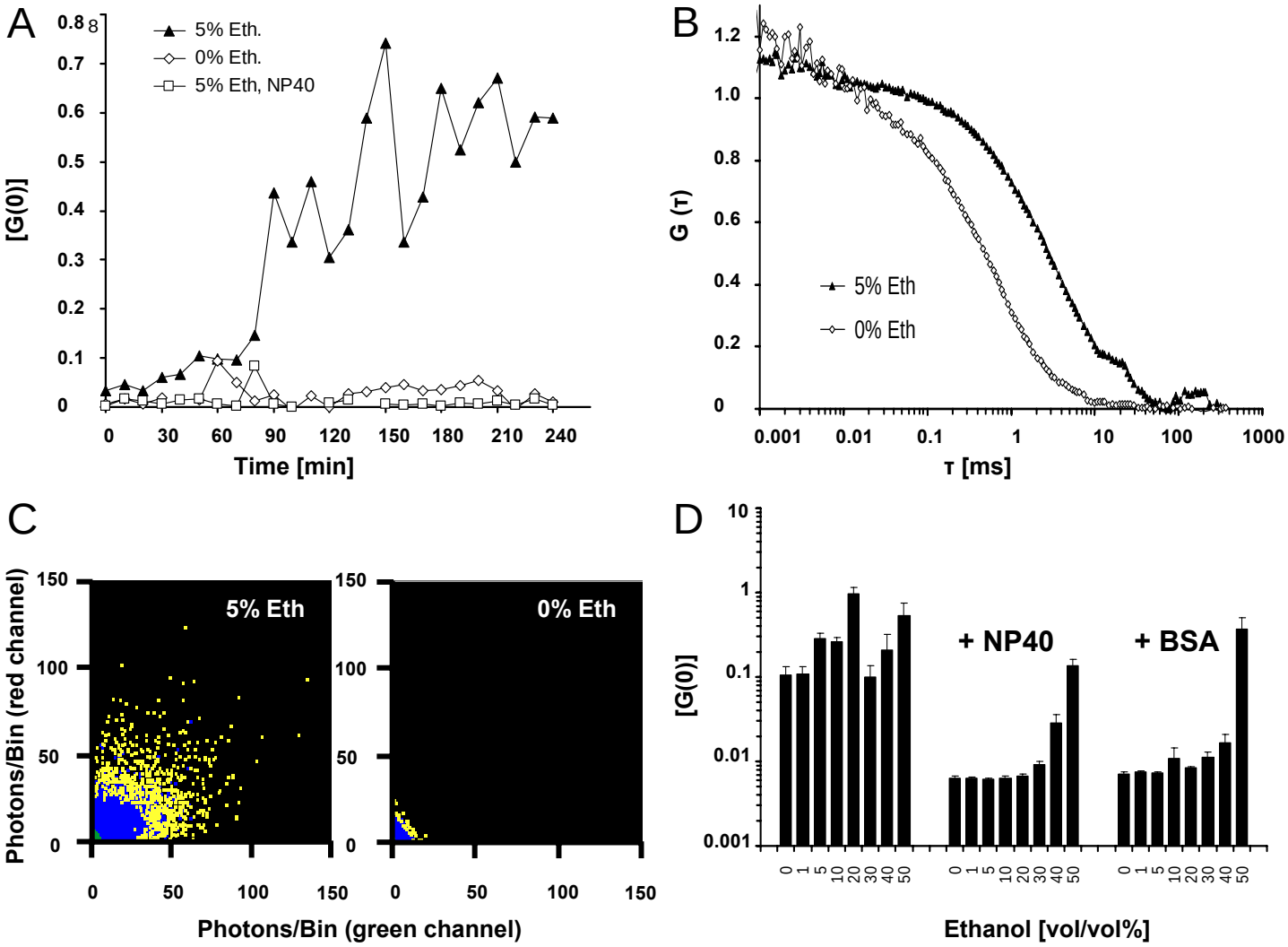
A
5% Eth.
0% Eth.
5% Eth, NP40
[G(0)]
Time [min]
B
G (τ)
5% Eth
0% Eth
τ [ms]
C
5% Eth
0% Eth
Photons/Bin (red channel)
Photons/Bin (green channel)
D
+ NP40
+ BSA
[G(0)]
Ethanol [vol/vol%]

Figure 2

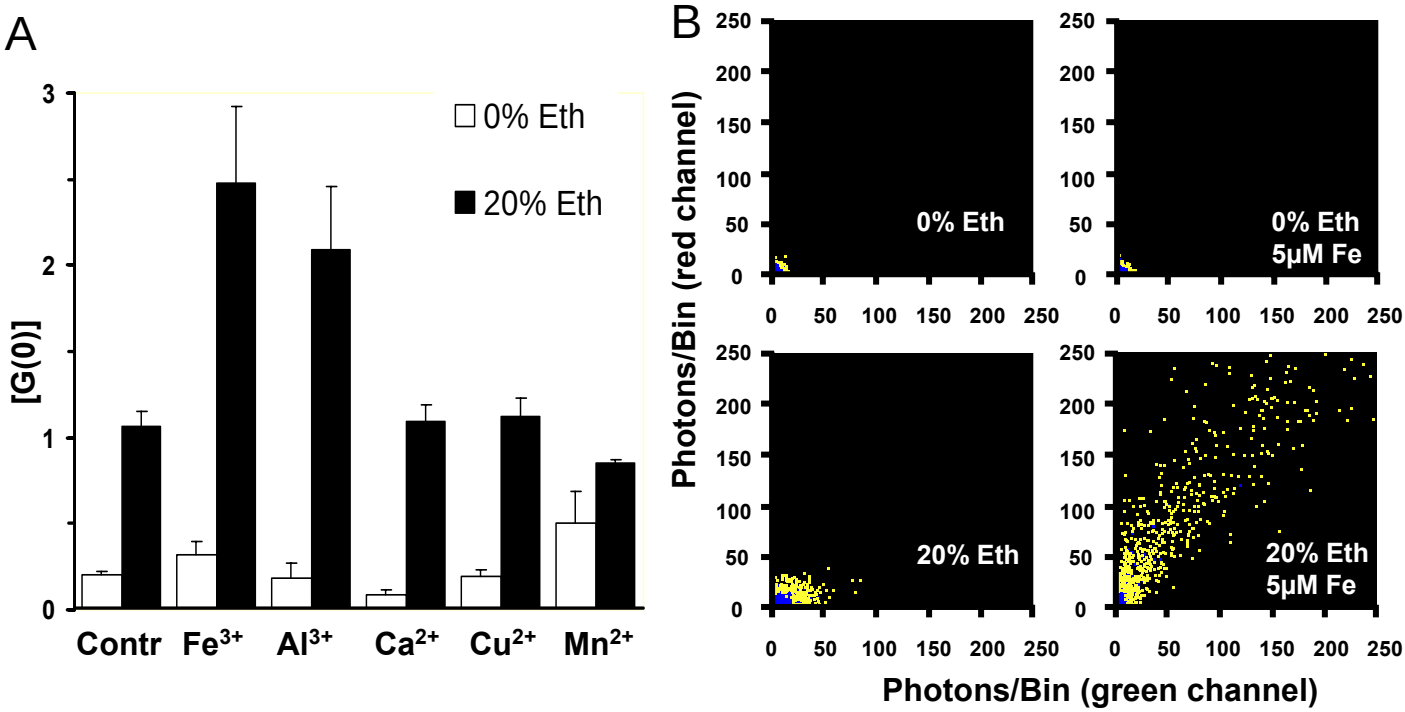
A
[G(0)]
0% Eth
20% Eth
Contr
Fe3+
Al3+
Ca2+
Cu2+
Mn2+
B
Photons/Bin (red channel)
Photons/Bin (green channel)
0% Eth
0% Eth 5µM Fe
20% Eth
20% Eth 5µM Fe

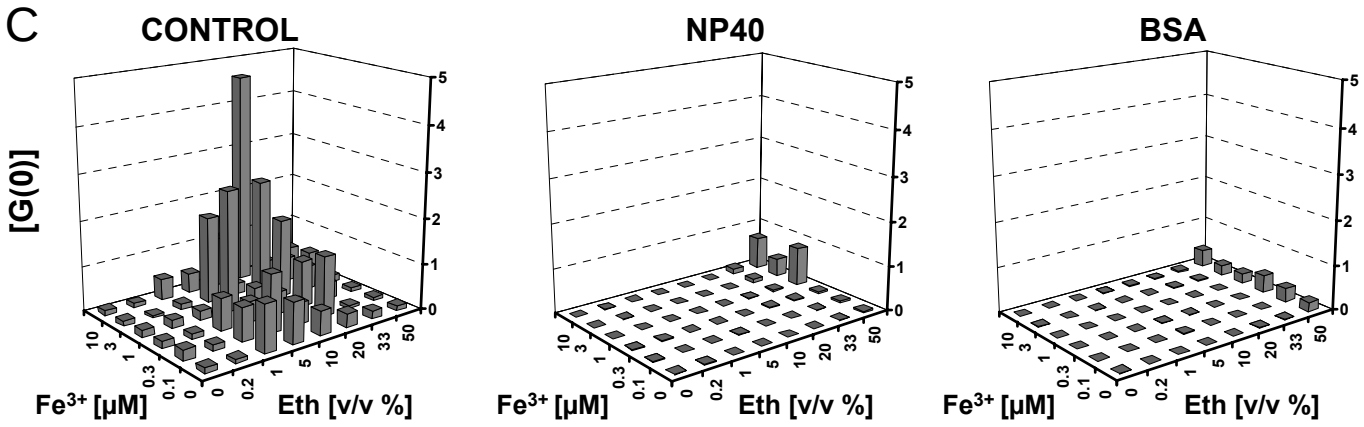
C
CONTROL
NP40
BSA
[G(0)]
Fe3+ [µM]
Eth [v/v %]

Figure 3

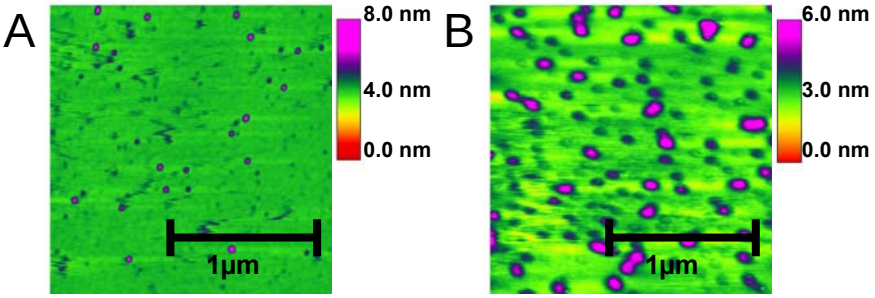
A
8.0 nm
4.0 nm
0.0 nm
1µm
B
6.0 nm
3.0 nm
0.0 nm
1µm

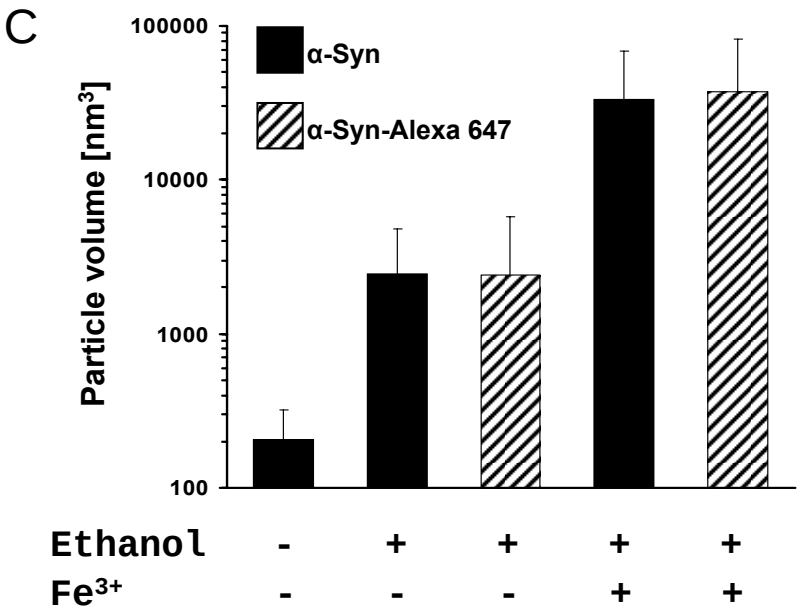
C
Particle volume [nm³]
100000
10000
1000
100
α-Syn
α-Syn-Alexa 647
Ethanol - + + + +
Fe3+ - - - + +

Figure 4

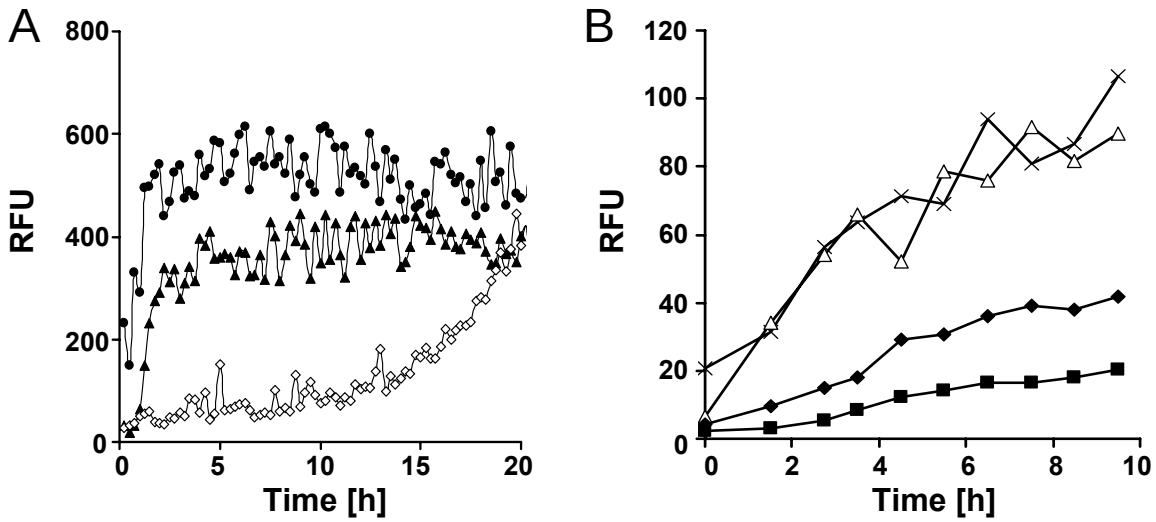
A
800
600
400
200
0
RFU
0
5
10
15
20
Time [h]
B
120
100
80
60
40
20
0
RFU
0
2
4
6
8
10
Time [h]

Figure 5

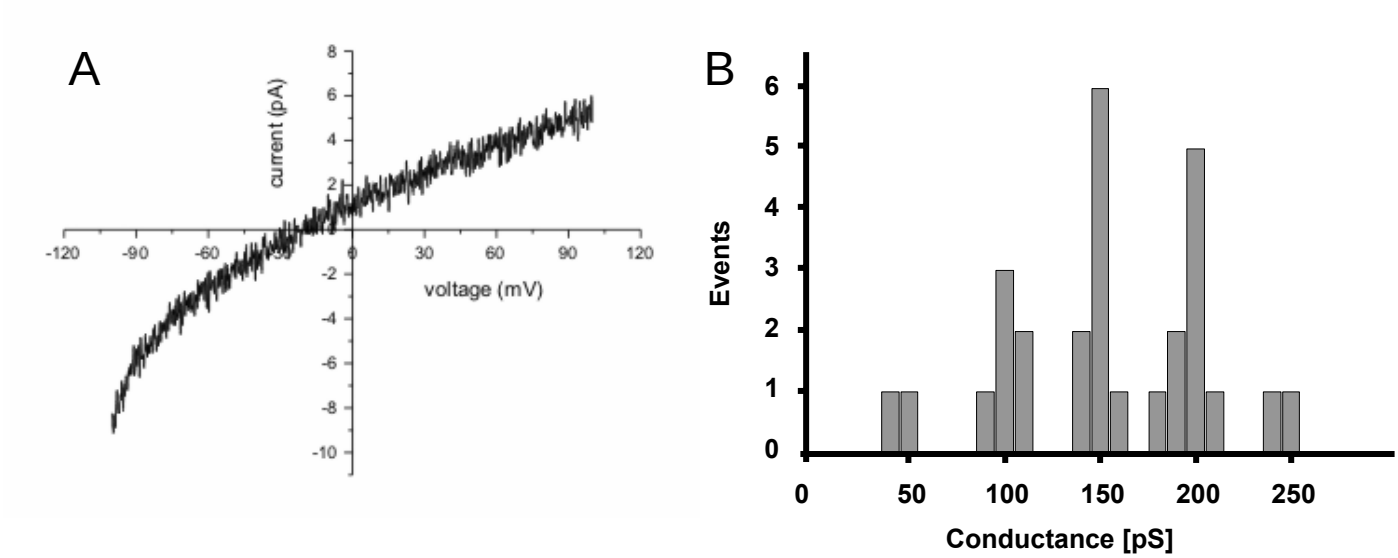
A
current (pA)
voltage (mV)
8
6
4
2
-2
-4
-6
-8
-10
-120
-90
-60
30
60
90
120
B
Events
0
1
2
3
4
5
6
0
50
100
150
200
250
Conductance [pS]

Figure 6

A

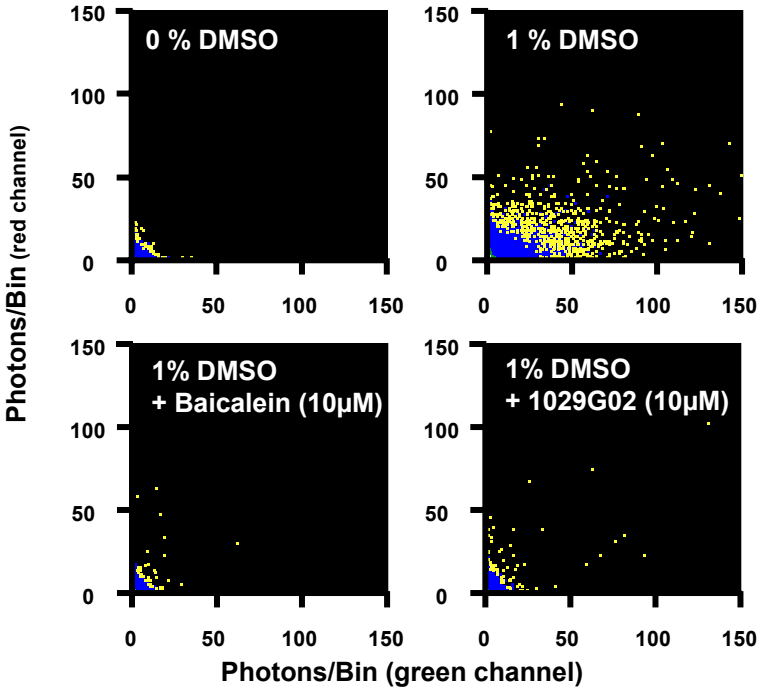

B Structure – Activity

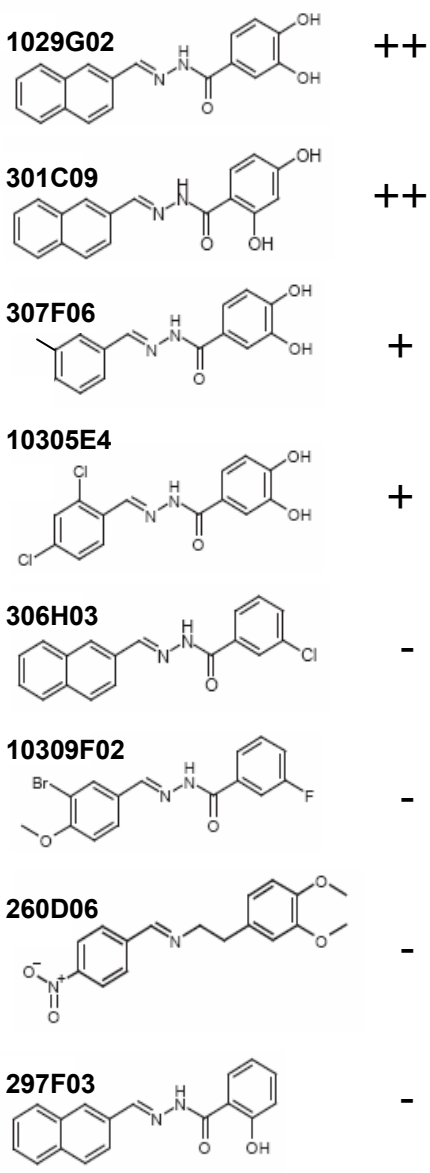

C

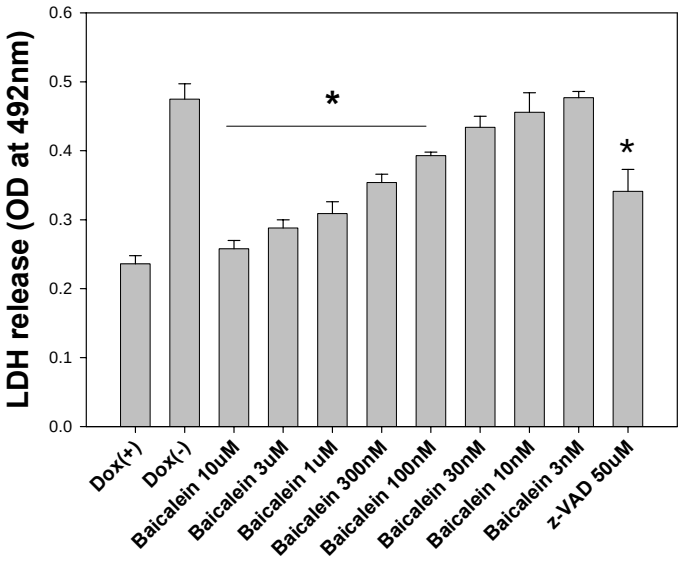

Table 1

Synuclein	**Synuclein-Alexa 488**	**Ethanol**	**20 µM $FeCl_3$**	**BSA**	**Fusion success-rate [%]**	**N**
-	-	-	-	-	0	42
+	-	-	-	-	0	42
-	+	-	-	-	0	42
-	-	up to 40%	-	-	0	42
-	-	-	+	-	0	42
-	-	-	-	+	0	42
+	-	20%	-	-	0	42
+	-	5%	+	-	0	42
+	-	20%	+	-	15	162
-	+	20%	+	-	12	84
+	-	20%	+	+	0	42

Table 2

	Fusion success-rate [%]	**N**
Synuclein	14	42
Synuclein + A11	0	42
Synuclein-Alexa488 + A11	0	42
Synuclein + asy1	0	42
Synuclein + 6E10	12	42

Figure S1

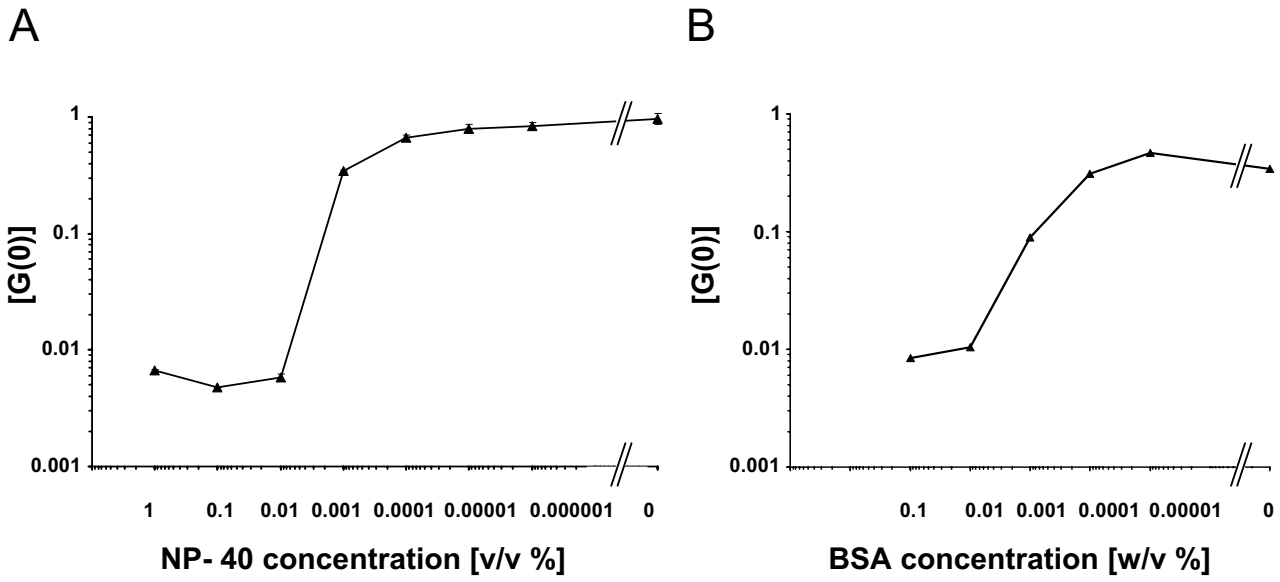

Figure S1:

Dose-response curve of the inhibition of α-syn oligomer formation by NP40 (A) and by BSA (B), respectively. Aggregation was monitored in a mixture of α-syn labeled with Alexa488 and α-syn labeled with Alexa647 in samples containing 20% ethanol in the presence of different concentrations of NP40 and BSA, respectively. Shown is the mean of triplicate measurements ± SEM of the cross-correlation amplitude [G(0)] in scanned measurements after 3-4 hours of incubation.

Figure S2

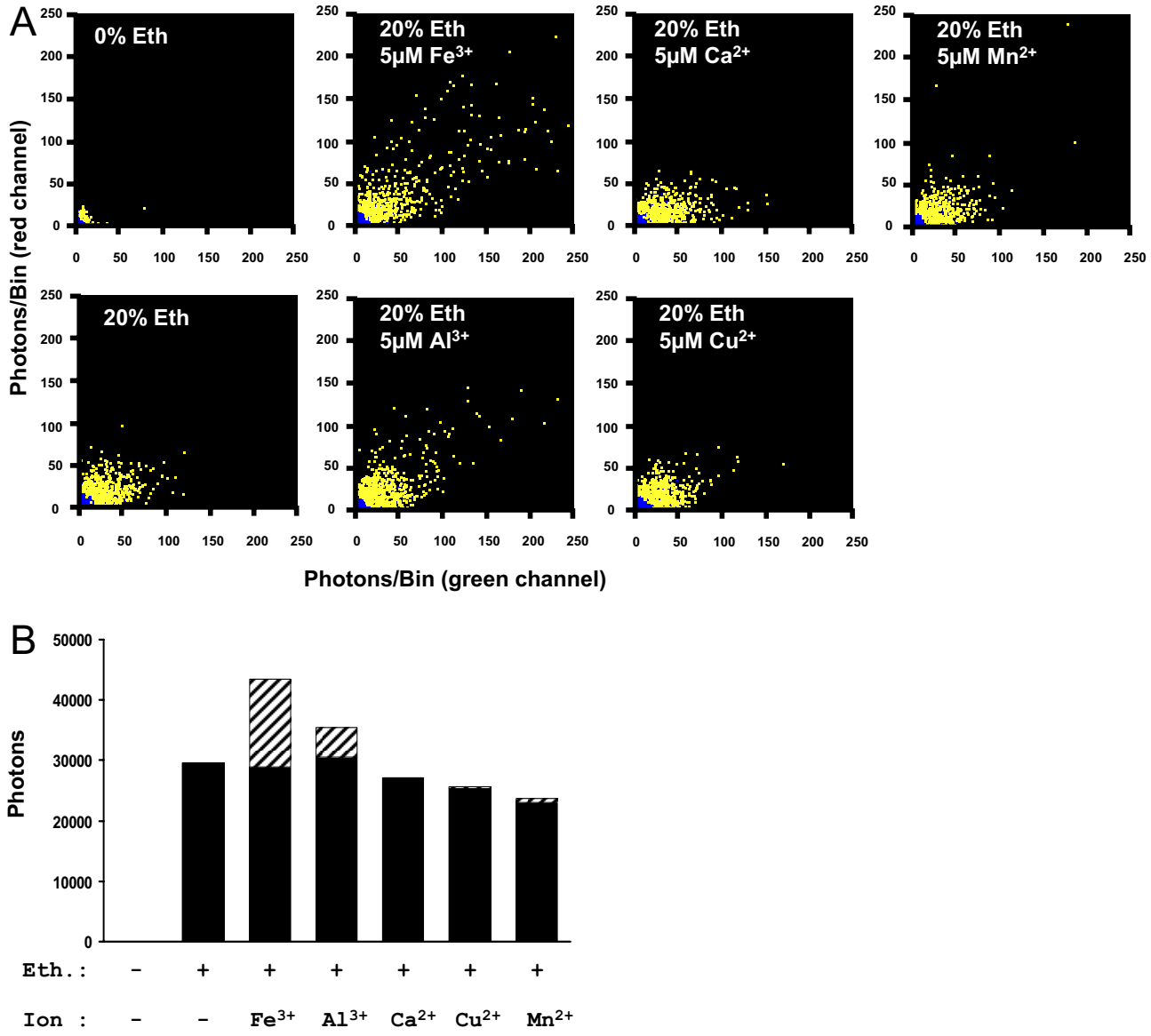

Figure S2:
Effect of Fe^{3+} and other metal ions on α-syn oligomerization. A) 2D intensity distribution histograms correspond to the experiment shown in Fig. 2A. Aggregation was analysed by SIFT measurements in a mixture of α-syn labeled with Alexa488 and α-syn labeled with Alexa647 in samples containing either no ethanol, 20% ethanol, or 20% ethanol plus $FeCl_3$, $AlCl_3$, $CaCl_2$, $CuCl_2$, and $MnCl_2$, respectively. Data were obtained after approximately 4 h of incubation. B) Quantitative SIFT analysis of the data shown in A of the fluorescent photon count obtained with threshold settings for either intermediate I (black bars) or intermediate II (hatched bars). Threshold settings for intermediate I: 20/20 < x < 150/110, and for intermediate II: x > 150/110.

Figure S3

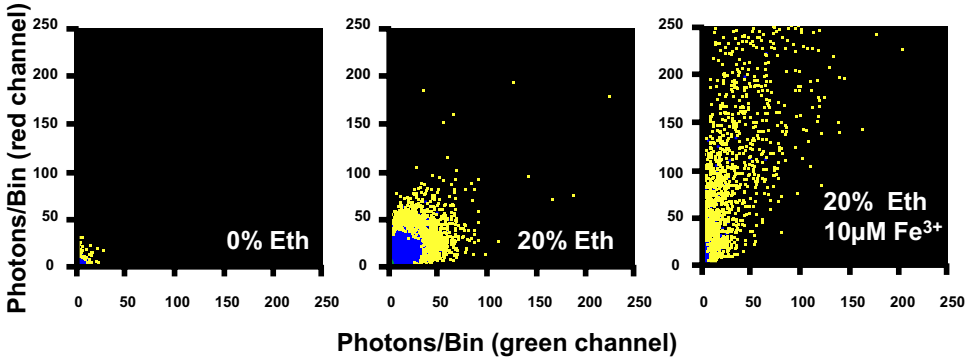

Figure S3:

Use of Tris buffer instead of sodium phosphate buffer. Aggregation of α-syn was performed in 50mM Tris buffer, pH 7.0 containing a mixture of α-syn monomers labeled with either Alexa488 or Alexa647 in presence of 0% ethanol, 20% ethanol or 20% ethanol / 10µM $FeCl_3$, respectively. Shown are 2D intensity distribution histograms obtained in scanned measurements after 4 h of incubation. Similar to the results obtained in sodium phosphate buffer (Fig. 2) the synergistic action of ethanol and Fe^{3+} results in the formation of much larger aggregates than found with ethanol alone.

Figure S4

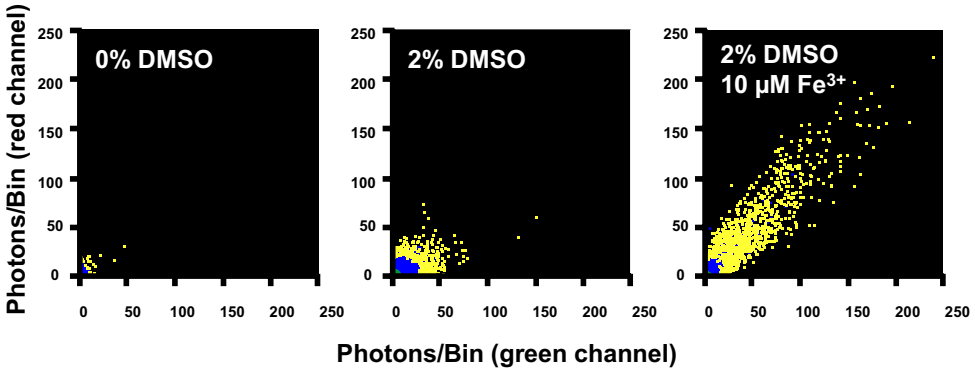

Figure S4:

Use of DMSO instead of ethanol for induction of aggregation. A mixture of α-syn labeled with Alexa488 and α-syn labeled with Alexa647 was aggregated in 50mM Tris buffer containing either no DMSO, 2% DMSO or 2% DMSO / 10µM $FeCl_3$, respectively. Shown are 2D intensity distribution histograms obtained in scanned measurements after 4 h of incubation. Results obtained with DMSO are similar to the data obtained in the ethanol dependent aggregation assay (cf. Fig 2, Fig S3).

Figure S5

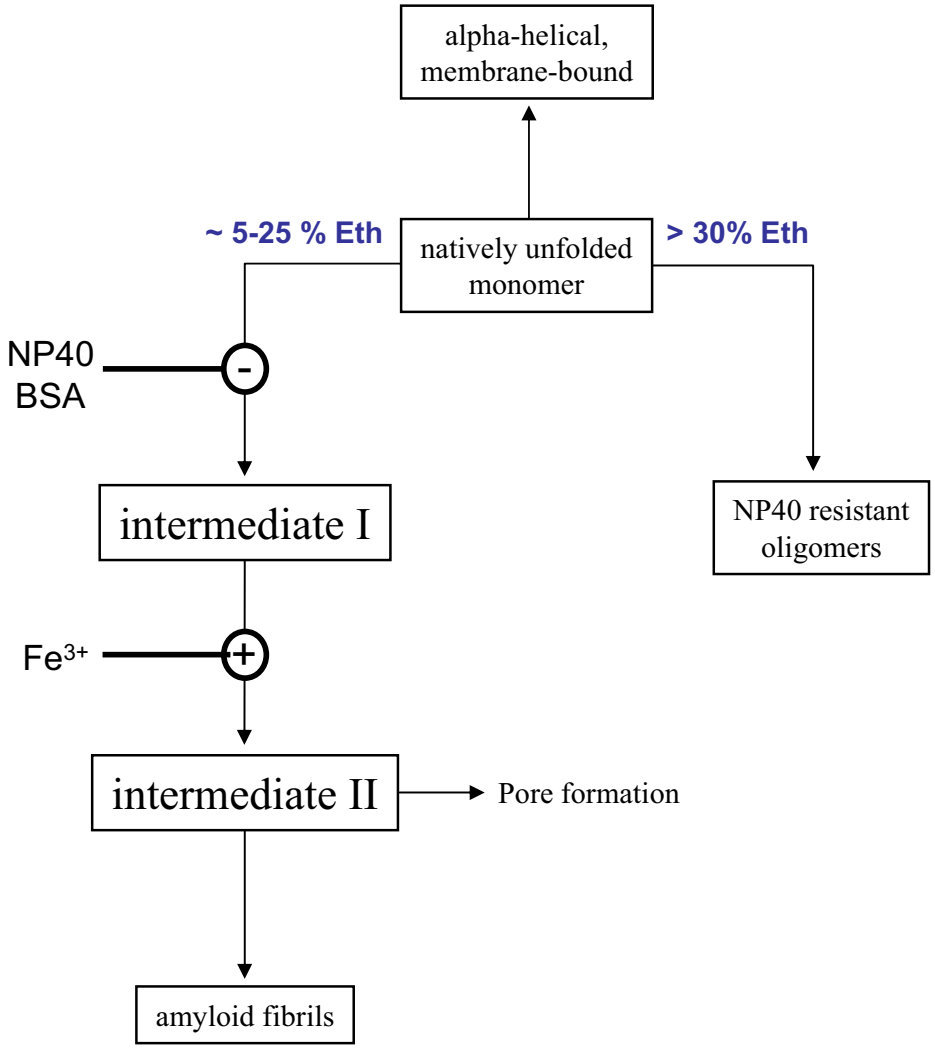

Figure S5:

Schematic representation of aggregation pathways of α-syn.

Table S1

Channel 1	Condition	C1	Q1 (kHz)	C2	Q2 (kHz)
1kfit	0 Eth	0.32	29.72	-	-
	0 Eth 5µM Fe^{3+}	0.40	29.72	-	-
2kfit	20 Eth	0.39	29.72	0.0054	259.69
	20 Eth 5µM Fe^{3+}	0.53	29.72	0.00051	2484.54

Channel 2	Condition	C1	Q1 (kHz)	C2	Q2 (kHz)
1kfit	0 Eth	0.59	23.27	-	-
	0 Eth 5µM Fe^{3+}	0.61	23.27	-	-
2kfit	20 Eth	0.81	23.27	0.0091	161.11
	20 Eth 5µM Fe^{3+}	0.85	23.27	0.00094	2358.98

Table S1:

Detailed quantitative FIDA analysis of aggregate concentration and brightness for the experiment shown in Figure 2B. Channel 1 provides the results for α-syn labeled with Alexa488 (=”green”), channel 2 provides the results for α-syn labeled with Alexa647 (=”red”). Brightness (Q1) and concentration (C1) of α-syn monomers were obtained from control measurements containing neither ethanol nor Fe^{3+}. These data were used for 2-component FIDA analysis in samples containing aggregates (aggregate brightness: Q2, aggregate concentration: C2). All data represent the mean of three independent measurements after 4h of incubation.

Table S2

			Ø Diameter [nm]	Ø Height [nm]	Volume [nm^3]
Syn	0 Eth	- Fe^{3+}	13.3	1.4	206
Syn	20 Eth	- Fe^{3+}	34.3	2.1	2460
Syn-Alexa 647	20 Eth	- Fe^{3+}	27.7	2.7	2418
Syn	20 Eth	+ Fe^{3+}	70.1	6.4	33214
Syn-Alexa 647	20 Eth	+ Fe^{3+}	91.9	3.7	37504

Table S2:

AFM data were obtained after incubation of 50 nM α-syn for 4 h at room temperature in the presence of 0%, 20% ethanol, and 20% ethanol / 20µM $FeCl_3$, respectively. Shown is the mean of measurements for n = 20 particles. For volume calculation, a cylindrical shape was assumed.

ï»¿

Different species of alpha synuclein oligomers induce calcium influx and seeding

Journal:	*Journal of Neuroscience*
Manuscript ID:	JN-RM-2617-07
Manuscript Type:	Regular Manuscript
Manuscript Section:	Neurobiology of Disease
Date Submitted by the Author:	08-Jun-2007

Complete List of Authors:	Danzer, Karin; Boehringer Ingelheim Pharma GmbH & Co KG, CNS researchHaasen, Dorothea; Boehringer Ingelheim Pharma GmbH & Co KG, Integrated Drug DiscoveryKarow, Anne; Boehringer Ingelheim Pharma GmbH & Co KG, CNS ResearchMoussaud, Simon; Boehringer Ingelheim Pharma GmbH & Co KG, CNS researchHabeck, Matthias; Ludwig-Maximilians Universität München, Zentrum für Neuropathologie und PrionforschungGiese, Armin; Ludwig-Maximilians Universität München, Zentrum für Neuropathologie und PrionforschungKretzschmar, Hans; Ludwig Maximilians University, Centre for NeuropathologyHengerer, Bastian; Boehringer Ingelheim Pharma GmbH & Co KG, CNS ResearchKostka, Marcus; Boehringer Ingelheim Pharma GmbH & Co KG, CNS Research
Keywords:	alpha synuclein, oligomers, pore-formation, neurodegeneration, Parkinson's disease, Toxicity
Themes & Topics:	t. Parkinson-s disease: Other <
Note: The following files were submitted by the to PDF. You must view these files (e.g. movies)	author for peer review, but cannot be converted online.
Supplemental_movie_1_.mpg Supplemental_movie_2_.mpg	

Neurobiology of Disease

Different species of alpha synuclein oligomers induce calcium influx and seeding

Karin M. Danzer[1], Dorothea Haasen[2], Anne R. Karow[1], Simon Moussaud[1], Matthias Habeck[3], Armin Giese[3], Hans Kretzschmar[3], Bastian Hengerer[1] and Marcus Kostka[1]

[1]CNS Research Boehringer Ingelheim Pharma GmbH & Co KG, 88397 Biberach, Germany

[2]Integrated Drug Discovery, Boehringer Ingelheim Pharma GmbH & Co KG, 88397 Biberach, Germany

[3]Zentrum für Neuropathologie und Prionforschung, Ludwig-Maximilians Universität München, Germany

Corresponding authors:

Karin Danzer

Boehringer Ingelheim Pharma GmbH & Co KG

CNS Research

Birkendorferstr. 65

88397 Biberach, Germany

Phone: ++49-7351-54-94041

Fax: ++49-7351-54-98928

Email: Karin.Danzer@bc.boehringer-ingelheim.com

Marcus Kostka

Boehringer Ingelheim Pharma GmbH & Co KG

Birkendorferstr. 65

88397 Biberach, Germany

Phone/Fax: ++49-7351-54-5415

Email: Marcus.Kostka@bc.boehringer-ingelheim.com

Keywords:

Parkinsons Disease, neurodegeneration, α-synuclein, pore-formation, oligomers, toxicity

Acknowledgements:

The authors are grateful to P. Kahle and C. Haass for providing α-syn plasmids and to F. Gillardon for suggestions concerning the manuscript. We also thank S. Eder for exquisite technical support for calcium measurements. The excellent technical assistance of P. Anding, S. Finger, W. Lemmer and M. Palchauchdhuri is gratefully acknowledged.

10 figures; 5 supplemental figures; 1 table; 45 pages

Abbreviated title: Different effects of α-synuclein oligomers

α-synuclein (α-syn); Parkinsons Disease (PD); fluorescence intensity distribution analysis (FIDA); atomic force microspcopy (AFM); Fluorescence Correlation Spectroscopy (FCS); room temperature (RT); standard error of mean (SEM); wildtype (wt)

Abstract:

Aggregation of α-synuclein (α-syn) has been linked to the pathogenesis of Parkinsons Disease (PD) and other neurodegenerative diseases. Increasing evidence suggests that prefibrillar oligomers and protofibrils, rather than mature fibrils of α-syn, are the pathogenic species in PD. Despite extensive effort on studying oligomerisation of α-syn, no studies have compared different oligomer species directly on a single particle level and investigated their biological effects on cells. In this study we applied a novel highly sensitive single molecule detection system that allowed a direct comparison of different oligomer types. Furthermore, we studied biological effects of different oligomer types on cells. For this purpose, we developed new oligomerisation protocols, that enabled the use of these different oligomers in cell culture.

We found that all of our three aggregation protocols resulted in heterogeneous populations of oligomers. Some types of oligomers induced cell death via disruption of cellular ion homeostasis by a presumably pore-forming mechanism. Other oligomer types could directly enter the cell resulting in increased α-syn aggregation. Based on our results we propose that under various physiological conditions heterogeneous populations of oligomeric forms will co-exist in an equilibrium. These different oligomer types lead directly or indirectly to cell damage. Our data indicate that inhibition of early α-syn aggregation events would consequently prevent all α-syn oligomer related toxicities. This has important implications for the development of disease modifying drugs for the treatment of PD and other synucleinopathies.

Introduction

Parkinson's disease (PD) is pathologically characterized by a selective loss of dopaminergic neurons in the substantia nigra and aggregated protein deposits termed Lewy bodies (Dauer and Przedborski, 2003). The main component of these intracellular deposits is aggregated alpha synuclein (α-syn) (Goedert, 2001). Gene multiplication in the α-syn gene (Singleton et al., 2003; Chartier-Harlin et al., 2004) and missense mutations (Polymeropoulos et al., 1997; Kruger et al., 1998; Zarranz et al., 2004) are linked to familial forms of PD. This supports the importance of α-syn in the pathogenesis of PD.

In vitro studies revealed that α-syn aggregation is a nucleation dependent process that occurs in a process ranging from monomer via oligomers to fibrils (Wood et al., 1999; Conway et al., 2000).

There is a growing body of evidence suggesting that the prefibrillar oligomers and protofibrils, rather than mature fibrils of α-syn, are the pathogenic species (Conway et al., 2000; Masliah et al., 2000; Goldberg and Lansbury, Jr., 2000; Gosavi et al., 2002; Auluck et al., 2002; Bucciantini et al., 2002; Park and Lansbury, Jr., 2003; Kayed et al., 2003; Bucciantini et al., 2004; Kayed et al., 2004; Bodner et al., 2006; El-Agnaf et al., 2006).

To date there are several protocols on oligomer preparation existing (Kayed et al., 2003; Lashuel and Grillo-Bosch, 2005). Whether these methods end up in the same type of oligomers is currently not clear. If and how oligomers differ structurally from each other on a single particle level, is not known. More importantly, biological effects of different types of oligomers on cells have not been studied directly. More importantly, the question arises if different types of oligomers induce different biological effects on cells.

To address these questions we developed novel standardized methods of α-syn oligomer generation and compared the samples directly on a single particle level. We applied fluorescence intensity distribution analysis (FIDA) (Kask et al., 1999; Kask et al., 2000; Zemanova et al., 2004; Levin et al., 2005) in a confocal single molecule detection system and compared our results with the fluorescence independent method atomic force microspcopy (AFM).

We exposed these differently generated oligomers to cells, to investigate, whether different types of oligomers have various biological effects on cells. We examined their respective actions on cytosolic calcium levels and their ability to seed intracellular aggregation of α-syn in SH-SY5Y cells and primary neurons. This study aims to elucidate the biological effects which might also occur in patients with PD or other synucleinopathies. The identification of pathologically relevant α-syn oligomer species forms therefore the basis for the identification of structural targets for anti-aggregatory compounds that will be of great importance to prevent these amyloidogenic diseases.

Materials and methods

Materials

All chemicals used were purchased from Sigma Aldrich, Inc., Munich, Germany unless stated otherwise.

Expression and Purification of Recombinant Wild-type α-syn

Expression and purification was preformed as Nuscher et al. (2004) previously described. Briefly, pET-5a/α–syn wt plasmid (a kind gift of Christian Haas and Philipp Kahle, LMU Munich, Germany) was used to transform Escherichia coli BL21(DE3) pLysS (Novagen, Madison, WI, USA). Expression was induced with isopropyl-ß-D-

thiogalactopyranose (Promega, Mannheim, Germany) for 4 h. Cells were harvested, resuspended in 20 mM Tris and 25 mM NaCl, pH 8.0 and lysed by freezing in liquid nitrogen followed by thawing. After 30 min of boiling, the lysate was centrifuged at 17600 g for 15 min at 4°C. Supernatant was filtered through 0,22 µm filter (Millex-GV, Millipore Corp., Bedford, MA, USA) before loaded onto a HiTrap Q HP column (5 ml, Amersham Biosciences, Munich, Germany) and eluted with a 25 mM to 500 mM NaCl salt gradient. The pooled α-syn peak passed over a Superdex 200 HR10/30 size exclusion column (Amersham Biosciences, Munich, Germany) using 20mM Tris, 25mM NaCl, pH 8,0 as running buffer. The pooled α-syn peak was concentrated using Vivaspin columns MWCO 5kD (Vivascience, Stonehouse, UK) and equilibrated to water. The protein concentration was determined using a BCA protein quantification kit (Pierce, Rockford, IL, USA). Aliquots were lyophilized and stored at -80°C.

Fluorescent labelling of α-syn

Protein labelling with the amino-reactive fluorescent dye Alexa Fluor-488-O-succinimidylester [Alexa488] (Molecular Probes, Inc., Eugene, USA) was performed according to the manufacturer's manual. Unbound fluorophores were separated by filtration steps in PD10 columns (Sephadex G25, Amersham Biosciences, Munich, Germany) equilibrated with 50 mM sodium phosphate pH 7.0. Quality control of labelled α-syn was performed by mass spectrometry and by Fluorescence Correlation Spectroscopy (FCS) measurements on an Insight Reader (Evotec-Technologies,Hamburg, Germany). The typical labelling ratio, was approximately 2 dye molecules per α-syn molecule. In order to remove preformed aggregates, the

stock solution of labelled α-syn was subjected to size exclusion chromatography (Sephadex 200, Amersham Biosciences, Munich, Germany).

Preparation of α-syn oligomers

a) Long incubation protocol (type A1 and A2)

Oligomers type A were prepared by dissolving lyophilized protein in 50 mM sodium phosphate buffer (pH 7.0) containing 20% ethanol to a final concentration of 7 µM. In case of oligomers type A2,10 µM of $FeCl_3$ (J.T. Baker, Griesheim, Germany) were additionally added, whereas oligomers type A1 were prepared without addition of $FeCl_3$. After 4h of shaking (GFL GmbH, Burgwedel, Germany), both types of oligomers were re-lyophilized and resuspended with a half of starting volume in 50 mM sodium phosphate buffer (pH 7.0) containing 10% ethanol. This was followed by shaking for 24h (stage 5, eppendorf thermomixer 5436, Wesseling-Berzdorf, Germany) at room temperature (RT) with open lids to evaporate residual ethanol. After 6 days incubation of both oligomers types at RT with closed lids, oligomers were used for characterisation studies, e.g. calcium influx and toxicity experiments. Alexa Fluor-488-O-succinimidylester labelled oligomers were prepared in the same manner as non-labelled oligomers by using Alexa-488 conjugated monomers.

b) Stirring incubation protocol (type B1 and B2)

Oligomers type B were prepared similar to oligomers type A by dissolving lyophilized protein in 50 mM sodium phosphate buffer (pH 7.0) containing 20% ethanol to a final concentration of 7 µM. In case of oligomers type B2,10 µM of $FeCl_3$ were additionally added, whereas oligomers type B1 were prepared without addition of $FeCl_3$. After 4h of shaking (GFL GmbH, Burgwedel, Germany) both oligomer types were re-lyophilized and resuspended with a half of starting volume of 50 mM sodium

phosphate buffer (pH 7.0) containing 10% ethanol. Additionally, after this procedure oligomers were stirred (RCT basic IKA Labortechnik, Staufen, Germany) with open lids using Teflon-coated microstirr bar (Fisherbrand, Pittsburgh, PA, USA) for 24h at RT. Alexa488 labelled oligomers were prepared in the same manner as non labelled oligomers by using Alexa488 fluorescent monomer.

a) Spin concentration protocol (type C1 and C2)

Oligomers type C were also prepared similar to oligomers type A by dissolving lyophilized protein in 50 mM sodium phosphate buffer (pH 7.0) containing 20% ethanol to a final concentration of 7 µM. In case of oligomers type C2,10 µM of $FeCl_3$ were additionally added, whereas oligomers type C1 were prepared without addition of $FeCl_3$. After overnight incubation at room temperature under continuously shaking (GFL GmbH, Burgwedel, Germany), oligomers were concentrated using ultracentrifugation (VivaSpin 500 columns, Vivascience, Germany). The oligomers were separated from monomer using a MWCO 30 kDa cut off filter. The oligomers were retained, while the monomeric protein passed through the filter as verified by FCS. Alexa-488 labelled oligomers were prepared in the same manner as non labelled oligomers by using Alexa-488 conjugated monomers.

Atomic Force Microscopy (AFM)

Sample preparation for AFM was carried out at RT. Typically 3-6 µl of different oligomers diluted in corresponding buffers to a working concentration of 1 µM were applied to a freshly cleaved muscovite mica substrate (Ted Pella, Redding, CA, USA) and incubated for 1min. The mica surface was then rinsed with 7x 200 µl double processed tissue culture water (Sigma Aldrich, Steinheim, Germany) to remove salts and loosely bound proteins. AFM-images were recorded on a MultiModeTM SPM

(Digital Instruments, Santa Barbara, CA, USA) equipped with an E-Scanner using etched silicon NanoProbes (model RTESP; Veeco Instruments, Mannheim, Germany). All measurements were carried out in the tapping mode with scan rates around 0.5 Hz. Images were processed using NanoScope software (Digital Instruments, Santa Barbara, CA, USA).

Confocal single particle analysis

FIDA measurements were carried out on an Insight Reader (Evotec-Technologies, Germany) with dual-colour excitation at 488nm and 633nm, using a 40x 1.2 NA microscope objective (Olympus, Japan) and a pinhole diameter of 70 µm at FIDA setting. Excitation power was 200 µW at 488 nm. Measurement time was 10 sec. Scanning parameters were set to 100 µm scan path length, 50 Hz beamscanner frequency, and 2000 µm positioning table movement. This is equivalent to approximately 10 mm/s scanning speed. All measurements were performed at RT. The fluorescence signal was analysed by FIDA using FCSPP Evaluation software version 2.0 (Evotec-Technologies, Germany). Fluorescence from the fluorophore Alexa-488 was recorded with a single photon detector. Photons were summed over time intervals of constant length (bins) using a bin length of 40 µs (Kask et al., 1999; Kask et al., 2000). Based on previous results the obtained data was analyzed by a 3-component-fit with two components fixed to a particle brightness Q of 20 and 50, respectively. For threshold setting, non-aggregated reference samples were used. This single molecule detection technology allows highly sensitive analysis of protein aggregation by slight changes in brightness of individual particles. FIDA is able to distinguish between differently bright species and as such gives indirect information about particle sizes.

Cell culture

SH-SY5Y human dopaminergic neuroblastoma cells were maintained at 37°C in 5% CO_2 in high glucose Dulbecco's modifed Eagle's medium (PAA Laboratories GmbH, Pasching, Austria) supplemented with 15% foetal bovine serum (Invitrogen GmbH, Karlsruhe, Germany) and 4 mM glutamine (Invitrogen GmbH, Karlsruhe, Germany).

To generate stable cell lines, SH-SY5Y cells were transfected using Metafectene (Cambio Ltd, Cambridge, U.K.) with pcDNA 3.1neo encoding α-syn[wt], α-syn[A30P] or α-syn[A53T] (plasmids were a kind gift of C. Haas and P. Kahle, LMU Munich, Germany). As mock vector controls, SH-SY5Y cells were transfected with plasmid pUHD15.1 encoding the transactivator protein for the tetracycline inducible expression system (Clontech, Saint-Germain-en-Laye, France). Mock transfected cells served as cells with endogenous level of α-syn.

Transfected cells were selected with 1000 µg/ml G418 (PAA Laboratories GmbH, Pasching, Austria) for 2–3 weeks until colonies emerged. Stable transfectants established from these colonies were tested for their α-syn expression levels using immunofluorescence and western blot analyses.

Cortical cell culture

Neuron-enriched cerebral cortical cells were prepared from embryonic brains (E14) of mice. Cortices were dissected from embryonic brain and the meninges was removed. The cells were dissociated by trypsinization and tituration. The dissociated cells were resuspended in serum free B27/neurobasal medium (Gibco-BRL, Invitrogen GmbH, Karlsruhe, Germany) and plated at a density of 1.25×10^5 cells / cm^2 on dishes pre-coated with Poly-D-Lysin/Laminin. Cells were maintained at 37°C in the presence of 10% CO_2/ 90% air in a humidified incubator. Medium was changed every third day.

Measurement of intracellular Ca2+

a) fluorescence imaging with fluorescent imaging plate reader (FLIPR)

For intracellular Ca2+ measurements using FLIPR primary cortical neurons were seeded at a density of 1.25 x 10^5 cells / cm^2 on 384-well black clear bottom microtiter plates (BD Biosciences, Heidelberg, Germany) pre-coated with Poly-D-Lysin/Laminin and cultured as described above. After 7 days cortical neurons were used for Ca2+ measurements. Mock transfected SH-SY5Y cells and α-syn[wt], [A30P] or [A53T] mutants were seeded into Collagen I coated 384-well black clear bottom microtiter plates (BD Biosciences, Heidelberg, Germany) at a density of 6000cells/well and cultured overnight. At the day of experiment cells were washed with Ringer buffer (130 mM NaCl, 5 mM KCl, 1 mM $CaCl_2$, 1 mM $MgCl_2$, 2 mM KH_2PO_4, 5 mM glucose, 20 mM HEPES) and loaded for 60 min with 2 µM of the cell-permeable Fluo-4 AM (Teflabs, Austin, TX, USA) in Ringer buffer containing 0.1% (w/v) pluronic acid F127 (Molecular Probes Inc., Eugene, USA). After removal of the fluorophore loading solution, cell layers were washed with Ringer buffer, incubated at room temperature for 30 min and washed again. The cell plates were then loaded into a fluorescence imaging plate reader (FLIPR TETRA TM, Molecular Devices, Wokingham, UK) together with a separate 384-well plate containing oligomers and controls. Treatment of cells was carried out with the following final concentrations: 7 µM oligomer type A1 and A2 (referring to moles of monomer starting concentration), 500 µg/ml Gramicidin D and 1.5 µM ionomycin as positive controls. Test compounds were distributed in a randomized pattern to minimize any cell plating effects due to well position. The fluorescence imaging plate reader (FLIPR) was programmed to transfer the test compounds and solvents simultaneously to all 384 wells 10 sec after commencement of recording of fluorescence (expressed as relative fluorescence units [RFU]). Fluorescence was excited at 488 nm and emission was measured at 510–560 nm.

Duration of recording was 10 min. Data are displayed as negative control corrected values, meaning signal response to oligomers including subtraction of corresponding solvent controls. The resulting signals were quantified by taking the maximum peak height of recording duration using Screenworks 1.2.0.73 software and are expressed as mean +/- SEM. Treatment effects were analyzed by unpaired t-test for each cell line. For the SH-SY5Y cell lines p-values were additionally adjusted for multiple testing using the Bonferroni-correction method. P-values less than 5% were considered as statistically significant. Differences (Δ) between treated and untreated cell lines were quantified by differences of mean values and corresponding 95% confidence intervals (CI). All cell lines were separately analyzed. For investigation of calcium source, calcium was omitted from Ringer buffer and experiments were performed as described above. To demonstrate a calcium ion channel independent effect of oligomers, 20 µM cobalt, a non-specific calcium channel blocker, was applied to cells 5 min before application of oligomers. Experimental setup was the same as described above.

b) fluorescence imaging with confocal microscopy

SH-SY5Y cells overexpressing α-syn[wt] were seeded into collagen I coated 96-well black µ-clear bottom microtiter plates (Greiner bio-one, Frickenhausen, Germany) at a density of 7500 cells/well and cultured overnight. Cortical neurons were seeded at a density of 6 x 10^4 cells / cm^2 on a 96-well black µ-clear bottom microtiter plates (Greiner bio-one, Frickenhausen, Germany)plate pre-coated with Poly-D-Lysin/Laminin and cultured as described above. After 7 days cortical neurons were used for Ca2+ measurements.

Cells were washed with Ringer buffer (130 mM NaCl, 5 mM KCl, 1 mM CaCl2, 1 mM MgCl2, 2 mM KH2PO4, 5 mM glucose, 20 mM HEPES) and loaded with 2 µM of the

cell-permeable Fluo-4 AM (Teflabs, Austin, TX, USA) in Ringer buffer containing 0.1 % (w/v) pluronic acid (Molecular Probes Inc., Eugene, USA) at 37°C for 60 min. After removal of the fluorophore loading solution, the cells were washed with Ringer buffer, incubated at room temperature for 30 min and washed again. The imaging system consisted of an inverted confocal microscope (Leica DM IRBE, Leica Mycrosystems GmbH, Wetzlar, Germany) equipped with a Leica 63x objective. Fluorescence excitation was performed with a 488 nm argon ion laser and emitted fluorescence (505nm<λ<530nm) was imaged by a scan head (Leica TCS SP, Leica Mycrosystems GmbH, Wetzlar, Germany). Time lapse pictures (1 frame per 2.5 sec) were captured using the Leica Confocal software package (Leica Mycrosystems GmbH, Wetzlar, Germany) and fluorescence intensities were measured from regions of interest centred on individual cells. Signals were expressed in relative fluorescence units (BU). Treatment of cells was carried out with the following final concentrations: 7µM monomer, 7µM oligomer type A1 and A2 (referring to moles of monomer starting concentration) and 6 µM ionomycin as a positive control. Treatments were applied by pipetting a fixed aliquot of 50 µl into the recorded well directly above the objective. Duration of recording was 150 sec or 300 sec. The 10-fold accelerated time lapse videos were made using windows movie maker software (microsoft).

Measurement of membrane potential changes using FLIPR

Primary cortical neurons were seeded at a density of 1.25 x 10^5 cells / cm^2 on 384-well black clear bottom microtiter plates (BD Biosciences, Heidelberg, Germany) pre-coated with Poly-D-Lysin/Laminin and cultured as described above. After 7 days cortical neurons were used for measurements of membrane potential. FLIPR membrane potential assay kit was performed according to manufacturers instructions. Briefly, cells were washed one time with assay buffer (1x Hanks' BSS

with 20 mM HEPES, pH 6). 20 µl of loading buffer (Molecular Devices, order number 8034, Sunnyvale, CA, USA), reconstituted as described in the product insert (final concentration= 20 µM) was added to each well. Cell plates were incubated for 30 min at 37°C. The cell plates were then loaded into a fluorescence imaging plate reader (FLIPR TETRA TM, Molecular Devices, Wokingham, UK) together with a separate 384-well plate containing oligomers and controls. Treatment of cells was carried out with the following final concentrations: 7 µM oligomer type A1 and A2 (referring to moles of monomer starting concentration), 500 µg/ml Gramicidin D as positive control. The fluorescence imaging plate reader (FLIPR) was programmed to transfer the test compounds and solvents simultaneously to all 384 wells 15 sec after commencement of recording of fluorescence (expressed as relative fluorescence units [RFU]). Fluorescence was excited at (510nm<λ<545nm) and emission was measured at (565nm<λ<625nm). Duration of recording was 10 min. Data are displayed as negative control corrected values, meaning signal response to oligomers including subtraction of corresponding solvent controls. The resulting signals were quantified by taking the maximum peak height of recording duration using Screenworks 1.2.0.73 software and are expressed as mean +/- SEM. Treatment effects for primary neurons were analyzed by one sample t-tests versus the hypothetical value 0 and quantified by mean values of differences (Δ) and corresponding 95% confidence intervals (CI).

Cell treatment and immunofluorescence staining

To investigate toxic effects or seeding properties of different oligomer preparations, SH-SY5Y overexpressing mutant α-syn[A53T] were seeded at 5000 cells/well using Collagen I coated 384-well black clear bottom microtiter plates (BD Biosciences Heidelberg, Germany). On the next day, cells were treated with 7 µM (referring to

moles of monomer) of different oligomers and the same volume of the corresponding solvent controls. After 2h treatment, oligomers were diluted 1:2 in culture medium for subsequent overnight treatment.

The treatment was stopped after overnight incubation using 2% formaldehyde and 1 µM Hoechst 33342^{TM} (Molecular Probes, Inc., Eugene, USA) in phosphate-buffered saline (PBS) as fixation solution. After washing, the cells were permeabilized and unspecific binding sites were blocked using 0.05% Saponin and 1% bovine serum albumine in PBS. After washing, the primary antibody (rabbit antibody against activated Caspase-3 (Asp175), Cell Signalling Technology, Beverly, MA, USA or rabbit antibody against α-syn (ASY-1, kind gift of Poul Henning Jensen, University of Aarhus, Denmark; described at Jensen et al., 2000)) was added for 1 h at 37°C, followed by another washing step and incubation with the secondary antibody (anti-rabbit antibody labelled with Alexa-Fluor 647, Molecular Probes, Inc., Eugene, USA) for 1 h at RT. After a final washing step of 50µl/well remained as residual volume.

Western Blotting of SH-SY5Y cell extracts

SH-SY5Y cells were scraped from 100 mm dishes and washed by centrifugation and resuspension in cold PBS. The cells were resuspended in STEN lysis buffer (250mM Tris, 750 mM NaCl, 10mM EDTA, 1% NP40, 25µg/ml Leupeptin, protease inhibitor mixture, pH 7.4) and incubated on ice for 30 min. After centrifugation at 1500 g for 10 min, protein concentrations of supernatants were quantified using the BCA assay (Pierce, Rockford, IL). Lysates (30 µg of protein) were resolved by electrophoresis on a 4-12 % Bis-Tris gradient gel (NuPAGE Novex Bis-Tris Gel, Invitrogen, Carlsbad, CA, USA) according to manufacturers instructions using NuPAGE MES buffer. After transfer to nitrocellulose membrane (Protran, Schleicher and Schuell, Whatman GmbH, Dassel, Germany) the blot was blocked for 1 h at RT with blocking buffer (I-

block, Tropix, Bedford, MA, USA). The blot was probed with ASY-1 antibody (1:500, kind gift of Poul Henning Jensen, University of Aarhus, Denmark) or anti-GAPDH (1:1000; Turku, Finland) for 1 h at RT. Bands were detected using alkaline phosphatase–conjugated secondary antibodies (1: 5000; Tropix, Bedford, MA, USA) and imaged with VersaDoc imaging system (Bio Rad laboratories GmbH, Munich, Germany).

Measurement of the assay plates in the IN Cell Analyzer 3000

Automated confocal fluorescence microscopy using the IN Cell Analyzer 3000™ (GE Healthcare Bio-Sciences, Little Chalfont, UK) has been described in detail (Wolff et al., 2006; Haasen et al., 2006). For our experiments, we employed the 364 laser line combined with a 450BP25 emission filter for Hoechst 33342™, the 647 nm laser line combined with a 695BP55 emission filter for Alexa Fluor 647, and the 488 nm laser line with a 535BP45 emission filter for Alexa Fluor 488. Fluorescence emission was recorded separately in the blue, red, and green channels, applying flat field correction for inhomogeneous illumination of the scanned area for each of the three channels.

Image analysis

Images stained for activated Caspase-3 were analyzed using the nuclear trafficking (TRF2) algorithm of the IN Cell Analyzer 3000™. Briefly, the algorithm identified the nuclei as pixel accumulations above a specified intensity threshold in the blue (nuclear) channel image. The number of nuclei correspond to the absolute cell number. In a specified dilated “cytoplasmic” mask region around these nuclei, the algorithm then searched for cells above a defined threshold in the red channel image, identifying cells stained for activated Caspase-3. The value “%positive cells” for each image was calculated as follows:

$$\% \text{ positive cells} = \frac{\text{number of positive cells in signal channel}}{\text{number of total cells in nuclear channel}} \times 100$$

For each treatment the numbers of % positive cells and total cells were normalized to the respective solvent controls to give % of control values [% CTL].

The mean and standard error of the mean for each analysis were calculated from the indicated number of images. Statistical significance was determined by unpaired t-test with $P<0.05$.

Statistical Analysis

Statistical analysis was performed as indicated as mentioned in the respective sessions for calcium measurements, measurement of membrane potential and image analysis using IN Cell Analyzer 3000.

Results

Aggregation of α-syn plays an important role in the pathogenesis of PD and other synucleinopathies. To characterize oligomers on a single particle level and to investigate their biological effects on both human neuroblastoma SH-SY5Y cells and primary cortical neurons, we developed three novel protocols for oligomer generation based on published observations. For the first time we compared the oligomers directly in shape, morphology and size using two single particle analysis methods. Finally, we investigated their bioactivity on cultured human cells.

The combination of ethanol and iron is sufficient to induce α-syn oligomerisation at very low protein concentrations (M. Kostka, T. Högen, K. Danzer and A. Giese, unpublished observation). In order to reduce ethanol concentrations that would interfere with subsequent cell culture experiments and to increase the oligomer yield, the aggregation conditions have been adapted and optimized. In the experiments described here we compared three different approaches:

First, we incubated oligomers for a period of six days after lyophylisation and resuspension in sodium phosphate buffer. This type of oligomers was termed type A. Second, based on the oligomer preparation protocol of Kayed et al. (2003) we used stirring bars to accelerate the aggregation process and to minimize ethanol concentrations, concurrently. We termed this oligomer type B. In the third approach, we used ultrafiltration to concentrate oligomers for use in cell culture. These oligomer type was named type C. Based on a finding that iron increases particle size of ethanol induced oligomers (M. Kostka, T. Högen, K. Danzer and A. Giese, unpublished observation), we investigated the influence of iron on all three oligomer types (A, B, C). Iron-free oligomers were termed type 1 oligomers and iron containing oligomers type 2.

To quantify and characterize the differently prepared oligomers, we used fluorescently labelled α-syn in nanomolar concentrations and applied FIDA with a confocal single molecule detection system.

CHARACTERISATION OF α-SYN OLIGOMERS TYPE A

Applying FIDA to characterize our oligomers, we found in the oligomers type A that nearly half of the overall particles appeared as monomers, whereas the other half was composed of small oligomeric particles. Although oligomers type A were incubated for several days, we found only small amounts of large oligomeric particles. There was no influence of iron on the particle size observed (Fig. 1*A*). In order to confirm our FIDA results, we used AFM as a fluorescence independent single molecule detection system.

AFM analysis showed that oligomers in the preparation type A appeared as heterogeneous population with globular and protofibrillar structures. Iron seemed to influence the aggregation process resulting in more extended protofibrillar structures (A2) whereas the iron-free preparation (A1) favours the generation of spherical structures (Fig 1*B*). Thus, small oligomer particles observed with FIDA could be confirmed with AFM analysis when compared to section analysis of monomers. As also described by Lashuel and co-workers (2002b), we observed annular structures with 40-45 nm in diameter in both preparations. Importantly, these annular structures were not found in monomer preparations (supplemental Fig. 1). In contrast to FIDA analysis almost no monomers were observed in oligomer preparations type A with our experimental AFM setup.

Taken together, using the complementary biophysical techniques FIDA and AFM, oligomers type A generated by long term incubation of low α-syn concentrations appeared as small, globular and annular structures.

CHARACTERISATION OF OLIGOMERS TYPE B

Oligomers type B were generated using stirring bars to facilitate ethanol evaporation. Applying FIDA for oligomer type B characterisation, we found in contrast to the preparation type A a higher conversion rate (80%) from monomers to small oligomers. This oligomer type B contained low monomeric percentages and only a small portion of large oligomeric particles. Additionally, there was no significant influence of iron on particle composition when comparing the FIDA analysis of the oligomer preparation B1 and B2 (Fig. 2 *A*).

Structural insight into oligomers type B was given by AFM analysis. Height images showed that oligomers type B appeared as a heterogeneous population (Fig. 2*B*). Also by stirring, globular structures have been detected, but no annular structures have been observed in any preparation. In contrast to FIDA analysis we saw an influence of iron on oligomer formation: iron-free prepared oligomers B1 appeared in a more compact spherical shape, while oligomers B2 prepared with iron showed up as amorphous structures.

Finally, the data demonstrate that oligomers type B were heterogeneous, globular oligomers, with low amounts of monomers and a majority of small oligomeric particles.

CHARACTERISATION OF OLIGOMERS TYPE C

The third kind of oligomers, oligomers type C, were prepared similar to the previous preparations and combined with an ultrafiltration step after the aggregation process.

With FIDA analysis we observed only in preparations type C an effect of iron administration: oligomers type C2 contained three times more small oligomeric forms than iron-free preparations (C1). Additionally, oligomer type C1 and C2 also differed

in the proportion of large particles. Here, large particles were present to a higher amount when compared with oligomers type A and B. Oligomers type C showed the lowest portion of monomers (Fig. 3*A*) among our three oligomer types A, B and C .

In contrast to the confocal fluorescence technique FIDA, the AFM analysis did not illustrate morphological differences in particle composition between oligomer type C1 and C2. Both oligomer types appeared as spherical particles with homogenous distribution of globular and protofibrillar structures (Fig. 3*B*). No annular structures like in the preparation type A were observed.

In summary, each of our novel protocols ended up in a heterogeneous oligomer population. We showed that changes in the aggregation protocols can lead to distinct forms of oligomers. We used these different oligomers to study the cellular responses to exogenously added oligomers.

INCREASE IN INTRACELLULAR CALCIUM MEDIATED BY OLIGOMERS TYPE A1 AND A2

It has been suggested that abnormal intracellular calcium homeostasis plays a crucial role in the pathogenesis of neurodegenerative disorders (Mattson and Chan, 2001). Moreover, we found that iron-induced oligomers were able to form pores in a synthetic bilayer pore forming assay (M. Kostka, T. Högen, K. Danzer and A. Giese, unpublished observation). Similarly, Volles and co-workers have shown pore-forming activity of α-syn protofibrils using synthetic vesicles (Volles et al., 2001; Volles and Lansbury, Jr., 2002). Therefore, we asked whether we could detect a calcium dysregulation in cells treated with oligomers type A. In contrast to monomer samples, oligomers type A1 and A2 evoked a rapid increase within seconds in calcium-dependent fluorescence in fluo-4-loaded singular SH-SY5Y cells using confocal microscopy (Fig. 4) and in a fluorometric imaging plate reader (FLIPR) (supplemental

Fig. 3*A*). The increase in intracellular calcium of singular SH-SY5Y cells is also demonstrated on a time lapse video (supplemental movie 2). As positive controls we used the channel-forming polypeptide ionophore gramicidin and the chelating calcium ionophore ionomycin, which allows calcium to diffuse passively through cellular membranes (Fig. 4; supplemental Fig. 3). In order to investigate whether the observed increase in intracellular calcium was dependent on cellular α-syn expression levels, we compared mock transfected SH-SY5Y cells expressing endogenous α-syn with cells stably overexpressing α-syn[wt] or mutant α-syn[A30P/A53T]. These cell lines exhibited comparable α-syn expression levels compared to the endogenous control as shown in supplemental Fig. 2. Again oligomers type A1 and A2 evoked a clear increase in calcium-dependent fluorescence compared to monomer and respective solvent controls. No clear differences in the calcium signal increase between mock transfected SH-SY5Y cells and overexpressing α-syn overexpressing SH-SY5Y cells have been observed (supplemental Fig. 3*)*. These data suggest that only the exogenously applied oligomers are responsible for the elevation of intracellular calcium and that the intracellular α-syn does not contribute to the effect in the time window investigated here.

In order to demonstrate also for primary neurons a elevation of intracellular calcium induced by oligomers type A, we performed the same experiments as described above for SH-SY5Y cells. Using confocal microscopy we confirmed also in primary neurons a significant increase in intracellular calcium (Fig. 5). A time lapse video of singular neurons shows also the calcium influx effect (supplemental movie 2). This was further confirmed by FLIPR measurements (supplemental Fig. 4).

In order to support a pore formation as possible mechanism responsible for the calcium influx we measured the membrane potential. Indeed, oligomers type A1 and

A2 showed in primary cortical neurons a depolarisation of the membrane potential as also shown for gramicidine (Fig. 6).

OLIGOMER TYPE A INDUCED CALCIUM ION INFLUX FROM EXTRACELLULAR SOURCES

To discriminate whether the observed increase in intracellular calcium induced by oligomers type A1 and A2 resulted from influx of extracellular calcium or emptying of intracellular calcium stores, we reduced the extracellular calcium concentration to very low levels by using calcium free buffer. In the absence of extracellular calcium the treatment of endogenous α-syn SH-SY5Y cells (Fig. 7*A*) completely abrogated the oligomer type A1 and A2 induced intracellular calcium increase. As expected, application of the channel-forming polypeptide gramicidin also no longer elicited an increase in intracellular calcium. Only ionomycin induced calcium signals were detectable. Thus, the increase of intracellular calcium levels induced by oligomers type A1, A2 and gramicidin resulted from extracellular sources, whereas the remaining ionomycin signal response was mediated by both influx of extracellular calcium and intracellular calcium release.

To rule out the possibility that endogenous calcium-permeable plasma membrane ion channels were affected by oligomers type A1 and A2, we added 20 µM cobalt, a non specific calcium channel blocker, to endogenous α-syn SH-SY5Y cells, prior to application of 7 µM oligomer type A1. Signal response in the presence of cobalt was of a comparable magnitude to that obtained in the absence of cobalt (Fig. 7*B*), suggesting that calcium influx through cobalt-sensitive calcium channels does not contribute to oligomer type A1 and A2 induced increase in intracellular calcium.

TOXICITY OF OLIGOMERS TYPE A

In order to investigate whether oligomers type A have toxic properties, we examined caspase 3 activation and determined cell number reduction after oligomer type A1 and A2 treatment. As there were no biological relevant differences in calcium response seen in SH-SY5Y cells expressing endogenous or elevated levels of α-syn, we performed toxicity assays only in mock transfected cells and in mutant α-syn[A53T] overexpressing cells.

Immunofluorescence staining for caspase 3 after oligomer type A1 treatment showed for both mock transfected and mutant α-syn [A53T] expressing SH-SY5Y cells a significant ($p<0.05$) increase in cleaved caspase 3 activity. Also treatment with oligomer type A2 resulted in a significant increase of caspase 3 activity in both cell lines, whereas the increase in caspase 3 activity seemed to be slightly higher in mutant α-syn[A53T] overexpressing cells than in cells with endogenous levels of α-syn (Fig. 8*A*). Treatment with oligomer type A1 caused in both cell lines a significant reduction in cell number, whereas mutant α-syn [A53T] overexpressing cells seemed to be more affected in cell number reduction than mock transfected cells. Although there was a lower caspase activation compared to the mock transfected cells, there was a stronger cell number reduction in this cell line. This discrepancy might be explained by non-apoptotic cell death. We observed a strong and significant cell number reduction in mutant α-syn[A53T] overexpressing cells treated with oligomers type A2. This is in accordance with the caspase 3 results. Although the cell number reduction in mock transfected cells treated with oligomers A2 is statistically not significant ($p=0.56$) compared to solvent control 2, oligomers type A2 seem to reduce cell number also in mock transfected cells (Fig. 8*B*).

In contrast to oligomers type A, our other types of oligomers, type B and type C, did not increase the level of intracellular calcium (data not shown). Moreover, we also did not detect a caspase activation or cell number reduction for oligomers type B and C. Thus, oligomers type A were the only oligomer type with annular structures and a calcium influx effect with a induction of cell death.

SEEDING CHARACTERISTICS OF OLIGOMERS TYPE B

It has been shown previously that aggregation of α-syn is a nucleation-dependent process, in which preformed aggregates function as seeds (Wood et al., 1999). To analyze whether exogenously added oligomers have the propensity to seed cytosolic α-syn, we treated SH-SY5Y cells stably overexpressing α-syn mutant [A53T] and mock transfected cells with endogenous levels of α-syn with Alexa-488-conjugated oligomers type B. Immunofluorescence staining showed co-localisation of Alexa-488-conjugated oligomers type B (green) and total amount of α-syn (red) in overlaid images. We found yellow coloured aggregates within cells after oligomer type B treatment in both α-syn mutant [A53T] and mock transfected cells. Confocal images demonstrated that cells treated with Alexa-488-conjugated oligomers type B2 displayed a reduction in cytoplasmic α-syn staining and an increase in yellow coloured intracellular aggregates (seeding), whereas solvent control treated cells showed homogenous cytoplasmic staining of α-syn (Fig. 9). Thus, exogenously added oligomers type B have entered the cell and seeded aggregation of cytosolic α-syn with a resulting increased protein aggregation in one local area.

Notably, these oligomers type B1 and B2 did not cause an increase in intracellular calcium (data not shown). This supports the idea that the oligomers type B are

different to the oligomers type A. Thus, oligomers type B and A differ not only in their biophysical properties, but this difference also translates into different cellular effects.

SEEDING CHARACTERISTICS OF OLIGOMERS TYPE C

Because also oligomers type C seemed to have different biophysical characteristics compared to oligomers type A and type B, we assumed also different biological effects on cells. First, we investigated again the effect on calcium homeostasis in neuroblastoma cells. In none of our assays oligomers type C caused an increase in intracellular calcium (data not shown).

We also investigated the seeding ability of oligomers type C as described for oligomers type B. Type C2 Alexa-488 oligomers induced as well a remarkable reduction in cytoplasmic staining of α-syn and a tremendous seeding effect in both α-syn mutant [A53T] and mock transfected cells with endogenous levels of α-syn (Fig. 10). Whereas, corresponding solvent control treated cells showed a homogeneous α-syn staining. Also, oligomers type C1 induced in both SH-SY5Y cell lines aggregate formation, whereas the seeding effect of oligomers type C2 was stronger. Also in primary neurons we were able to demonstrate a reduction in cytoplasmic α-syn staining and a tremendous “yellow” aggregate formation near the nucleus after oligomer type C2 treatment. Corresponding solvent control treated neurons showed a homogeneous cytoplasmic staining of α-syn (Fig. 10*C*). Thus, also oligomers type C had the propensity to seed cytosolic α-syn by accumulation of intracellular α-syn within one local area after exogenous application in both SH-SY5Y cell lines and primary neurons.

Notably, oligomers type A had in none of our approaches any seeding propensity (data not shown).

All together, our data provide evidence that several different types of oligomers can be formed under various conditions, which differ in shape, morphology and size. Consequently, these different types of oligomers have distinct biological effects on cells (summarized in table 1).

Discussion

In this study we have shown that depending on aggregation conditions heterogeneous populations of α-syn oligomers are forming, which can be differentiated based on their biophysical properties and cellular effects. Type A oligomers induced an increased membrane permeability and trigger cell death. Type B and C oligomers were able to enter cells directly and to seed intracellular α-syn aggregation.

Many protocols of oligomer preparation have been described in the literature, but all were characterized with different methods, making it difficult to compare the different approaches. Here, we directly compared various types of oligomers by two single particle analysis methods, AFM and FIDA, and cellular readouts. The influence of iron on in vitro aggregation of α-syn has been reported by (Uversky et al., 2001). These findings formed the basis for our present work.

Characterisation of our oligomers type A with AFM revealed spherical oligomers from 2 to 6 nm in height. This is consistent with observations of other groups (Rochet et al., 2000; Conway et al., 2000; Volles et al., 2001; Hoyer et al., 2004; Apetri et al., 2006), although these studies were carried out with far higher protein concentrations. Wood et al (1999) had previously determined 28 µM as the critical concentration for α-syn aggregation. Our approaches used 4 times less protein. This was possible due to the application of the highly sensitive FIDA analysis in contrast to the standard techniques used in the other studies. The method of oligomer generation used by Jensen and co-workers (2000) required protein concentrations 10-fold higher than our approaches and resulted mostly in fibrils after 7 days of incubations. In contrast, our samples still consisted mainly of oligomers and monomers at this time point, with no fibrils yet apparent. Prolonged incubation, however, lead to fibril formation (supplemental Fig. 2), suggesting that our oligomers were on pathway to fibrils.

Kayed et al described the generation of homogeneous oligomer populations using a greatly differing protocol starting with seedless stock solutions (Kayed and Glabe, 2006). In contrast, our oligomer preparations turned out to be heterogeneous mixtures: FIDA data demonstrated that almost 50% of α-syn contained in type A oligomers was in the monomeric form. An obvious explanation for the relatively high proportion of monomers in the preparations type A is an equilibrium between monomers and oligomers type A. After ultrafiltration in order to separate the monomer fraction and the oligomer type A fraction, monomers re-appeared in the oligomer fraction (data not shown). The α-syn monomers were, however, not seen by AFM, most probably because the monomers were washed off during the AFM sample preparation.

In addition to the generation and biophysical characterisation of different oligomer types, we also investigated their biological effects following application to cells. We found that two types of our oligomers (B and C) entered into cells and seeded intracellular α-syn aggregation. Our other type of oligomers (type A) did not enter into cells. Instead they seemed to act at the cellular membrane where they initiated an elevation of intracellular calcium. This increase in intracellular calcium occurred only in the presence of calcium in the extracellular buffer suggesting that this effect is due to an influx from extracellular sources. We have also shown that this calcium influx is independent of cobalt-sensitive calcium channels. This is in contrast to Adamczyk and Strosznajder (2006), who suggested that α-syn induces a calcium influx via N-type voltage-dependent Ca2+ channels. Their study differs greatly in two aspects. First, their model system is comprised of rat synaptoneurosomes, and second, they used monomeric α-syn for their investigations. Therefore, the data of Adamczyk and Strosznajder (2006) are not directly comparable to our data.

Several mechanisms have been suggested to underlie the increase in intracellular calcium induced by amyloidogenic proteins: increase in membrane permeability (Demuro et al., 2005), insertion into the membrane and formation of a pore (Kawahara et al., 2000; Arispe, 2004; Lashuel and Lansbury, Jr., 2006), and a direct interaction with membrane components to destabilize the membrane structure (Muller et al., 1995; Mason et al., 1996; Avdulov et al., 1997; Green et al., 2004). Although we can not exclude an increase in membrane permeability or mechanisms destabilizing the membrane structure, our data support the amyloid pore hypothesis suggested by Lashuel and Lansbury (2006). They demonstrated with synthetic vesicles a pore-forming mechanism of α-syn protofibrils (Volles et al., 2001; Volles and Lansbury, Jr., 2002; Lashuel et al., 2002a). The influx of extracellular calcium observed in our experiments suggests that α-syn pore-formation occurs also in living cells. In addition, the calcium influx pattern of bacterial toxin gramicidin closely resembled the α-syn oligomer type A induced calcium influx. Thus, the pore forming mechanism mediated by oligomers type A could be similar to that of membrane spanning pores formed by known protein toxins (e.g. hemolysin, latroxin and aerolysin) (Valeva et al., 1997; Orlova et al., 2000; Wallace et al., 2000). Moreover, we also found a change in membrane potential in primary neurons after oligomer type A treatment. The observed depolarisation could be the consequence of ion fluxes through pores in the membrane. Intriguingly, only oligomers type A contained annular structures. Recently, Tsigelny et al. (2007) have shown by utilizing molecular modelling and molecular dynamics simulations that α-syn can form pentamers and hexamers forming a ring-like structure that can incorporate in the membrane. Direct evidence for the existence of amyloid pore-like structures in vivo has been provided by the extraction of annular α-syn structures from post mortem brain tissues from a multiple system atrophy patient (Pountney et al., 2005). Our annular oligomers type A

with 45 nm in diameter were similar to those extracted oligomers that ranged from 30 to 50 nm in diameter.

These results suggest a disruption of cellular ion homeostasis followed by caspase activation and cell death via membrane spanning pores as one possible pathogenic mechanism of α-syn oligomers that might also occur in vivo. A disruption of calcium homeostasis has been proposed for several related amyloidogenic oligomers, including amyloid ß-peptide, prion, islet amyloid polypeptide, polyglutamine and lysozyme (Demuro et al., 2005). Even prefibrillar aggregates of non-disease related proteins have been shown to be internalized into cells followed by a rise of free calcium levels (Bucciantini et al., 2004). These findings strengthen the idea of a common mechanism of disruption of calcium homeostasis mediated by different pre-fibrillar aggregates of disease-related and non-disease related proteins.

Our data demonstrate that oligomers type A evoked increase in intracellular calcium was similar in cells overexpressing α-syn[wt, A30P, A53T] and cells expressing only endogenous level of α-syn. This suggests that intracellular α-syn does not contribute under these experimental conditions to the pore formation, although other studies have shown that cells expressing mutant α-syn[A53T] have a higher plasma membrane permeability (Furukawa et al., 2006).

In contrast, oligomers type B and C did not increase intracellular calcium (data not shown), but these oligomers could directly enter the cell and promote intracellular aggregate formation.

Effects of extracellular oligomers on cells might play an important role, also under pathophysiological conditions, since intriguing findings have recently shown that α-syn aggregates could be secreted from cells and therefore possibly insult neighbouring cells (Lee et al J Neurosci 2005). However, as α-syn is an intracellular

protein, the in vivo situation can still differ from this model, as there could also be other mechanisms involved not considered in this study.

Earlier studies have shown that monomeric α-syn and prefibrillar aggregates from non-disease related proteins can translocate into cells, although the mechanism of aggregate internalisation to date remains unclear (Bucciantini et al., 2004; Ahn et al., 2006). We were able to confirm that oligomers type B and C could also be internalized into cells and deploy then their seeding properties. A previous study has shown that membrane bound α-syn can seed intracellular α-syn (Lee et al., 2002). The seeding effect observed in our study could be similar to the effect shown by Lee and co-workers. Oligomers type B and C might resemble nucleating species as described also in cell-free studies (Hoyer et al., 2002). Seeding could also be one underlying mechanism for the ascending progression of α-syn pathology within the brains of Parkinson's patients (Braak et al., 2003).

In our experimental setup oligomers type B and C did not induce caspase activation or cell loss (data not shown). This correlates with the lack of an increase in intracellular calcium. We hypothesize that although oligomers type B and C seed intracellular aggregation of α-syn, the resulting progression in aggregate formation in cell culture models is so fast due to the high levels of α-syn overexpression that the nucleating species immediately end up as large aggregates, bypassing the toxic oligomeric intermediates. Therefore, it might well be that oligomers with seeding properties could still trigger toxic neurodegenerative processes in synucleinopathies, where α-syn is present at physiological concentrations.

In conclusion, this study suggests that the aggregation process of α-syn results in distinct populations of oligomeric forms with different cellular effects. The cellular effects of α-syn oligomers described here in cell culture could resemble events that

take place in PD patients. However, further studies are needed to characterize the pathophysiologically relevant oligomeric forms in the brains of PD patients. Preventing the early events in oligomer formation might be a novel approach for the development of effective drugs for the treatment of PD and other synucleinopathies.

Fig. 1 : Characterisation of long-term incubated of α-syn oligomers (type A1 and A2)

A, FIDA analysis of two oligomeric α-syn forms generated after long-term incubation (6 days) in 50 mM sodium phosphate buffer. The influence of ferrous chloride has been worked out (type A1 without ferrous chloride and type A2 with ferrous chloride). Means +/- SEM of five measurements are shown. ***B,*** AFM images (500 nm x 500 nm) of type A1 and A2 oligomeric α-syn forms generated after long-term incubation (6 days) in 50 mM sodium phosphate buffer. Section analysis revealed globular or protofibrilar oligomers from 2 to 6 nm in height. Also annular structures (arrows) were found in both oligomer types A1 and A2. AFM images are representative examples of several AFM images of independent oligomer preparations.

Fig. 2 : Characterisation of α-syn oligomers type B1 and B2 generated with stirring bars

A, Single particle analysis revealed two oligomeric forms generated with stirring bars. The influence of ferrous chloride has been worked out (type B1 without ferrous chloride and type B2 with ferrous chloride).***B***, AFM images (1 μm^2) of two oligomeric forms generated with stirring bars. Oligomers appeared as heterogenous population with particles from 3-23 nm in height using section analysis. Oligomer type B1 appeared in a more compact spherical form than oligomer type B2. AFM images are representative examples of several AFM images of independent oligomer preparations.

Fig. 3 : Characterisation of α-syn oligomers (type C1 and C2)

A, Single particle analysis of two oligomeric α-syn forms generated by overnight incubation and ultrafiltration. The influence of ferrous chloride has been analyzed

(type C1 without ferrous chloride and type C2 with ferrous chloride).***B***, AFM images (1 μm^2) of two oligomeric α-syn forms generated by overnight incubation and ultracentrifugation. Images showed globular and protofibrillar oligomer structures with 4-10 nm in height. Using AFM analysis there were no significant morphological differences detectable between oligomer type C1 and oligomer type C2. AFM images are representative examples of several AFM images of independent oligomer preparations.

Fig. 4: $[Ca^{2+}]$ elevation by α-syn oligomers type A1 and A2 in SH-SY5Y cells

Traces show $[Ca^{2+}]$ dependant fluorescence of single SH-SY5Y cells overexpressing α-syn[wt] in response to 6 µM ionomycin, 0.1 mg/ml monomer, 0.1 mg/ml oligomer type A1 and A2 with respective solvent controls. Oligomers type A1 and A2 evoked a clear increase in intracellular $[Ca^{2+}]$. Fluorescence records illustrating typical responses to different treatments starting at the time point of application. The inset images of the cell were captured at the times indicated during the trace and are depicted on a pseudo colour scale with “warmer” colours on a rainbow scale corresponding to higher fluorescence. The inset images show representatives of a single cell.

Fig. 5: $[Ca^{2+}]$ elevation by α-syn oligomers type A1 and A2 in primary neurons

Traces show $[Ca^{2+}]$ dependant fluorescence of single cortical neurons in response to 6 µM ionomycin, 0.1 mg/ml monomer, 0.1 mg/ml oligomer type A1 and A2 with respective solvent controls. Oligomers type A1 and A2 evoked a clear increase in intracellular $[Ca^{2+}]$. Fluorescence records illustrating typical responses to the different treatments starting at the time point of application. The inset images show pseudo colour representatives of a single cell, captured at the times indicated by the trace.

Fig. 6: Depolarisation of membrane potential induced by oligomers type A1 and A2

A, Kinetic plots illustrating typical signal responses to application of 0.1 µg/µl α-syn monomer, oligomers type A1 and A2, and 500 µg/ml gramicidin as positive control. Oligomers type A1 and A2 showed a clear depolarisation of membrane potential. Each trace shows the negative control corrected mean fluorescence of 1.25 x 10^5 primary neurons. ***B***, Quantification of fluorescence intensity in response to oligomer type A1 and A2 induced depolarisation in primary neurons compared to solvent control. Values are the mean +/- SEM; n=3, *P<0.002, one sample t-test against hypothetical value 0. A1 treated neurons: Δ= 286.8 (95% CI: 277.4-296.2); A2 treated neurons: Δ= 345.2 (95% CI: 286.2-404.2)

Fig. 7: α-syn oligomer type A1 and A2 induced intracellular [Ca2+] increase via influx of extracellular [Ca^{2+}] sources

A, Kinetic plots illustrating typical signal responses to application of 0.1 µg/µl α-syn oligomers type A1 and A2, and positive controls 1.5 µM ionomycin and 500 µg/ml gramicidin in [Ca^{2+}] free extracellular buffer. Each trace shows the mean fluorescence of 6000 mock transfected SH-SY5Y cells expressing endogenous α-syn. Intracellular [Ca^{2+}] signals evoked by oligomers type A1, A2 and gramicidin were completely abolished when cells were incubated in [Ca^{2+}] free extracellular buffer, whereas ionomycin induced [Ca^{2+}] signals were persistent. ***B***, [Ca^{2+}] signals evoked by oligomer type A1 and A2 are not reduced by cobalt, a non specific Ca^{2+} channel blocker. Each trace shows typical mean fluorescence of 6000 mock transfected SH-SY5Y cells following addition of oligomers type A1 in the presence and absence of cobalt. Oligomers type A showed a clear calcium channel independent increase in

intracellular [Ca2+]. This experiment was repeated 2 times and showed similar results.

Fig. 8 : Toxicity of α-syn oligomers type A1 and A2

A, Quantification of Caspase 3 activation normalized to corresponding solvent controls; values are the mean +/- SEM; n=3. Treatment of mock transfected SH-SY5Y cells or cells overexpressing α-syn mutant A53T with 0.1 mg/ ml oligomers type A1 and A2 lead to a significant activation of Caspase 3, unpaired t test, *P<0.05 compared with data from corresponding solvent controls: Oligomer type A1 treated: mock: Δ=151 (95% CI: 83.3-218.6); α-syn[A53T]: Δ=75.8 (95% CI: 5.8-145.9); oligomer type A2 treated: mock: Δ=90.9 (95% CI: 54.6-127.2); α-syn[A53T]: Δ=288.9 (95% CI: 147.3-430.5). ***B***, Quantification of cell number reduction normalized to corresponding solvent controls. Values are the mean +/- SEM; n=3. Oligomers type A1 evoked on both mock transfected and stably overexpressing mutant α-syn[A53T] SH-SY5Y cell lines a significant reduction in cell number. Oligomers type A2 led on overexpressing mutant α-syn[A53T] SH-SY5Y cells to a significant reduction in cell number, unpaired t-test, *P<0.05 compared with data from corresponding solvent controls: Oligomer type A1 treated: mock: Δ=-56 (95% CI: -91.5 to -20.5); α-syn [A53T]: Δ=-79.3 (95% CI: -104.9 to -53.62); oligomer type A2 treated: mock: Δ=-34.6 (95% CI: -75.6 to-6.5); α-syn[A53T]: Δ=-72.1 (95% CI: -99.4 to- 44.7). Both oligomer types mediated their toxicity after 24h.

Fig. 9: Seeding effect of α-syn oligomers type B1 and B2

Immunocytochemical staining of α-syn with ASY-1 antibody (in red) after treatment with 0.1 mg/ml Alexa-488 labelled oligomers type B1 and B2 (in green) or solvent

controls. Confocal images showed a reduction in cytoplasmic staining of α-syn and an increase in cell associated aggregates (seeding) in SH-SY5Y stably overexpressing α-syn[A53T] (***A***) or mock transfected SH-SY5Y with endogenous expression of α-syn (***B***) when treated with oligomer type B2. Oligomer type B2 had a higher potential to seed aggregate formation than oligomer type B1. This experiment was repeated two times and showed similar results.

Fig. 10 : Seeding effect of α-syn oligomers type C1 and 2

Immunocytochemical staining of α-syn with ASY-1 antibody (in red) after treatment with 0.1 mg/ml Alexa-488 labelled oligomers type C1 and C2 (in green) or solvent controls. Confocal images showed a reduction in cytoplasmic staining of α-syn and an increase in cell associated aggregates (seeding) in SH-SY5Y stably overexpressing α-syn mutant A53T (***A***) or mock transfected SH-SY5Y cells (***B***) treated with oligomer type C2. Oligomer type C2 had a higher potential to trigger aggregate formation than oligomer type C1. This experiment was repeated two times and showed similar results. ***C***, Also primary cortical neurons showed a decrease in cytoplasmic staining of α-syn (red) and remarkable cell associated α-syn aggregate formation (yellow).

Supplemental Fig. 1: AFM image of monomeric α-syn

A, The lyophilized protein was freshly dissolved in 50mM sodium phosphate buffer at a concentration of 1 nM. The corresponding height images (1 μm^2) showed almost exclusively particles of 0.8 -1 nm in height. ***B***, Size distribution of monomeric α-syn Quantitative size distribution analysis of α-syn particles reveal average heights of 1 nm indicating that monomeric species had adsorbed on muscovite mica surface.

Particle analysis was performed by the NanoScope data processing software (Digital Instruments, Santa Barbara, CA, USA) corrected for tilting and bowing of the substrate.

Supplemental Fig. 2: Expression levels of α-syn in SH-SY5Y cells

A, Mock transfected and SH-SY5Y cells overexpressing α-syn[wt, A30P, A53T] were lysed, and proteins were resolved by 4-12% SDS PAGE. Lysates were Western blotted using polyclonal α-syn antibody ASY-1. Equal protein loading was verified using an anti GAPDH antibody (loading control). ***B***, Laser confocal microscope images of mock transfected and SH-SY5Y cells overexpressing α-syn[wt, A30P, A53T]. Cells were immunostained with the α-syn antibody ASY-1 (red).

Supplemental Fig. 3: $[Ca^{2+}]$ elevation by α-syn oligomers type A1 and A2 in SH-SY5Y cells

A, Kinetic plots illustrating typical signal responses to application of 0.1 µg/µl α-syn monomer, oligomers type A1 and A2, and 1.5 µM ionomycin and 500 µg/ml gramicidin as positive controls. Oligomers type A1 and A2 evoked a clear increase in intracellular calcium. Each trace shows the negative control corrected mean fluorescence of 6000 mock transfected SH-SY5Y cells expressing endogenous level of α-syn. ***B,*** Quantification of $[Ca^{2+}]$ elevation in mock transfected SH-SY5Y cells, cells overexpressing α-syn[wt, A30P, A53T] induced by different treatments. All cell lines showed a clear increase of intracellular $[Ca^{2+}]$ after oligomer treatment compared to the respective solvent controls and α-syn monomeric form. Values are the mean +/- SEM; n=3 ; *P < 0.0001. Bonferroni adjusted p-value for pair wise comparisons versus corresponding solvent controls. Oligomer type A1 treated: mock:

Δ=153 (95% CI: 126.6-179.3); α-syn[wt]: Δ=140.8 (95% CI: 114.5-167.1); α-syn[A30P]: Δ=106.6 (95% CI: 80.3-132.9); α-syn[A53T]: Δ=112.5 (95% CI: 86.13-138.8). Oligomer type A2 treated: mock: Δ=118.6 (95% CI: 78.85-158.4); α-syn[wt]: Δ=122.1 (95% CI: 82.31-161.9); α-syn[A30P]: Δ=137.7 (95% CI: 97.96-177.5); α-syn [A53T]: Δ=145.4 (95% CI: 105.6-185.2). The experiments were repeated 4 times, all experiments showed similar results.

Supplemental Fig. 4: [Ca2+] elevation by α-syn oligomers type A1 and A2 in primary cortical neurons

A, Kinetic plots illustrating typical signal responses to application of 0.1 µg/µl α-syn monomer, oligomers A1 and 2, and 1.5 µM ionomycin and 500 µg/ml gramicidin as positive controls. Both oligomer types A1 and A2 increased intracellular [Ca2+] to the same extend compared to the respective solvent controls and α-syn monomeric form. Each trace shows the negative control corrected mean fluorescence of 1.25 x 10^5 primary neurons. ***B***, Quantification of [Ca^{2+}] elevation induced by different treatments. Values are the mean +/- SEM; n=3 ; *P < 0.0001, unpaired t test. Oligomer type A1 treated neurons: Δ= 218.5 (95% CI: 201.0-235.9); Oligomer type A2 treated neurons: Δ= 219.5 (95% CI: 181.7-257.2).

Supplemental Fig. 5: α-syn fibrils

A, AFM image of α-syn fibrils. Fibrils of the A type after 1 week prolonged incubation (15days) in 50 mM sodium phosphate buffer. ***B***, Negatively stained transmission electron micrographs of α-syn fibrils after 15 days incubation of approach type A.

References

Adamczyk A, Strosznajder JB (2006) Alpha-synuclein potentiates Ca2+ influx through voltage-dependent Ca2+ channels. Neuroreport 17:1883-1886.

Ahn KJ, Paik SR, Chung KC, Kim J (2006) Amino acid sequence motifs and mechanistic features of the membrane translocation of alpha-synuclein. Journal of Neurochemistry 97:265-279.

Apetri MM, Maiti NC, Zagorski MG, Carey PR, Anderson VE (2006) Secondary structure of alpha-synuclein oligomers: characterization by raman and atomic force microscopy. J Mol Biol 355:63-71.

Arispe N (2004) Architecture of the Alzheimer's A beta P ion channel pore. J Membr Biol 197:33-48.

Auluck PK, Chan HY, Trojanowski JQ, Lee VM, Bonini NM (2002) Chaperone suppression of alpha-synuclein toxicity in a Drosophila model for Parkinson's disease. Science 295:865-868.

Avdulov NA, Chochina SV, Igbavboa U, Warden CS, Vassiliev AV, Wood WG (1997) Lipid binding to amyloid beta-peptide aggregates: preferential binding of cholesterol as compared with phosphatidylcholine and fatty acids. J Neurochem 69:1746-1752.

Bodner RA, Outeiro TF, Altmann S, Maxwell MM, Cho SH, Hyman BT, McLean PJ, Young AB, Housman DE, Kazantsev AG (2006) Pharmacological promotion of

inclusion formation: a therapeutic approach for Huntington's and Parkinson's diseases. Proc Natl Acad Sci U S A 103:4246-4251.

Braak H, Del TK, Rub U, de Vos RA, Jansen Steur EN, Braak E (2003) Staging of brain pathology related to sporadic Parkinson's disease. Neurobiol Aging 24:197-211.

Bucciantini M, Calloni G, Chiti F, Stefani M, Formigli L, Nosi D, Dobson CM (2004) Prefibrillar amyloid protein aggregates share common features of cytotoxicity. J Biol Chem 279:31374-31382.

Bucciantini M, Giannoni E, Chiti F, Baroni F, Formigli L, Zurdo J, Taddei N, Ramponi G, Dobson CM, Stefani M (2002) Inherent toxicity of aggregates implies a common mechanism for protein misfolding diseases. Nature 416:507-511.

Chartier-Harlin MC, Kachergus J, Roumier C, Mouroux V, Douay X, Lincoln S, Levecque C, Larvor L, Andrieux J, Hulihan M (2004) [alpha]-synuclein locus duplication as a cause of familial Parkinson's disease. The Lancet 364:1167-1169.

Conway KA, Lee SJ, Rochet JC, Ding TT, Williamson RE, Lansbury PT, Jr. (2000) Acceleration of oligomerization, not fibrillization, is a shared property of both alpha-synuclein mutations linked to early-onset Parkinson's disease: implications for pathogenesis and therapy. Proc Natl Acad Sci U S A 97:571-576.

Dauer W, Przedborski S (2003) Parkinson's disease: mechanisms and models. Neuron 39:889-909.

Demuro A, Parker I, Glabe CG, Mina E, Kayed R, Milton SC (2005) Calcium dysregulation and membrane disruption as a ubiquitous neurotoxic mechanism of soluble amyloid oligomers. J Biol Chem 280:17294-17300.

El-Agnaf OM, Salem SA, Paleologou KE, Curran MD, Gibson MJ, Court JA, Schlossmacher MG, Allsop D (2006) Detection of oligomeric forms of alpha-synuclein protein in human plasma as a potential biomarker for Parkinson's disease. FASEB J 20:419-425.

Furukawa K, Matsuzaki-Kobayashi M, Hasegawa T, Kikuchi A, Sugeno N, Itoyama Y, Wang Y, Yao PJ, Bushlin I, Takeda A (2006) Plasma membrane ion permeability induced by mutant alpha-synuclein contributes to the degeneration of neural cells. J Neurochem 97:1071-1077.

Goedert M (2001) Alpha-synuclein and neurodegenerative diseases. Nat Rev Neurosci 2:492-501.

Goldberg MS, Lansbury PT, Jr. (2000) Is there a cause-and-effect relationship between alpha-synuclein fibrillization and Parkinson's disease? Nat Cell Biol 2:E115-E119.

Gosavi N, Lee HJ, Lee JS, Patel S, Lee SJ (2002) Golgi fragmentation occurs in the cells with prefibrillar alpha-synuclein aggregates and precedes the formation of fibrillar inclusion. J Biol Chem 277:48984-48992.

Green JD, Kreplak L, Goldsbury C, Li B, X, Stolz M, Cooper GS, Seelig A, Kistler J, Aebi U (2004) Atomic force microscopy reveals defects within mica supported lipid

bilayers induced by the amyloidogenic human amylin peptide. J Mol Biol 342:877-887.

Haasen D, Wolff M, Valler MJ, Heilker R (2006) Comparison of G-protein coupled receptor desensitization-related beta-arrestin redistribution using confocal and non-confocal imaging. Comb Chem High Throughput Screen 9:37-47.

Hoyer W, Antony T, Cherny D, Heim G, Jovin TM, Subramaniam V (2002) Dependence of alpha-synuclein aggregate morphology on solution conditions. J Mol Biol 322:383-393.

Hoyer W, Cherny D, Subramaniam V, Jovin TM (2004) Rapid Self-assembly of alpha-Synuclein Observed by In Situ Atomic Force Microscopy. J Mol Biol 340:127-139.

Jensen PH, Islam K, Kenney J, Nielsen MS, Power J, Gai WP (2000) Microtubule-associated protein 1B is a component of cortical Lewy bodies and binds alpha-synuclein filaments. J Biol Chem 275:21500-21507.

Kask P, Palo K, Fay N, Brand L, Mets U, Ullmann D, Jungmann J, Pschorr J, Gall K (2000) Two-dimensional fluorescence intensity distribution analysis: theory and applications. Biophys J 78:1703-1713.

Kask P, Palo K, Ullmann D, Gall K (1999) Fluorescence-intensity distribution analysis and its application in biomolecular detection technology. Proc Natl Acad Sci U S A 96:13756-13761.

Kawahara M, Kuroda Y, Arispe N, Rojas E (2000) Alzheimer's beta-amyloid, human islet amylin, and prion protein fragment evoke intracellular free calcium elevations by

a common mechanism in a hypothalamic GnRH neuronal cell line. J Biol Chem 275:14077-14083.

Kayed R, Edmonds B, Milton SC, Glabe CG, Sokolov Y, Hall JE, McIntire TM (2004) Permeabilization of lipid bilayers is a common conformation-dependent activity of soluble amyloid oligomers in protein misfolding diseases. J Biol Chem 279:46363-46366.

Kayed R, Glabe CG (2006) Conformation-dependent anti-amyloid oligomer antibodies. Methods Enzymol 413:326-344.

Kayed R, Head E, Thompson JL, McIntire TM, Milton SC, Cotman CW, Glabe CG (2003) Common structure of soluble amyloid oligomers implies common mechanism of pathogenesis. Science 300:486-489.

Kruger R, Kuhn W, Muller T, Woitalla D, Graeber M, Kosel S, Przuntek H, Epplen JT, Schols L, Riess O (1998) Ala30Pro mutation in the gene encoding alpha-synuclein in Parkinson's disease. Nat Genet 18:106-108.

Lashuel HA, Grillo-Bosch D (2005) In vitro preparation of prefibrillar intermediates of amyloid-beta and alpha-synuclein. Methods Mol Biol 299:19-33.

Lashuel HA, Hartley D, Petre BM, Walz T, Lansbury PT, Jr. (2002a) Neurodegenerative disease: amyloid pores from pathogenic mutations. Nature 418:291.

Lashuel HA, Lansbury PT, Jr. (2006) Are amyloid diseases caused by protein aggregates that mimic bacterial pore-forming toxins? Q Rev Biophys 39:167-201.

Lashuel HA, Petre BM, Wall J, Simon M, Nowak RJ, Walz T, Lansbury PT, Jr. (2002b) Alpha-synuclein, especially the Parkinson's disease-associated mutants, forms pore-like annular and tubular protofibrils. J Mol Biol 322:1089-1102.

Lee HJ, Choi C, Lee SJ (2002) Membrane-bound alpha-synuclein has a high aggregation propensity and the ability to seed the aggregation of the cytosolic form. J Biol Chem 277:671-678.

Levin J, Bertsch U, Kretzschmar H, Giese A (2005) Single particle analysis of manganese-induced prion protein aggregates. Biochemical and Biophysical Research Communications 329:1200-1207.

Masliah E, Rockenstein E, Veinbergs I, Mallory M, Hashimoto M, Takeda A, Sagara Y, Sisk A, Mucke L (2000) Dopaminergic loss and inclusion body formation in ?-synuclein mice: Implications for neurodegenerative disorders. Science 287:1265-1269.

Mason RP, Trumbore MW, Pettegrew JW (1996) Molecular membrane interactions of a phospholipid metabolite. Implications for Alzheimer's disease pathophysiology. Ann N Y Acad Sci 777:368-373.

Mattson MP, Chan SL (2001) Dysregulation of cellular calcium homeostasis in Alzheimer's disease: bad genes and bad habits. J Mol Neurosci 17:205-224.

Muller WE, Koch S, Eckert A, Hartmann H, Scheuer K (1995) beta-Amyloid peptide decreases membrane fluidity. Brain Res 674:133-136.

Nuscher B, Kamp F, Mehnert T, Odoy S, Haass C, Kahle PJ, Beyer K (2004) Alpha-synuclein has a high affinity for packing defects in a bilayer membrane: a thermodynamics study. J Biol Chem 279:21966-21975.

Orlova EV, Rahman MA, Gowen B, Volynski KE, Ashton AC, Manser C, van HM, Ushkaryov YA (2000) Structure of alpha-latrotoxin oligomers reveals that divalent cation-dependent tetramers form membrane pores. Nat Struct Biol 7:48-53.

Park JY, Lansbury PT, Jr. (2003) Beta-synuclein inhibits formation of alpha-synuclein protofibrils: a possible therapeutic strategy against Parkinson's disease. Biochemistry 42:3696-3700.

Polymeropoulos MH, Lavedan C, Leroy E, Ide SE, Dehejia A, Dutra A, Pike B, Root H, Rubenstein J, Boyer R, Stenroos ES, Chandrasekharappa S, Athanassiadou A, Papapetropoulos T, Johnson WG, Lazzarini AM, Duvoisin RC, Di IG, Golbe LI, Nussbaum RL (1997) Mutation in the alpha-synuclein gene identified in families with Parkinson's disease. Science 276:2045-2047.

Pountney DL, Voelcker NH, Gai WP (2005) Annular alpha-synuclein oligomers are potentially toxic agents in alpha-synucleinopathy. Hypothesis. Neurotox Res 7:59-67.

Rochet JC, Conway KA, Lansbury PT, Jr. (2000) Inhibition of fibrillization and accumulation of prefibrillar oligomers in mixtures of human and mouse alpha-synuclein. Biochemistry 39:10619-10626.

Singleton AB, et al. (2003) alpha-Synuclein locus triplication causes Parkinson's disease. Science 302:841.

Tsigelny IF, Bar-On P, Sharikov Y, Crews L, Hashimoto M, Miller MA, Keller SH, Platoshyn O, Yuan JX, Masliah E (2007) Dynamics of alpha-synuclein aggregation and inhibition of pore-like oligomer development by beta-synuclein. FEBS J 274:1862-1877.

Uversky VN, Li J, Fink AL (2001) Metal-triggered structural transformations, aggregation, and fibrillation of human alpha-synuclein. A possible molecular NK between Parkinson's disease and heavy metal exposure. J Biol Chem 276:44284-44296.

Valeva A, Palmer M, Bhakdi S (1997) Staphylococcal alpha-toxin: formation of the heptameric pore is partially cooperative and proceeds through multiple intermediate stages. Biochemistry 36:13298-13304.

Volles MJ, Lansbury PT, Jr. (2002) Vesicle permeabilization by protofibrillar alpha-synuclein is sensitive to Parkinson's disease-linked mutations and occurs by a pore-like mechanism. Biochemistry 41:4595-4602.

Volles MJ, Lee SJ, Rochet JC, Shtilerman MD, Ding TT, Kessler JC, Lansbury PT, Jr. (2001) Vesicle permeabilization by protofibrillar alpha-synuclein: implications for the pathogenesis and treatment of Parkinson's disease. Biochemistry 40:7812-7819.

Wallace AJ, Stillman TJ, Atkins A, Jamieson SJ, Bullough PA, Green J, Artymiuk PJ (2000) E. coli hemolysin E (HlyE, ClyA, SheA): X-ray crystal structure of the toxin and observation of membrane pores by electron microscopy. Cell 100:265-276.

Wolff M, Haasen D, Merk S, Kroner M, Maier U, Bordel S, Wiedenmann J, Nienhaus GU, Valler M, Heilker R (2006) Automated high content screening for

phosphoinositide 3 kinase inhibition using an AKT 1 redistribution assay. Comb Chem High Throughput Screen 9:339-350.

Wood SJ, Wypych J, Steavenson S, Louis JC, Citron M, Biere AL (1999) alpha-synuclein fibrillogenesis is nucleation-dependent. Implications for the pathogenesis of Parkinson's disease. J Biol Chem 274:19509-19512.

Zarranz JJ, Alegre J, Gomez-Esteban JC, Lezcano E, Ros R, Ampuero I, Vidal L, Hoenicka J, Rodriguez O, Atares B, Llorens V, Gomez TE, del Ser T, Munoz DG, de Yebenes JG (2004) The new mutation, E46K, of alpha-synuclein causes Parkinson and Lewy body dementia. Ann Neurol 55:164-173.

Zemanova L, Schenk A, Hunt N, Nienhaus GU, Heilker R (2004) Endothelin receptor in virus-like particles: ligand binding observed by fluorescence fluctuation spectroscopy. Biochemistry 43:9021-9028.

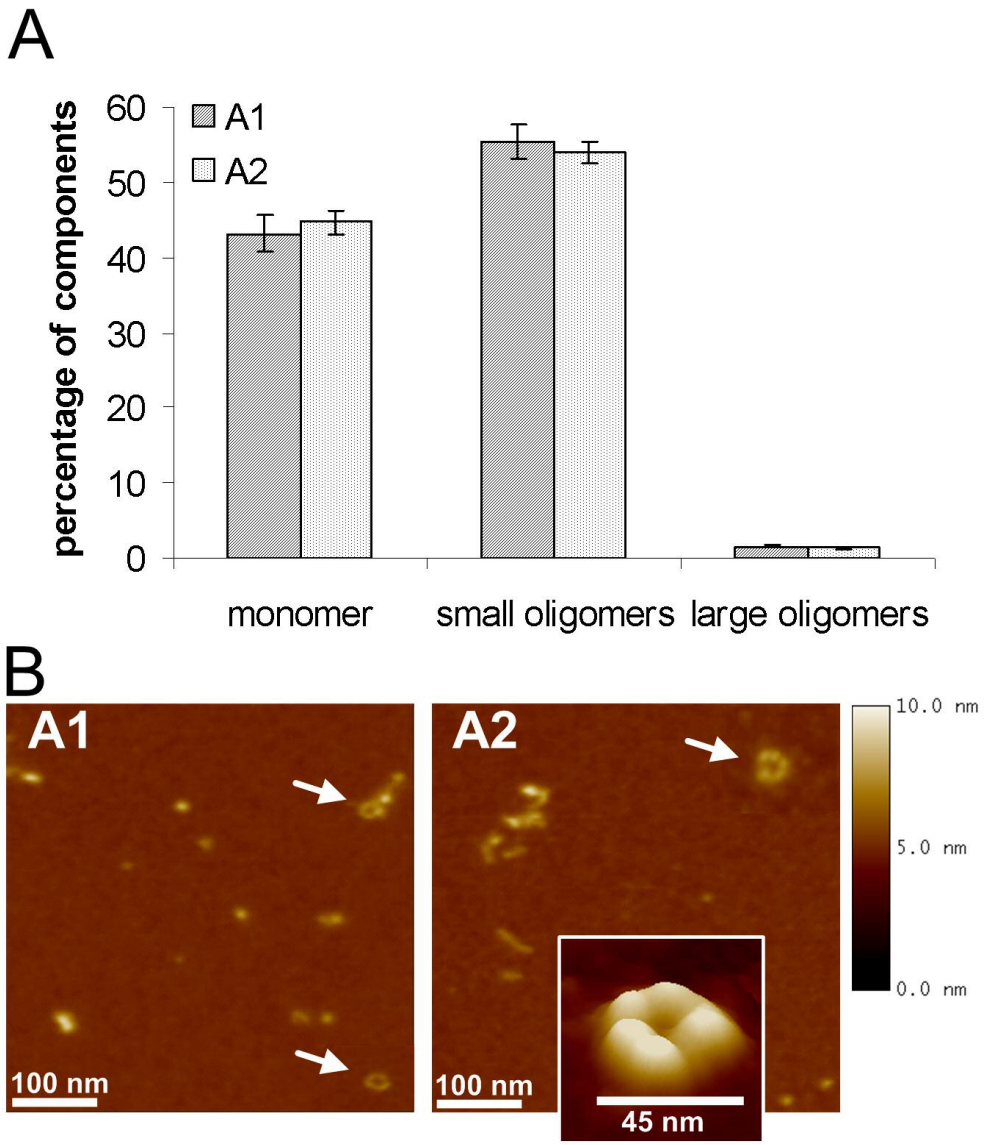

Fig. 1 : Characterisation of long-term incubated of α-syn oligomers (type A1 and A2) A, FIDA analysis of two oligomeric α-syn forms generated after long-term incubation (6 days) in 50 mM sodium phosphate buffer. The influence of ferrous chloride has been worked out (type A1 without ferrous chloride and type A2 with ferrous chloride). Means +/- SEM of five measurements are shown. B, AFM images (500 nm x 500 nm) of type A1 and A2 oligomeric α-syn forms generated after long-term incubation (6 days) in 50 mM sodium phosphate buffer. Section analysis revealed globular or protofibrilar oligomers from 2 to 6 nm in height. Also annular structures (arrows) were found in both oligomer types A1 and A2. AFM images are representative examples of several AFM images of independent oligomer preparations.

85x103mm (400 x 400 DPI)

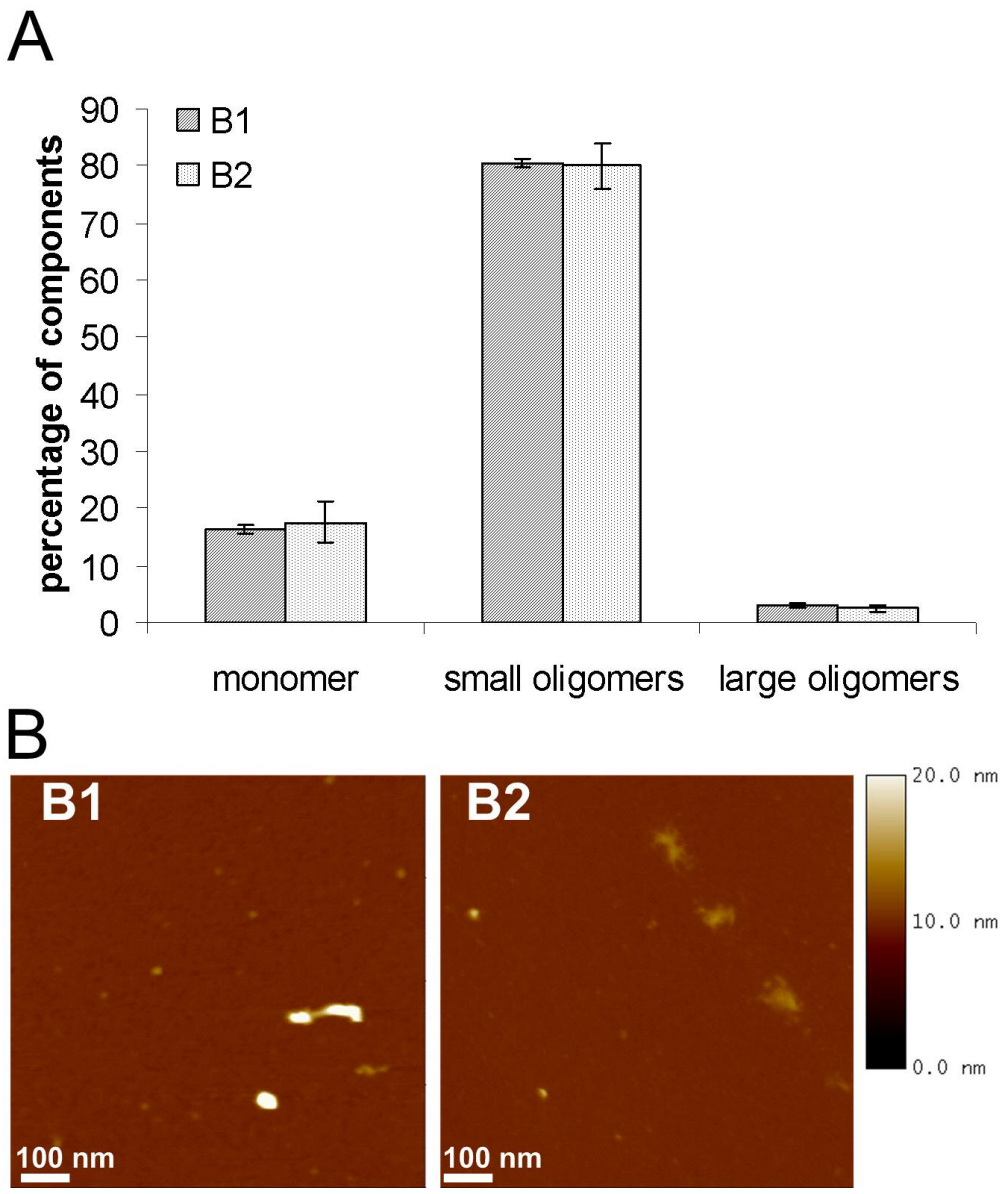

Fig. 2 : Characterisation of α-syn oligomers type B1 and B2 generated with stirring bars A, Single particle analysis revealed two oligomeric forms generated with stirring bars. The influence of ferrous chloride has been worked out (type B1 without ferrous chloride and type B2 with ferrous chloride).B, AFM images (1 µm2) of two oligomeric forms generated with stirring bars. Oligomers appeared as heterogenous population with particles from 3-23 nm in height using section analysis. Oligomer type B1 appeared in a more compact spherical form than oligomer type B2. AFM images are representative examples of several AFM images of independent oligomer preparations.
85x102mm (400 x 400 DPI)

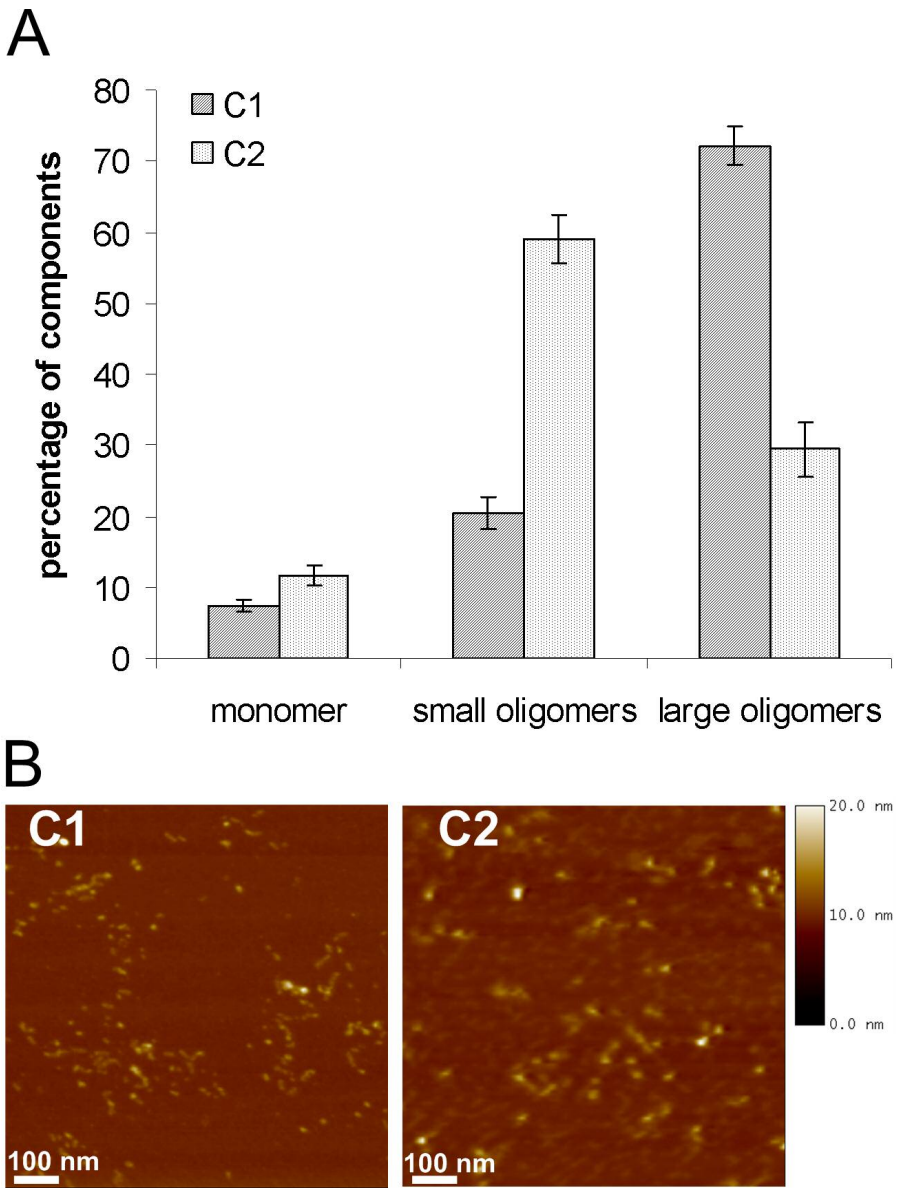

Fig. 3 : Characterisation of α-syn oligomers (type C1 and C2) A, Single particle analysis of two oligomeric α-syn forms generated by overnight incubation and ultrafiltration. The influence of ferrous chloride has been analyzed (type C1 without ferrous chloride and type C2 with ferrous chloride).B, AFM images (1 µm2) of two oligomeric α-syn forms generated by overnight incubation and ultracentrifugation. Images showed globular and protofibrillar oligomer structures with 4-10 nm in height. Using AFM analysis there were no significant morphological differences detectable between oligomer type C1 and oligomer type C2. AFM images are representative examples of several AFM images of independent oligomer preparations.
85x110mm (400 x 400 DPI)

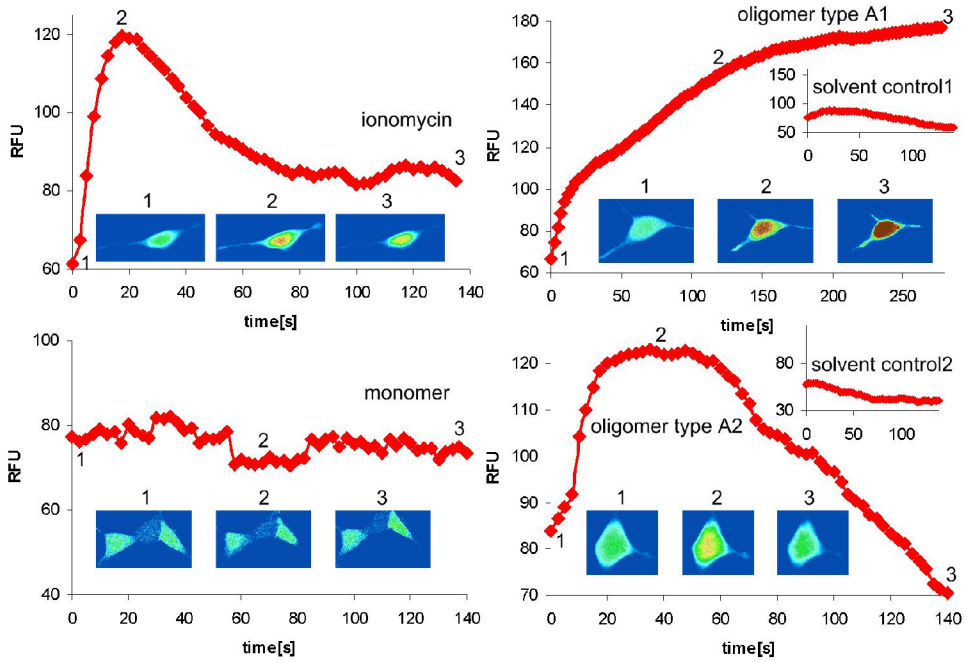

Fig. 4: [Ca2+] elevation by α-syn oligomers type A1 and A2 in SH-SY5Y cells Traces show [Ca2+] dependant fluorescence of single SH-SY5Y cells overexpressing α-syn[wt] in response to 6 µM ionomycin, 0.1 mg/ml monomer, 0.1 mg/ml oligomer type A1 and A2 with respective solvent controls. Oligomers type A1 and A2 evoked a clear increase in intracellular [Ca2+]. Fluorescence records illustrating typical responses to different treatments starting at the time point of application. The inset images of the cell were captured at the times indicated during the trace and are depicted on a pseudo colour scale with □warmer□ colours on a rainbow scale corresponding to higher fluorescence. The inset images show representatives of a single cell.
116x81mm (400 x 400 DPI)

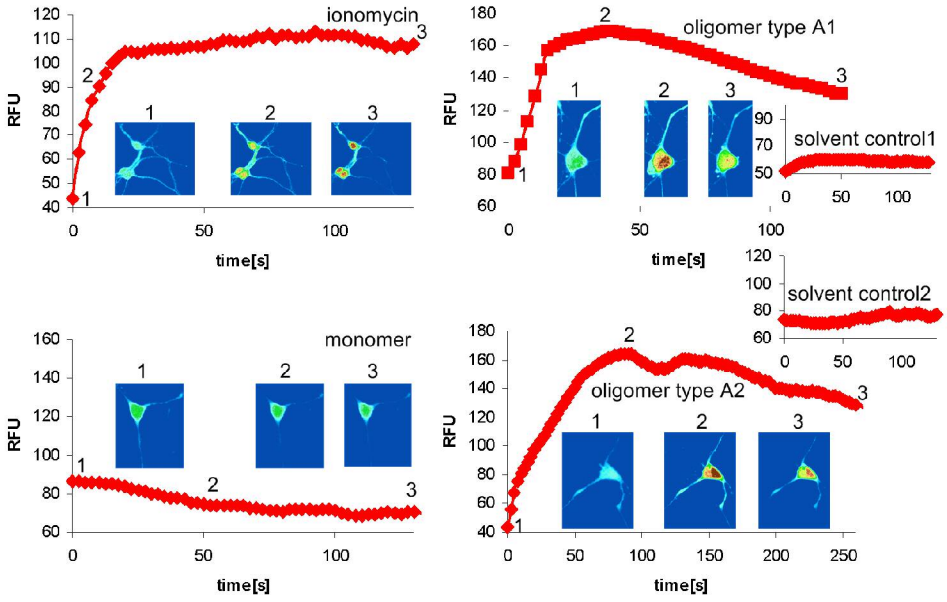

Fig. 5: [Ca2+] elevation by α-syn oligomers type A1 and A2 in primary neurons Traces show [Ca2+] dependant fluorescence of single cortical neurons in response to 6 µM ionomycin, 0.1 mg/ml monomer, 0.1 mg/ml oligomer type A1 and A2 with respective solvent controls. Oligomers type A1 and A2 evoked a clear increase in intracellular [Ca2+]. Fluorescence records illustrating typical responses to the different treatments starting at the time point of application. The inset images show pseudo colour representatives of a single cell, captured at the times indicated by the trace.
116x74mm (400 x 400 DPI)

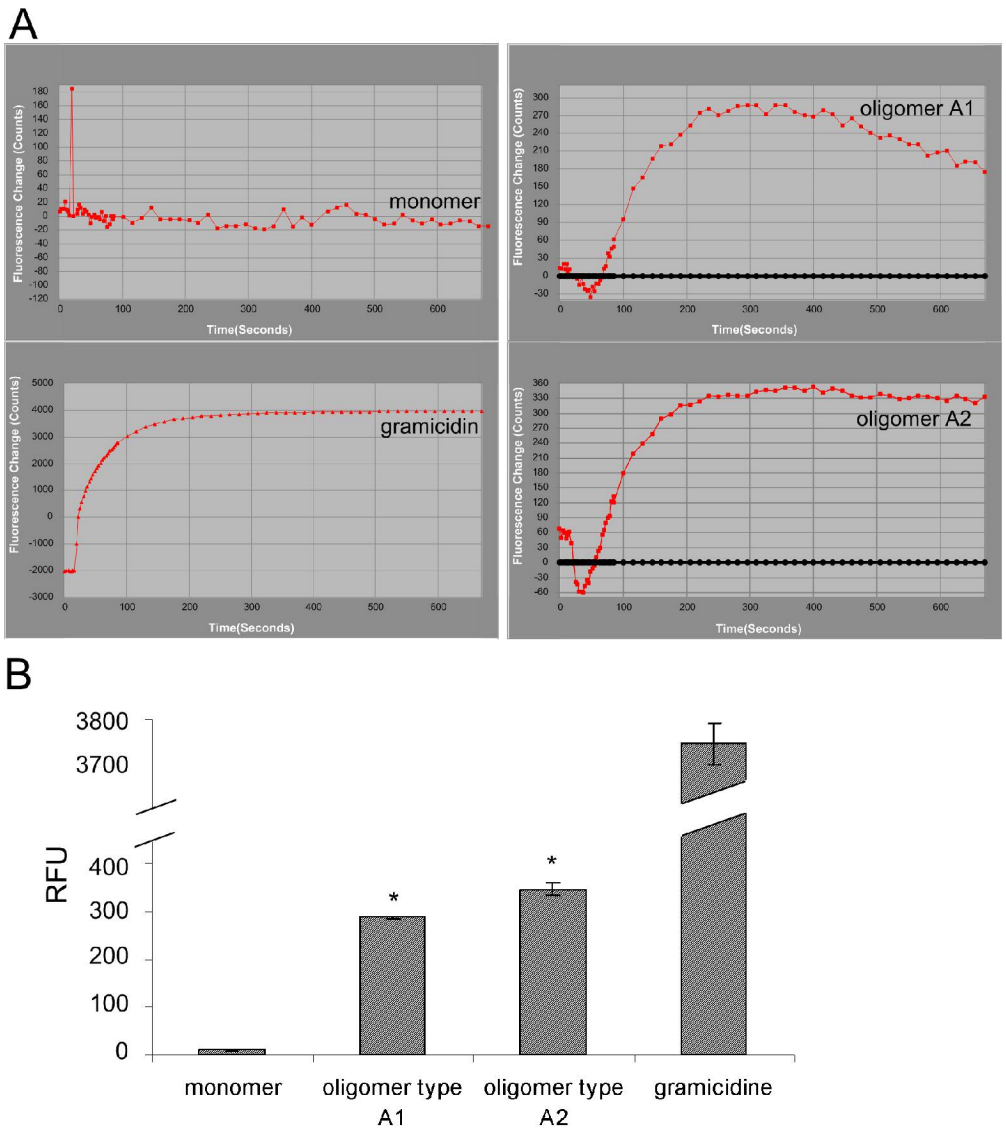

Fig. 6: Depolarisation of membrane potential induced by oligomers type A1 and A2 A, Kinetic plots illustrating typical signal responses to application of 0.1 µg/µl α-syn monomer, oligomers type A1 and A2, and 500 µg/ml gramicidin as positive control. Oligomers type A1 and A2 showed a clear depolarisation of membrane potential. Each trace shows the negative control corrected mean fluorescence of 1.25 x 10 5 primary neurons. B, Quantification of fluorescence intensity in response to oligomer type A1 and A2 induced depolarisation in primary neurons compared to solvent control. Values are the mean +/- SEM; n=3, *P<0.002, one sample t-test against hypothetical value 0. A1 treated neurons: Δ= 286.8 (95% CI: 277.4-296.2); A2 treated neurons: Δ= 345.2 (95% CI: 286.2-404.2)

116x134mm (400 x 400 DPI)

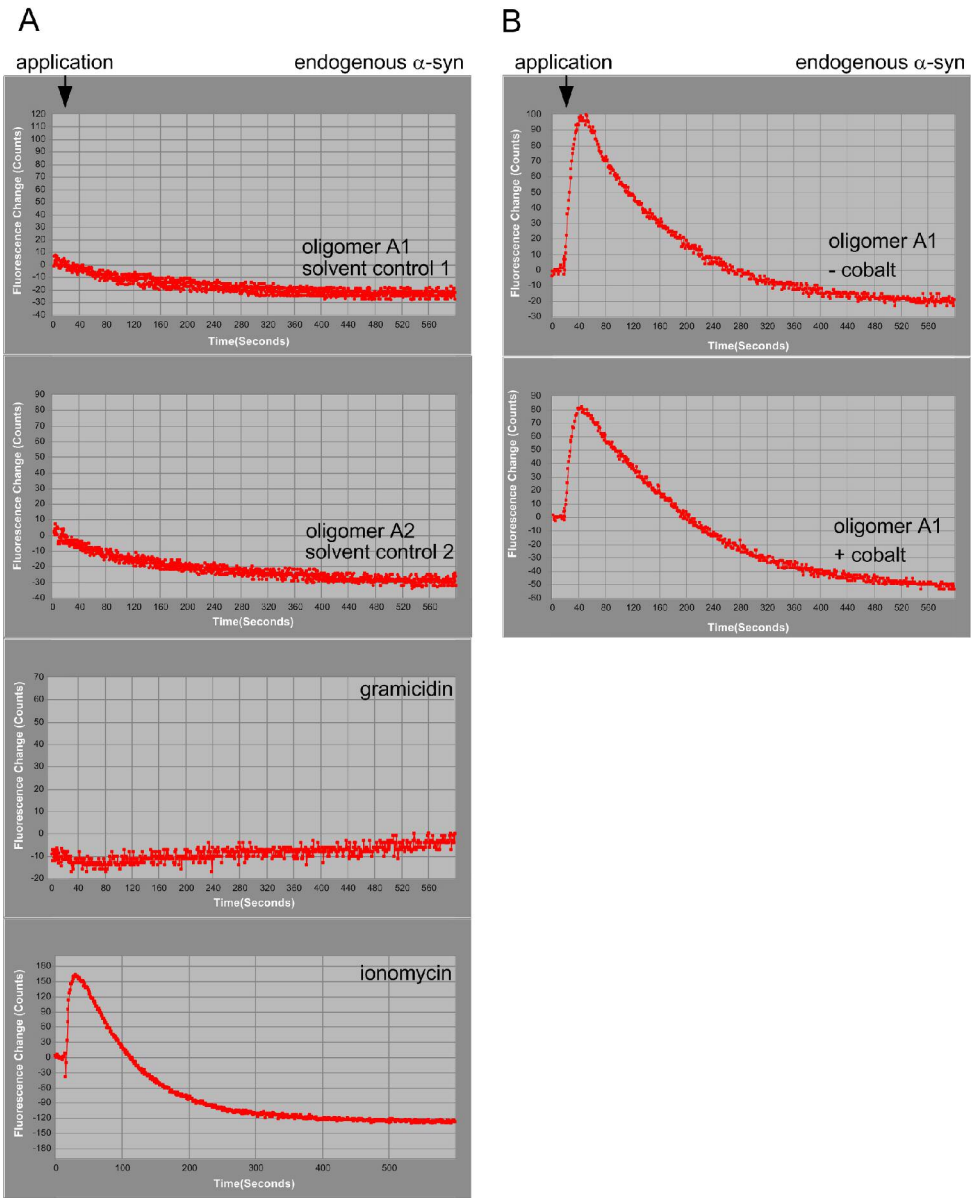

Fig. 7: α-syn oligomer type A1 and A2 induced intracellular [Ca2+] increase via influx of extracellular [Ca2+] sources A, Kinetic plots illustrating typical signal responses to application of 0.1 µg/µl α-syn oligomers type A1 and A2, and positive controls 1.5 µM ionomycin and 500 µg/ml gramicidin in [Ca2+] free extracellular buffer. Each trace shows the mean fluorescence of 6000 mock transfected SH-SY5Y cells expressing endogenous α-syn. Intracellular [Ca2+] signals evoked by oligomers type A1, A2 and gramicidin were completely abolished when cells were incubated in [Ca2+] free extracellular buffer, whereas ionomycin induced [Ca2+] signals were persistent. B, [Ca2+] signals evoked by oligomer type A1 and A2 are not reduced by cobalt, a non specific Ca2+ channel blocker. Each trace shows typical mean fluorescence of 6000 mock transfected SH-SY5Y cells following addition of oligomers type A1 in the presence and absence of cobalt. Oligomers type A showed a clear calcium channel independent increase

in intracellular [Ca2+]. This experiment was repeated 2 times and showed similar results.
116x143mm (400 x 400 DPI)

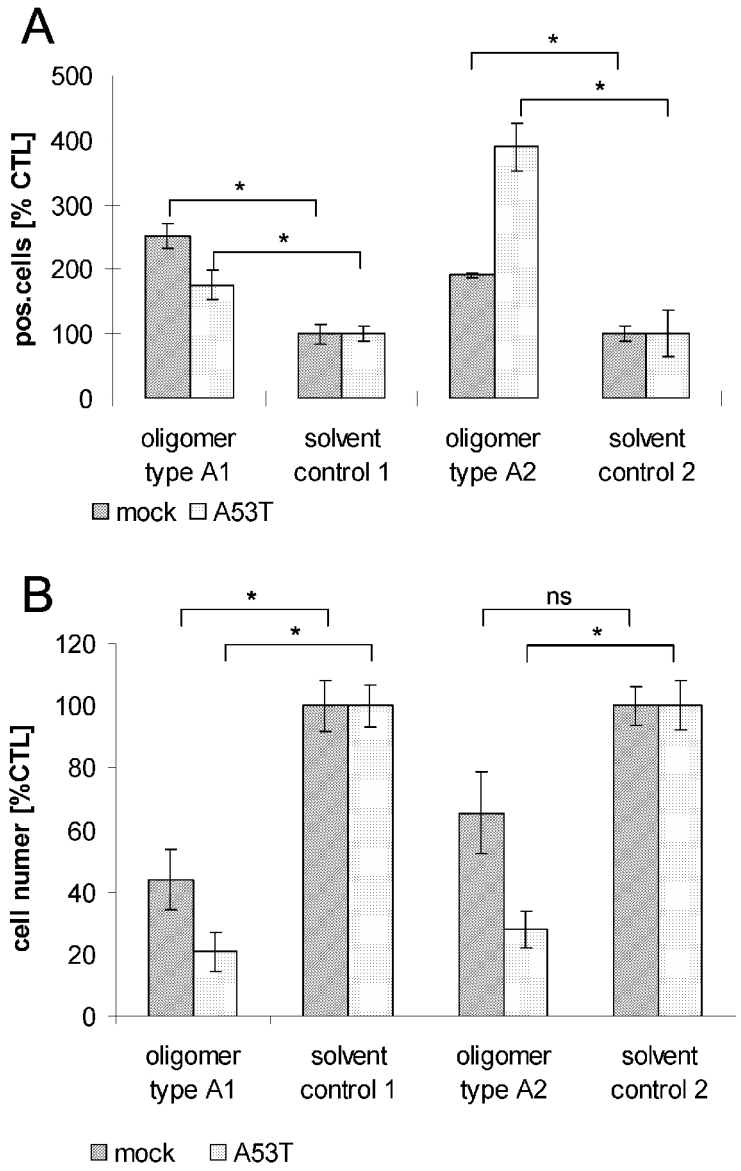

Fig. 8 : Toxicity of α-syn oligomers type A1 and A2 A, Quantification of Caspase 3 activation normalized to corresponding solvent controls; values are the mean +/- SEM; n=3. Treatment of mock transfected SH-SY5Y cells or cells overexpressing α-syn mutant A53T with 0.1 mg/ ml oligomers type A1 and A2 lead to a significant activation of Caspase 3, unpaired t test, *P<0.05 compared with data from corresponding solvent controls: Oligomer type A1 treated: mock: Δ=151 (95% CI: 83.3-218.6); α-syn[A53T]: Δ=75.8 (95% CI: 5.8-145.9); oligomer type A2 treated: mock: Δ=90.9 (95% CI: 54.6-127.2); α-syn[A53T]: Δ=288.9 (95% CI: 147.3-430.5). B, Quantification of cell number reduction normalized to corresponding solvent controls. Values are the mean +/- SEM; n=3. Oligomers type A1 evoked on both mock transfected and stably overexpressing mutant α-syn[A53T] SH-SY5Y cell lines a significant reduction in cell number. Oligomers type A2 lead on overexpressing mutant α-syn[A53T] SH-SY5Y cells to a significant

reduction in cell number, unpaired t-test, *P<0.05 compared with data from corresponding solvent controls: Oligomer type A1 treated: mock: Δ=-56 (95% CI: -91.5 to -20.5); α-syn [A53T]: Δ=-79.3 (95% CI: -104.9 to -53.62); oligomer type A2 treated: mock: Δ=-34.6 (95% CI: -75.6 to-6.5); α-syn[A53T]: Δ=-72.1 (95% CI: -99.4 to- 44.7). Both oligomer types mediated their toxicity after 24h.

85x125mm (600 x 600 DPI)

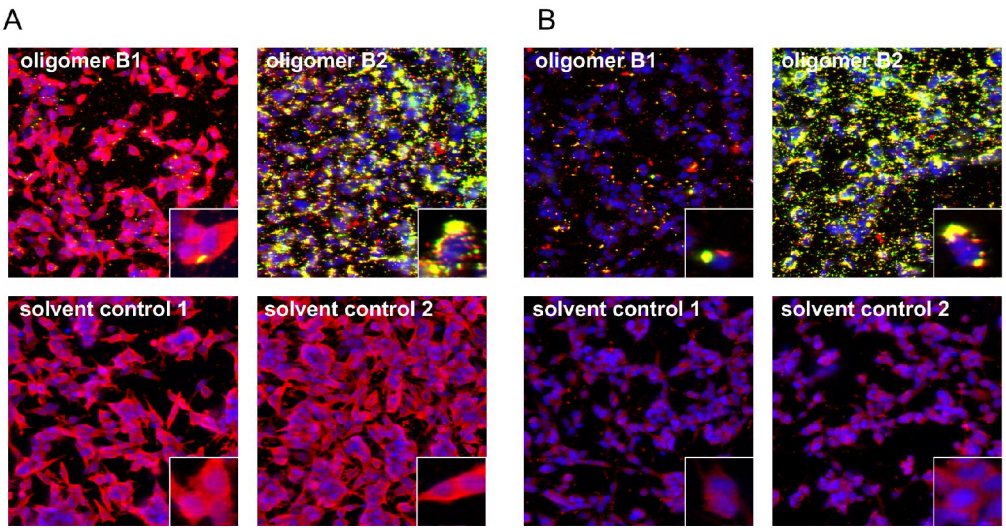

Fig. 9: Seeding effect of α-syn oligomers type B1 and B2 Immunocytochemical staining of α-syn with ASY-1 antibody (in red) after treatment with 0.1 mg/ml Alexa-488 labelled oligomers type B1 and B2 (in green) or solvent controls. Confocal images showed a reduction in cytoplasmic staining of α-syn and an increase in cell associated aggregates (seeding) in SH-SY5Y stably overexpressing α-syn[A53T] (A) or mock transfected SH-SY5Y with endogenous expression of α-syn (B) when treated with oligomer type B2. Oligomer type B2 had a higher potential to seed aggregate formation than oligomer type B1. This experiment was repeated two times and showed similar results.
116x61mm (400 x 400 DPI)

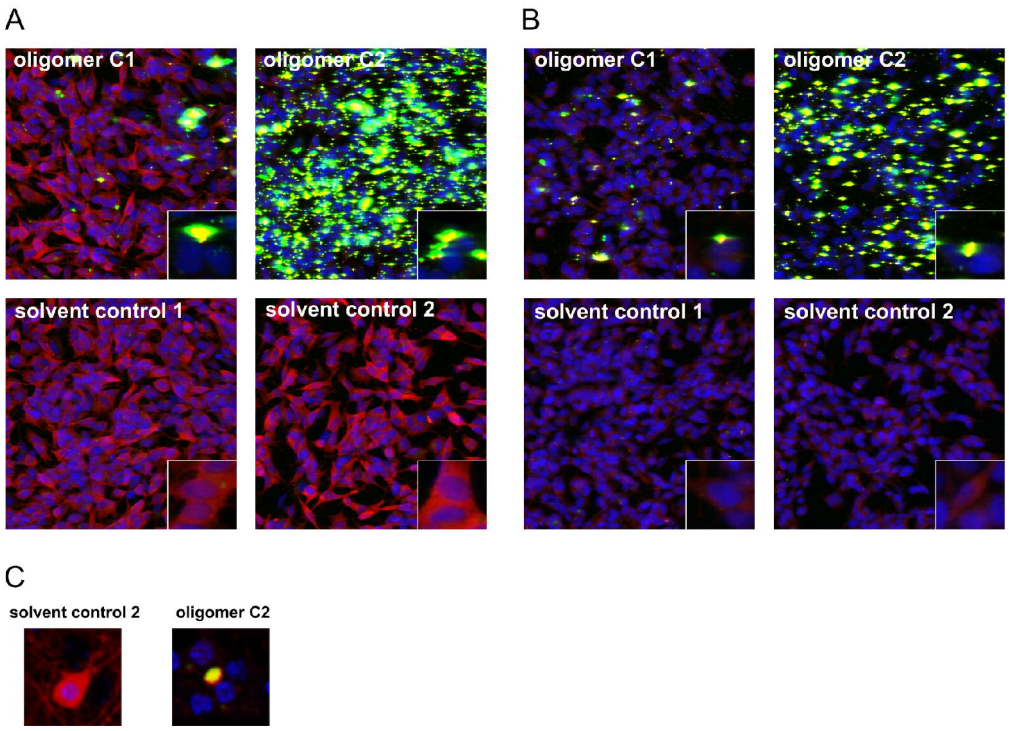

Fig. 10 : Seeding effect of α-syn oligomers type C1 and 2 Immunocytochemical staining of α-syn with ASY-1 antibody (in red) after treatment with 0.1 mg/ml Alexa-488 labelled oligomers type C1 and C2 (in green) or solvent controls. Confocal images showed a reduction in cytoplasmic staining of α-syn and an increase in cell associated aggregates (seeding) in SH-SY5Y stably overexpressing α-syn mutant A53T (A) or mock transfected SH-SY5Y cells (B) treated with oligomer type C2. Oligomer type C2 had a higher potential to trigger aggregate formation than oligomer type C1. This experiment was repeated two times and showed similar results. C, Also primary cortical neurons showed a decrease in cytoplasmic staining of α-syn (red) and remarkable cell associated α-syn aggregate formation (yellow).
116x84mm (400 x 400 DPI)

oligomer type	annular structures	particles >5 nm in height	calcium influx	cell death	caspase activation	seeding
A1	+	-	+	+	+	-
A2	+	-	+	+	+	-
B1	-	+	-	-	-	+
B2	-	+	-	-	-	++
C1	-	+	-	-	-	+
C2	-	+	-	-	-	++

116x30mm (600 x 600 DPI)

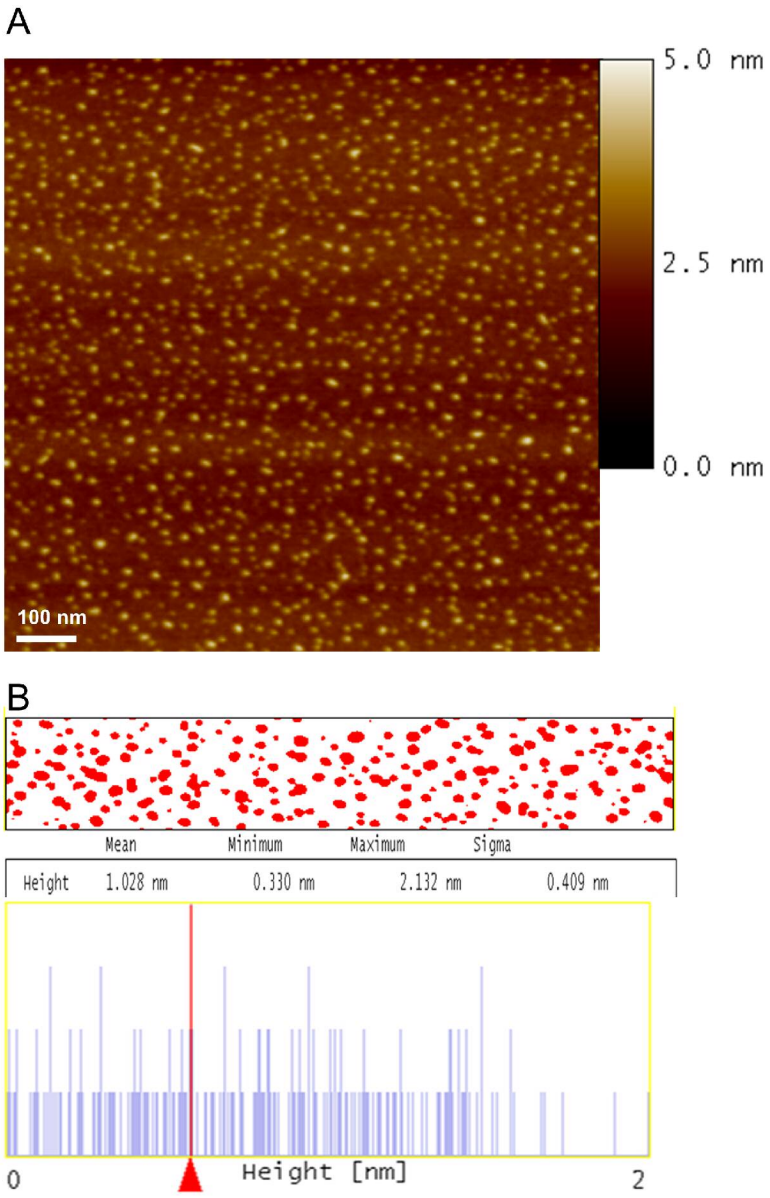

Supplemental Fig. 1: AFM image of monomeric α-syn A, The lyophilized protein was freshly dissolved in 50mM sodium phosphate buffer at a concentration of 1 nM. The corresponding height images (1 µm2) showed almost exclusively particles of 0.8 -1 nm in height. B, Size distribution of monomeric α-syn Quantitative size distribution analysis of α-syn particles reveal average heights of 1 nm indicating that monomeric species had adsorbed on muscovite mica surface. Particle analysis was performed by the NanoScope data processing software (Digital Instruments, Santa Barbara, CA, USA) corrected for tilting and bowing of the substrate.
116x172mm (400 x 400 DPI)

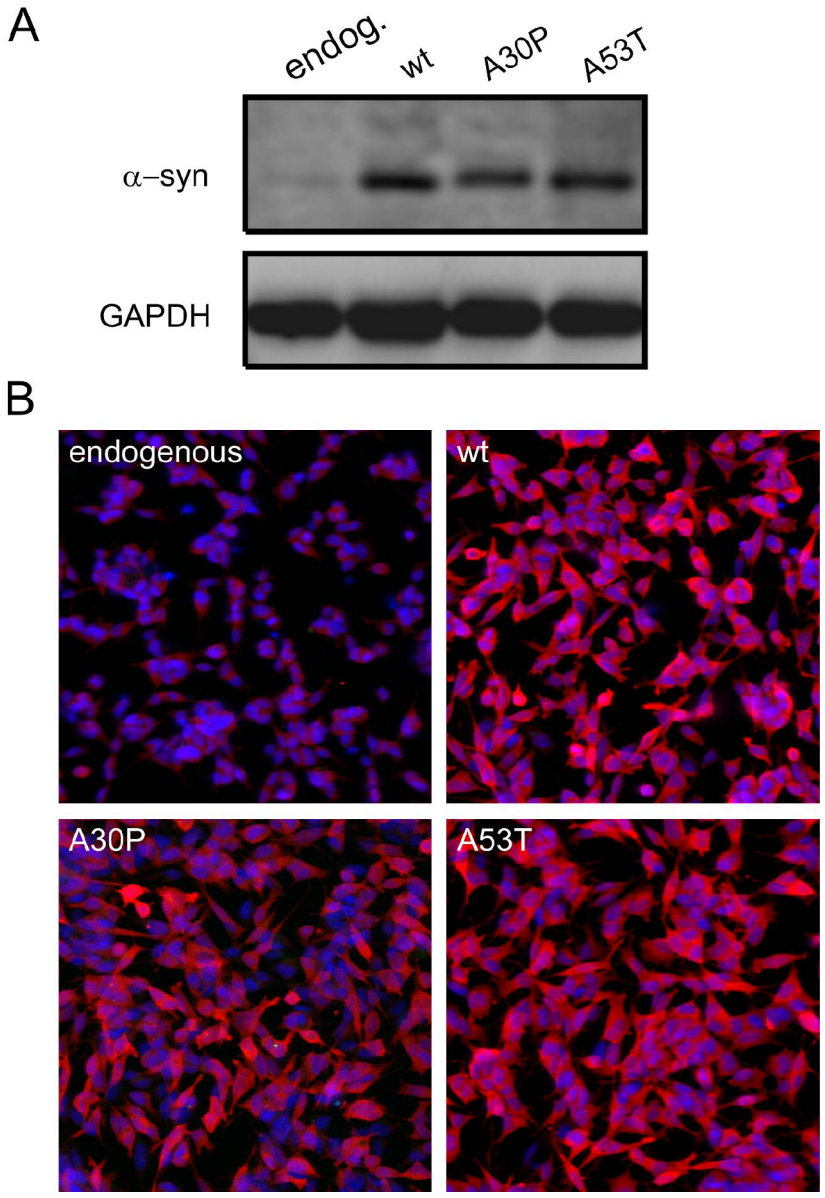

Supplemental Fig. 2: Expression levels of α-syn in SH-SY5Y cells A, Mock transfected and SH-SY5Y cells overexpressing α-syn[wt, A30P, A53T] were lysed, and proteins were resolved by 4-12% SDS PAGE. Lysates were Western blotted using polyclonal α-syn antibody ASY-1. Equal protein loading was verified using an anti GAPDH antibody (loading control). B, Laser confocal microscope images of mock transfected and SH-SY5Y cells overexpressing α-syn[wt, A30P, A53T]. Cells were immunostained with the α-syn antibody ASY-1 (red).
85x125mm (400 x 400 DPI)

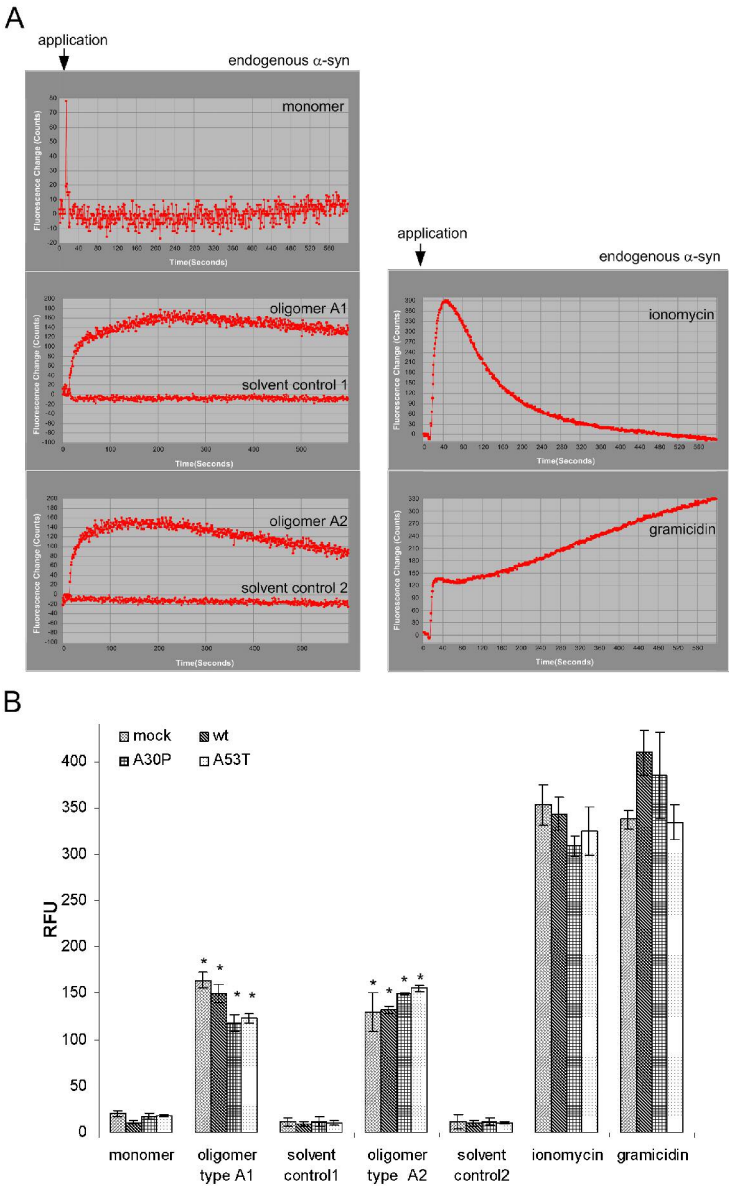

Supplemental Fig. 3: [Ca2+] elevation by α-syn oligomers type A1 and A2 in SH-SY5Y cells A, Kinetic plots illustrating typical signal responses to application of 0.1 µg/µl α-syn monomer, oligomers type A1 and A2, and 1.5 µM ionomycin and 500 µg/ml gramicidin as positive controls. Oligomers type A1 and A2 evoked a clear increase in intracellular calcium. Each trace shows the negative control corrected mean fluorescence of 6000 mock transfected SH-SY5Y cells expressing endogenous level of α-syn. B, Quantification of [Ca2+] elevation in mock transfected SH-SY5Y cells, cells overexpressing α-syn[wt, A30P, A53T] induced by different treatments. All cell lines showed a clear increase of intracellular [Ca2+] after oligomer treatment compared to the respective solvent controls and α-syn monomeric form. Values are the mean +/- SEM; n=3 ; *P < 0.0001. Bonferroni adjusted p-value for pair wise comparisons versus corresponding solvent controls. Oligomer type A1 treated: mock: Δ=153 (95% CI: 126.6-179.3); α-syn[wt]: Δ=140.8

(95% CI: 114.5-167.1); α-syn[A30P]: Δ=106.6 (95% CI: 80.3-132.9); α-syn[A53T]: Δ=112.5 (95% CI: 86.13-138.8). Oligomer type A2 treated: mock: Δ=118.6 (95% CI: 78.85-158.4); α-syn[wt]: Δ=122.1 (95% CI: 82.31-161.9); α-syn[A30P]: Δ=137.7 (95% CI: 97.96-177.5); α-syn [A53T]: Δ=145.4 (95% CI: 105.6-185.2). The experiments were repeated 4 times, all experiments showed similar results.

116x191mm (400 x 400 DPI)

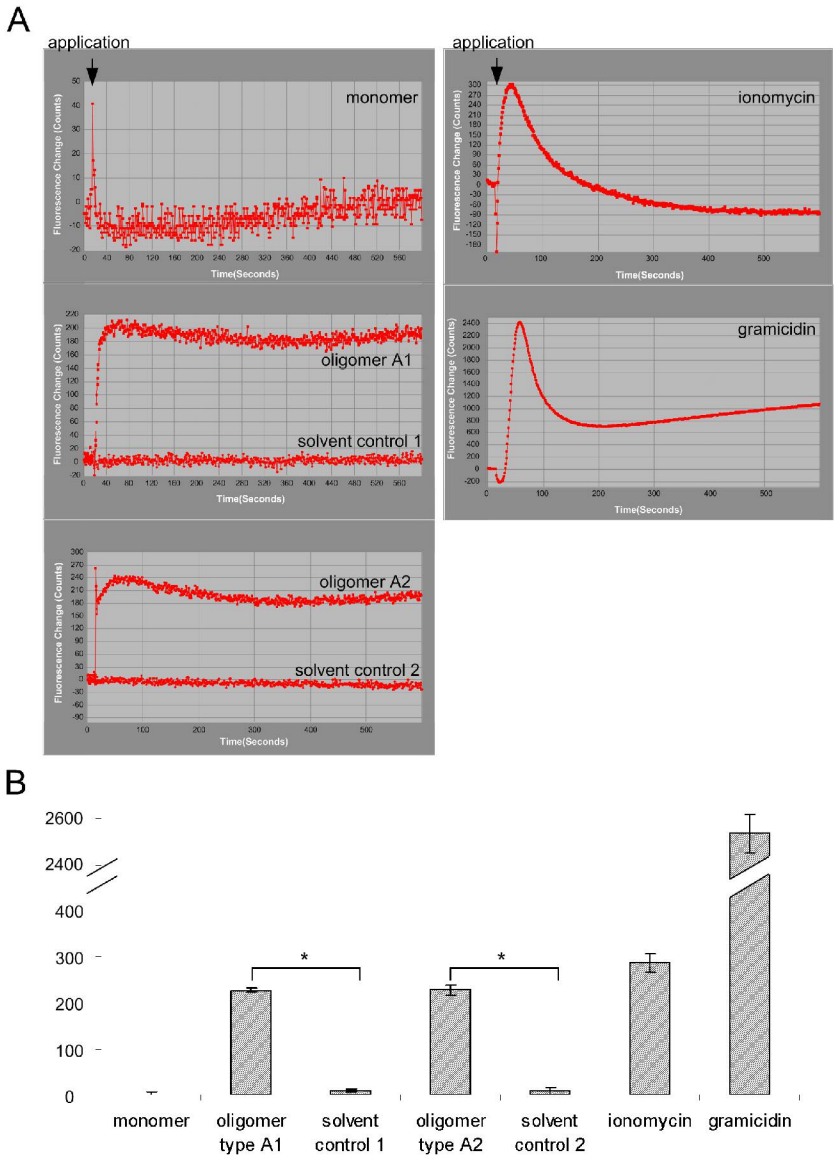

Supplemental Fig. 4: [Ca2+] elevation by α-syn oligomers type A1 and A2 in primary cortical neurons A, Kinetic plots illustrating typical signal responses to application of 0.1 µg/µl α-syn monomer, oligomers A1 and 2, and 1.5 µM ionomycin and 500 µg/ml gramicidin as positive controls. Both oligomer types A1 and A2 increased intracellular [Ca2+] to the same extend compared to the respective solvent controls and α-syn monomeric form. Each trace shows the negative control corrected mean fluorescence of 1.25 x 10 5 primary neurons. B, Quantification of [Ca2+] elevation induced by different treatments. Values are the mean +/- SEM; n=3 ; *P < 0.0001, unpaired t test. Oligomer type A1 treated neurons: Δ= 218.5 (95% CI: 201.0-235.9); Oligomer type A2 treated neurons: Δ= 219.5 (95% CI: 181.7-257.2).
116x164mm (400 x 400 DPI)

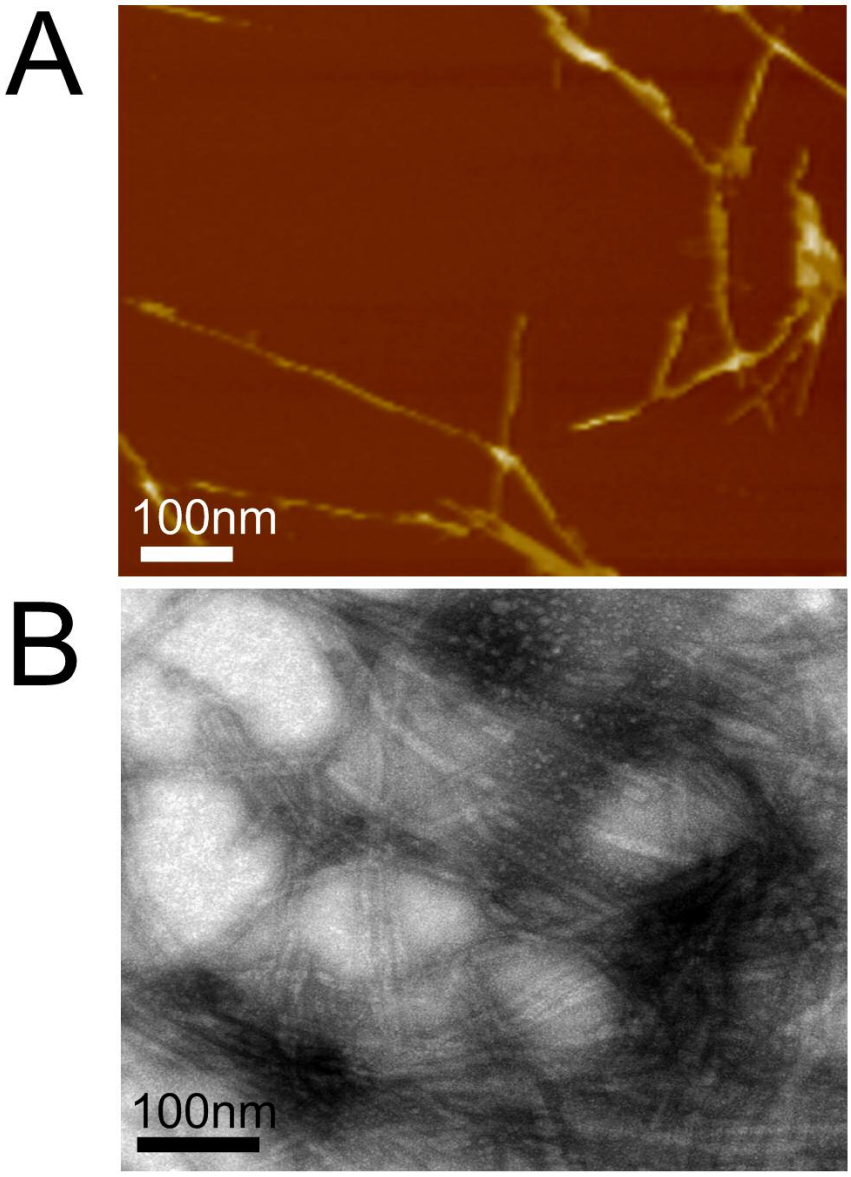

Supplemental Fig. 5: α-syn fibrils A, AFM image of α-syn fibrils. Fibrils of the A type after 1 week prolonged incubation (15days) in 50 mM sodium phosphate buffer. B, Negatively stained transmission electron micrographs of α-syn fibrils after 15 days incubation of approach type A.
61x87mm (400 x 400 DPI)

Functional protein kinase arrays reveal inhibition of p-21 activated kinase 4 by α-synuclein oligomers

Journal:	*Journal of Neurochemistry*
Manuscript ID:	JNC-E-2007-0603.R1
Manuscript Type:	Original Article
Date Submitted by the Author:	n/a
Complete List of Authors:	Danzer, Karin; Boehringer Ingelheim Pharma, CNS Research Schnack, Cathrin; Boehringer Ingelheim Pharma, CNS Research Sutcliffe, Andrew; Procognia, Procognia Hengerer, Bastian; Boehringer Ingelheim Pharma, CNS Research Gillardon, Frank; Boehringer Ingelheim Pharma, CNS Research
Keywords:	Parkinson's disease, protein array, alpha-synuclein, oligomers, p21-activated kinase, LIM kinase

Functional protein kinase arrays reveal inhibition of p-21 activated kinase 4 by α-synuclein oligomers

Karin M. Danzer,[1*] Cathrin Schnack,[1*] Andrew Sutcliffe,[2] Bastian Hengerer,[1] and Frank Gillardon[1]

[1] Boehringer Ingelheim Pharma GmbH & Co KG, 88397 Biberach, Germany

[2] Procognia Limited, Maidenhead, Berkshire SL6 7RJ, UK

[*] these authors contributed equally

Address correspondence to: Dr. Frank Gillardon, Boehringer Ingelheim Pharma GmbH & Co. KG, CNS Research, Birkendorfer Str. 65, 88397 Biberach an der Riss, Germany , Tel.: ++49-7351-548460, Fax: ++49-7351-5498928, E-mail: Frank.Gillardon@bc.boehringer-ingelheim.com

Abstract

There is increasing evidence that aggregation of α-synuclein contributes to the functional and structural deterioration in the central nervous system of Parkinson's disease patients and transgenic animal models. α-Synuclein binds to various cellular proteins and aggregated α-synuclein species may affect their physiological function. In the present study, we used protein arrays spotted with 178 active human kinases for a large scale analysis of the effects of recombinant α-synuclein on kinase activities. Incubation with globular α-synuclein oligomers significantly inhibited autophosphorylation of p21-activated kinase 4 compared to treatment with monomeric α-synuclein or β-synuclein. A concentration-dependent inhibition was also observed in a solution-based kinase assay. To show *in vivo* relevance, we analyzed brainstem protein extracts from α-synuclein(A30P) transgenic mice where accumulation of α-synuclein oligomers has been demonstrated. By immunoblotting using a phospho-specific antibody, we detected a significant decline in phosphorylation of LIM kinase 1, a physiological substrate for p21-activated kinase 4. Suppression of p21-activated kinase activity by amyloid-β oligomers has recently been reported in Alzheimer's disease. Thus, p21-activated kinases may represent a target for various neurotoxic protein oligomers, and signaling deficits may contribute to the behavioural defects in chronic neurodegenerative diseases.

Keywords: Parkinson's disease, protein array, α-synuclein, oligomers, p21-activated kinase, LIM kinase, transgenic mice

Abbreviations: AD, Alzheimer's disease; AFM, atomic force microscopy; LIMK, LIM kinase; MAPK, mitogen-activated protein kinase; PAK, p21-activated kinase; PD, Parkinson's disease; PKC, protein kinase C; ROCK, Rho-associated kinase; SDS-PAGE, sodium dodecyl sulfate-polyacrylamide gel electrophoresis

Introduction

α-Synuclein is a major component of Lewy bodies in Parkinson's disease (PD) and dementia with Lewy bodies, and of glial cytoplasmic inclusions in multiple system atrophy (Goedert 2001; Shults 2006). In the healthy brain, α-synuclein is a natively unfolded, abundant protein that may be involved in neurotransmitter vesicle release. Missense mutations in α-synuclein (A30P, E46K, A53T) are associated with autosomal dominant, familial PD. Mutations in α-synuclein promote formation of oligomeric or fibrillar aggregates *in vitro* (Dev et al. 2003; Lundvig et al. 2005; Shults 2006). Transgenic flies and mice that overexpress mutant α-synuclein in neurons exhibit behavioural and structural alterations that partially mimic PD. The neurotoxic mechanisms of aggregated α-synuclein and the molecular species (oligomers, protofibrils, fibrils) involved are not completely understood. Recent studies have focussed on impairment of the proteasome and lysosome system or dysfunction of mitochondria. On the other hand, numerous proteins have been identified that interact with α-synuclein or become sequestered in Lewy bodies (Dev et al. 2003; Zhou et al. 2004). These interacting proteins may influence aggregation of α-synuclein. Alternatively, their physiological function or subcellular location may be affected depending on the conformation of α-synuclein.

By co-immunopreciptiation or affinity chromatography several protein kinases were shown to bind to α-synuclein. Some of them (e.g. G-protein-coupled receptor kinase 5, dual specificity tyrosine-regulated kinase 1A) phosphorylate α-synuclein, thus enhancing aggregation and neurotoxicity (Arawaka et al. 2006; Kim et al. 2006). By contrast, the activity of other kinases that interact with α-synuclein (e.g. extracellular signal-regulated kinase 1/2, p38 mitogen-activated protein kinase, c-Jun N-terminal kinase, and various protein kinase C isoforms) is suppressed in overexpressing cell lines suggesting that attenuation of kinase signaling may contribute to α-synuclein-mediated neurodegeneration (Ostrerova et al. 1999; Iwata et al. 2001). Notably, a loss-of-function mutation in protein kinase C γ (PKCγ) in rats causes a Parkinsonian syndrome (Craig et al. 2001). The conformation of α-synuclein in these

transfected cell lines has not been investigated in detail. Overexpression of wildtype and mutant α-synuclein inhibited kinase activity with similar efficacy, and only monomeric α-synuclein was detected in cell lysates by sodium dodecyl sulfate-polyacrylamide gel electrophoresis (SDS-PAGE) and immunoblotting (Ostrerova et al. 1999; Iwata et al. 2001). However, it is conceivable that SDS-sensitive α-synuclein oligomers were formed in these overexpressing cells as has been shown by others (Mazzulli et al. 2006). In order to understand the putative pathophysiological effects of α-synuclein on kinase signaling pathways in more detail, it is important to know whether monomeric and aggregated α-synuclein affects kinase activity differentially. Moreover, a technique that permits simultaneous functional assessement of numerous kinases in the presence of α-synuclein under identical experimental conditions would be advantageous.

Very recently, protein arrays containing 178 unique full-length human protein kinases have become available (Kinome 1.0 protein function arrays, Procognia, Maidenhead, UK). We have tested autophosphorylation of the arrayed kinases in the presence of monomeric or oligomeric recombinant α-synuclein and radioactive ATP. Furthermore, we have assessed protein interaction using fluorescently labeled α-synuclein preparations. Finally, α-synuclein-mediated changes in kinase activity were also evaluated in mutant α-synuclein transgenic mice.

Material and methods

Transgenic mice

Generation of (Thy1)-human[A30P] α-synuclein transgenic mice and their behavioural and biochemical analysis have been described in detail elsewhere (Freichel et al. 2006). Homozygous mice were produced after backcrossing into C57Bl/6 mice. Three female transgenic mice and wildtype control animals 12 months of age were used. All animal procedures were approved by the Federal Animal Care Committee.

Animals were killed by cervical dislocation followed by decapitation. The brains were rapidly removed and placed into ice-cold homogenization buffer containing 50 mM MOPS, pH 7.4, 320 mM sucrose, 0.2 mM dithiothreitol, 100 mM KCl, 0.5 mM $MgCl_2$, 0.01 mM EDTA, 1 mM EGTA, and phosphatase / protease inhibitor cocktails (Roche, Mannheim, Germany). All subsequent steps were performed at 4°C. The brainstem, where α-synuclein oligomers acumulate (Freichel et al. 2006), was microdissected and homogenized in 1:10 (w/v) homogenization buffer with 12 strokes in a Teflon-glass douncer. The homogenate was centrifuged for 10 min at 800xg. An aliquot of the supermatant was taken for protein determination using the modified Bio-Rad protein assay (Bio-Rad, München, Germany) before freezing the sample at -80°C.

Expression of recombinant α-synuclein

Expression and purification of wildtype α-synuclein was performed as previously desribed (Nuscher et al. 2004; Giese et al. 2005). Briefly, a pET-5a/α–synuclein plasmid was used to transform *Escherichia coli* BL21(DE3) pLysS. Expression was induced with isopropyl-ß-D-thiogalactopyranose (Promega, Mannheim, Germany) for 4 h. Cells were harvested, resuspended in 20 mM Tris and 25 mM NaCl, pH 8.0 and lysed by freezing in liquid nitrogen followed by thawing. After boiling for 30 min, the lysate was centrifuged at 17600xg for 15 min at 4°C. The supernatant was passed through a 0.22 µm filter (Millex-GV, Millipore Corp., Bedford, MA, USA), loaded onto a HiTrap Q HP column (5 ml, Amersham Biosciences, Munich, Germany) and eluted with a NaCl gradient (25 mM to 500 mM). The pooled α-synuclein peak fractions were further purified on a Superdex 200 HR10/30 size exclusion column (Amersham Biosciences, Munich, Germany) using 20mM Tris, 25 mM NaCl, pH 8.0 as running buffer. The pooled α-synuclein fractions were concentrated using Vivaspin columns (MWCO 5 kDa, Vivascience, Stonehouse, UK) and equilibrated to water. The protein concentration was determined using a BCA protein quantification kit (Pierce, Rockford, IL, USA). Aliquots were lyophilized and stored at -80°C.

Fluorescent labeling of α-synuclein

Protein labeling using the amino-reactive fluorescent dye Alexa Fluor-488-O-succinimidylester (Molecular Probes Inc., Eugene, USA) was performed according to the manufacturer's protocol. Unbound fluorophores were separated by filtration on PD10 columns (Sephadex G25, Amersham Biosciences, Munich, Germany) equilibrated with 50 mM sodium phosphate pH 7.0. In order to remove preformed aggregates, the stock solution of labeled α-synuclein was subjected to size exclusion chromatography (Sephadex 200, Amersham Biosciences, Munich, Germany).

Preparation of α-synuclein oligomers

Oligomeric α-synuclein (type A2) was prepared as described in detail by Danzer et al. (2007). In short, lyophilized recombinant protein was dissolved to a final concentration of 7 μM in 50 mM Na_2HPO_4 buffer (pH 7.0) containing 20% ethanol and 10 μM $FeCl_3$ (J.T. Baker, Griesheim, Germany). After shaking for 4h, oligomers were re-lyophilized and resuspended in 50 mM Na_2HPO_4 buffer (pH 7.0) containing 10% ethanol. This was followed by shaking for 24h at room temperature in Eppendorf cups with open lids to evaporate residual ethanol. After 6 days incubation at room temperature without shaking and with closed lids, α-synuclein oligomers were analyzed by atomic force microscopy or immunoblotting and subsequently used for kinase assays. Alexa-488 labeled oligomers were prepared using the same protocol from Alexa-488 conjugated monomers.

Atomic Force Microscopy (AFM)

3-6 μl of different α-synuclein preparations diluted to 1 μM were applied to a freshly cleaved muscovite mica substrate (Ted Pella, Redding, USA). After 1 min at room temperature, the mica surface was rinsed several times with 200 μl double distilled water to remove salts and weakly bound proteins. AFM images were recorded on a MultiModeTM SPM (Digital

Instruments, Santa Barbara, USA) equipped with an E-Scanner using etched silicon RTESP NanoProbes (Veeco Instruments, Mannheim, Germany). All measurements were carried out in the tapping mode with scan rates of 0.5 Hz. Images were processed using NanoScope software (Digital Instruments, Santa Barbara, USA).

Functional protein kinase arrays

Full-length human kinases tagged with a biotin-carboxyl carrier protein are expressed in insect cells. The tag is biotinylated only when the fusion protein is correctly folded and enables oriented immobilization on streptavidin-coated glass slides. The development of this approach, using a tag derived from the *E. coli* biotin carboxyl carrier protein, has been described elsewhere (Boutell et al. 2004; Blackburn et al. 2005). Content for the Kinome 1.0 arrays was selected from a set of human proteins with known or predicted kinase activity, defined as the kinome (Manning et al. 2002).

The Kinome 1.0 arrays were treated according to the manufacturer's protocol (Procognia, Maidenhead, UK). In short, the arrays were washed twice for 5 min at 4°C in assay buffer (1.4 mM KH_2PO_4, 4.3 mM Na_2HPO_4, 135 mM NaCl, 2.7 mM KCl, 5% glycerol, 5 mM $MgCl_2$, 1% BSA, pH 7.4). Thereafter, the arrays were overlaid with monomeric or oligomeric α-synuclein (3.5 μM) plus 10 μC_i/μl [γ^{33}]-ATP in 120 μl assay buffer. Monomer preparations were spiked with $FeCl_3$ (10 μM final concentration) immediately before array incubation. The slides were covered with plastic Hybrislips (Grace Biolabs, USA) and incubated at 25°C for 30 min. Subsequently, the arrays were washed with assay buffer and ultra pure water followed by centrifugation at 240xg for 2 min and exposure to phosphoscreens (GE Healthcare, Freiburg, Germany) or X-ray films (Kodak, Rochester, USA).

The phosphoscreens were scanned on a Typhoon 9400 laser scanner (GE Healthcare, Freiburg, Germany) at a resolution of 25 μm. Scanning parameters were optimized to give images in which none of the spots were saturated, but where required additional scanning at higher gain or laser power was performed to visualize weaker spots. 16 bit TIFF images of

the arrays were analysed using Array-Pro Analyzer Version 4.5.1.48 (Media Cybernetics, Silver Spring, USA). The median signal intensity of all spots on the array was exported to a spreadsheet package where the data was pre-processed. A signal to background ratio was calculated for all kinase spots on the array. A background intensity value was generated for each array by calculating the average value of the median intensity for all the negative control replicate spots on the array. For each array the median intensity of all kinase spots was divided by the background value specific for each array to generate the spot specific signal to background ratio. The pre-processed data was then imported into the spreadsheet software supplied with the protein arrays and data analysis was completed. The signal to background ratio was used for all subsequent calculations which involved determining the percentage inhibition of kinase autophosphorylation. The four replicates of all proteins on the array enabled comparison of monomer versus oligomer treatment using a two-tailed paired t-test.

Solution-based kinase assay

Autophosphorylation of GST-tagged p21-activated kinase 4 (PAK4) or His-tagged Rho-associated kinase (ROCK) was assessed in assay buffer (1.4 mM KH_2PO_4, 4.3 mM Na_2HPO_4, 135 mM NaCl, 2.7 mM KCl, 5% glycerol, 5 mM $MgCl_2$, 1% BSA, pH 7.4) containing 1 µM human recombinant kinase, synuclein monomers or oligomers (1 µM, 2 µM, and 5 µM, respectively), and 10 μC_i/µl [γ^{33}]-ATP at 25°C for 30 min. Monomer preparations were spiked with $FeCl_3$ (10 µM final concentration) immediately before administration. The reaction was stopped by adding 4x Laemmli buffer and heating the solution to 70°C for 10 min. Proteins were separated on a 10% SDS-polyacrylamide minigel. Finally, the gel was dried at 70°C in a vacuum gel dryer (Bio-Rad, München, Germany) and exposed to a phosphoscreen (GE Healthcare, Freiburg Germany) for 24 h at -80°C. For colloidal Coomassie post-staining, dried gels were rehydrated in 200 ml rehydration buffer (30% glycerol, 20% methanol, 10% acetic acid) for 1h at room temperature. Thereafter, gels were

fixed in 40% ethanol, 10% acetic acid for 1 hour, and subsequently washed twice with distilled water for 10 min. Protein dye stock solution was diluted 1:4 in 20% methanol and gels were stained in dye working solution (0.025% Coomassie Briliant Blue G250, 0.5% ortho-phosphoric acid, 2.5% ammonium sulphate) overnight. Following several washing steps in 0.1% acetic gels were scanned using a GS-700 imaging densitometer (BioRad, München, Germany).

Immunoblotting

Proteins (20 μg per lane) were separated on 12% polyacrylamide minigels and subsequently transferred to nitrocellulose membranes using a wet transfer system (Bio-Rad, München, Germany). After blocking in buffer containing 20 mM Tris, pH 7.4, 500 mM NaCl, 0.1% Tween 20, and 5% BSA for 90 min, the membranes were incubated overnight with rabbit polyclonal antibodies against phospho-LIM kinase 1(Thr508) or total LIM kinase 1 (LIMK1) (1:1000, Cell Signaling Technology, Beverly, USA) or with rabbit antibodies against full-length α-synuclein (1:500, ASY-1, Jensen et al. 2000). Horseradish peroxidase-conjugated secondary antibodies and enhanced chemiluminescence reagents (ECL kit; GE Healthcare, Freiburg, Germany) were used for detection. Membranes were subsequently stripped in buffer containing 62.5 mM Tris-HCl, pH 6.8, 2% SDS, 100 mM β-mercaptoethanol for 1.5 h at 70°C, washed ten times in Tris-buffered saline and re-probed with a mouse monoclonal anti-glyceraldehyde-3-phosphate dehydrogenase antibody (5 μg/ml, Biotrend, Köln, Germany) as loading control. Densitometric analysis of immunoblots was performed using Quantity One (Bio-Rad, München, Germany).

Results

α-Synuclein oligomers were prepared from recombinant α-synuclein monomers and extensively characterized by biophysical methods (Danzer et al. 2007). Using atomic force microscopy (AFM) globular structures up to 5 nm in height became detectable after

incubation for 6 days (Fig. 1A). Fibrillar structures were only detected after prolonged incubation for 14 days (Fig. 1A). Similar structures were observed by AFM using fluorophore-labeled α-synuclein. Fluorophore labeling and stability of α-synuclein oligomers in array buffer was confirmed by a modified fluorescence correlation spectroscopy technique originally described by Giese et al. 2005 (Fig. 1B). Recombinant α-synuclein preparations were also characterized by immunoblotting where bands of α-synuclein dimers and oligomers were clearly detectable (Fig. 1B). This band pattern resembles data published from α-synuclein(A30P) transgenic mice (Freichel et al. 2006). Using these methods, a mixure of α-synuclein monomers and oligomers (about 50% each) could be detected in the oligomer preparations. Administration of these oligomers (7 μM) to SH-SY5Y cell cultures led to a massive calcium influx, whereas α-synuclein monomers had no effect (Danzer et al. 2007).

Effects on kinase autophosphorylation *in vitro* were assessed by incubating Kinome 1.0 arrays with either monomeric or oligomeric α-synuclein (3.5 μM) and radiolabeled ATP. As shown in Figure 2, α-synuclein oligomers significantly ($p<0.001$, t-test) inhibited autophosphorylation of quadruplicate spots of PAK4 and PKCφ by 80.4 ± 1.4% and 74.5 ± 7.1%, respectively, whereas activities of neighbouring kinases were not affected compared to arrays treated with monomeric α-synuclein. Inhibition of PAK4 activity by α-synuclein oligomers (by 48.9 ± 0.9%) could be confirmed in an independent experiment, whereas attenuation of PKCζ autophosphorylation did not reach significance in the second run. Autophosphorylation of other family members that were present on the arrays (e.g. PAK2, PKCζ) was not significantly suppressed. Treatment with β-synuclein also did not alter activity of arrayed PAK4 and PKCφ (101.4 ± 7.6% and 100.8 ± 1.5%, respectively) compared to monomeric α-synuclein. Alexa Fluor-488 labeled α-synuclein could not be detected on the protein arrays after three washing steps demonstrating that binding to the arrayed kinases is reversible.

A concentration-dependent suppression of PAK4 autophosphorylation (ranging from 40% to 80%) was also detected in two independent solution-based kinase assays where recombinant human PAK4 (1 μM) was incubated with different concentrations of oligomeric α-synuclein and monomeric synucleins (α and β), respectively (Fig. 3A). Phosphorylated synucleins were not detectable in this assay. Autophosphorylation of Rho-associated kinase (ROCK) was not affected by α-synuclein oligomers up to 5 μM (Figure 3B).

In order to demonstrate *in vivo* relevance, we analyzed phosphorylation of the PAK4 substrate LIMK1 (Dan et al. 2001; Zhao et al. 2005) in brains from α-synuclein(A30P) transgenic mice and wildtype controls. Protein lysates were prepared from brainstem tissue, where α-synuclein oligomers have been detected in 12 months old transgenic mice (Freichel et al. 2006). Immunoblotting with antibodies specific for phospho-LIMK1(Thr508) and total LIMK1, respectively, revealed a decline in the ratio of phospho-LIMK1 to total LIMK1 by 74.4 ± 12.0% (mean ± SD, n = 3 per group) in α-synuclein(A30P) overexpressing mice compared to non-transgenic controls (Fig. 4).

Discussion

In previous studies using α-synuclein overexpressing cell lines, a reduction in MAPK and PKC signaling was detected (Ostrerova et al. 1999; Iwata et al. 2001). Here, we used protein arrays containing 178 human protein kinases for a comprehensive *in vitro* analysis of the inhibitory effects of monomeric and oligomeric α-synuclein on kinase activity. The data presented illustrate a novel application of functional protein arrays in basic research and drug discovery (Templin et al. 2003). Our assay is based on the autophosphorylation of the arrayed kinases in the presence of radioactive ATP. Some kinases on the arrays exhibit only weak autophosphorylating activity, probably due to the absence of activating binding partners (e.g. cyclin-dependent kinases) or a high Michaelis-Menten constant for ATP (e.g. p38 MAPK), making analysis difficult. Nevertheless, we could demonstrate that α-synuclein oligomers, but not monomers, suppress autophosphorylation of PKCφ and PAK4. Although

we routinely tested the structure and toxicity of our α-synuclein preparations before application onto kinase arrays, we cannot exclude some variability in the percentage of oligomer species present in different preparations which may explain why inhibition of PKCφ did not reach significance in a second experiment. Autophosphorylation of arrayed PAK4 however, was reproducibly and maximally inhibited by oligomeric α-synuclein compared to monomeric α-synuclein. α-Synuclein level in the cytosolic protein fraction from total brain homogenates amounts to approximately 1.0% (Iwai et al. 1995). Thus, the low micromolar concentrations used in our study may represent physiological concentrations within central neurons. As an additional control we tested β-synuclein which has an identical negatively charged C-terminal domain as α-synuclein, but is not prone to aggregation, since it lacks part of the hydrophobic intermediate region (Goedert, 2001). Inhibition of PAK4 activity by oligomeric α-synuclein was also confirmed in a solution-based kinase assay. In this assay, radiolabeled α-synuclein could not be detected by subsequent SDS-PAGE demonstrating that α-synuclein is not a substrate for PAK4. It remains uncertain, whether α-synuclein aggregates generated in test tubes represent the toxic protein species accumulating in PD brains. Inhibition of PAK signaling in α-synuclein transgenic mice brains (see below) however, indicates that both species target the same kinase.

PAKs were originally identified in a screen for Rho GTPase binding partners in rat brain cytosol. They are classified as conventional (also termed group A) PAKs, consisting of PAK1, PAK2, and PAK3, and non-conventional (group B) PAKs including PAK4, PAK5, and PAK6 (Zhao et al. 2005). Non-conventional PAKs are highly similar in their GTPase-binding domain and kinase domain, but share only about 50% identity with conventional PAKs in these domains. Outside these domains, non-conventional PAKs are completely different from each other and from conventional PAKs. Importantly, non-conventional PAKs lack the kinase inhibitory domain that binds and auto-inhibits the catalytic domain of conventional PAKs (Abo et al. 1998; Qu et al. 2003; Zhao et al. 2005). These differences in primary and secondary structure may underlie the inhibition of PAK4, but not PAK2, on protein kinase arrays by α-

synuclein oligomers. In contrast to conventional PAKs, binding of the GTPase Cdc42 does not stimulate activity of PAK4, but recruits active PAK4 to the Golgi apparatus where it may be involved in controlling of vesicle transport (Abo et al., 1998). Interestingly, fragmentation of the Golgi apparatus has been shown in α-synuclein transduced COS-7 cells containing small prefibrillar aggregates (Gosavi et al. 2002), and an early defect in Golgi vesicular trafficking has recently been reported in α-synuclein overexpressing yeast which was restored by co-expression of a Rab GTPase (Cooper et al. 2006).

Only few substrates for PAK4 have so far been identified. Overexpression of PAK4 in NIH 3T3 cells moderately enhanced activity of c-Jun N-terminal kinase and extracellular signal-regulated kinase (Abo et al. 1998) which may contribute to the reduction of MAPK signaling in α-synuclein overexpressing neuronal cell lines shown by others (Iwata et al. 2001). More importantly, immunopurified PAK4 phosphorylated and activated LIMK1 more strongly than PAK1, and dominant-negative LIMK1 inhibited most of the the cellular changes induced by a constitutively active PAK4 mutant (Dan et al. 2001) demonstrating that LIMK1 is a major downstream effector of PAK4. PAKs phosphorylate LIMK1 at the conserved threonine 508 residue in the activation loop. Using a phospho-specific antibody, we could demonstrate a significant reduction in LIMK1(Thr508) phosphorylation in brainstem lysates from α-synuclein(A30P) overexpressing mice. In adult mutant mice, α-synuclein oligomers accumulate in brainstem areas (Freichel et al. 2006) strongly suggesting that aggregated α-synuclein also inhibits the PAK4 – LIMK1 signaling pathway *in vivo*. LIMK1 is not spotted on the Kinome 1.0 arrays, however, its closest relative LIMK2 is arrayed. Since incubation with α-synuclein oligomers did not affect LIMK2 autophosphorylation, a direct inhibition of LIMK1 by α-synuclein aggregates in these mouse mutants seems unlikely. LIMK1 also becomes phosphorylated at Thr508 by ROCK and similar to PAKs, activity of ROCK is modulated by interaction with Rho family GTPases (Ohashi et al. 2000). On the other hand, autophosphorylation of ROCK was not affected by α-synuclein oligomers in our solution-based kinase assay, and thus, an involvement of ROCK can be excluded.

What are the functional consequences of a loss of PAK4 - LIMK1 signaling? Targeted gene disruption of PAK4 in mice led to embryonic lethality by day 11.5 (Qu et al. 2003). PAK4-deficient embryos show severe defects in the fetal heart and nervous system. Neurite outgrowth and neuronal migration is massively impaired which is probably due to the role for PAK4 in the regulation of the cytoskeleton and the formation of filopodia. Gene knockout of the PAK4 substrate LIMK1 is not lethal, since its expression is mainly restricted to neurons. Adult LIMK1-deficient mice show abnormal spine morphology and altered postsynaptic long-term potentiation, but also changes in presynaptic function pointing to a reduction in neurotransmitter release (Meng et al. 2002). Notably, LIMK1 knockout mice exhibit enhanced locomotor activities, impaired spatial learning, and prolonged freezing in a fear response task which is similar to the behavioural changes in α-synuclein(A30P) overexpressing mice (Freichel et al., 2006). Expression of a dominant-negative PAK transgene in the postnatal forebrain of mice also caused alterations in spine morphology and impairment in memory retention (Hayashi et al. 2004).

Spine loss and memory impairment in mouse mutants with deficits in PAK signaling recently led Cole and coworkers to investigate the PAK pathway in Alzheimer's disease (AD) (Zhao et al. 2006). In their hypothesis-driven approach they concentrated on the conventional PAK isoforms 1, 2, and 3. By immunoblotting using phospho-specific antibodies, they showed a significant reduction in activated PAKs in brain lysates from AD patients and Tg2576 mice overexpressing mutant amyloid precursor protein. Importantly, lowering the brain levels of soluble amyloid-β oligomers in transgenic mice by passive immunization significantly increased the levels of phosphorylated PAK. Moreover, intracerebroventricular infusion with a PAK inhibitor caused memory deficits in adult mice strongly suggesting that PAK signaling defects caused by oligomeric amyloid-β contribute to cognitive dysfunction in AD (Zhao et al. 2006). By protein array technology, we could demonstrate an inhibition of the non-conventional PAK4 by recombinant α-synuclein oligomers and a decline in LIMK1 phosphorylation in α-synuclein(A30P) transgenic mice. Taken together, suppression of PAK

activity may represent a common downstream pathomechanism for various toxic protein oligomer species and a potential therapeutic target both in AD and PD.

Acknowledgements

The authors are grateful to Prof. Christian Haass and Prof. Philipp Kahle for providing α-synuclein transgenic mice and pET-5a plasmids, and to Prof. Philip Cohen for providing recombinant kinases. We thank Anne Karow and Udo Heinzelmann for help with AFM, Armin Giese for help with spectroscopy, and Sandra Felk and Susanne Zach for excellent technical assistance. Karin Danzer thanks Marcus Kostka for scientific support.

References

Abo A., Qu J., Cammarano M. S., Dan C., Fritsch A., Baud V., Belisle B. and Minden A. (1998) PAK4, a novel effector for Cdc42Hs, is implicted in the reorganization of the actin cytoskeleton and in the formation of filopodia. EMBO J. 17, 6527-6540.

Arawaka S., Wada M., Goto S., Karube H., Sakamoto M., Ren C. H., Koyama S., Nagasawa H., Kimura H., Kawanami T., Kurita K., Tajima K. and Kato T. (2006) The role of G-protein-coupled receptor kinase 5 in pathogenesis of sporadic Parkinson's disease. J. Neurosci. 26, 9227-9238.

Blackburn J. M. and Hart D. J. (2005) Fabrication of protein function microarrays for systems-oriented proteomic analysis. Methods Mol. Biol. 310, 197-216.

Boutell J. M., Hart D. J., Godber B. L., Kozlowski R. Z. and Blackburn J. M. (2004) Functional protein microarrays for parallel characterisation of p53 mutants. Proteomics 4, 1950-1958.

Cooper A. A., Gitler A. D., Cashikar A., Haynes C. M., Hill K. J., Bhullar B., Liu K., Xu K., Strathearn K. E., Liu F., Cao S., Caldwell K. A., Caldwell G. A., Marsischky G., Kolodner R. D., LaBaer J., Rochet J. C., Bonini R. M. and Lindquist S. (2006) α-Synuclein blocks ER-Golgi traffic and Rab1 rescues neuron loss in Parkinson's models. Science (in press).

Craig N. J., Alonso M. B. D., Hawker K. L., Shiels P., Glencorse T. A., Campbell J. M., Bennett N. K., Canham M., Donald D., Gardiner M., Gilmore D. P., MacDOnald R: J., Maitland K., McCallion A. S., Russell D., Payne A. P., Sutcliffe R. G. and Davies R. W. (2001) A candidate gene for human neurodegenerative disorders: a rat PKCγ mutation causes a Parkinsonian syndrome. Nat. Neurosci. 4, 1061-1062.

Dan C., Kelly A., Bernard O. and Minden A. (2001) Cytoskeletal changes regulated by the PAK4 serine/theonine kinase are mediated by LIM kinase 1 and cofilin. J. Biol. Chem. 276, 32115-32121.

Danzer K., Haasen, D., Karow A., Moussaut S., Habeck M., Kretzschmar H., Giese A., Hengerer B. and Kostka M. (2007) Different species of alpha-synuclein oligomers induce calcium influx and seeding. J. Neurosci., in press.

Dev K. K., Hofele K., Barbieri S., Buchman V. L. and van der Putten H. (2003) α-Synuclein and its molecular pathophysiological role in neurodegenerative disease. Neuropharmacol. 45, 14-44.

Freichel C., Neumann M., Ballard T., Müller V., Woolley M., Ozmen L., Borroni E., Kretzschmar H. A., Haass C., Spooren W. and Kahle P. J. (2006) Age-dependent cognitive decline and amygdala pathology in α-synuclein transgni mice. Neurobiol. Aging (in press).

Giese A., Bader B., Bieschke J., Schaffar G., Odoy S., Kahle P. J., Haass C. and Kretzschmar H. (2005) Single particle detection and characterization of synuclein co-aggregation. Biochem. Biophys. Res. Comm. 333, 1202-1210.

Goedert M. (2001) Alpha-synuclein and neurodegenerative diseases. Nature Rev. Neurosci. 2, 492-501.

Gosavi N., Lee H. J., Lee J. S., Patel S. and Lee S. J. (2002) Golgi fragmentation occurs in the cells with prefibrillar α-synuclein aggregates and precedes the formation of fibrillar inclusions. J. Biol. Chem. 277, 48984-48992.

Hayashi M. L., Choi S. Y., Rao B. S. S., Jung H. Y., Lee H. K., Zhang D., Chattarji S., Kirkwood A. and Tonegawa S. (2004) Altered cortical synaptic morphology and impaired memory consolidation in forebrain-specific dominant-negative PAK transgenic mice. Neuron 42, 773-787.

Iwai A., Masliah E., Yoshimoto M., Ge N., Flanagan L., Rohan de Silva H. A., Kittel A. and Saitoh T. (1995) The precursor protein of non-Aβ component of Alzheimer's disease amyloid is a presynaptic protein of the central nervous system. Neuron 14, 467-475.

Iwata A., Maruyama M., Kanzawa I. and Nukina N. (2001) α-Synuclein affects the MAPK pathway and accelerates cell death. J. Biol. Chem. 276, 45320-45329.

Jensen P. H., Islam K., Kenney J., Nielsen M. S., Power J. and Gai W. P. (2000) Microtubule-associated protein 1B is a component of cortical Lewy bodies and binds α-synuclein filaments. J. Biol. Chem. 275, 21500-21507.

Kim E. J., Sung J. Y., Lee H. J., Rhim H., Hasegawa M., Iwatsubo T., Min D. S., Kim J., Paik S. R. and Chung K. C. (2006) Dyrk1A phosphorylates α-synuclein and enhances intracellular inclusion formation. J. Biol. Chem. 281, 33250-33257.

Lundvig D., Lindersson E. and Jensen P. H. (2005) Pathogenic effects of α-synuclein aggregation. Mol. Brain Res. 134, 3-17.

Manning G., Whyte D. B., Martinez R., Hunter T. and Sudarsanam S. (2002) The protein kinase complement of the human genome. Science 298, 1912-1934.

Mazzulli J. R., Mishizen A. J., Giasson B. I., Lynch D. R., Thomas S. A., Nakashima A., Nagatsu T., Ota A. and Ischiropoulos H. (2006) Cytosolic catechols inhibit α-synuclein aggregation and facilitate the formation of intracellular soluble oligomeric intermediates. J. Neurosci. 26, 10068-10078.

Meng Y., Zhang Z., Tregoubov W., Janus C., Cruz L., Jackson M., Lu W. Y., MacDonald J. F., Wang J. Y., Falls D. L. and Jia Z. (2002) Abnormal spine morphology and enhanced LTP in LIMK-1 knockout mice. Neuron 35, 121-133.

Nuscher B., Kamp F., Mehnert T., Odoy S., Haass C., Kahle P. J. and Beyer K. (2004) α-Synuclein has a high affinity for packing defects in a bilayer membrane. J. Biol. Chem. 279, 21966-21975.

Ohashi K., Nagata K., Maekawa M., Ishizaki T., Narumiya S., and Mizuno K. (2000) Rho-associated kinase ROCK activates LIM-kinase 1 by phosphorylation at threonine 508 within the activation loop. J. Biol. Chem. 275, 3577-3582.

Ostrerova N., Petrucelli L., Farrer M., Mehta N., Choi P., Hardy J. and Wolozin B. (1999) α-Synuclein shares physical and functional homology with 14-3-3 proteins. J. Neurosci. 19, 5782-5791.

Qu J., Li X., Novitch B. G., Zheng Y., Kohn M., Xie J. M., Kozinn S., Bronson R., Beg A. A. and Minden A. (2003) PAK4 kinase is essential for embryonic viability and for proper neuronal development. Mol. Cell. Biol. 23, 7122-7133.

Shults C. W. (2006) Lewy bodies. Proc. Natl. Acad. Sci. USA 103, 1661-1668.

Templin M. F., Stoll D., Schwenk J. M., Potz O., Kramer S. and Joos T.O. (2003) Protein microarrays: promising tools for proteomic research. Proteomics 3, 2155-2166.

Zhao Z. S. and Manser E. (2005) PAK and other Rho-associated kinases – effectors with surprisingly diverse mechanisms of regulation. Biochem. J. 386, 210-214.

Zhao L., Ma Q. L., Calon F., Harris-White M. E., Yang F., Lim G. P., Morihara T., Ubeda O. J., Ambegaokar S., Hansen J. E., Weisbart R. H., Teter B., Frautschy S. A. and Cole G. M. (2006) Role of p21-activated kinase pathway defects in the cognitive deficits of Alzheimer disease. Nat. Neurosci. 9, 234-242.

Zhou Y., Gu G., Goodlett D. R., Zhang T., Pan C., Montine T. J., Montine K. S., Aebersold R. H. and Zhang J. (2004) Analysis of α-synuclein-associated proteins by quantitative proteomics. J. Biol. Chem. 279, 39155-39164.

Figure Legends

Figure 1. (A) Monomeric, oligomeric, and fibrillar preparations of recombinant human α-synuclein visualized by atomic force microscopy in the tapping mode (each panel 0.5 x 0.5 μm). (B) Fluorophore-conjugated recombinant α-synuclein analyzed by a modified fluorescence correlation spectroscopy method at day 0 (left panel) and after aggregation for 6 days (middle panel). The presence of oligomeric aggregates carrying multiple fluorophores results in an increased number of bins with higher fluorescence intensity.
(Right panel) Immunoblot analysis of α-synuclein oligomer preparations showing the presence of several α-synuclein immunoreactive, high molecular weight bands (lane 1, 2), whereas a predominant monomer band is visible at 14 kDa in an α-synuclein monomer preparation (lane 3).

Figure 2. Magnified section of Kinome 1.0 arrays where autophosphorylation of arrayed kinases has been tested following incubation with recombinant α-synuclein monomers and oligomers, respectively. A decrease in signal intensity is visible on the oligomer-treated array in the four replicate spots of protein kinase C φ (upper row, right sub-array) and p21-activated kinase 4 (middle row, right sub-array). Autophosphorylation of adjacent kinases is unchanged.

Figure 3. (A) (Upper panel) Gel electrophoretic analysis of a solution-based kinase assay where p21-activated kinase 4 (1 μM) was incubated with monomeric α-synuclein (lane 1, 4, 7), oligomeric α-synuclein (lane 2, 5, 8) or monomeric β-synuclein (lane 3, 6, 9) at the concentrations indicated. Autophosphorylation of GST-tagged p21-activated kinase (approximately 90 kDa) is concentration-dependently inhibited by α-synuclein oligomers. (Lower panel) Coomassie post-staining confirms that similar amounts of p21-activated kinase were used.

(B) (Left panel) Activity of Rho-associated kinase is not inhibited by α-synuclein oligomers (lane 2) compared to α-synuclein monomers (lane 1) or β-synuclein (lane 3) (5 μM each). (Right panel) Coomassie post-staining reveals that similar enzyme amounts were tested.

Figure 4. Representative immunoblot analysis of brainstem protein extracts from a α-synuclein(A30P) transgenic (tg) mouse and a wildtype (wt) control animal using antibodies against phospho-LIM kinase 1 and total LIM kinase 1 (LIMK1), respectively. Phosphorylation of LIM kinase 1 at threonine 508, which becomes phosphorylated by p21-activated kinases, is decreased in transgenic mice. Glyceraldehyde-3-phosphate dehydrogenase (GAPDH) was assessed as loading control.

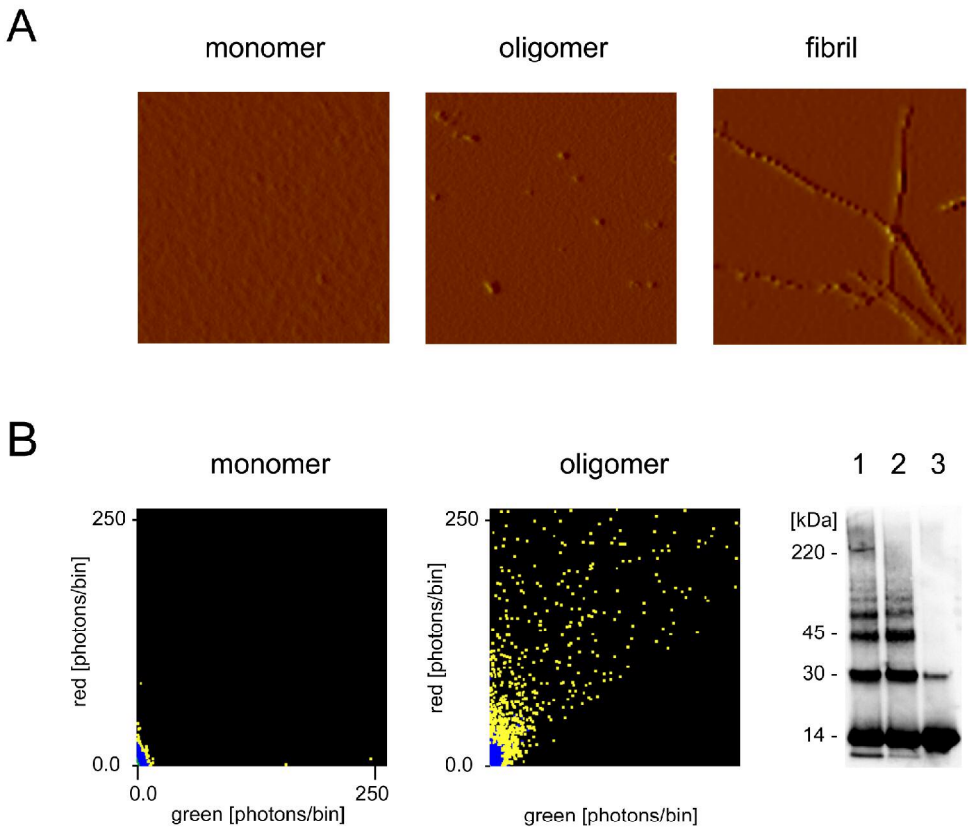
A
monomer
oligomer
fibril
B
monomer
oligomer
1 2 3
250
red [photons/bin]
0.0
0.0
250
green [photons/bin]
250
red [photons/bin]
0.0
green [photons/bin]
[kDa]
220 -
45 -
30 -
14 -

Fig. 1

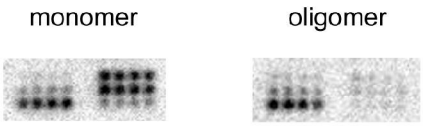

Fig. 2

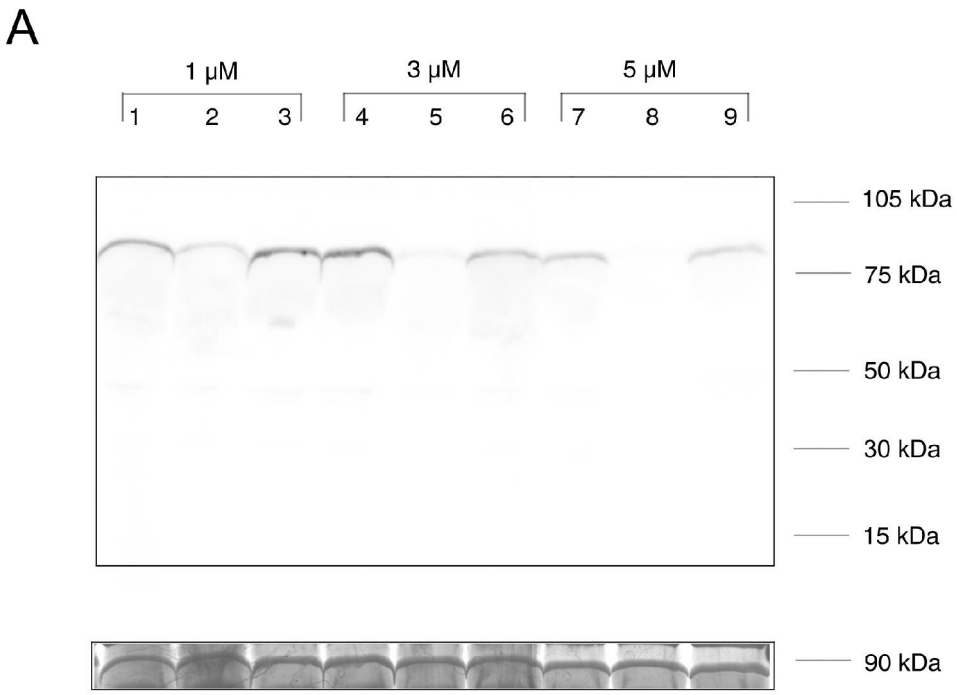
A
1 µM
3 µM
5 µM
1 2 3 4 5 6 7 8 9
105 kDa
75 kDa
50 kDa
30 kDa
15 kDa
90 kDa

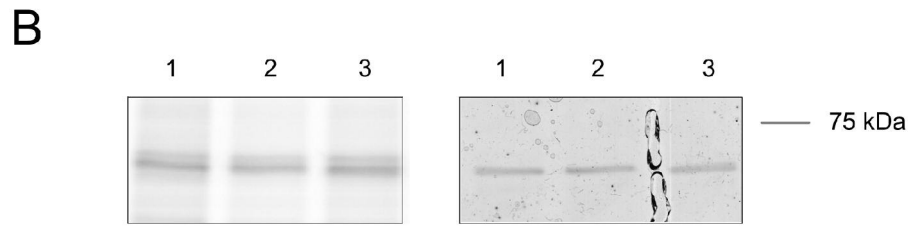
B
1 2 3 1 2 3
75 kDa

Fig. 3

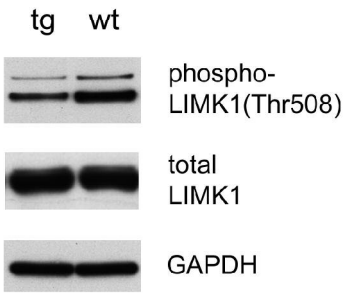

Fig. 4

Danksagung

Mein erster großer Dank gilt meinem Betreuer Dr. Marcus Kostka, der diese Dissertation ins Leben gerufen und mich immer voll und ganz sowohl wissenschaftlich als auch moralisch unterstützt hat. Er stand mir immer mit Rat und Tat zur Seite und seine sehr hilfreichen und zielgerichteten Vorschläge haben mir stets geholfen, zügig und effektiv zu arbeiten.

Bei Herrn apl. Prof. Dr. Wolfgang Weidemann möchte ich mich für die Übernahme des Erstgutachtens bedanken.

Herrn Prof. Dr. Spindler und Herrn PD Dr. Frank Gillardon danke ich für ihre wissenschaftliche Begutachtung in ihrer Funktion als Zweit- bzw. Drittgutachter.

Ich danke ebenso unserer Kollaborationspartnern PD Dr. med. Armin Giese und Tobias Högen für die fruchtbare Zusammenarbeit.

Ein herzliches Dankeschön gilt auch dem Leiter unserer Gruppe Dr. Bastian Hengerer für die nette Aufnahme in seine Gruppe, seine Unterstützung und die anregenden Diskussionen. Es hat Spaß gemacht, in der Parkinson Gruppe zu arbeiten.

Auch Peter Anding, Sabine Finger und Monika Palchaudhuri gilt ein von Herzen kommendes Dankeschön! Vielen Dank für die Unterstützung bei der täglichen Laborarbeit und die schöne Zeit im Labor.

Ein Dankeschön auch an meine Kollegen Dr. Lothar Kussmaul und Sebastian Eder für die guten Diskussionen. Daraus haben sich einige sehr gute Experimente entwickelt.

Auch bei meinen Eltern und Geschwistern Simone, Constanze und Wolfgang, sowie meinen Freunden vor allem Isa möchte ich mich bedanken. Sie hatten immer viel Verständnis und haben mich während der ganzen Studienzeit begleitet.

Mein besonderer Dank gilt meinem Mann Michael, der mir während der letzten Jahre so viel Einfühlungsvermögen, Geduld, Unterstützung und Liebe entgegenbrachte. Er schenkt mir Kraft, Mut und macht mein Herz froh, was die Grundlage war, damit diese Arbeit gelingen konnte.

Lebenslauf

Persönliche Angaben

Name:	Karin Danzer, geb. Ruf
Geburtsdatum:	26. November 1978
Adresse:	Büchsengasse 7
	89073 Ulm
Geburtsort:	Biberach/Riss
Staatsangehörigkeit:	deutsch
Familienstand:	verheiratet
Email:	karin.danzer@bc.boehringer-ingelheim.com

Ausbildung:

2004-2007	**Dissertation in der Abteilung Zentrales Nervensystem, Boehringer Ingelheim Pharma GmbH & Co. KG und Abteilung Allgemeine Zoologie und Endokrinologie, Universität Ulm**
2003	**Diplomarbeit in der Abteilung Physiologische Chemie, Universität Ulm**
2000-2003	**Hauptstudium Diplombiologie an der Universität Ulm,** Hauptfächer: Mikrobiologie, Humangenetik, Pharmakologie und Chemie
1999-2000	Fortsetzung des **Grundstudiums Diplombiologie** an der Universität Ulm
1998-1999	Beginn des **Grundstudiums Diplombiologie** an der Julius-Maximilians-Universität in Würzburg
1998	**Abitur** am Pestalozzi-Gymnasium in Biberach/Riss

Praktika:

2005	• vierwöchiger Forschungsaufenthalt an der University of California, Irvine, Department of Molecular Biology and Biochemistry, USA, Prof. Charles Glabe
2002	• dreimonatiges Praktikum am Institute of Medical Genetics Cardiff, University of Cardiff, U.K., Prof. Upadhyaya
2002	• Wissenschaftliche Hilfskraft am Interdisziplinären Zentrum für Klinische Forschung Abteilung Neurologie in Ulm (2 Monate)
2001	• Sechswöchiges Praktikum bei Boehringer Ingelheim Pharma GmbH & Co KG in der Abteilung Onkologie
2000-2002	• Wissenschaftliche Hilfskraft in der Abteilung Allgemeine Zoologie und Endokrinologie an der Universität Ulm, Prof. Spindler

Präsentationen, Vorträge und Preise

2007	• AD/PD Award, sponsored by Karger, erhalten auf der internationalen Alzheimer und Parkinson Konferenz in Salzburg
	• AD/PD Kongress, Salzburg, Poster: Different a-Synuclein Oligomers-the Toxic Species in Parkinson's Disease
2006	• Forum of European Neuroscience, Wien, Poster: Oligomeric Forms of Proteins
	• MDS, Kyoto, Vortrag in der Young Scientists Best Posters Session: a-Synuclein Oligomers-the Toxic Species in Parkinson's Disease
	• MDS, Kyoto, Poster: a-Synuclein Oligomers-the Toxic Species in Parkinsons Disease
2005	• FENS/Hertie Winter School, Kitzbühel, Poster: Identification of Pathological Relevant a-Synuclein Species in Parkinson's Disease and Synucleinopathies

Publikationen:

- **K.Danzer** and M.Kostka: Different species of alpha synuclein oligomers induce calcium influx and seeding. Accepted *Journal of Neuroscience* on 21st June 2007
- **K.Danzer,** C.Schnack and F.Gillardon: Functional protein kinase arrays reveal inhibition of p-21 activated kinase 4 by a-synuclein oligomers. Revised version submitted to *Journal of Neurochemistry* on 28th June 2007
- M.Kostka, **K.Danzer**, T.Högen, and A.Giese: Single particle characterisation of pore forming a-Synuclein Aggregates. Submitted to *European Molecular Biology organisation (EMBO)* on 13th May 2007
- F.Gillardon, W.Rist, L.Kussmaul, J.Vogel, M.Berg, **K.Danzer**, N.Kraut and B.Hengerer: Proteomic and functional alterations in brain mitochondria from Tg2576 mice occur before amyloid plaque deposition. *Proteomics*. 2007 Feb;7(4):605-16.

Ulm, den 2. Juli 2007

Karin Danzer

Erklärung:

Hiermit versichere ich, dass ich die vorliegende Arbeit selbstständig angefertigt habe und keine anderen als die angegebenen Quellen und Hilfsmittel benutzt, sowie die wörtlich und inhaltlich übernommenen Stellen als solche kenntlich gemacht habe.

Ulm, den 2. Juli 2007

Karin Danzer